

UC Berkeley

UC Berkeley Electronic Theses and Dissertations

Title

Pleistocene-Recent Thermal and Faunal Change in California's Coastal Marine Habitats

Permalink

<https://escholarship.org/uc/item/3x63m4tp>

Author

Orzechowski, Emily Ann

Publication Date

2019

Peer reviewed|Thesis/dissertation

Pleistocene-Recent Thermal and Faunal Change in California's
Coastal Marine Habitats

By

Emily A. Orzechowski

A dissertation submitted in partial satisfaction of the
requirements for the degree of

Doctor of Philosophy

in

Integrative Biology

in the

Graduate Division

of the

University of California, Berkeley

Committee in charge:

Professor Seth Finnegan, Chair
Professor Charles Marshall
Professor John Chiang

Summer 2019

Abstract

Pleistocene-Recent Thermal and Faunal Change in California's

Coastal Marine Habitats

by

Emily A. Orzechowski

Doctor of Philosophy in Integrative Biology

University of California, Berkeley

Professor Seth Finnegan, Chair

The Pleistocene Epoch (2,588,000 – 11,700 years ago) was characterized by cyclical global change: warming and cooling, sea level rises and subsequent falls. Terraced above the shores of California, coastal uplift has raised and preserved the remains of Pleistocene beaches. Over 150 years of research on this “marine terrace” record has uncovered a dynamic history of climatic and consequent biogeographical change. As such, California's marine terrace record provides an empirical framework for understanding how thermal change drives biogeographic shifts. But our knowledge of the magnitude of Pleistocene coastal thermal changes, and, the extent to which species' ranges were impacted, has been limited by the difficulty of precisely dating marine terraces and independently reconstructing their paleoenvironments.

Here, I leverage recent advances in geochronology and paleo-thermometry to revisit the marine terraces of California. In Chapter I, I introduce this classic paleoecological system and review its major contributions to natural history. In Chapter II, I use bulk and clumped stable isotope paleo-thermometry to provide clarity on the magnitude of thermal change observed within coastal marine habitats during several Pleistocene climate states, including the Marine Isotope Substages (MIS) 5a (~80,000 years ago) and 5e (~120,000 years ago). In Chapter III, I compare paleo-temperature reconstructions to their associated mollusk communities to test whether species lived within their present-day thermal niches during the Pleistocene. In Chapter IV, I compile marine terrace localities radiometrically dated to MIS 5e—the warmest climate state of the last 300,000 years—to analyze the environmental characteristics of presently extralimital species. And finally, in Chapter V, I synthesize my findings in the context of contemporary change.

I find that Pleistocene paleo-temperatures were ~2.5°C cooler than present for MIS 5a and similar to at present for MIS 5e open-coast habitats. All fossil species occurrences fall well inside their present-day thermal niches, thereby indicating that coastal marine mollusks have tracked stable thermal niches over Pleistocene timescales. I further find that ~15% of species found in southern California during MIS 5e have since been extirpated to warmer southern waters and that these species range into cooler subtropical regions at higher rates than their conterminous faunas. Taken together, these findings portend that contemporary climate change will welcome the establishment of subtropical invasive species once regional warming suffices to allow southern mollusks to track their thermal ranges up California's coast.

Dedication

For my family

Acknowledgements

A million thanks to my research adviser and dissertation chair, Seth Finnegan. Your energy, patience, and remarkable talent for seeing patterns in a haze of data never cease to inspire me. I would also like to thank my qualifying and dissertation committee members Anthony Barnoksy, John Chiang, Dave Lindberg, Charles Marshall, and Ian Wang. Each of you broadened my perspective, sharpened my research methods, and shaped my questions. And finally, a sincere and special thanks to Dan Muhs, Jere Lipps, Jim Valentine, Dave Lindberg (again), and Charles Powell, II: your expertise and guidance in understanding the geology and biogeography of California's marine terraces (and some basins) has been truly indispensable.

My dissertation research was enabled by generous funding from the National Science Foundation, the UC Museum of Paleontology, American Natural History Museum, American Philosophical Society, Conchologists of America, Evolving Earth Foundation, National Geographic Society Young Explorers Program, Natural History Museum of Los Angeles County, Northern California Geological Society, Sigma Xi, and the Western Society of Malacologists; stipend and fellowship support was provided by the National Science Foundation, UC Museum of Paleontology, and the Exploring California Biodiversity GK-12 Program.

An exceptional experience doing fieldwork on San Nicolas Island was made possible by the generous advice and assistance of the U.S. Navy, Lisa Thomas, and Daniel Muhs. Austin Hendy, Mary Stecheson, and Erica Clites provided invaluable assistance while I studied museum specimens at the Los Angeles County Museum of Invertebrate Paleontology and UC Museum of Paleontology. Jessica Bean, Zev Brooks, Bob Gaines, John Grimsich, Timothy Teague, Daniel Stolper, and Wenbo Yang were immensely helpful in X-ray diffractometry and isotope analyses.

I'd further like to thank my colleagues at the Paleontological Society for their professional mentoring, most especially thank you Arnie Miller, Rowan Lockwood, Steve Holland, and Bruce MacFadden, and thank you also to Sharon McMullen, Lucy Chang, and Kris Kusnerik for your camaraderie while serving as Student Representatives to Council. Additional thanks go to my Finnegan Lab comrades Larry Taylor, Joshua Zimmt, and Sara Kahanamoku-Snelling, for their support and bad puns (just Josh); and to my Graduate Assembly peers for their inspiring leadership. I'd also like to thank my K-12 education mentors and colleagues: Betsy Mitchell, Jessica Bean, Candy Blesse, Karina Klonoski, Leslie McGinnis, and Lisa White.

Finally, sincere thanks to my undergraduate research thesis, apprentice, and work-study students. Alyssa Barbosa, your work ethic and expertise in taxonomy was truly indispensable. Chloe Golde, thank you for bringing your hilarious sense of humor and amazing grasp of marine science content to the lab. Leyla Namazie, your sharp insights and quick learning are sure to serve you well in science. Max Titcomb, you brought an infectious curiosity and laughter to the lab. Stephanie Wang, your delightful levity and keen interest was such a joy to work with. Nina Jaeger, your interest in the higher terraces and your collaborative spirit led to some amazing discoveries. Zev Brooks, it was an honor to work with you; I can't wait to see what you uncover in graduate school and beyond. Sydney Mingos, thank you for being there from the start and helping me through the initial difficulties. Our fieldwork trip with Jackson was *the* highlight of my dissertation work.

Table of Contents

Dedication.....	i
Acknowledgements	ii
Table of Contents	iii
List of Figures.....	iv
List of Tables.....	v
Chapters:	
I. An introduction to the Pleistocene marine terraces of California	1
II. Late Pleistocene coastal marine temperatures in California	11
III. Pleistocene-present thermal niche tracking in Californian coastal mollusks	38
IV. Extralimitals from the Marine Isotope Substage 5e in coastal marine California.....	53
V. Lessons from the Pleistocene and predictions for the present.....	72
References	73
Appendices:	
I. Bulk isotopes and $\delta^{18}\text{O}$ paleo-temperatures	89
II. Clumped isotopes and Δ_{47} paleo-temperatures	112
III. Pleistocene faunas of Isla Vista, Palos Verdes Hills, and San Nicolas Island	115
IV. Present-day ranges of Pleistocene mollusks from California.....	120
V. Marine Isotope Substage 5e fossil localities.....	132
VI. Marine Isotope Substage 5e extralimital mollusc occurrences	134
VII. Present-day ranges of Northern Panamic region mollusks	136

List of Figures

1.1 Reconstructed Pleistocene localities in southern California	6
1.2 San Nicolas Island marine terrace locality map	7
1.3 Average annual sea surface temperatures for Pacific Northeast	8
1.4 Average winter sea surface temperatures for Pacific Northeast.....	9
1.5 Average summer sea surface temperatures for Pacific Northeast	10
2.1 Δ_{47} Temperatures for Late Pleistocene climate states.....	25
2.2 Δ_{47} Temperatures for Late Pleistocene climate states by <i>C. biplicata</i> specimens	26
2.3 Δ_{47} & $\delta^{18}\text{O}_{\text{seawater}}$ for reconstructed locations and climate states	27
2.4 Late Pleistocene-Modern $\delta^{18}\text{O}_{\text{aragonite}}$	28
2.5 Late Pleistocene-Modern $\delta^{18}\text{O}$ temperature.....	29
2.6 Late Pleistocene-Modern $\delta^{18}\text{O}$ temperature on San Nicolas Island by specimen	30
2.7 Modern $\delta^{18}\text{O}$ and modern buoy-measured temperatures.....	31
2.8 Late Pleistocene-modern $\delta^{13}\text{C}_{\text{aragonite}}$ and $\delta^{18}\text{O}_{\text{aragonite}}$	32
2.9 Late Pleistocene-modern $\delta^{13}\text{C}_{\text{aragonite}}$	33
2.10 Late Pleistocene-Modern $\delta^{18}\text{O}$ temperature on Palos Verdes Hills by specimen	34
2.11 Late Pleistocene-Modern $\delta^{18}\text{O}$ temperature on Isla Vista by specimen	35
3.1 Δ_{47} temperatures for Early Pleistocene terraces on San Nicolas Island.....	45
3.2 Δ_{47} and $\delta^{18}\text{O}_{\text{seawater}}$ for Early Pleistocene marine terraces on San Nicolas Island.....	46
3.3 $\delta^{18}\text{O}$ temperatures for Early Pleistocene terraces on San Nicolas Island	47
3.4 Contemporary thermal niche tracking on San Nicolas Island	48
3.5 Late Pleistocene thermal niche tracking on San Nicolas Island.....	49
3.6 Early Pleistocene thermal niche tracking on San Nicolas Island	50
3.7 Thermal niche tracking at Palos Verdes Hills during MIS 5a and 5e	51
3.8 Thermal niche tracking at Isla Vista during MIS 3a	52
4.1 California & Northern Panamic region map with MIS 5e fossil localities	64
4.2 Best-supported MIS 5e extralimital model species probabilities	65
4.3 Best-supported MIS 5e extralimital model species probabilities	66

List of Tables

2.1 $\delta^{18}\text{O}$ Temperature for Late Pleistocene climate states.....	36
2.2 $\delta^{18}\text{O}$ temperature Tukey's Honest Significance Test.....	37
4.1 Paleo-protected vs. paleo-open coast MIS 5e extralimital occurrences	67
4.2 Environmental and geographic predictors correlation matrix	68
4.3 AICc model comparisons for range-limiting regression models.....	69
4.4 AICc model comparisons for range-through regression models.....	70
4.5 Parameter estimates for the best-supported logistic regression models	71

Chapter I

An introduction to the Pleistocene marine terraces of California

"Modern species that are found as fossils beyond their present geographic range are generally held to be indicators of a corresponding shift of the environment, due to climatic or other change. In the absence of conflicting evidence that inference is plausible. The late Pliocene and Pleistocene marine molluscan faunas of California, however, present conflicting evidence as indicators of past temperature. Species that are north of their present geographic range are found in direct association with species that are south of their present range.

This conflicting evidence might be resolved by postulating subsequent evolution in physiological characters that shows no correlation with evolution in morphological characters available to paleontologists, or by postulating the rise and extinction of local subspecies-or species differentiated by physiological characters unknown and unknowable to paleontologists.

It is suggested that determinations of temperature coefficient, based on the ratio of the isotopes O^{18} to O^{16} in the calcium carbonate of the fossils, should show whether the conflicting evidence is as irreconcilable as it now appears to be."

W.P. Woodring, *Science (abstracts)*, 1951, from
"Basic assumption underlying paleoecology."

1.1 A classic paleoecological study system

Along the coast of southern California, the uplifted remnants of Pleistocene fossil beaches, known as "marine terraces," are ubiquitous geomorphological features which have inspired the curiosity of generations of paleontologists (e.g., Conrad 1855; Dall 1921; Crickmay 1929; Valentine 1961; Veddar and Norris 1963; Kennedy et al 1982; Lindberg and Lipps 1993; Roy et al 1993; Powell 2000; Muhs and Groves 2018). Studies dating to the late nineteenth century (see Conrad 1855 and review of early work in Valentine 1961) have shaped and enforced the foundation of paleoecology, and in the process, built a wealth of knowledge relating to this classic paleoecological system (Valentine 1973). Foundational studies in taphonomy interrogated the depositional characteristics of fossil assemblages and showed how they reflect paleo-habitats (Johnson 1960a, 1960b, 1962, 1965b) and environmental conditions (Johnson 1965a, 1967; Schopf 1978). The 1989 paper entitled "How Good is the Fossil Record?" further used marine terraces as the basis to affirm the strength of the fossil record (~80% of hard-shelled species known to occur in California are found as fossils in the terrace and basin records) and to highlight the species which it fails to faithfully record, i.e. small-bodied and rare animals

(Valentine 1989). A preponderance of biogeographic evidence supported the cyclical rhythms of glacial and interglacial climate states and showed that species shifted their ranges up and down the coast of California in apparent accordance with thermal regimes (Valentine 1961; Kennedy et al 1982; Roy et al 1995, 1996). And finally, a striking lack of extinctions in the Pleistocene marine terrace record (Valentine 1989b; Linberg and Lipps 1993; Holland 2013) — even in the face of rapid and substantive global changes — helped form the concept of "background" extinctions and inspired the theory of global continental configurations in dictating biodiversity collapses and buffering (Valentine and Moores 1970; Valentine 1973; Valentine 1989b).

Complementary to the blossoming of research focused on the fossilized constituents of prehistoric beaches, naturalists from institutions throughout the Pacific coastal regions of the U.S. studied, in great detail, the life histories, ecologies, and distributions of intertidal and shallow subtidal coastal marine invertebrates (Ricketts et al 1939; Keen 1971; Morris et al 1980; Coan et al 2000; Coan and Valentich-Scott 2012). Most widely known of these naturalists was Ed Ricketts, whose persona John Steinbeck canonized in his 1951 "The Log from the Sea of Cortez" and whose natural history of intertidal habitats, "Between Pacific Tides" (1939), remains a desk-side companion for both scientists and amateurs alike. These naturalist efforts built reservoirs of knowledge (Ricketts et al 1939; Keen 1971; Morris et al 1980; Coan et al 2000; Coan and Valentich-Scott 2012) that enabled paleontological investigations that cut across disciplines and have most recently been brought to bear on some of the most curious features of the marine terrace record (Roy et al 1995, 2001).

1.2 Faunal-based paleoenvironmental reconstructions, extralimitals, and thermally disjunct assemblages

The majority of work on California's marine terraces has focused on applying the geological axiom that "the present is the key to the past" by leveraging modern data on species' geographic ranges to interpret paleo-thermal regimes (Arnold 1903; Woodring et al 1946; Valentine 1961; Addicott 1966; Kennedy et al 1982; Powell 2001; Powell et al 2004, 2009). This important body of research — which largely concentrated on sites in the rapidly developing urban regions around Los Angeles but also encompassed remote regions in the Channel Islands (Figures 1.1 and 1.2) — worked on the basis that coastal California's geography is largely north-south trending, and as such latitudinal variation in geographic distributions corresponds strongly to annual and seasonal thermal isobars (Figures 1.3, 1.4, and 1.5). By drawing lines of evidence between the contemporary thermal ranges of species found as fossils, researchers computed bounds on pre-historic thermal maxima and minima, thereby enabling the incorporation of these geomorphologically complex features into an emerging stratigraphic and paleo-climate framework (e.g., Valentine 1961; Powell 1994, 2000, 2001, 2004; Hall 2002; Powell and Ponti 2007). "Extralimitals," i.e. species that occurred in California during the Pleistocene but today reside exclusively to the north or south, formed the basis of these paleoenvironmental reconstructions, with warm paleo-temperatures inferred by the presences of southern extralimitals and cool paleo-temperatures inferred by the presences of northern extralimitals

(Kanakoff and Emerson 1959; Valentine 1961; Veddar and Norris 1963; Powell 1994, 2000, 2001, 2004; Hall 2002; Powell and Ponti 2007).

But as the opening quote by Wendell Phillips Woodring encapsulates, such faunal based paleoenvironmental reconstructions were not without critics (Woodring 1951; Johnson 1960a). As these critics stated: using modern ranges to draw inferences about paleo-environmental conditions is based on an assumption of thermal niche stability. Thus, this assumption would be violated in instances of niche evolution, thereby leading to uninterpretable and misleading paleoenvironmental results. Moreover, studies that used the faunas to infer paleo-conditions, and then used those inferences to draw conclusions about biogeography, ran the risk of circular reasoning (Dincauze 1987).

The presence of thermally disjunct, or "anomalous" assemblages, at several sites throughout California seemed to call into question the validity of faunal based reconstructions (Woodring 1951; Valentine and Emerson 1961; Lindberg and Lipps 1996). These assemblages, in which both northern and southern extralimitals co-occurred in close association, showed evidence of paleo-habitats with no modern analog, and hence, implied some degree of (realized) thermal niche evolution over Pleistocene timescales (Valentine and Meade 1961; Zinsmeister 1974; Lindberg et al 1980; Lindberg and Lipps 1996). However, several researchers intuited that these thermally disjunct assemblages were not evidence of thermal niche evolution (Lindberg and Lipps 1993), but that instead they represented complex environmental conditions ranging from inter-annual (Zinsmeister 1974) and inter-centennial variability (Roy et al 1996) to localized upwelling and enhanced seasonality (Valentine 1955, 1958; Emerson 1956a, 1956b; Valentine and Emerson 1961). From this standpoint, thermally disjunct assemblages merely symbolized poorly understood paleo-environments requiring independent paleoenvironmental evidence to clarify (Woodring 1951; Valentine and Emerson 1961; Valentine 1973).

1.3 Advances in marine terrace geochronology and paleo-thermometry

Recent innovations in marine terrace geochronology have called into question the century-old discussion of thermally disjunct assemblages and enlightened the biogeographic framework of southern California's terraces. These studies built a uranium-thorium radiometric dating model using the solitary coral *Balanophyllia elegans* (Muhs 1992; Muhs et al 1994, 2002, 2006, 2012, 2015, 2014). Such radiometric dating is the first comprehensive approach that is based on direct dating and independent of faunal evidence (as opposed to correlative dating approaches, such as amino acid racemization; Wehmiller 1977; Kennedy et al 1982, 1992) to be leveraged in the marine terrace system and has enabled a new regional geochronology (Muhs et al 2002, 2006, 2012, Muhs and Groves 2018). As uplifted marine terraces primarily preserve sea level highstands (Johnson 1988, 1992; but see Powell 1994, Powell and McGann 2008, and Powell et al 1992 for discoveries of submerged wave-cut platforms formed during sea level lowstands) and uranium-thorium dating is constrained to within the Late Pleistocene window, the majority of marine terraces have been dated to the three Marine Isotope Stage 5 highstands (Shackleton and

Opdike 1973; Martinson 1987): the 5e (~120,000 years ago; Johnson and Libbey 1997), 5c (~105,000 years ago), and 5a (~80,000 years ago).

The new marine terrace geochronology has clarified questions regarding the ages, uplift rates, and paleo-sea level histories of southern California's Late Pleistocene coastal marine fossil record (Muhs et al 2002, 2006, 2012, 2014, Muhs and Groves 2018). It has also helped resolve the conditions under which thermally disjunct assemblages formed: whereas the majority of marine terrace localities show clear evidence of dating to a particular MIS 5 substage, when several fossils are dated from thermally disjunct assemblages these fossils show a bimodal age distribution — with some fossils dating to MIS 5e and others dating to the 5c (Muhs et al 2012, 2014; Muhs and Groves 2018). Such evidence implies that the same terrace surface was flooded during two different sea level highstands (MIS 5e and 5c), which caused millennial scale time-averaging (Muhs et al 2012, 2014; Muhs and Groves 2018). This hypothesis for thermally disjunct assemblages contains a testable proposition: fossils from thermally disjunct sites should show a bimodal distribution of paleo-temperatures, with some fossils reconstructing relatively warm conditions (presumably deposited during the globally warmer-than-present MIS 5e state) and others reconstructing cooler conditions (presumably deposited during the globally cooler-than-present MIS 5c climate state).

The magnitude of Late Pleistocene thermal changes in coastal marine California is at present poorly understood. Early attempts to utilize geochemical paleo-temperature proxies have generally produced conflicting or inconclusive results, in part due to inherent difficulties in applying bulk oxygen isotope composition to reconstruct paleo-temperatures during climate states with unknown seawater compositions (Valentine and Meade 1961; Muhs and Kyser 1987). Fortunately, recent advances in clumped isotope paleo-thermometry allow the reconstruction of paleo-temperature independent of seawater composition (Ghosh et al 2006; Schauble et al 2006; Eiler 2007, 2011), thus enabling a renewed investigation of Late Pleistocene climate change in coastal California.

1.4 Revisiting the marine terraces of coastal California

Here I revisit the classic paleoecological system of California's marine terrace record. Specifically, I leverage recent geochronologies (Muhs et al 2002, 2006, 2012, Muhs and Groves 2018) and introduce new paleo-temperature reconstructions based on independent methodologies (Ghosh et al 2006; Schauble et al 2006; Eiler 2007, 2011) to answer several unresolved questions and interpret their importance in the context of contemporary climate change.

In Chapter II, I present paleo-temperature reconstructions for several marine terrace sites along the Californian coast (Figures 1.1 and 1.2) spanning MIS 5e (~120,000 years ago), 5c (~105,000 years ago), 5a (~80,000 years ago), and 3a (~50,000 years ago). These paleo-temperatures provide clarity on the magnitude of Late Pleistocene thermal changes, speak to an ongoing debate about the relationship between regional warming and upwelling in California and other

Eastern Boundary Current Systems (Bakun 1990; Bakun et al 2015; Sydeman et al 2014; Wang et al 2015), and help distinguish the temporal mixing in certain thermally disjunct assemblages. In Chapter III, I apply my paleo-temperature reconstructions to construct a test of thermal niche evolution and thermal niche tracking in Late and Early Pleistocene fossil assemblages. In Chapter IV, I analyze the characteristics of extralimital species from the warmest climate state of the last 300,000 years —MIS 5e — and synthesize the regional biogeography and paleoclimate for this ancient analog climate. I close in Chapter V by synthesizing my findings in the context of contemporary climate change in coastal marine California.

Chapter I Figures

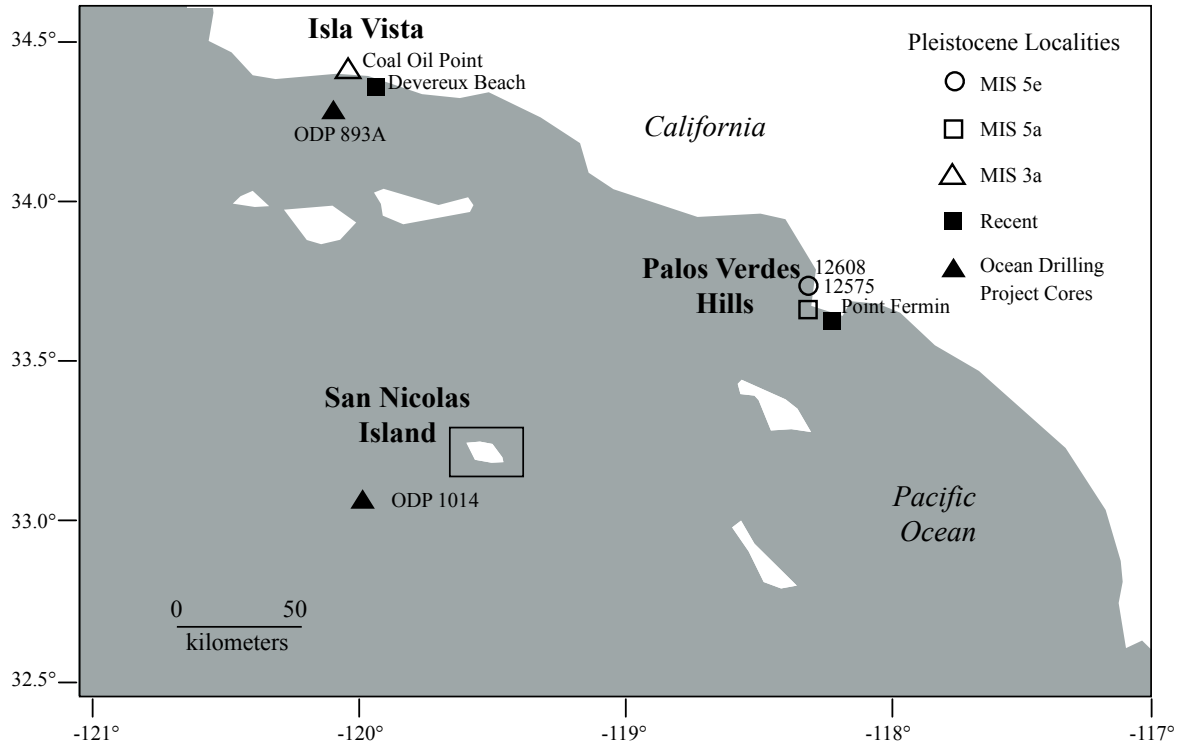


Figure 1.1: Reconstructed Pleistocene localities in southern California. Both modern and fossil collections were made at each location: San Nicolas Island, Palos Verdes Hills, and Isla Vista. See Figure 1.2 for localities on San Nicolas Island. Age of localities is indicated; MIS = Marine Isotope Substage; ODP= Ocean Drilling Project Core.

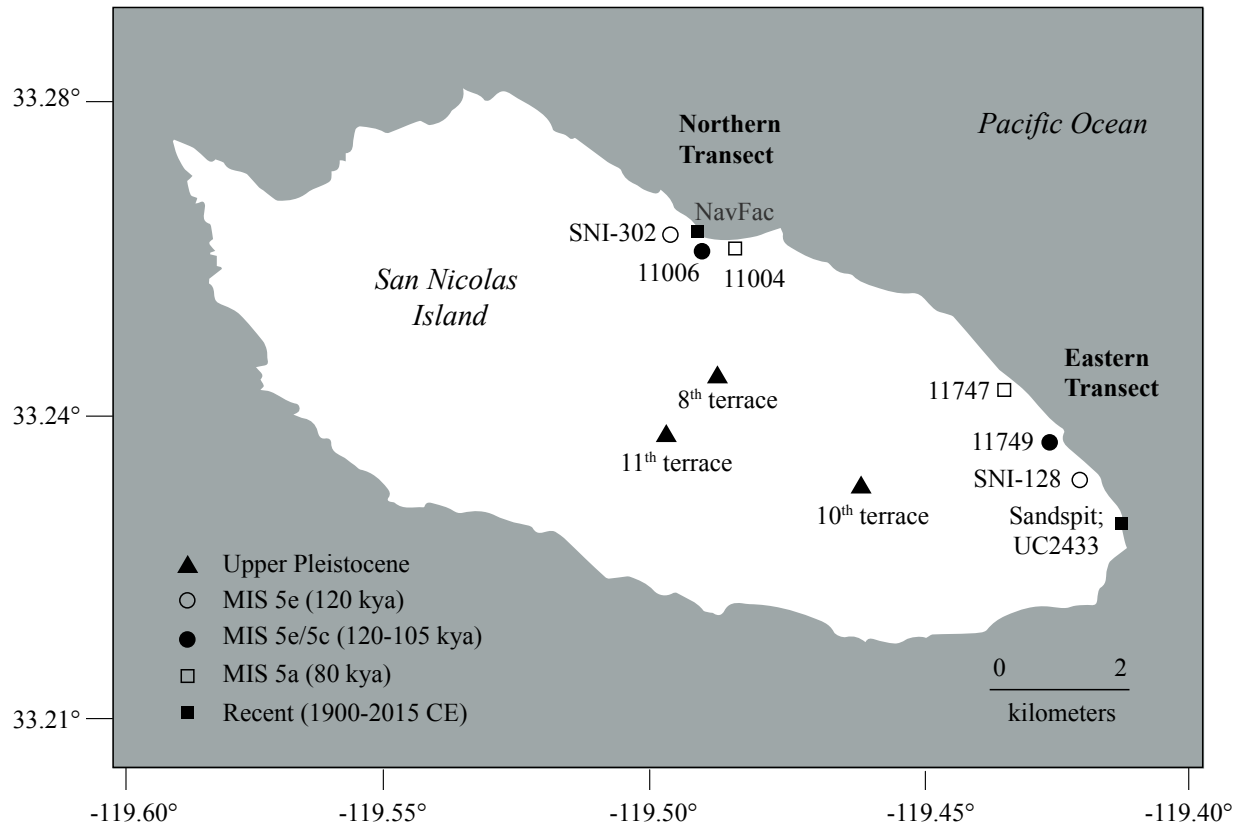


Figure 1.2: San Nicolas Island marine terrace locality map. Two Late Pleistocene-modern transects, each containing modern, MIS 5a, 5e/5c, and 5e localities, were made along the northern and eastern sides of the island. Early Pleistocene localities made on higher marine terraces are located in the island's interior. Age of localities is indicated; MIS = Marine Isotope Substage.

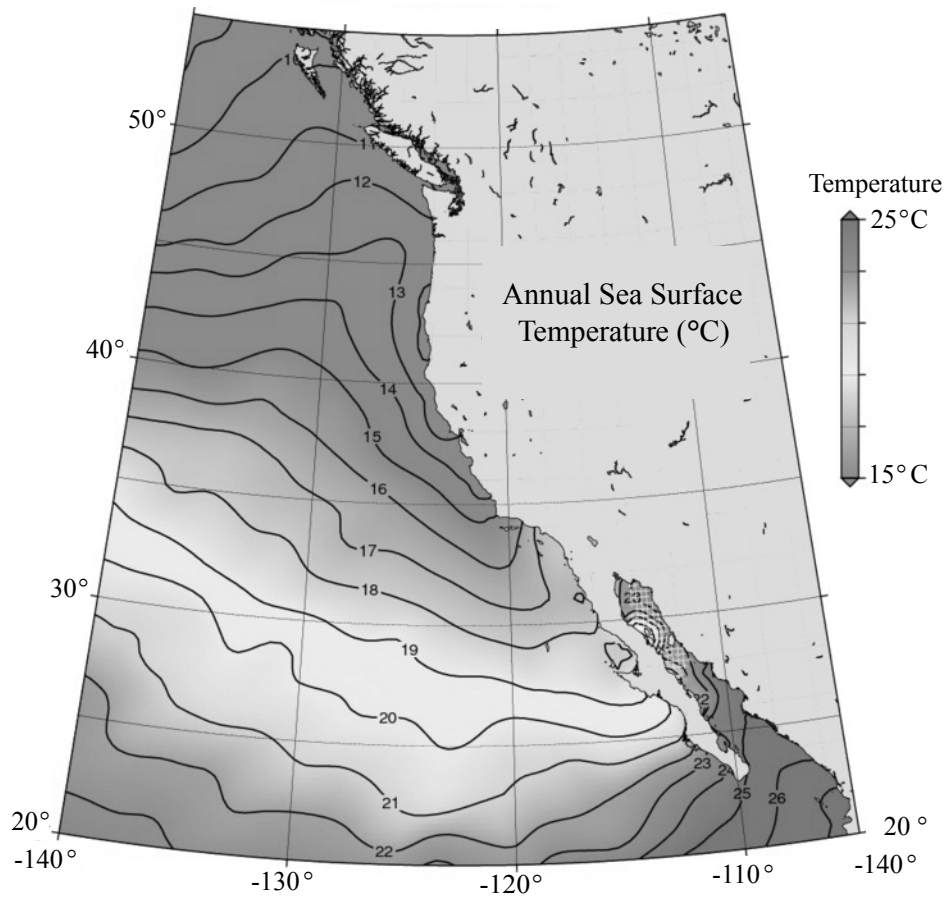


Figure 1.3: Average annual sea surface temperatures for the Pacific Northeast. Annual sea surface temperatures averaged over 1955-2018 and at quarter-degree resolution; thermal isobars from 26°C-10°C indicated. Data and figure modified from the National Oceanographic and Atmospheric Administration’s World Ocean Atlas 2018 (nodc.noaa.gov/cgi-bin/OC5/woa18f/woa18f). Contemporary average annual temperatures in southern California range between 15°C-18°C.

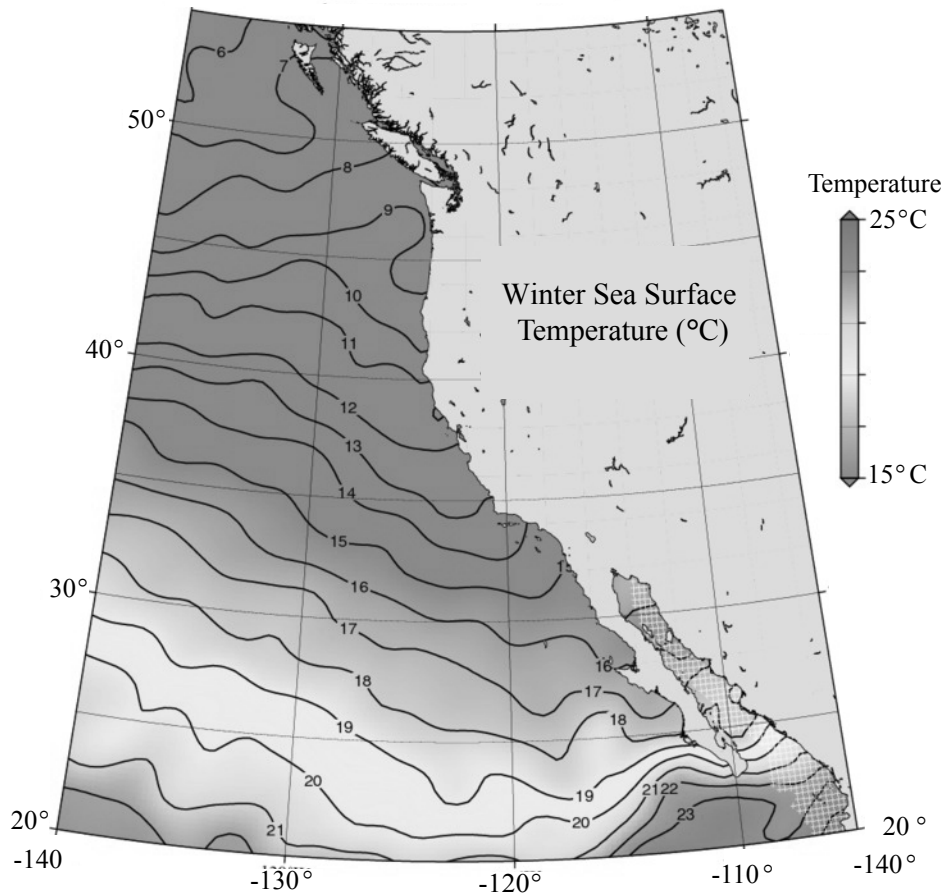


Figure 1.4: Average winter sea surface temperatures for the Pacific Northeast. Winter sea surface temperatures averaged over 1955-2018 and at quarter-degree resolution; thermal isobars from 26°C-10°C indicated. Data and figure modified from the National Oceanographic and Atmospheric Administration’s World Ocean Atlas 2018 (nodc.noaa.gov/cgi-bin/OC5/woa18f/woa18f). Contemporary average winter temperatures in southern California range between 13°C-16°C.

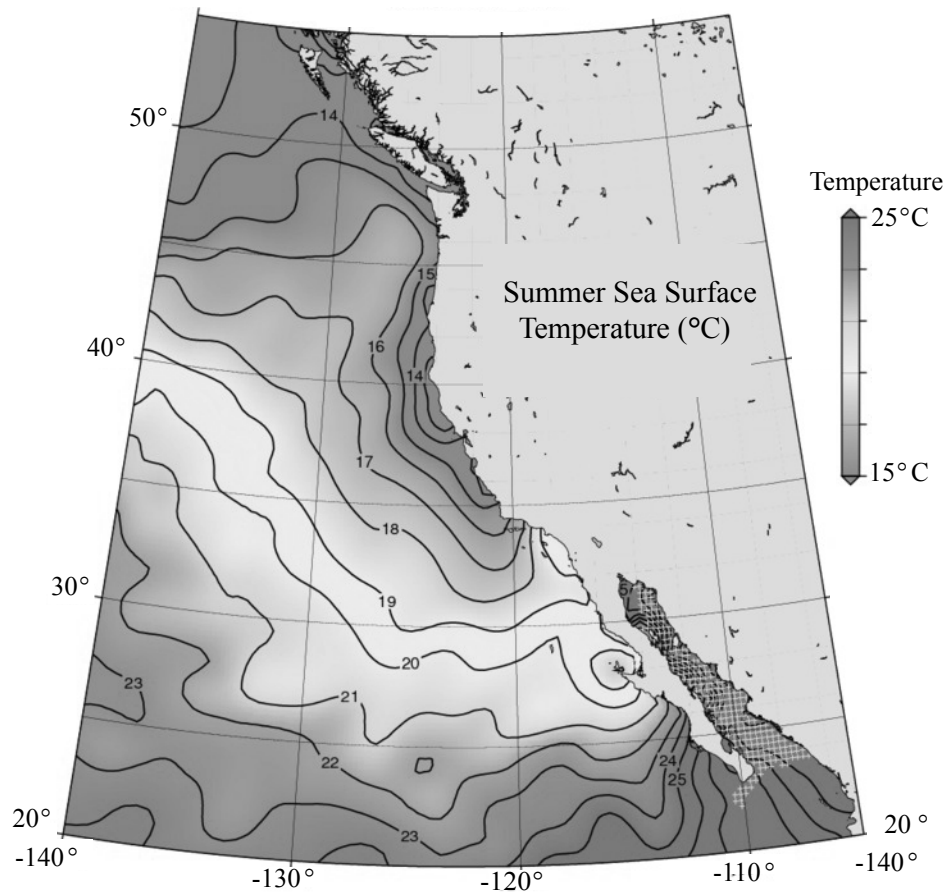


Figure 1.5: Average summer sea surface temperatures for the Pacific Northeast. Summer sea surface temperatures averaged over 1955-2018 and at quarter-degree resolution; thermal isobars from 26°C-10°C indicated. Data and figure modified from the National Oceanographic and Atmospheric Administration’s World Ocean Atlas 2018 (nodc.noaa.gov/cgi-bin/OC5/woa18f/woa18f). Contemporary average summer temperatures in southern California range between 17°C-19°C.

Chapter II

Late Pleistocene coastal marine temperatures in California

2.1 Abstract

Marine terraces – the uplifted remains of wave-cut platforms from prehistoric sea level highstands – are excellently preserved in southern California and enable the reconstruction of Late Pleistocene climate states in coastal marine habitats. Here, I use clumped (Δ_{47}) and bulk ($\delta^{18}\text{O}$) stable isotope paleo-thermometry on well-preserved shells of the marine gastropod *Callianax biplicata* to reconstruct temperatures at three locations along the California coast: San Nicolas Island, Palos Verdes Hills, and Isla Vista, which together span the Marine Isotope Substages (MIS) 5e (~120,000 years ago), 5c (105,000 years ago), 5a (80,000 years ago), and 3a (50,000 years ago). At each location, both modern and fossil temperatures were reconstructed, allowing for the comparison of modern stable isotope-based temperatures to directly measured buoy temperature data. I find strong correspondence between stable isotope-based temperature reconstructions on modern shells and directly measured buoy data. I further find that both Δ_{47} and Δ_{47} -constrained $\delta^{18}\text{O}$ reconstructions yield similar paleo-temperature conditions for all localities analyzed. Both approaches reconstruct the MIS 5e as similar to present conditions and the MIS 5a as ~2.5°C cooler than at present. Interestingly, an MIS 3a fossil locality at Isla Vista is reconstructed as being quite warm (~15°C), despite being from a relatively cold interstadial period; however, reconstructed $\delta^{18}\text{O}_{\text{seawater}}$ compositions show evidence that the site is a paleo-embayment, which is further bolstered by sedimentological data. These results suggest a moderate degree of thermal stability in southern California's coastal marine habitats, perhaps caused by the stabilizing effects of an interplay between upwelling and coastal geomorphology.

2.2 Introduction

Global climate proxy compilations show significant differences in the magnitudes of climate change during specific Late Pleistocene climate states (Lisiecki and Raymo 2005; Turney and Jones 2010; McKay et al 2011). Marine Isotope Substage 5e (~120,000 years ago), for instance, globally is reconstructed as only slightly warmer than present-day (Turney and Jones 2010; McKay et al 2011). However, in mid-latitude areas some regions reached 4°C above present levels (Turney and Jones 2010; McKay et al 2011). Within the classic paleoecological study system of California's Pleistocene marine terraces (i.e., uplifted wave-cut platforms), MIS 5e shows seemingly contradictory faunal evidence of being both warmer and cooler than present day, even at nearby sites dated to the same time periods (Valentine and Meade 1961; Muhs and Kyser 1986; Muhs et al 2012; Muhs and Groves 2018).

Here I employ clumped (Δ_{47}) and bulk ($\delta^{18}\text{O}$) stable isotope paleo-thermometry to reconstruct the magnitude of Late Pleistocene thermal change in coastal marine habitats during MIS 5e

(~120,000 years ago), 5c (~105,000 years ago), 5a (~80,000 years ago), and 3a (~50,000 years ago). I focus on three locations (Figures 1.1 and 1.2) – San Nicolas Island, Palos Verdes Hills, and Isla Vista – where marine terrace outcrops are excellently preserved and independently dated using uranium-thorium radiometric analyses. At each locality, I scrutinize the accuracy of this approach by comparing reconstructed isotope-based temperatures to modern directly measured coastal sea surface temperatures. Taken together, these paleo-temperature data provide clarity on the degree of Late Pleistocene thermal change within coastal marine habitats of southern California and help to discriminate between Pleistocene climate change scenarios for the region.

2.3 Background

2.3.1 Marine terrace localities

The marine terrace localities chosen for paleoenvironmental reconstruction at Isla Vista (Figure 1.1), Palos Verdes Hills (Figure 1.1), and San Nicolas Island (Figures 1.1 and 1.2) were selected due to their good fossil preservation, well-studied mollusk faunas, and independent age constraints. These sites include terraces formed during MIS 5e, 5c, 5a, and 3a. Most reconstructed localities represent paleo-open coast environments that range from rocky intertidal to sandy shoal environments. One potential paleo-embayment, at Isla Vista, is also included in the present geochemical reconstructions.

San Nicolas Island: San Nicolas Island's fourteen marine terraces are one of the best Quaternary records of coastal marine habitats in the North America (Veddar and Norris 1963; Lindberg and Lipps 1996; Muhs et al 2012). The lowest two terraces have been radiometrically dated at several locations along the island's northern and eastern shores (Valentine and Veeh 1969; Muhs et al 1992, 1994, 2006, 2012). The lowest terrace yields MIS 5a dates and a number of extralimital northern species at fossil localities LACMIP 11004/ 11005, and 11747. Dating at numerous sites on the second terrace yields two distinctive age groups of MIS 5e and MIS 5c at elevations between 33-28 meters (terrace 2b) and exclusively MIS 5e dates at elevations of 38-36 meters (terrace 2a) above present-day sea level. Fossils from terrace 2b (LACMIP 11749 and 11006) contain a mixture of northern and southern extralimital species whereas terrace 2a contains only southern extralimital species (SNI-302 and 128; Muhs et al 2012). This evidence suggests that the “thermally disjunct” terrace 2b is a composite terrace that was deposited during MIS 5e and then re-occupied and mixed during the subsequent MIS 5c; the slightly higher terrace 2a was apparently not reoccupied, presumably because sea levels during MIS 5c did not reach that level (Muhs et al 2012). Because MIS 5e is thought to have been warmer than at present, and MIS 5c similar or slightly cooler than the present day, this terrace reoccupation hypothesis explains the observed pattern of northern and southern species on the time-averaged terrace 2b surface (Muhs et al 2012, 2014, 2018).

Palos Verdes Hills: The lowest two terraces at Palos Verdes Hills, the Paseo del Mar (fossil locality LACMIP 12575; Figure 1.1) and Gaffey terraces (fossil locality LACMIP 12608; Figure

1.1), preserve rocky, exposed coastal settings. Uranium-thorium radiometric dating and amino acid correlation date these localities to MIS 5a and 5e, respectively (Muhs et al 2006, 2018). The fossil fauna at 12575 contains extralimital northern species and thus suggests cooler-than-present conditions during MIS 5a; the fauna at 12608 contains no extralimital species, thereby suggesting that thermal conditions during MIS 5e were comparable to at present (Muhs et al 2006).

Isla Vista: The Coal Oil Point fossil locality at Isla Vista (Figure 1) is unusual in the marine terrace record because it records an interstadial climate state that was deposited when sea levels were well below present-day levels (Trecker et al 1999; Gurrola et al 2013). As such, it provides a rare glimpse into coastal marine habitats during a climate state that was significantly colder than at present (Wright 1972; Barrick et al 1989). Uranium-thorium dating places the deposits to MIS 3a (~47,000 years ago) when global sea level was ~64 meters below present (Gurrola et al 2013). Paleoenvironmental reconstructions based on foraminifera, mollusks, and sediments suggest a shallow (< 5 meter depth) coastal environment with rocky and protected sandy habitats. The presence of several extralimital northern species suggests conditions that were distinctively cooler than present-day.

2.3.2 *Callianax biplicata*

Abundance & ubiquity: *C. biplicata* (Sowerby, 1825; formerly *Olivella*) is a lower intertidal-shallow subtidal marine gastropod with an affinity for rubbly soft-bottom habitats (Ricketts et al 1985). It is the most ubiquitous marine mollusc found along California's coasts today and is the most common fossil found in California's marine terrace record (Valentine 1961; 1980). Presently, it ranges from Magdalena Bay, Mexico to Vancouver Island, Canada and is known to occur on offshore islands, including the Channel Islands (Morris et al 1980). In its preferred habitats of protected and semi-protected open coast habitats (e.g., lees of headlands) it can form aggregations that commonly exceed 1000 individuals per square meter (Onuf 1972; Stohler 1969; Valentine 1961; 1980). These habitats, which are relatively shielded from erosive wave-energy and serve as the sites of coastal sediment accumulation, are also the depositional environments that are most commonly represented in the Pleistocene marine terrace record (Valentine 1980).

Ecology: *C. biplicata*'s living populations have been studied extensively (e.g. Edwards 1968, 1969a, 1969b; Phillips 1977), and local population densities appear to be largely driven by the availability of food (they are omnivorous and have been observed suspension-feeding, rasping algae, and consuming dead and live prey; [Hickman and Lipps 1983]), availability of soft substrates, and protection from intense wave action (Edwards 1969). They are also known to live in rocky, exposed intertidal habitats, but in far fewer numbers. However, rocky intertidal hermit crabs show a strong preference for *C. biplicata*'s relatively large and sturdy shells, and as such they are also quite numerous within rocky intertidal death assemblages (Valentine 1980; Walker 1988, 1989). *C. biplicata* burrows into the sediments just below the surface during the day and

emerges from the subsurface at twilight, when they become more active (Phillips 1977); this shallow semi-infaunal burrowing behavior is not deep enough to offer a buffer from temperature extremes or heat stress (Johnson 1965a; Edwards 1969b) but does offer some protection from receding water levels at low tides (Edwards 1969b; Phillips 1977). *C. biplicata* reproduces year-round; within studied populations in southern California and Oregon, there are no observable changes in size or age class structure throughout the year (Edwards 1968, 1969a, 1969b).

Growth & reproduction: A long-term study of *C. biplicata*'s growth in San Diego revealed no relationship between growth and time of year (Stohler 1962, 1969). Growth is not continuous, however. Indeed, Stohler found that one individual grew only 0.1 mm while another grew 9.7 mm in the same year and at the same site (Stohler 1969). Another individual grew from 14 to 26 mm in a 5-year time span (Stohler 1969). From this, Stohler interpreted that individuals likely grow in relation to the availability of food, and do not exhibit any observable biases with respect to season (Stohler 1969). Individuals reach sexual maturity at 16 mm and typically do not grow beyond 30 mm (Edwards 1968; Stohler 1962, 1969). It is estimated that individuals reach sexual maturity at 4-5 years age, and can live lifespans in excess of 10 years (Edwards 1968; Edwards 1969; Stohler 1962, 1969). An investigation of growth lines within *C. biplicata*'s shell also revealed no annual or seasonal patterns, and in this case it again appears that growth line color and thickness may be related to food availability or source, and not annual or seasonal environmental change (Stohler 1962, 1969).

Shell mineralogy & preservation: *C. biplicata*'s shell mineralogy is 100% biogenic aragonite (Krinsley 1960). Aragonite is a thermodynamically unstable polymorph of calcium carbonate that recrystallizes to calcite at temperatures as low as 125°C (Staudigel and Swart 2016). Recrystallized calcite can distort both stable and clumped isotope ratios, biasing results towards lighter stable isotope values and warmer clumped isotope-derived temperature reconstructions at as little as 10% calcite recrystallization (Staudigel and Swart 2016). In contrast to other marine mollusks with calcite or mixed calcite-aragonite shell mineralogy, *C. biplicata*'s pure aragonite shell, and hence, high vulnerability to diagenetic alteration, can be viewed as a strength for isotope paleo-thermometry because the absence of calcite recrystallization strongly indicates good shell preservation conditions, and therefore, paleo-temperature reconstructions that are relatively unbiased by diagenesis. Several studies investigating the preservation of Pleistocene *C. biplicata* have found very low (< 5 %) levels of calcite recrystallization (Krinsley 1960; Trecker et al 1998).

Utility as a paleo-temperature recorder: *C. biplicata*'s pristine shell preservation on Pleistocene timescales, ubiquity in nearly all Californian coastal marine habitats, abundance in the marine terrace record, relatively long lifespan, and shell growth that shows no evidence of being biased by seasonal preferences together make this species a strong system for paleoenvironmental reconstruction. However, it's relatively slow and apparently discontinuous growth likely precludes the possibility of consistently reconstructing high-resolution (e.g. daily or weekly resolution as seen in other mollusks) environmental maxima and minima. Instead, *C. biplicata*'s

shells show promise as multi-year records of average seasonal and annual growth temperature conditions (Trecker et al 1998).

2.3.3 Bulk stable isotope ratios in mollusc shells & the $\delta^{18}\text{O}$ paleo-thermometer

Mollusks precipitate their calcium carbonate (CaCO_3) shells in isotopic equilibrium with the dissolved CO_2 content of seawater. Since mollusks exhibit continuous growth, the carbonate content of their shells contains a chronological record of the animal's growing conditions. (Note that some mollusks, however, show evidence of metabolic "vital effects" that create an isotopic disequilibrium between seawater composition and their carbonate shells. *C. biplicata* does not appear to exhibit strong vital effects [Trecker et al 1998].) When biogenic carbonate shell material is reacted with orthophosphoric acid (H_3PO_4) it produces CO_2 gas in isotopic equilibrium (but with a constant offset based on reaction temperature that is accounted for through standard corrections) with the original biogenic carbonate (Equation 2.1; see Burman et al 2005 for orthophosphoric acid preparation techniques). The resulting CO_2 gas can then be measured for both oxygen ($\delta^{18}\text{O}$) and carbon ($\delta^{13}\text{C}$) stable isotope ratios.



$\delta^{18}\text{O}$ is the ratio of bulk stable oxygen isotopes with atomic weights 18 and 16 ($^{18}\text{O}:^{16}\text{O}$) whereas $\delta^{13}\text{C}$ is the ratio of bulk stable carbon isotopes with atomic weights 13 and 12 ($^{13}\text{C}:^{12}\text{C}$). $\delta^{18}\text{O}$ (Equation 2.2) and $\delta^{13}\text{C}$ in aragonite are represented in reference to the Vienna Pee Dee Formation Belemnite (VPDB) international reference standard in parts per thousand (‰).

$$\delta^{18}\text{O} \text{ ‰ VPDB} = \left(\frac{\left(\frac{^{18}\text{O}}{^{16}\text{O}}\right)_{\text{sample}}}{\left(\frac{^{18}\text{O}}{^{16}\text{O}}\right)_{\text{VPDB standard}}} - 1 \right) \times 1000 \quad (\text{Equation 2.2})$$

$\delta^{13}\text{C}$ & paleo-upwelling isotope signatures: Along the California coast, $\delta^{13}\text{C}$ captures variation in seawater composition that is largely driven by productivity and upwelling (Takesue and Geen 2004). Upwelled waters are drawn from depth and contain higher amounts of respired carbon, which is isotopically light (i.e. depleted in ^{13}C) due to isotopic fractionation that occurs during respiration; in contrast, productive waters are isotopically enriched due to isotopic fractionation whereby ^{12}C is preferentially taken up by marine primary producers, thus leaving surrounding waters enriched with ^{13}C . Despite the fact that upwelling brings nutrients to the surface and hence stimulates coastal productivity (which has an opposite isotope signature), upwelling has been shown to correspond to an average depletion in $\delta^{13}\text{C}$ by -0.5 to -0.7‰ in coastal California (Killingley and Berger 1979; Takesue and Geen 2004). These isotopically light $\delta^{13}\text{C}$ upwelling signatures are accompanied by enriched $\delta^{18}\text{O}$, as upwelled waters are drawn from depth and as such are colder and more saline than coastal surface waters (Takesue and Geen 2004).

$\delta^{18}\text{O}$ paleo-thermometry: $\delta^{18}\text{O}$ precipitated in carbonates ($\delta^{18}\text{O}_{\text{aragonite}}$) records both the effects of temperature and seawater composition. The former relationship is caused by temperature-

dependent fractionation that occurs during carbonate precipitation in which ^{18}O is preferentially incorporated into the solid phase at colder temperatures (Urey 1947; Epstein et al 1953). This $\delta^{18}\text{O}$ paleo-thermometry relationship has been determined empirically in the aragonite shells of marine mollusks (Grossman and Ku 1986; Hudson and Anderson 1989):

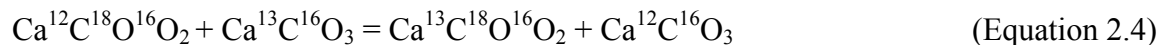
$$T (\text{°C}) = 19.7 - 4.34 (\delta^{18}\text{O}_{\text{aragonite}} - \delta^{18}\text{O}_{\text{seawater}}) \quad (\text{Equation 2.3})$$

where, $\delta^{18}\text{O}_{\text{aragonite}}$ is cast in terms of VPBD and $\delta^{18}\text{O}_{\text{seawater}}$ is cast in terms of the international standard Vienna Standard Mean Ocean Water (VSMOW).

Because the bulk stable isotope paleo-thermometer (Equation 2.3) is dependent on the starting isotopic composition of seawater ($\delta^{18}\text{O}_{\text{seawater}}$), temperature cannot be reconstructed based on $\delta^{18}\text{O}_{\text{aragonite}}$ alone. $\delta^{18}\text{O}_{\text{seawater}}$ varies substantially in both time (see review in Grossman 2012) and space (Schmidt et al 1999), in large part, due to an isotopic fractionation that occurs during evaporation in which water molecules including ^{16}O are preferentially evaporated (Gat 1996). Hence, $\delta^{18}\text{O}$ of meteoric water is depleted. On Pleistocene timescales, enhanced meteoric water storage in ice caps causes $\delta^{18}\text{O}_{\text{seawater}}$ to be enriched during glacial intervals, and ice cap melting causes $\delta^{18}\text{O}_{\text{seawater}}$ to be lighter during interglacial intervals (Grossman 2012). Within California's coastal marine habitats, freshwater input can result in sizable depletions in $\delta^{18}\text{O}_{\text{seawater}}$ near rivers and enrichments in deeper and more saline waters (Schmidt et al 1999).

2.3.4 Clumped stable isotopes in carbonates & the Δ_{47} paleo-thermometer

Unlike the $\delta^{18}\text{O}$ paleo-thermometer, carbonate clumped isotope paleo-thermometry provides a $\delta^{18}\text{O}_{\text{seawater}}$ -independent temperature reconstruction (Ghosh et al 2006; Schauble et al 2006; Eiler 2007, 2011). The method is based on a thermodynamic relationship between carbonate precipitation and the 'clumping,' or state-ordering, of carbon and oxygen isotopes distributed in the carbonate crystal lattice (Ghosh et al 2006; Schauble et al 2006; Eiler 2007, 2011). At thermodynamic equilibrium, carbonate crystals contain $^{13}\text{C}^{18}\text{O}^{16}\text{O}_2^{2-}$ ionic group abundances described by the homogenous equilibrium (Equation 2.4; Schauble et al 2006):



Thus, as temperatures warm isotopes incorporated into the carbonate crystal lattice approach a stochastic mixture; hence, greater "clumping" of heavy isotopes corresponds to cooler temperatures whereas less clumping corresponds to warmer temperatures.

As with stable isotope analyses, clumped isotope analyses begin by reacting carbonate material with orthophosphoric acid to release CO_2 (Equation 2.1) in isotopic equilibrium (but with a consistent offset due to reaction temperature) with the original carbonate. CO_2 isotopologues of molecular masses 44 through 49 are then measured using mass spectrometry (e.g., the CO_2 isotopologue with mass 47 is composed of $^{13}\text{C}^{18}\text{O}^{16}\text{O}$, $^{12}\text{C}^{17}\text{O}^{18}\text{O}$, or $^{13}\text{C}^{17}\text{O}_2$).

The excess abundance of carbonate isotopologues of molecular mass 47 containing heavy stable isotopes of carbon (^{13}C) and oxygen (^{18}O) relative to the expected stochastic distribution (reached at > 1000 °C) of this combination is captured in the parameter Δ_{47} (Ghosh et al 2006; Affek and Eiler 2006; Equation 2.5).

$$\Delta_{47}\text{‰} = \left[\left(\frac{R^{47}}{R^{47*}} - 1 \right) - \left(\frac{R^{46}}{R^{46*}} - 1 \right) - \left(\frac{R^{45}}{R^{45*}} - 1 \right) \right] \times 1000 \quad (\text{Equation 2.5})$$

where,

$$R^{\text{isotopologue}} = \frac{\text{mass isotopologue}}{\text{mass 44}} \quad (\text{Equation 2.5.1})$$

and, $R^{\text{isotopologue}*}$ is the same relationship as Equation 2.5 but with the ratios for the same sample with a stochastic distribution of isotopologues (Ghosh et al 2006; Affek and Eiler 2006).

The relationship between Δ_{47} and temperature as derived in Ghosh et al 2006 and cast in terms of temperature (°C) is described as:

$$T^{\circ\text{C}} = \sqrt{\frac{(10^6 \times 0.0449)}{(\Delta_{47} - 0.167)}} - 273.15 \quad (\text{Equation 2.6})$$

Once $\delta^{18}\text{O}_{\text{aragonite}}$ and temperature are reconstructed, $\delta^{18}\text{O}_{\text{seawater}}$ can be calculated following a reordering of Equation 2.3:

$$\delta^{18}\text{O}_{\text{seawater}} = \delta^{18}\text{O}_{\text{aragonite}} + (0.23041475 * T(^{\circ}\text{C})) - 4.539171 \quad (\text{Equation 2.7})$$

2.4. Methods

2.4.1 Shell collection & preservation analyses

Modern and fossil *C. biplicata* shells were collected from fossil localities (Figures 1.1 and 1.2) through fieldwork from 2015-2017 in southern California and on San Nicolas Island. Subsurface specimens were collected by first removing bulk sediments exposed at the surface. Modern specimens were collected from beaches immediately adjacent to fossil sites. Historical specimens from a ~1900 field expedition to San Nicolas Island were collected from the University of California Museum of Paleontology (UCMP 2433; Veddar and Norris 1963; Figures 1.1 and 1.2).

2.4.2 Shell preservation analyses

X-ray diffractometry (XRD) was used to detect the presence of calcite recrystallization in fossil *C. biplicata* specimens. Specimens were prepared for XRD by releasing aragonite powder from shells with a hand Dremel set to lowest speed. All samples were taken from sections of the shell that were also used for isotope and clumped analyses. Powders weighing approximately 4–8 milligrams were mixed with acetone and dried on silicon and quartz zero-background plates. XRD scans were constructed to capture major and minor calcite and aragonite peaks.

2.4.3 Bulk ($\delta^{18}\text{O}$) stable isotope analyses

Aragonite powders weighing between 20 and 100 micrograms were released from well-preserved *C. biplicata* shells using a Dremel hand drill set on the lowest speed to avoid accidental calcite recrystallization that can be caused by heating due to mechanical stress (Staudigel and Swart 2016). These microsamples were drilled in nearly overlapping intervals through a cross-section of the shell's inner growth layers; this method thus samples most of the shell's growing conditions. Between 10 and 35 microsamples were taken from each specimen depending on specimen (or fragment) size. Samples were digested with orthophosphoric acid (H_3PO_4) at 90°C (Equation 2.1) and then measured for both oxygen ($\delta^{18}\text{O}$) and carbon ($\delta^{13}\text{C}$) stable isotope ratios.

Bulk stable isotope ratios were determined using a GV IsoPrime mass spectrometer with Dual-Inlet and MultiCarb systems in the Center for Stable Isotope Biogeochemistry in the University of California, Berkeley's Department of Integrative Biology. Several replicates of the international standard NBS19 and two laboratory standards (CaCO_3 -I & II) were measured during each sample measurement run; overall external analytical precision is about $\pm 0.05\text{‰}$ for $\delta^{13}\text{C}$ and about $\pm 0.07\text{‰}$ for $\delta^{18}\text{O}$. A correction was applied to $\delta^{18}\text{O}_{\text{aragonite}}$ values to account for an apparent vital effect (0.5‰) for *C. biplicata*.

2.4.4 Clumped (Δ_{47}) stable isotope analyses

C. biplicata powdered aragonite samples weighing between 8–12 mg were reacted with orthophosphoric acid at 90°C to release CO_2 (Equation 2.3). Resulting sample CO_2 was purified by passage through successive cryogenic traps that included a Porapak-Q gas chromatograph column at -20°C . Purified CO_2 gas was then introduced to a Finnigan Thermo MAT 253 mass spectrometer using a custom-built autoline described in detail in Passey et al 2010 at the University of California, Berkeley in the Department of Earth and Planetary Sciences. Mass 44-normalized ion ratios of all stable CO_2 isotopologue masses (i.e., 45/44, 46/44, 47/44, 48/44, 49/44) were measured, with nine measurement acquisitions assessed for each sample. To account for pressure re-equilibration in the measurement gas bellows, the y-intercept and slope of the linear regression with time was used to calculate pressure-balance corrected Δ_{47} . A $+0.082\text{‰}$ correction was applied to Δ_{47} data to account for the difference in phosphoric acid reaction temperature (90°C) and that of the original temperature calibration (25°C ; Ghosh et al 2006). In-house (travertine and Carrara marble) and international (ETH1-ETH4; Bernasconi 2018)

standards were run alongside *C. biplicata* samples. $\delta^{13}\text{C}$ and $\delta^{18}\text{O}$ values analyzed alongside Δ_{47} measurements were compared to continuously analyzed international standards (ETH1-ETH4; Bernasconi 2018); corrections based on the slope and intercept of measured standard values were applied to *C. biplicata* $\delta^{13}\text{C}$ and $\delta^{18}\text{O}$ values to account for consistent offsets in $\delta^{13}\text{C}$ and $\delta^{18}\text{O}$ measured standard values through time (Appendix II).

2.4.5 Statistical analyses

Summary statistics and statistical analyses were generated using Δ_{47} and $\delta^{18}\text{O}$ measurements that excluded statistical outliers showing signs of organic contamination (i.e. high Δ_{48} excess) or measurement error. In the case of $\delta^{18}\text{O}$, measurements that were enriched or depleted by greater than 3.5‰ relative to the statistical mean for each specimen were excluded from analyses; this reduced the dataset by only a marginal amount (17 out of 875 measurements were excluded). Differences in $\delta^{18}\text{O}$ reconstructed temperatures between climate states were assessed using two-sample t-tests and one-way Analysis of Variance (ANOVA) for contrasts of two or greater than two sample means, respectively (Sokal 2011). Statistically significant ANOVA results were additionally tested using the post-hoc Tukey Honest Significant Differences (HSD) test, which provides measures of statistical differences between each pair of mean comparisons in an ANOVA (Tukey 1949; Sokal 2011).

2.5 Results

2.5.1 Shell preservation X-ray Diffraction (XRD) analyses

None of the fossil ($n = 24$) or modern ($n = 3$) *C. biplicata* analyzed using XRD showed evidence of substantial calcite recrystallization; though, two shells do show minor recrystallization of less than 3%. This minor degree of recrystallization is equivalent to previous shell mineralogy studies (up to ~5% calcite recrystallization found in Krinsley 1960 and Trecker et al 1998) and lower than the 10% calcite recrystallization threshold for biasing stable and clumped isotope ratios (Staudigel and Swart 2016), and hence, no shells analyzed for XRD analyses were excluded from clumped or bulk stable isotope ratio analyses.

2.5.2 Stable isotopes & paleo-thermometry

San Nicolas Island: Average paleo-temperature estimates derived from Δ_{47} paleo-thermometry for MIS 5e, MIS 5e/5c, and MIS 5a are 16°C (standard error = 0.9; $n = 4$ specimens; 14 measurements), 14.3°C (standard error = 0.85; $n = 4$ specimens; 13 measurements), and 13.4°C (standard error = 0.7; $n = 4$ specimens; 17 measurements), respectively (Figures 2.1 and 2.2). Average reconstructed $\delta^{18}\text{O}_{\text{seawater}}$ values for these climate states are 0.3‰ (MIS 5e; standard error = 0.25), 0.55‰ (standard error = 0.18; MIS 5e/5c), and 0.45‰ (standard error = 0.15; MIS 5a; Figure 2.3). This 0.3-0.55‰ for Late Pleistocene climate states is relatively enriched in comparison to modern $\delta^{18}\text{O}_{\text{seawater}}$ values for the San Nicolas Island region of ~-0.1‰ (Grossman

and Ku 1986). $\delta^{18}\text{O}$ paleo-thermometry reconstructions average 16.8°C, 15.2°C, 13.8°C, and 16.5°C for MIS 5e (n = 7 specimens; 78 measurements), 5e/5c (n = 8 specimens; 105 measurements), 5a (n = 8 specimens; 108 measurements), and modern (shells collected from 1900-2015; n = 12 specimens; 105 measurements) climate states, respectively (see Figure 2.4 for $\delta^{18}\text{O}_{\text{aragonite}}$ values; Figures 2.5 and 2.6; Table 2.1). MIS 5e and modern climate states are not statistically distinguishable, thus suggesting that MIS 5e conditions were quite similar to present day (Figure 2.5; Tables 2.1 and 2.2); MIS 5a conditions average 2°C cooler than the modern (Figure 2.5; Tables 2.1 and 2.2). $\delta^{18}\text{O}$ and Δ_{47} stable isotope paleo-thermometry estimates are comparable for MIS 5e (terrace 2a) and 5a, but, differ by ~1°C for terrace 2b, which contains assemblages dating to both MIS 5e and 5c (Figures 2.1 and 2.5). $\delta^{18}\text{O}$ paleo-thermometry reconstructions for modern shells (collected between 1900-2015) further show a close correspondence to contemporary (2010-2016) sea surface temperature data recorded in an offshore buoy (National Data Buoy Center Station 46219; Figure 2.7). $\delta^{13}\text{C}$ and $\delta^{18}\text{O}_{\text{aragonite}}$ show no general trend between climate states on San Nicolas Island (Figure 2.8), although $\delta^{13}\text{C}$ ratios for modern specimens are bimodally distributed: specimens collected between 2000-2015 show a distinctively lighter (~1‰) signature in comparison to specimens collected from 1900, which are more similar to Late Pleistocene $\delta^{13}\text{C}$ values (Figures 2.8 and 2.9).

Palos Verdes Hills: Δ_{47} paleo-temperatures for MIS 5e (n = 2 specimens; 6 measurements) and MIS 5a (n = 2 specimens; 8 measurements) at Palos Verdes Hills average 16.2°C and 13.2°C, respectively (Figures 2.1 and 2.2). Reconstructed $\delta^{18}\text{O}_{\text{seawater}}$ values for these climate states are not significantly different and average 0.6-0.35‰; as is also the case on San Nicolas Island, these values are more enriched in comparison to modern seawater composition of ~-0.1‰ for surface waters of the southern Californian region (Grossman and Ku 1986; Figure 2.3). $\delta^{18}\text{O}$ temperatures (see Figure 2.4 for $\delta^{18}\text{O}_{\text{aragonite}}$ values) average 16.8°C, 13.6°C, and 16°C for MIS 5e (n = 4 specimens; 76 measurements), 5a (n = 4 specimens; 59 measurements), and modern (shells collected from 2015-16; n = 4 specimens; 50 measurements) climate states, respectively (Figures 2.5, 2.6, and 2.10; Table 2.2). $\delta^{18}\text{O}$ paleo-temperatures show a close correspondence to contemporary buoy data from nearshore San Pedro Bay (National Data Buoy Center Station 46222; Figure 2.7). $\delta^{13}\text{C}$ values are distinctively heavier for MIS 5e and comparable for the modern and MIS 5e, with $\delta^{13}\text{C}$ showing a ~0.5‰ lighter signature (Figure 2.8) of 1‰ VPDB which further aligns with shells collected on San Nicolas Island from 2000-2015 (Figure 2.9).

Isla Vista: Δ_{47} paleo-temperatures for MIS 3a (n = 2 specimens; 9 measurements) at Isla Vista average 15°C (Table 2.1; Figures 2.1 and 2.2), with a fairly large variance (standard error = 1.5). Reconstructed $\delta^{18}\text{O}_{\text{seawater}}$ values have a high variance and average 0.11‰ (standard error = 0.35). In contrast to other Late Pleistocene climate states at San Nicolas Island and Palos Verdes Hills, MIS 3a $\delta^{18}\text{O}_{\text{seawater}}$ is fairly depleted in ^{13}C and more closely resemble modern open-coast $\delta^{18}\text{O}_{\text{seawater}}$ values for the region (~-0.1‰; Grossman and Ku 1986). $\delta^{18}\text{O}$ temperatures (see Figure 2.4 for $\delta^{18}\text{O}_{\text{aragonite}}$ values) average 14.5°C and 16.6°C for MIS 3a (n = 6 specimens; 96 measurements) and modern (shells collected from 2015-16; n = 6 specimens; 66 measurements) climate states, respectively (Figures 2.5, 2.6, and 2.11; Table 2.2). $\delta^{18}\text{O}$ temperatures show a

close correspondence to contemporary buoy data from offshore eastern Santa Barbara (National Data Buoy Center Station 46053; Figure 2.7). $\delta^{13}\text{C}$ values are heavier for MIS 3a compared to the modern, with $\delta^{13}\text{C}$ showing the same $\sim 1\text{‰}$ lighter offset (Figures 2.8 and 2.9) between Late Pleistocene and contemporary shells in Palos Verdes Hills and San Nicolas Island (Figure 2.9).

2.6 Discussion

2.6.1 The promise of Δ_{47} and $\delta^{18}\text{O}$ paleo-thermometry in *Callianax biplicata*

Comparison of vital-effect (+0.5‰) corrected *C. biplicata* $\delta^{18}\text{O}$ temperatures and directly measured buoy data yields a promising indication that *C. biplicata* is a strong recorder of coastal sea surface temperature as both produce similar average temperature conditions (Figure 2.7). Moreover, both Δ_{47} and $\delta^{18}\text{O}$ reconstruct statistically indistinguishable paleo-temperatures (Figures 2.1 and 2.5). The only exception to this agreement is on San Nicolas Island's terrace 2b, in which $\delta^{18}\text{O}$ and Δ_{47} diverge slightly (Figures 2.1 and 2.5). Taken together, these results imply that *C. biplicata* is a faithful recorder of paleo-temperature conditions, at least at the averaged sub-annual to inter-annual scales analyzed here.

2.6.2 $\delta^{13}\text{C}$ and the Suess effect

Bulk $\delta^{13}\text{C}$, $\delta^{18}\text{O}$, and Late Pleistocene upwelling: Within Pleistocene climate states, $\delta^{13}\text{C}$ and $\delta^{18}\text{O}$ show several notable patterns. First, MIS 5e fossil sites are lighter in both $\delta^{13}\text{C}$ and $\delta^{18}\text{O}$ than MIS 5e/5c and MIS 5a fossil sites. These findings align with planktonic $\delta^{13}\text{C}$ from the Tanner Basin record (near San Nicolas Island), which also indicate lighter bulk isotope values during MIS 5e relative to MIS 5a (Ocean Drilling Project Site 1014; Hendy and Kennett 2000; Figure 1.1). However, drawing direct comparisons between the deep sea and coastal records is not straightforward because vertical stratification has varied substantively between Late Pleistocene climate states (Hendy and Kennett 2000). Depleted MIS 5e $\delta^{13}\text{C}$ may indicate enhanced upwelling conditions were present during this relatively warm interglacial climate state (Killingley and Berger 1979; Takesue and Geen 2004). Such a scenario (i.e., of enhanced upwelling) is posited for warming intervals in Eastern Boundary Currents: during warming intervals a greater land-ocean temperature disparity drives enhanced alongshore winds, which in turn cause upwelling (Bakun 1990; Bakun et al 2015; Sydemann et al 2014). MIS 5a, on the hand, does not show strong evidence of enhanced upwelling (which is accompanied by $\delta^{13}\text{C}$ depletions of 0.5-0.7‰), but could have had greater surface water productivity (Takesue and Geen 2004; Figures 2.8 and 2.9). Similarly, the fossil site at Isla Vista shows evidence of being a productive paleo-habitat (Takesue and Geen 2004; Figures 2.8 and 2.9).

The Suess effect: *C. biplicata* specimens collected between 2000-2015 at San Nicolas Island, Palos Verdes Hills, and Isla Vista all show average $\delta^{13}\text{C}$ centered between 1-0.7‰, values which are notably depleted relative to Late Pleistocene *C. biplicata* specimens (Figures 2.8 and 2.9). On San Nicolas Island, the pattern is more striking: specimens collected between 2000-2015 show

~1‰ depletion relative to specimens collected during a ~1900 C.E. expedition to the island (Figures 2.8 and 2.9). This 1‰ offset over the last century aligns with the global "Suess effect" offset between contemporary and pre-industrial $\delta^{13}\text{C}$ in the atmosphere and oceans (Suess 1953, 1955) caused by the anthropogenic release of CO_2 in fossil fuels (and other human activities), which is depleted in $\delta^{13}\text{C}$ (Quay et al 1992).

2.6.3 Δ_{47} and $\delta^{18}\text{O}$ paleo-thermometry

MIS 5e marine terrace localities: I reconstruct MIS 5e marine terraces at Palos Verdes Hills and San Nicolas Island (terrace 2a) as $\sim 16^\circ\text{C}$ on average, which is similar to present conditions in both locations (Figures 2.1, 2.5, 2.6, and 2.10; Tables 2.1 and 2.2). This reconstruction is slightly cooler than faunal based temperature inferences imply (Muhs et al 2012). For instance, SNI-302 contains several southern extralimital mollusks, which paleontologists have traditionally used to infer warmer-than-present conditions since these mollusks are extirpated to the south today (Muhs et al 2012). However, using extralimitals to infer paleo-temperatures on offshore islands, in particular, is complicated because offshore islands show mixed faunal affinities (i.e. species which are latitudinally disjunct on the mainland coast co-occur) compared to maincoast assemblages (Valentine 1966; Lindberg et al 1980; McLean and Coan 1996). Moreover, notable variation in coastal temperatures occurs between paleo-embayments, which reach warmer temperatures, and open-coast habitats (Valentine 1961; Muhs et al 2018).

MIS 5e/5c and thermally disjunct assemblages: Shells from terrace 2b on San Nicolas Island, which houses multiple so-called "thermally disjunct" fossil assemblages (i.e., assemblages in which both southern and northern extralimitals co-occur) shows evidence of being occupied by two wave-cut platforms during MIS 5e and 5c climate states (Muhs et al 2012; Muhs et al 2014; Muhs and Groves 2018). My paleo-temperature reconstructions for these thermally disjunct sites average slightly cooler than present (by $\sim 1^\circ\text{C}$; Figures 2.1, 2.5, and 2.6; Tables 2.1 and 2.2). However, individual shells appear to show a bimodal distribution in $\delta^{18}\text{O}$ temperatures: five specimens cluster quite close to MIS 5a temperature conditions and three specimens cluster within MIS 5e temperature conditions (Figure 2.6). This bimodal distribution might be driven by differential ages of the fossils, with the former group dating to MIS 5c (which globally is slightly cooler than present-day) and the latter group dating to MIS 5e (Figure 2.6). A previous study conducted by Muhs and Kyser (1987) that used uplift rates to estimate $\delta^{18}\text{O}_{\text{seawater}}$ computed paleo-temperatures on par with my reconstructed values for terrace 2b. (Note that Muhs and Kyser 1987 was published before the discovery of terrace reoccupation between MIS 5e and 5c on San Nicolas Island's terrace 2b. Thus, the authors believed terrace 2b to have been deposited exclusively during MIS 5e and thereby interpreted their findings to imply that MIS 5e temperatures were cooler than at present.)

MIS 5a marine terrace localities: At Palos Verdes Hills and on San Nicolas Island both Δ_{47} and $\delta^{18}\text{O}$ temperature reconstructions indicate a distinctively cool ocean ($\sim 2.5^\circ\text{C}$) during MIS 5a highstand (Figures 2.1 2.5, 2.6, and 2.10; Tables 2.1 and 2.2). This finding corresponds well with

faunal based reconstructions of other MIS 5a sites, which estimated $\sim 3^{\circ}\text{C}$ offsets in temperature conditions between MIS 5a and today on the basis of several fossil occurrences with northern extralimital ranges (Emerson 1956; Valentine and Emerson 1961; Valentine and Meade 1960; Kern 1971; Kennedy 1978; Kennedy et al 1982; Muhs et al 2002, 2006, 2012). Foraminiferal data from the Santa Barbara Basin Ocean Drilling Project (Site 893A; Figure 1.1) and pollen data from northern California similarly agree with my reconstruction of a cool ocean (Adam 1988; Kennett and Venz 1995), as do global climate model and proxy compilations (Kennett and Venz 1995; Hendy and Kennett 2000; Lisiecki and Raymo 2005).

MIS 3a marine terrace at Isla Vista: The MIS 3a locality at Isla Vista (the "Coal Oil Point" fossil locality) is one of the only remains of an interstadial wave-cut terrace that is preserved above present-day sea level (Wright 1972; Trecker et al 1999; Gurrola et al 2014). In comparison to MIS 5e, 5c, and 5a, MIS 3a represents the coldest interval preserved in California's uplifted Late Pleistocene marine terrace record (Trecker et al 1999; Gurrola et al 2014). Notably, my paleo-temperature reconstructions are only $\sim 2\text{-}3^{\circ}\text{C}$ cooler than at present (Figures 2.5, 2.7, and 2.12; Table 2.1), a result that is warmer than expected and similar to my MIS 5a reconstructions (Figures 2.5 and 2.7; Tables 2.1 and 2.2).

However, the MIS 3a "Coal Oil Point" locality also shows evidence of being a paleo-embayment: fine-grained below-wave base sediments (Wright 1972; Belanger 2004) combined with megainvertebrate fossils of mixed depth-affinities (i.e., an indicator of paleo-embayments; e.g., Kanakoff and Emerson 1959; Valentine 1961; Kern 1971; Powell 2001) and shallow subtidal water foraminifera taxa (Barrick et al 1989), provide sedimentological and faunal evidence consistent with the location being a paleo-embayment (rather than conclusive evidence of a sublittoral marine habitat, as was inferred by Wright 1972). Further, my reconstructed $\delta^{18}\text{O}_{\text{seawater}}$ values show a range of both very light and enriched values, together averaging to be quite depleted at $\sim 0.3\text{‰}$; as paleo-embayments receive significant seasonal freshwater inputs (Schmidt et al 1999), these relatively depleted $\delta^{18}\text{O}_{\text{seawater}}$ values further bolster the paleo-embayment hypothesis for this locality (Figure 2.3). Because paleo-embayments can reach temperatures distinctively warmer than adjacent open-coast habitats (Valentine 1961; Ricketts 1985; Bakun 1990; Bakun et al 2005), these paleo-temperature reconstructions likely capture the warmer upper-end of coastal marine habitats during MIS 3a. The presence of many cold-water northern extralimital species at the fossil locality further indicates that nearby open-coast habitats were likely cooler than suggested on the basis of this fossil locality alone (Wright 1972; Belanger 2004).

2.7 Conclusions

C. biplicata shows evidence of being a faithful recorder of averaged temperature conditions and exhibits good correspondence between Δ_{47} and $\delta^{18}\text{O}$ paleo-temperatures (Figures 2.1, 2.5, and 2.7). A notable $\sim 1\text{‰}$ depletion in $\delta^{13}\text{C}$ between contemporary and ~ 1900 specimens (Figure 2.9)

is consistent with the globally recognized Suess effect (Suess 1953, 1955; Quay et al 1992) and further highlights the promise of *C. biplicata* as a faithful paleoenvironmental recorder.

I reconstruct open-coast MIS 5e sites, deposited during the peak of the last interglacial complex, as thermally similar to at present (Figures 2.1 and 2.5). Evidence of thermal conditions similar to present-day, combined with $\delta^{13}\text{C}$ evidence (Figure 2.9) is consistent with enhanced upwelling (Killingley and Berger 1979; Takesue and Geen 2004), which may corroborate the climate scenario posited in Bakun 1990 that global warming can coincide with enhanced upwelling along some Eastern Boundary Currents (Bakun 1990; Bakun et al 2015; Sydeman et al 2014; Wang et al 2015). Specimens from terrace 2b on San Nicolas Island, which represents a time-averaged surface occupied by MIS 5e and 5c climate states (Muhs et al 2012, 2014; Muhs and Groves 2018), show evidence of climate state mixing — with some specimens reconstructing MIS 5e-like conditions and others reconstructing cooler than at present conditions (Figure 2.6). I reconstruct MIS 5a as $\sim 2.5^\circ\text{C}$ cooler than at present (Figure 2.1 and 2.5) and $\delta^{13}\text{C}$ signatures suggest that these cool surface waters may have coincided with enhanced primary productivity (Takesue and Geen 2004). I reconstruct MIS 3a at Isla Vista as $\sim 2.5^\circ\text{C}$ cooler than at present (Figures 2.1, 2.5, and 2.11). However, this fossil site shows evidence of being a paleo-embayment (Wright 1972; Belanger 2004), an inference which both warmer-than-expected reconstructed temperatures (with a wider thermal range) and depleted reconstructed $\delta^{18}\text{O}_{\text{seawater}}$ values support (Figures 2.1, 2.3, and 2.5); thus, these temperature reconstructions likely represent a habitat considerably warmer than adjacent open-coast MIS 3a habitats.

Chapter II Figures

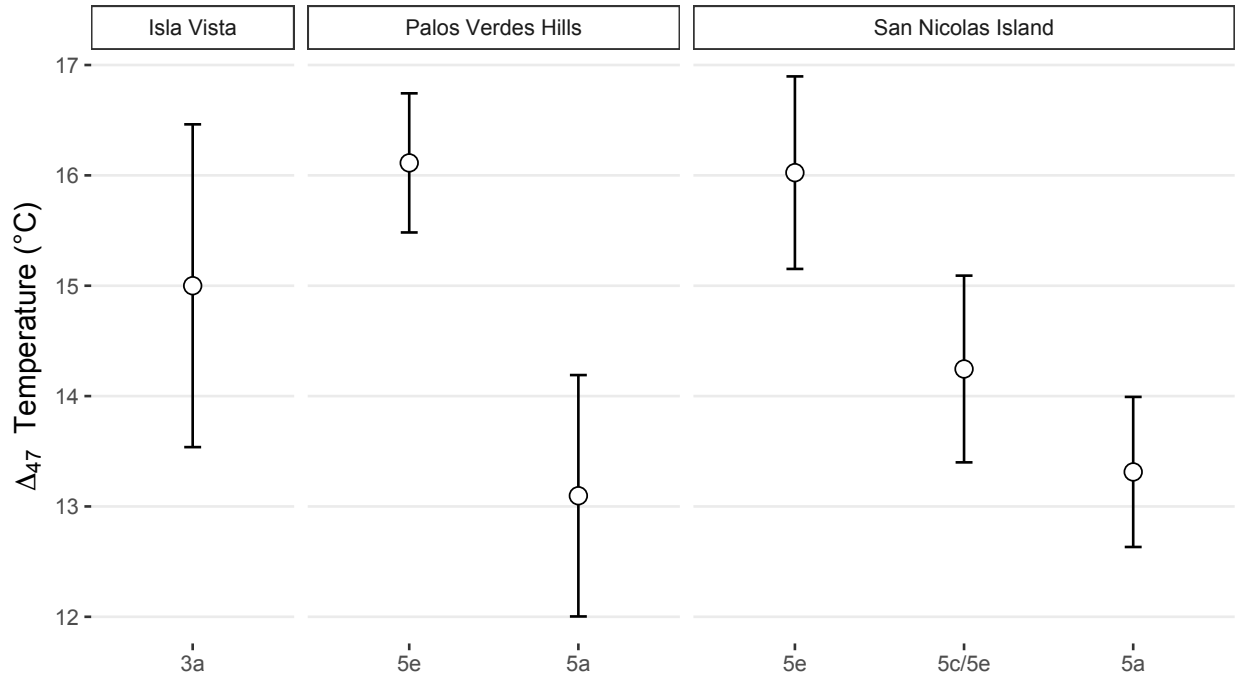


Figure 2.1: Δ_{47} temperatures for Late Pleistocene climate states. Means represented as points bracketed by the standard error of the mean estimate; $n = 70$. MIS 5e and MIS 5a on both San Nicolas Island and Palos Verdes Hills are reconstructed at $\sim 16^\circ\text{C}$ and $\sim 13^\circ\text{C}$, respectively. MIS 3a, which is dated to a cool interstadial period, is reconstructed at 15°C , but with a relatively large degree of uncertainty. See Appendix II for Δ_{47} data.

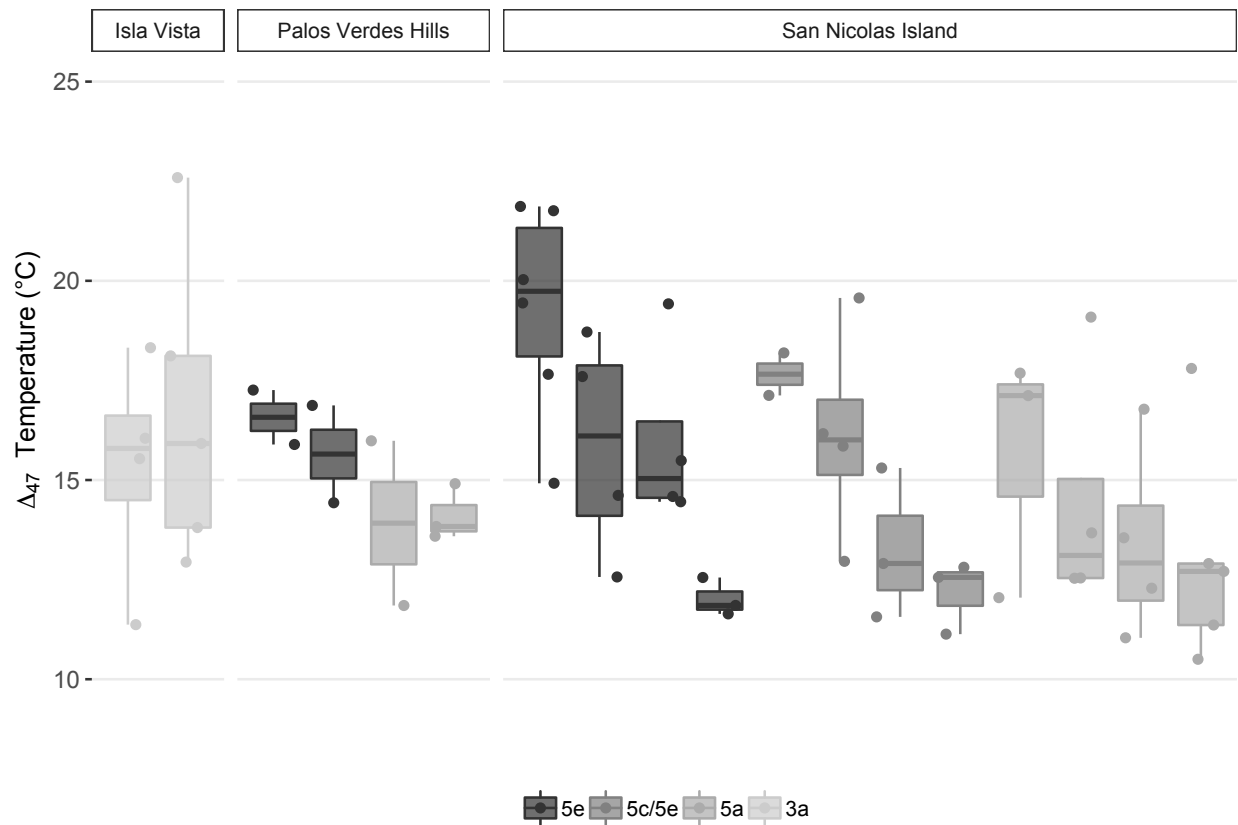


Figure 2.2: Δ_{47} temperatures for Late Pleistocene climate states by *Callinax biplicata* specimens. Boxplots represent median (horizontal lines) and interquartile range (upper and lower 25% represented by boxplot whiskers) for each Late Pleistocene specimen; individual points represent measured Δ_{47} values; n = 70. See Appendix II for Δ_{47} data.

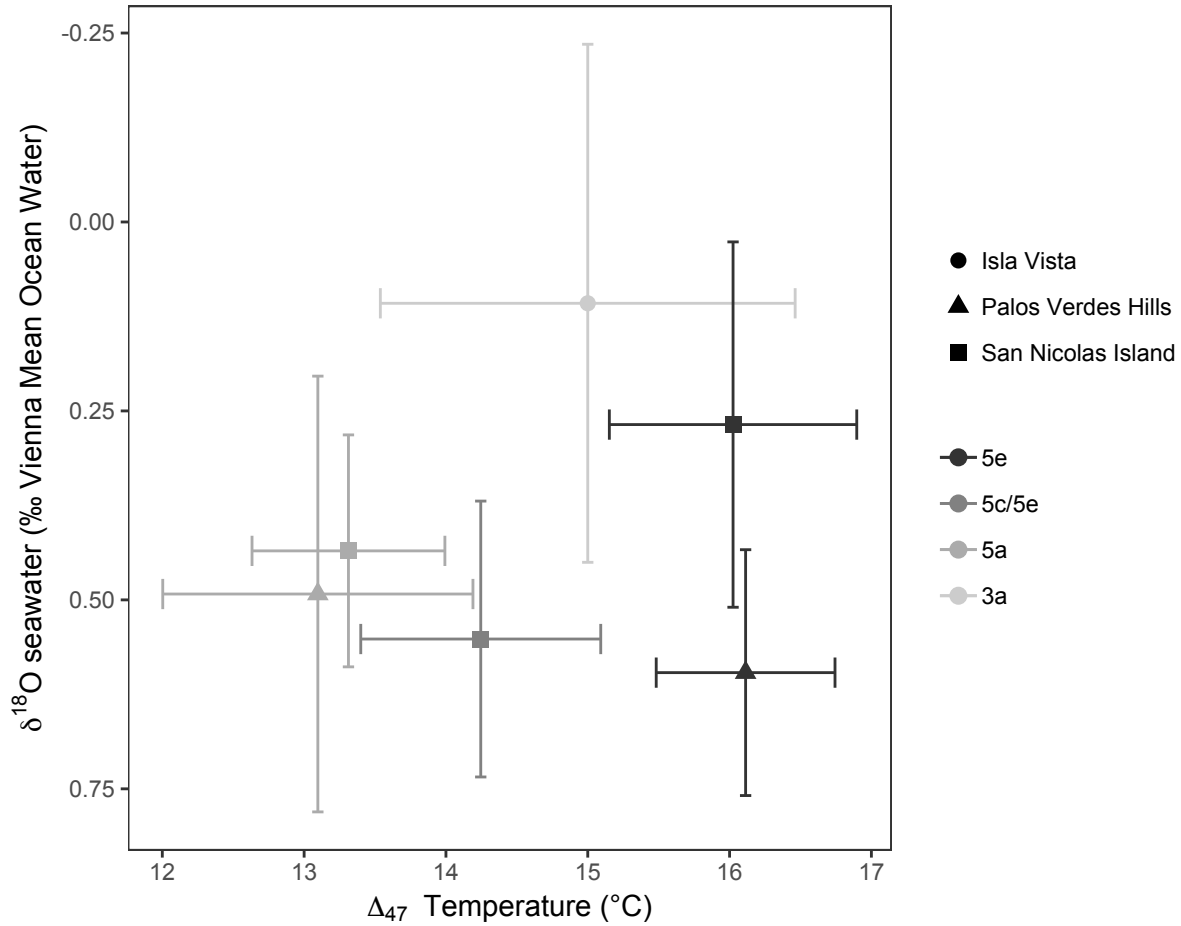


Figure 2.3: Δ_{47} & $\delta^{18}\text{O}_{\text{seawater}}$ for reconstructed locations and climate states. Points represent means; horizontal and vertical bars represent the standard error of the mean for Δ_{47} and $\delta^{18}\text{O}_{\text{seawater}}$, respectively; $n = 70$. Please note that Δ_{47} and $\delta^{18}\text{O}_{\text{seawater}}$ errors are (inversely) correlated because Δ_{47} is used to construct $\delta^{18}\text{O}_{\text{seawater}}$ estimates (Equation 2.7). See Appendix II for Δ_{47} data.

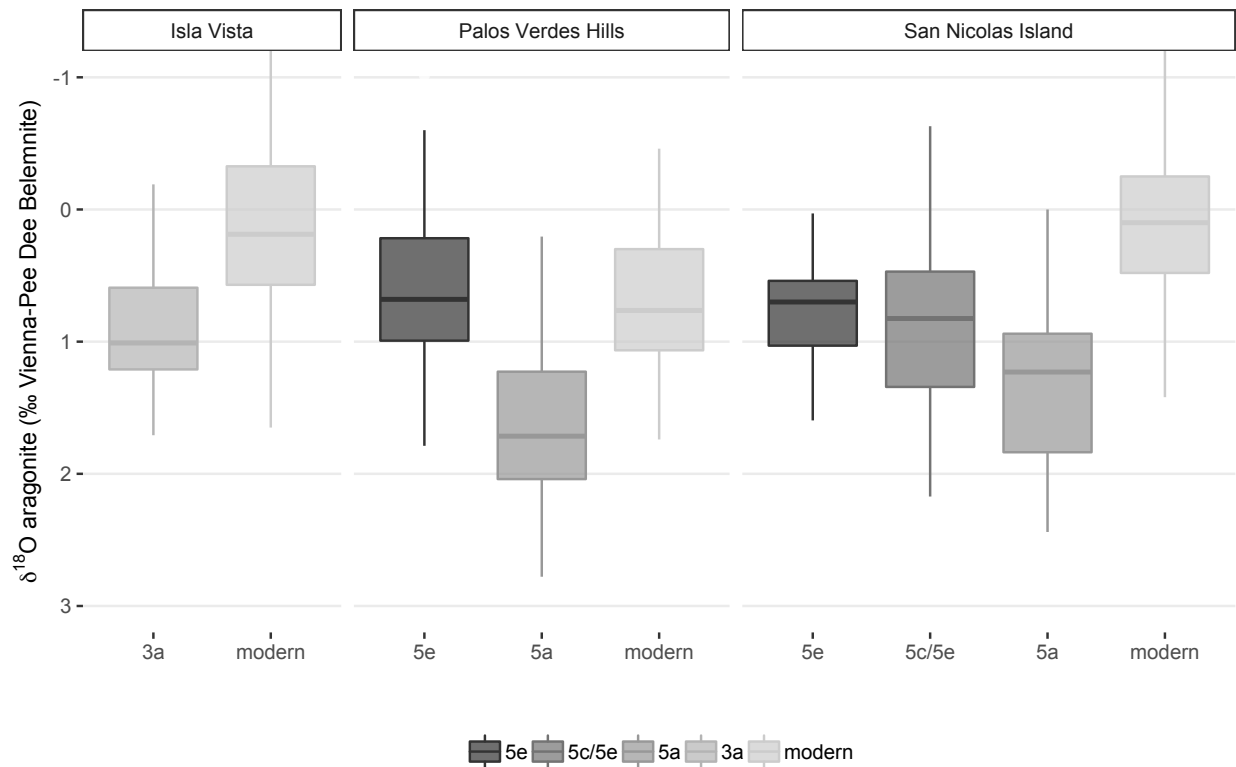


Figure 2.4: Late Pleistocene-Modern $\delta^{18}\text{O}_{\text{aragonite}}$. Boxplots represent median (horizontal lines) and interquartile range (upper and lower 25% represented by boxplot whiskers) for each Late Pleistocene climate state analyzed; $n = 858$. See Appendix I for $\delta^{18}\text{O}$ data.

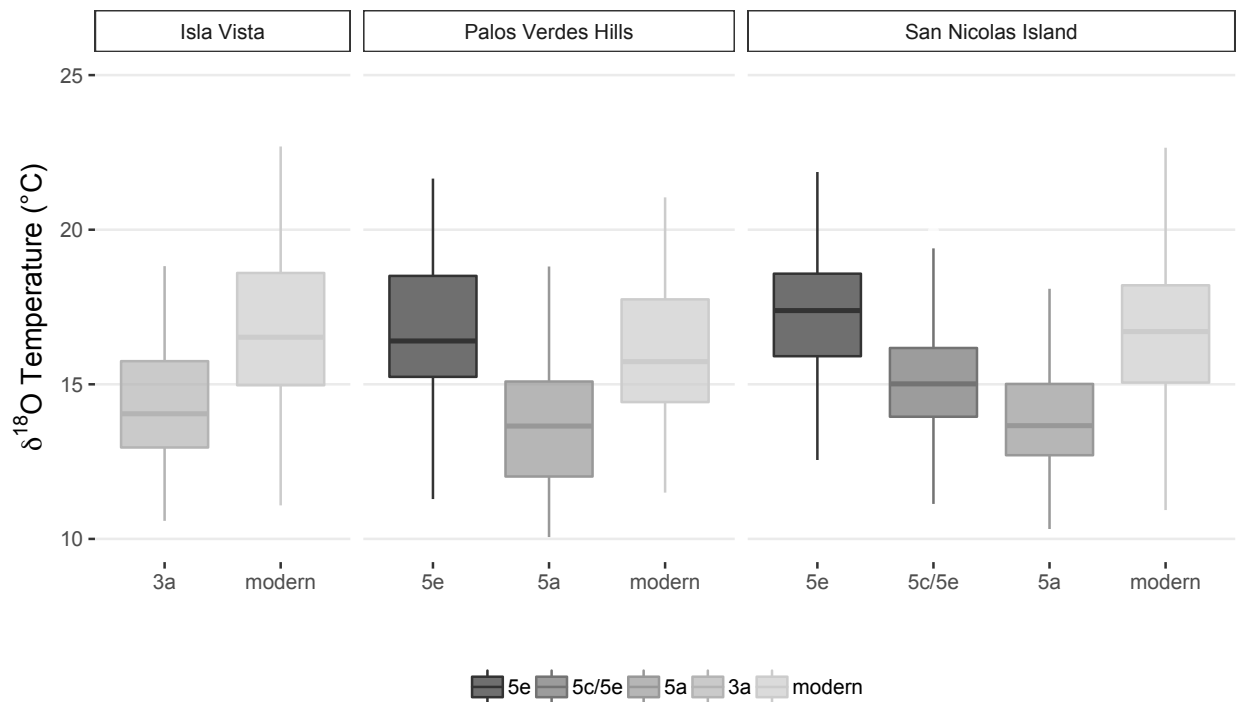


Figure 2.5: Late Pleistocene-Modern $\delta^{18}\text{O}$ temperature. Boxplots represent median (horizontal lines) and interquartile range (upper and lower 25% represented by boxplot whiskers) for each climate state analyzed. MIS 5e on both San Nicolas Island and at Palos Verdes Hills are reconstructed as similar to modern-day; MIS 5a is reconstructed as 2.5°C cooler than present; n = 858. See Appendix I for $\delta^{18}\text{O}$ data.

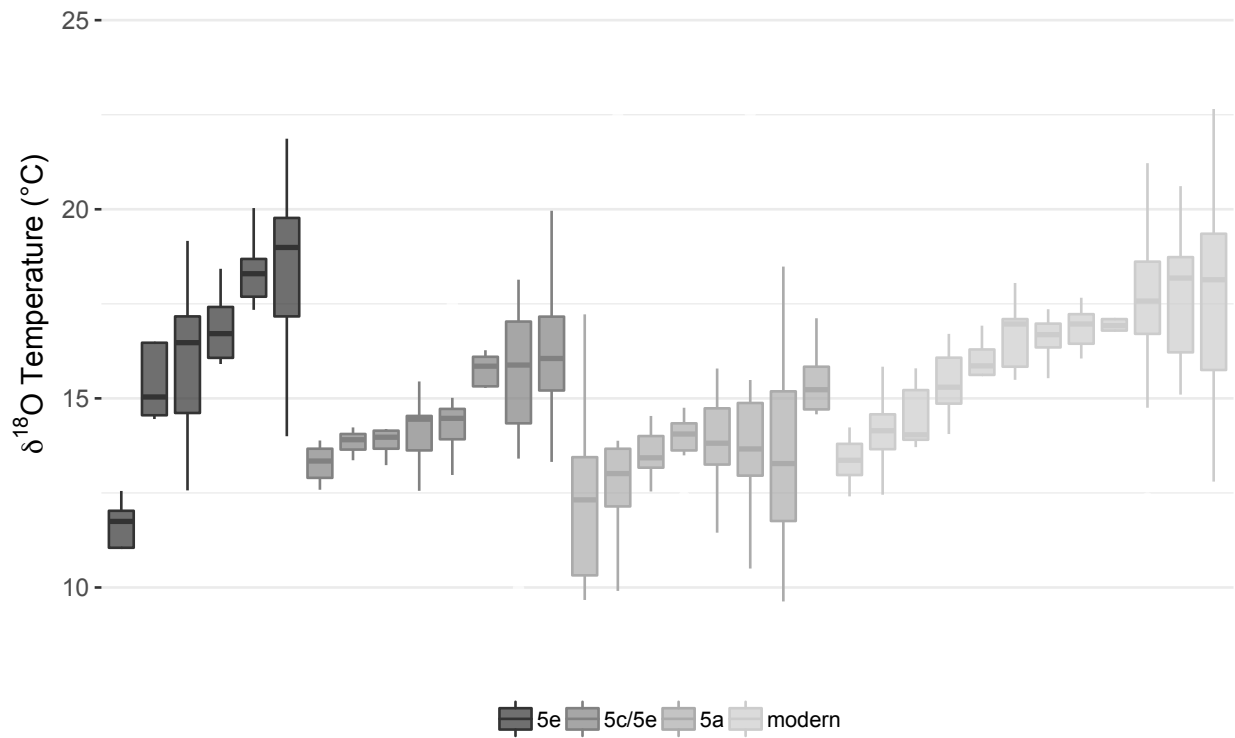


Figure 2.6: Late Pleistocene-Modern $\delta^{18}\text{O}$ temperature on San Nicolas Island by *Callianax biplicata* specimens. Boxplots represent medians (horizontal lines) and interquartile range (upper and lower 25% represented by boxplot whiskers) for each Late Pleistocene and modern specimen analyzed; n = 461. See Appendix I for $\delta^{18}\text{O}$ data.

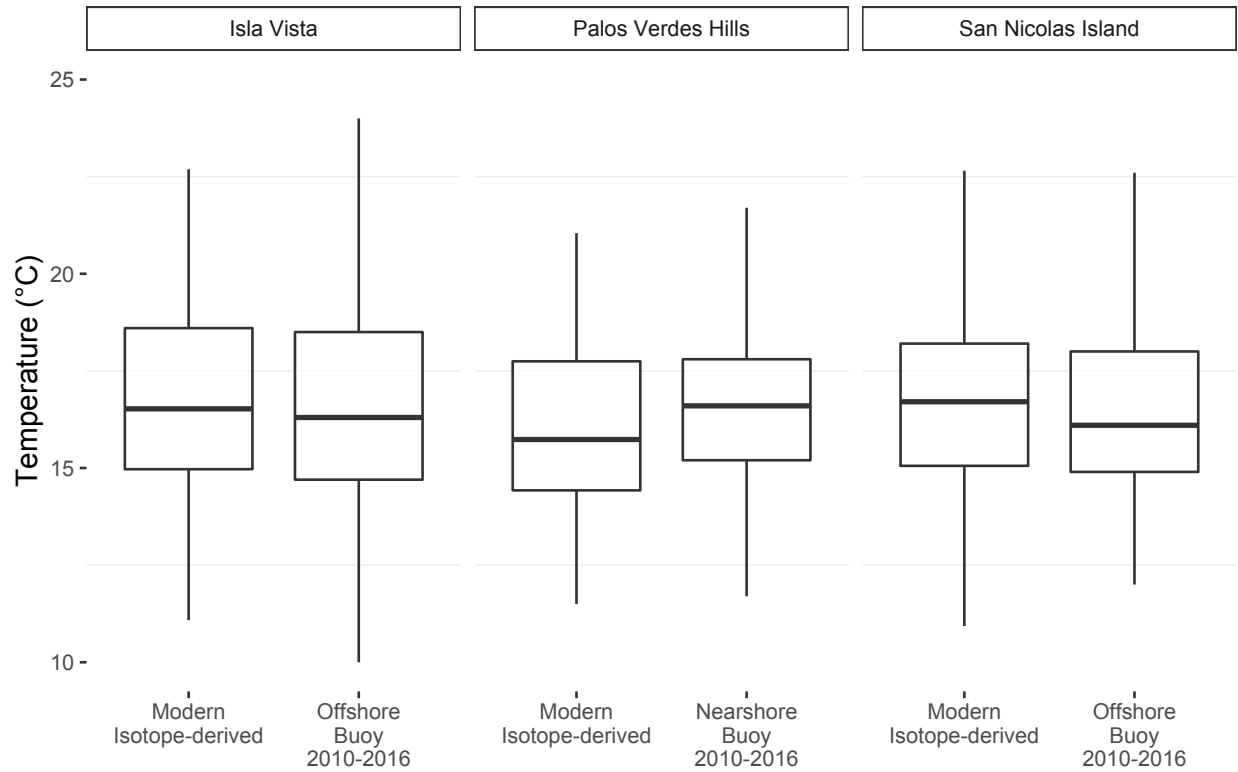


Figure 2.7: Modern $\delta^{18}\text{O}$ & modern buoy-measured temperatures. Boxplots represent median (horizontal lines) and interquartile range (upper and lower 25% represented by boxplot whiskers). Modern $\delta^{18}\text{O}$ temperatures and directly measured sea surface temperatures from nearshore (San Pedro Bay near Palos Verdes Hills) and offshore (San Nicolas Island and Isla Vista) buoy data closely correspond. Isla Vista buoy data accessed from: ndbc.noaa.gov/station_page.php?station=46053; Palos Verdes Hills buoy data accessed from: ndbc.noaa.gov/station_page.php?station=46222; San Nicolas Island buoy data accessed from: ndbc.noaa.gov/station_page.php?station=46219. Please note that the isotope-derived temperatures have been corrected by 0.5‰ to account for an apparent vital effect in *C. biplicata*, uncorrected isotope-derived temperatures are ~0.25-0.5°C warmer than shown above. See Appendix I for $\delta^{18}\text{O}$ data.

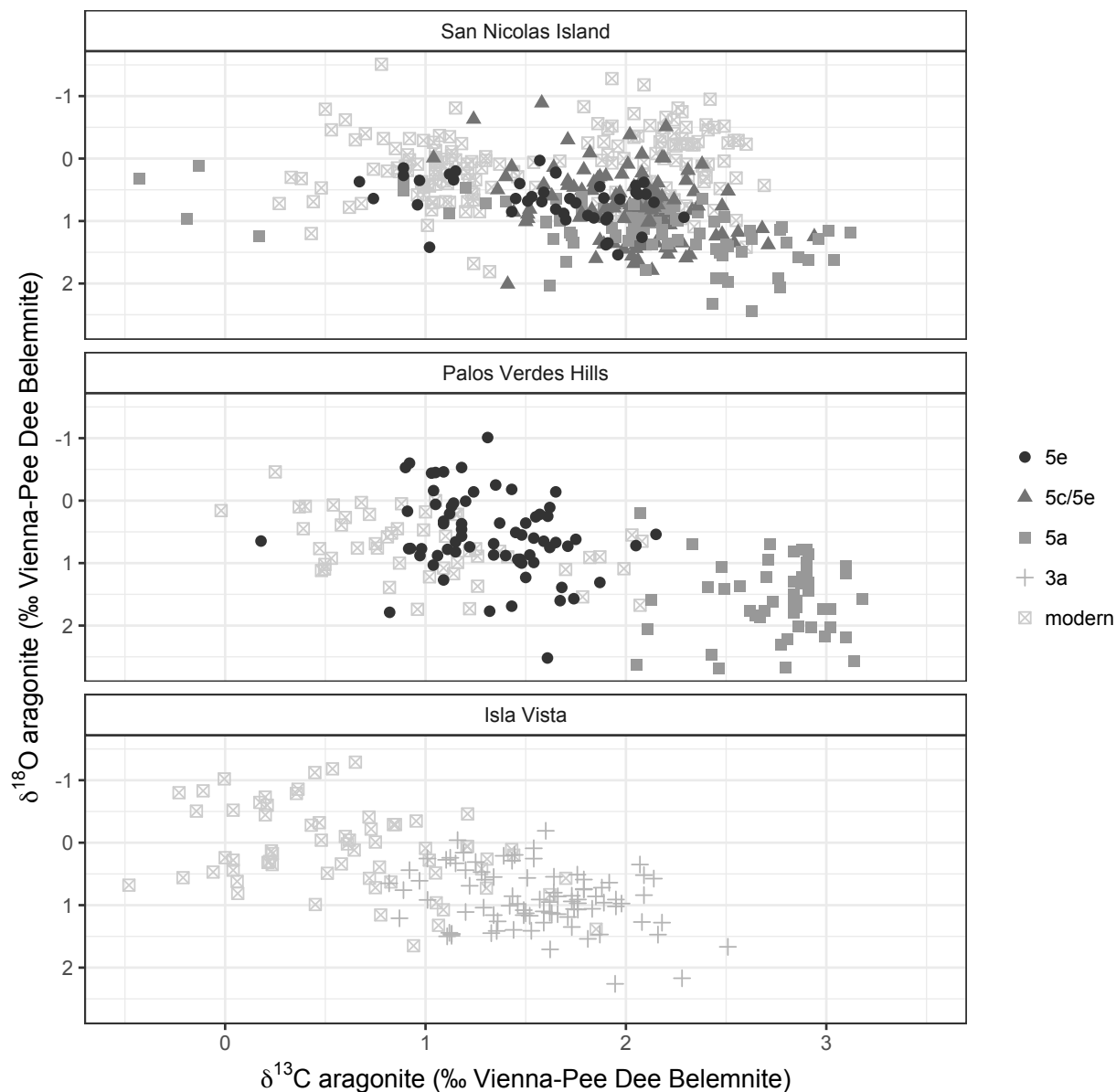


Figure 2.8: Late Pleistocene-modern $\delta^{13}\text{C}_{\text{aragonite}}$ and $\delta^{18}\text{O}_{\text{aragonite}}$. Points represent individual values analyzed. On San Nicolas Island and Palos Verdes Hills, lighter $\delta^{13}\text{C}_{\text{aragonite}}$ and $\delta^{18}\text{O}_{\text{aragonite}}$ correspond to MIS 5e and MIS 5a, respectively; $n = 858$. At all locations, the lightest $\delta^{13}\text{C}$ and $\delta^{18}\text{O}_{\text{aragonite}}$ values are modern (though, MIS 5e values at Palos Verdes Hills are quite similar to modern values; see also Figure 2.10), with the notable exception of a cluster of modern San Nicolas Island values, which are significantly enriched in $\delta^{13}\text{C}_{\text{aragonite}}$ and were collected in ~ 1900 . See Figure 2.12 for the temporal separation of modern $\delta^{13}\text{C}_{\text{aragonite}}$ values at San Nicolas Island. See Appendix I for $\delta^{18}\text{O}$ and $\delta^{13}\text{C}$ data.

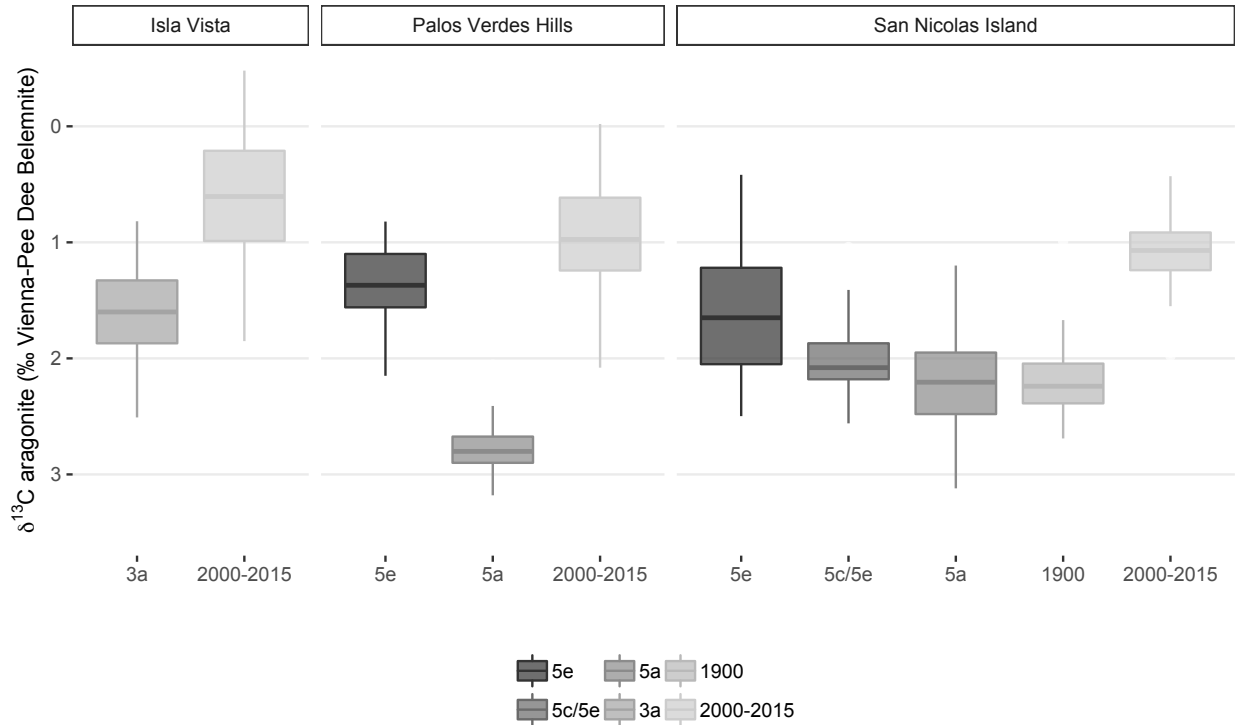


Figure 2.9: Late Pleistocene-modern $\delta^{13}\text{C}_{\text{aragonite}}$. Boxplots represent median (horizontal lines) and interquartile range (upper and lower 25% represented by boxplot whiskers); $n = 858$. Modern shells collected between 2000-2015 are distinctively lighter compared to Late Pleistocene shells. Shells collected in ~1900 on San Nicolas Island closely align with Late Pleistocene values, with a ~1‰ offset between shells collected ~1900 and between 2000-2015. See Appendix I for $\delta^{13}\text{C}$ data.

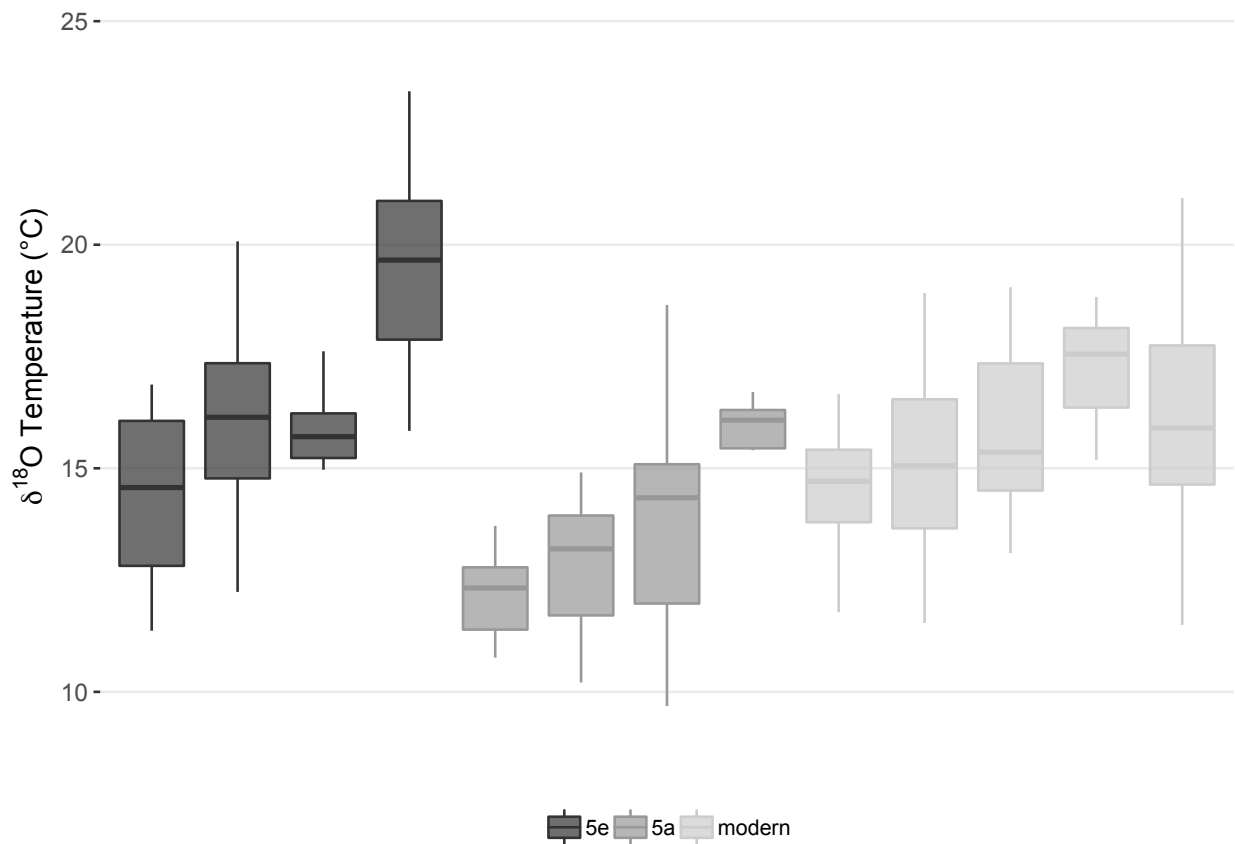


Figure 2.10: Late Pleistocene-Modern $\delta^{18}\text{O}$ temperature on Palos Verdes Hills by specimen. Boxplots represent median (horizontal lines) and interquartile range (upper and lower 25% represented by boxplot whiskers) for each MIS 5e, MIS 5a, and modern specimen analyzed; $n = 186$. See Appendix I for $\delta^{18}\text{O}$ data.

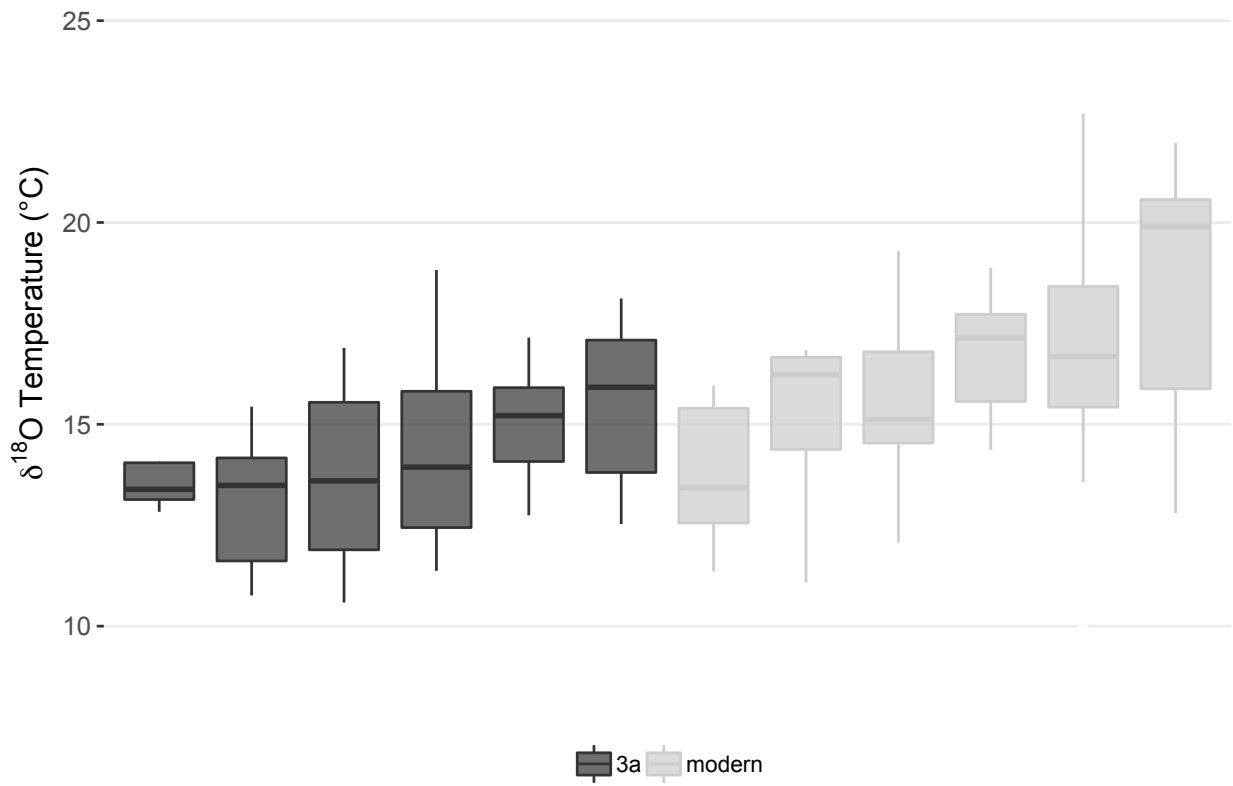


Figure 2.11: Late Pleistocene-Modern $\delta^{18}\text{O}$ temperature on Isla Vista by specimen.

Boxplots represent median (horizontal lines) and interquartile range (upper and lower 25% represented by boxplot whiskers) for each MIS 3a and modern specimen analyzed; n = 169. See Appendix I for $\delta^{18}\text{O}$ data.

Chapter II Tables

Location	<i>t</i>	Mean Square	Sum of Squares	<i>F</i>	df	<i>p</i>	Mean 5e	Mean 5e/5c	Mean 5a	Mean 3a	Mean modern
San Nicolas Island	-	177 [5.2]	706.5 [2354]	34.1	4 [454]	<0.001	16.8	15.1	13.8	-	16.5
Palos Verdes Hills	-	165 [5.9]	331 [1029]	28.1	2 [175]	<0.001	16.8	-	13.6	-	15.9
Isla Vista	5.2	-	-	-	122	<0.001	-	-	-	14.5	16.6

Table 2.1: $\delta^{18}\text{O}$ temperature for Late Pleistocene climate states. Analysis of Variance (ANOVA) results for San Nicolas Island and Palos Verdes Hills; t-test results for Isla Vista $\delta^{18}\text{O}$ Late Pleistocene temperatures. Both ANOVA and t-tests assess whether sample means are drawn from the same population (null hypothesis) or different populations (alternative hypothesis). See Table 2.2 for Tukey’s Honest Significance Test results for significant ANOVA analyses. *F*: F-test statistic; *t*: t-test statistic; df: degrees of freedom. For ANOVA results, residual values are in brackets.

Location	Contrast	Difference	Lower CI	Upper CI	<i>p</i>
San Nicolas island	5e-5e/5c	1.76	0.79	2.73	< 0.001
	5e-5a	3.08	2.07	4.1	<0.0001
	5e-modern	-0.48	-1.55	0.59	0.73
	5e/5c-5a	1.32	0.49	2.15	< 0.001
	5e/5c-modern	-2.2	-3.14	-2.24	< 0.001
	5a-modern	3.6	-4.5	-2.63	<0.0001
Palos Verdes Hills	5e-5a	3.2	2.19	4.24	<0.0001
	5e-modern	0.88	-0.17	1.93	0.12
	5a-modern	-2.33	-3.46	-1.21	<0.0001

2.2: $\delta^{18}\text{O}$ temperature Tukey's Honest Significance Tests. Post-hoc test results for significant ANOVA analyses (Table 2.1) for Palos Verdes Hills and San Nicolas Island. “Difference”: difference of means; “Lower and Upper CI”: lower and upper 95% confidence intervals of the difference in means between comparisons.

Chapter III

Pleistocene-present thermal niche tracking in Californian coastal mollusks

3.1 Abstract

How global biodiversity responds to contemporary climate change will depend, in part, on whether species can keep pace with climate change and track their thermal niches across wide distances and biogeographic barriers. Those species that cannot shift their geographic ranges will need to adapt or face extinction. Here, I examine the extent to which coastal marine mollusks tracked, or conversely, evolved, their thermal niches in response to Quaternary climate change. I focus on understanding the responses of coastal marine mollusk communities to climate change in southern California, with an emphasis on San Nicolas Island, where extensive marine terraces of Pleistocene sea level highstands preserve a sequence of environmental conditions and mollusk communities during key climate states over the last million years. Utilizing stable bulk ($\delta^{18}\text{O}$) and clumped (Δ_{47}) isotope analyses of well-preserved gastropods (*Callianax biplicata*) from these terraces, I reconstruct paleo-temperatures and pair these data with Pleistocene mollusk assemblages to determine the extent to which coastal marine mollusks have tracked their thermal niches over the last million years. At each Late and Early Pleistocene fossil site analyzed, I find that the contemporary thermal niches of all species overlap with reconstructed paleo-temperatures. These findings imply that coastal marine mollusks have tracked stable thermal niches over Pleistocene timescales in southern California.

3.2 Introduction

Along southern California's coast the uplifted remains of Pleistocene beaches, known as “marine terraces”, preserve the shells of coastal marine mollusk species which no longer live in the region today and instead live in cooler or warmer far to the north or south (Valentine 1961; Valentine and Jablonski 1993; Roy et al 1996). The wide offsets between fossil occurrences and modern geographic ranges, combined with the curious presence of “thermally disjunct” marine terrace localities that contain a mixture of cool and warm-water species (Arnold 1903; Woodring et al 1946; Valentine 1955; Emerson 1956; Valentine and Lipps 1967; Addicott 1966; Lipps et al 1968; Zinmeister 1974; Marincovich 1976; Lindberg and Lipps 1996; Roy et al 1995, 1996; Muhs et al 2012, 2014, 2018), appears to call into question the assumption that species have stable thermal niches and instead suggests that substantive niche evolution may have occurred on Pleistocene timescales (Valentine and Meade 1961; Zinsmeister 1974; Lindberg et al 1980; Lindberg and Lipps 1996). However, a lack of comprehensive and unambiguous paleo-temperature reconstructions for these fossil localities (but see earlier attempts which produced conflicting results in Valentine and Meade 1961; Dodd 1966; Muhs and Kyser 1986) makes it difficult to determine the extent to which mollusks may have tracked stable thermal niches into southern California in response to Late Pleistocene climate changes.

Recent research in species distribution modeling as well as species monitoring efforts on contemporary timescales has shown emerging support for niche tracking in response to contemporary climate change (Barry et al 1995; Zacherl et al 2003; Sanford et al 2019). On geological timescales, however, the results tend to be more mixed: while a majority of fossil occurrences are well predicted by paleo-species distribution models, many are not, even on Quaternary timescales (Martinez-Meyer and Peterson 2006; Pearman et al 2008; Veloz et al 2012; Saupe et al 2014, 2015; Jackson and Blois 2015). At face value, these paleo-species distribution models may support a role for environmental niche evolution (Svenning et al 2011; Veloz et al 2012; Stigall 2014; Saupe et al 2014; Jackson and Blois 2015; Patzkowsky and Holland 2016). However, interpreting the results of such models in the context of niche evolution and niche tracking is not straightforward (see review in Peterson 2011). For instance, many paleo-species distribution models pair highly localized fossil occurrences, some with uncertain ages, with global paleo-climate models that represent specific climate state scenarios (see a review of recent methodologies in Haywood et al 2019). This could generate spurious outcomes when fossil occurrences are naturally time-averaged or analytically binned into coarse intervals that span substantial climatic variability (Roy et al 1996; Haywood et al 2019) and when global paleo-climate models do not accurately predict the conditions at the local scale of fossil occurrences — which occurs especially in transitional areas and other areas characterized by substantial climate variation over short spatial scales (Holt et al 2017; see also IPCC reviews in Randall et al 2007 and Flato et al 2013).

Coastal marine habitats in southern California are characterized by highly localized climates influenced by the confluence of ocean currents and complexities in coastal geomorphology that produce considerable surface temperature differences over short distances (Valentine 1961; Ricketts et al 1985). The marine terrace record, which preserves the fossilized remains of Pleistocene marine mollusks, is time-averaged at a scale of 10,000 years (Valentine 1989; Kidwell and Bosence 1991; Russell 1991; but see Powell 2013) but in some cases, can be averaged at a scale of greater than 20,000 years when the same terrace surfaces were occupied during subsequent sea level highstands (Muhs et al 2012, 2014, 2018). Given the scales of time-averaging and spatial variability present within coastal California, paleo-species distribution modeling based on global climate models would not provide appropriate tests of thermal niche evolution and tracking.

Here I test the thermal niche evolution and thermal niche tracking hypotheses by employing stable isotope paleo-thermometry (Chapter II) and comparing resultant paleo-temperature reconstructions with the contemporary thermal ranges of species found as fossils at these sites. I focus on San Nicolas Island, where an excellently preserved flight of marine terraces provides an unparalleled opportunity to test thermal niche evolution and tracking over Late-Early Pleistocene timescales (over one million to 80,000 years ago; Lindberg and Lipps 1996; Muhs et al 2002, 2006, 2012, 2014). I further analyze two maincoast marine terrace localities at Palos Verdes

Hills and Isla Vista from open-coast and paleo-embayment localities (Muhs et al 2006; Trecker et al 1999).

3.3 Methods

3.3.1 Paleo-temperature reconstructions

Stable bulk and clumped isotope paleo-thermometry: Paleo-temperatures were reconstructed for sites on San Nicolas Island (Figures 1.1 and 1.2), Palos Verdes Hills (Figure 1.1), and Isla Vista (Figure 1.1) using clumped (Δ_{47}) and Δ_{47} -constrained bulk ($\delta^{18}\text{O}_{\text{aragonite}}$) stable isotope paleo-thermometry as outlined in Chapter II (Tables 2.1 and 2.2; Figures 2.1 and 2.5). In brief, well-preserved *C. biplicata* shells were sampled from each fossil site and adjacent modern area; clumped isotope paleo-thermometry on coarsely sampled parts of the shell were used to generate independent constraints on temperature at each site during each time period (Equation 2.6). These temperatures were used to reconstruct the oxygen isotope composition of paleo-seawater at that site (Equation 2.7), which was then used in the paleo-thermometer equation (Equation 2.3) to reconstruct higher-resolution bulk $\delta^{18}\text{O}_{\text{aragonite}}$ paleo-temperatures.

Early Pleistocene terraces on San Nicolas Island: Fossils from the 8th, 10th, and 11th terraces on San Nicolas Island are exceptionally well preserved and offer the opportunity to test the stability of coastal marine mollusc niches on deeper Quaternary timescales. Unfortunately, these terraces fall outside the zone of uranium-thorium dating and have yet to be comprehensively dated using other geochronology methods. Available evidence indicates that the 8th and 10th terraces may correlate with mid-early Pleistocene Marine Isotope Substages 21 and 31 (Muhs et al 2015; Daniel Muhs, personal communication 2019). The 11th terrace was likely deposited over 1 million years ago (Pearse 1988; Lindberg and Lipps 1996; Muhs et al 2012).

3.3.2 Faunal lists

Faunal lists for each fossil site (Figures 1.1 and 1.2) were assembled by surveying the published literature, taxonomically identifying fossils collected during field expeditions from 2015-2017, and studying museum collections at the Los Angeles County of Invertebrate Paleontology (LACMIP) and the University of California of Museum of Paleontology. Species names were taxonomically standardized using the World Register of Marine Species (WoRMS 2019), with updates or corrections when necessary (e.g., Zoosymposia 2019). In total, the database contains 56 bivalve and 105 gastropod species.

3.3.3 Contemporary species thermal ranges

Contemporary species' thermal ranges were calculated by compiling satellite-based sea surface temperature (SST) data across a species' coastal geographic distributions. Species' distributions along the Pacific mainland and Gulf of California coasts, as well as major offshore Pacific islands (Channel, Guadalupe, Rocas Alijos, Tres Marías, Revillagigedo, Clipperton Atoll, Coco,

Malpelo, and Galapagos islands) were collected from published faunal surveys, monographs, and scientific papers (Appendix IV). Bathymetry and SST data were taken from the ETOPO1 Global Relief Model (Amante and Eakins 2009) and National Oceanic and Atmospheric Administration's World Ocean Atlas 2018 at the quarter-degree grid cell resolution data for all averaged decades available (1955-2017; Locarnini et al 2018), respectively. Only coastal marine grid cells that average less than 5 meters below mean sea level were analyzed in the present study to approximate the same intertidal-shallow subtidal depths preserved within the marine terrace record localities at San Nicolas Island, Palos Verdes Hills, and Isla Vista (Chapter II; Figures 1.1 and 1.2). Two SST values were extracted for each quarter-degree grid cell: summer and winter SSTs. Average summer SSTs are the average SST observed during the Northern and Southern Hemisphere's summer months (i.e., July-September and December-March, respectively) for all measured years; average winter SSTs are the average SST observed during the Northern and Southern Hemisphere's winter months. Contemporary species ranges were computed using average winter SST as the lower thermal limit and average summer SST as the upper thermal limit. This method is conservative in that it will tend towards underestimating each species thermal tolerances, as sub-seasonal (i.e. daily-monthly) temperatures commonly reach levels much cooler and warmer than captured in the seasonally averaged values.

3.4 Results

3.4.1 Δ_{47} & $\delta^{18}\text{O}$ paleo-thermometry for Early Pleistocene terraces on San Nicolas Island

Δ_{47} paleo-temperatures for the 11th, 10th, and 8th terraces on San Nicolas Island average 16.2°C (standard error = 1.5), 16.5°C (standard error = 0.7), and 16.6°C (standard error = 0.8), respectively (Figure 3.1). Reconstructed $\delta^{18}\text{O}_{\text{seawater}}$ values average between 0.7‰-1.1‰ and are enriched compared to present-day $\delta^{18}\text{O}_{\text{seawater}}$ for offshore San Nicolas Island of ~-0.1‰ (Figure 3.2). The 11th terrace has a wide range of reconstructed $\delta^{18}\text{O}_{\text{seawater}}$ and Δ_{47} paleo-temperatures; $\delta^{18}\text{O}_{\text{seawater}}$ for the 8th terrace is reconstructed as distinctively lighter than the 10th terrace, although the two have similar reconstructed temperatures (Figure 3.2). Bulk stable isotope ($\delta^{18}\text{O}_{\text{aragonite}}$) temperatures are similar to Δ_{47} paleo-temperatures for the 11th and 10th terraces, but differ markedly for the 8th terrace, which $\delta^{18}\text{O}$ paleo-thermometry reconstructs as being quite warm (17.6°C) in comparison to the Δ_{47} measurements of 16.6°C (Figure 3.3).

3.4.2 Thermal niche tracking

All species found on San Nicolas Island today have modern realized thermal niches that overlap with $\delta^{18}\text{O}$ and Δ_{47} reconstructed temperatures taken from shells collected between 1900-2015 (Figure 3.4). Fossil mollusks from late Pleistocene (MIS 5e, 5c/5e, 5a, and 3a) and Early Pleistocene (terraces 8, 10, and 11) marine terrace localities show evidence of stable thermal niche tracking at all locations analyzed (San Nicolas Island [Figures 3.5 and 3.6], Palos Verdes Hills [Figure 3.7], and Isla Vista [Figure 3.8]): the contemporary thermal ranges of all species found as fossils at 8 fossil localities overlap with locality-specific reconstructed paleo-temperatures (Figures 3.5 and 3.6). On the 11th and 10th terraces of San Nicolas Island, one

species (*Lirabuccinum dirum*, Reeve 1846) falls slightly outside the reconstructed $\delta^{18}\text{O}$ paleo-temperatures, but for both of these sites this species does range into Δ_{47} paleo-temperatures, which are reconstructed as slightly cooler than $\delta^{18}\text{O}$ temperatures (Figure 3.6). Because Δ_{47} temperatures are direct reconstructions, whereas $\delta^{18}\text{O}$ is based on Δ_{47} -constrained $\delta^{18}\text{O}_{\text{seawater}}$ inferences, the Δ_{47} data provide the more authoritative reconstruction in cases where both approaches diverge. Hence, the Early Pleistocene fossil assemblages on San Nicolas Island also appear to strongly support the thermal niche tracking hypothesis.

3.5 Discussion

3.5.1 Early Pleistocene climate states of San Nicolas Island's upper marine terraces

Although they are not as well-constrained at the lower terraces, existing geochronological data suggest that the 8th, 10th, and 11th terraces on San Nicolas Island correlate with Mid-Early Pleistocene highstands between 866,000 and ~1 million years ago (Muhs et al 2015; Muhs, personal communication, 2019). Δ_{47} and $\delta^{18}\text{O}$ paleo-temperatures reconstruct conditions that are similar to present for each upper terrace, although Δ_{47} values reconstruct a wider range of cool and warm temperatures for the 11th terrace (Figures 3.1 and 3.3). Faunas from these higher terraces contain several extralimital species, but since both northern and southern extralimital species are present, it is difficult to draw any conclusions from faunal-based temperature reconstructions (Veddar and Norris 1963). Although it is outside the scope of the present study, an area worthy of future research would be to determine whether these upper terraces on San Nicolas Island show evidence of terrace re-occupation, as has been shown to be present on the island's second terrace (terrace 2b; Muhs et al 2012), where two highstands cut platforms into the same terrace surface and hence deposited a mixture of both northern and southern extralimital species referred to as "thermally disjunct" assemblages (Muhs et al 2012, 2014; Muhs and Groves 2018).

3.5.2 Thermal niche tracking over a million years in southern California

Contemporary proof-of-principle: The contemporary thermal ranges of all species collected on San Nicolas Island's modern beaches from ~1900 to 2016 overlap with my reconstructed $\delta^{18}\text{O}$ paleo-temperatures (Figure 3.4, see also Figure 2.7). This overlap provides a proof-of-principle for my study because it confirms that *C. biplicata* $\delta^{18}\text{O}$ paleo-temperatures reconstruct accurate thermal conditions. Moreover, it produces contemporary thermal ranges (which uses seasonal winter and summer average conditions from the World Ocean Atlas; Figures 1.4 and 1.5) on a scale comparable to my reconstructed paleo-temperatures.

Late-Early Pleistocene thermal niche tracking: At all Early and Late Pleistocene sites analyzed, the contemporary thermal ranges of every fossil species known from the site overlaps with my reconstructed paleo-temperatures (Figures 3.5, 3.6, 3.7, and 3.8). The fossil sites analyzed include both southern and northern extralimitals (Appendix III and IV), as well as thermally

disjunct assemblages containing both northern and southern extralimitals in close association (Figures 3.5, 3.6, 3.7, and 3.8; Appendix III and V; Veddard and Norris 1963; Muhs et al 2012). Only one species (*Lirabuccinum dirum*) on the 10th and 11th terraces of San Nicolas Island shows evidence of occurring in $\delta^{18}\text{O}$ paleo-temperatures slightly outside its contemporary thermal range (Figure 3.6). However, when Δ_{47} temperatures (Figure 3.1), as opposed to in $\delta^{18}\text{O}$ paleo-temperatures (Figure 3.3), are analyzed, the *Lirabuccinum* fossil occurrence is well within its contemporary thermal range. This remarkable pattern of complete paleo-temperature and contemporary thermal range correspondence strongly suggests that coastal marine mollusks have tracked stable thermal niches over the Pleistocene in southern California.

My finding of stable thermal niche tracking in coastal marine mollusks contrasts with some paleo-species distribution modeling studies conducted on terrestrial plants and animals which found less clear evidence of (realized) niche stability over Quaternary timescales (Martinez Meyer et al 2004; Pearman et al 2008a, 2008b; Veloz et al 2012; Worth et al 2014). This contrast may underscore fundamental differences in physiology and life history between terrestrial and marine species (e.g., Sunday et al 2011). For instance, terrestrial ectotherms show evidence of filling their thermal niches to a lesser degree than marine ectotherms, the latter of which tend to occupy latitudinal ranges that fully realize their thermal tolerances (Sunday et al 2012). In this sense, marine ectotherms, such as those analyzed herein, are "thermal-range conformers" whose latitudinal ranges closely capture their thermal ranges. A corollary of this thermal-conformer hypothesis is that marine ectotherms should show high sensitivities to climate change at their northern and southern range endpoints (Sunday et al 2012). The analyses herein — conducted during several distinctive climate states over the last million years — show such evidence of thermal-range conformance: southward or northward range extensions and contractions were in-step with fluctuating Pleistocene climates because all Pleistocene occurrences, including extralimitals, analyzed experienced paleo-temperatures well within their contemporary ranges (Figures 3.5, 3.6, 3.7, and 3.8).

Implications for faunal-based paleo-temperature reconstructions & thermally-disjunct assemblages: Since the late 1800's, the modern-day distributions of species found as fossils in California's marine terrace record have been used to make inferences about maximum and minimum paleo-temperature conditions (e.g., Woodring et al 1946; Valentine 1961; Addicott 1966; Lipps 1967; Wright 1972; Kennedy et al 1982; Powell 2001; Powell et al 2004, 2009). Mostly, these studies based their inferences on the present-day latitudinal ranges, and in some cases depth ranges, of extralimital species to build their temperature reconstructions (Valentine and Meade 1960; Valentine 1961; Addicott 1966; Lipps 1967; Wright 1972; Powell 2001; Powell et al 2004, 2009). However, using faunal-based paleotemperature reconstructions requires an assumption of thermal niche stability over Pleistocene timescales (Woodring 1951; Johnson 1960a; Valentine and Emerson 1956). My finding of stable niche tracking over Late-Early Pleistocene timescales provide some evidence that this assumption may indeed be justified, at least in this Pleistocene coastal marine mollusc system.

With respect to thermally disjunct assemblages, however, my paleo-temperature results and interpretations diverge materially from many faunal-based interpretations because these studies tended to take at face value that thermally disjunct species co-occurred in life (Arnold 1903; Woodring et al 1946; Woodring 1951; Valentine 1955; Emerson 1956; Valentine and Lipps 1967; Addicott 1966; Lipps et al 1968; Zinmeister 1974; Marinovich 1976; Lindberg and Lipps 1996; but see Crickmay 1929), and hence, interpreted their paleo-environments as representing no-analog habitats with either strong seasonality, unusual upwelling regimes, or some combination of other environmental factors (e.g., Valentine 1955, 1958, 1961; Emerson 1956a; Valentine and Emerson 1961; Zinmeister 1974). My study, however, reconstructs the paleo-temperatures of thermally disjunct assemblages as merely encompassing both warm and cool temperatures, which may be caused by centennial variation (e.g., Roy et al 1996), or perhaps more likely, millennial variation caused by terrace reoccupation and coincident time-averaging of distinctively different climate states (Muhs et al 2012, 2014; Muhs and Groves 2018; see also Chapter II discussion of terrace 2b on San Nicolas Island). However, thermally disjunct assemblages represent only a minority of faunal-based environmental reconstruction studies. Encouragingly, my results for Late-Early Pleistocene climate states, which vary from ~3°C cooler to < 1°C warmer than at present for open-coast habitats, largely align with previous faunal-based reconstructions, and hence, support their continued use as paleo-environmental inferential tools, especially in cases where geochemical reconstructions are outside the scope of study or unwarranted (e.g. poor fossil preservation).

3.6 Conclusions

Marine mollusks found at twelve fossil sites in southern California spanning 50,000-1,000,000 years ago show evidence of stable thermal niche tracking: all fossil species, including those with presently extralimital ranges, lived within paleo-temperatures encompassed by their contemporary thermal niches (Figures 3.5, 3.6, 3.7, and 3.8). I interpret these results to be robust, as a test of my methods using the modern occurrences of species on San Nicolas Island demonstrates the expected pattern of correspondence between contemporary ranges and stable isotope *C. biplicata*-based temperature reconstructions (Figure 3.4). The pattern of complete correspondence between paleo-temperatures and contemporary thermal ranges challenges the notion that extralimital species and thermally disjunct assemblages represent cases of thermal niche evolution or no-analog conditions, at least on the Pleistocene timescales analyzed herein (Valentine and Meade 1961; Zinsmeister 1974; Lindberg et al 1980; Lindberg and Lipps 1996). Instead, my findings suggest that coastal marine mollusks are thermal-range conformers (Sunday et al 2012) and have shifted their latitudinal distributions to keep pace with changing climates over Pleistocene timescales.

Chapter III Figures

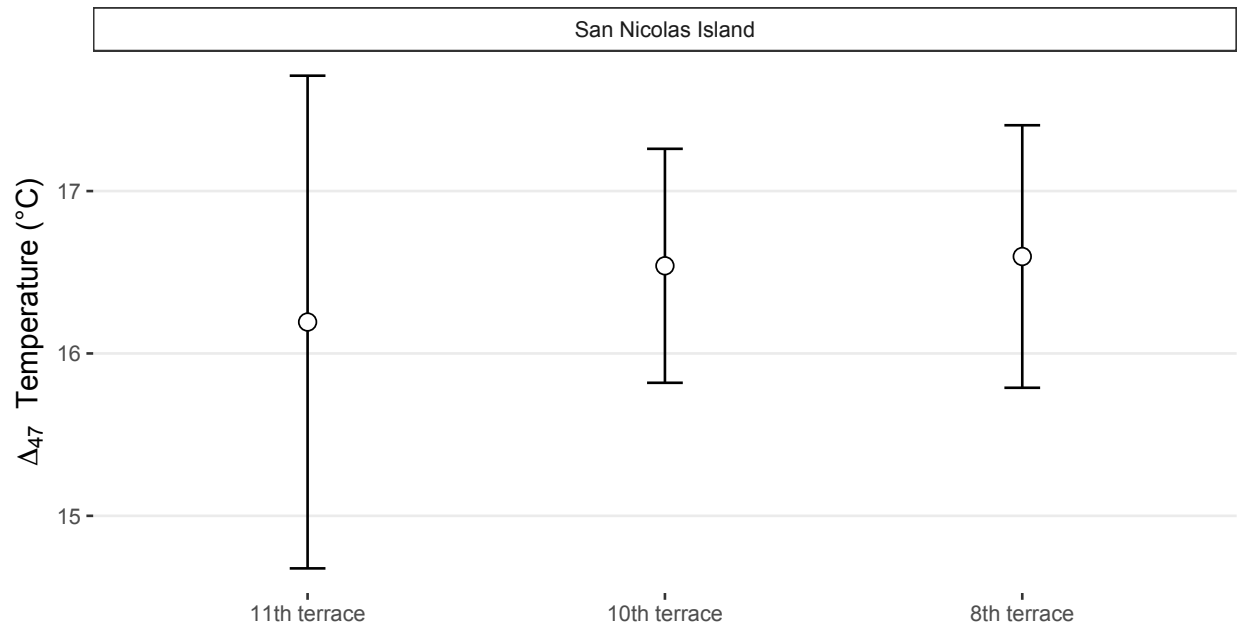


Figure 3.1: Δ_{47} temperatures for Early Pleistocene terraces on San Nicolas Island. Means represented as points bracketed by the standard error of the mean estimate. The 11th terrace has greater variance in reconstructed temperatures compared to the 10th and 8th, both of which have reconstructed paleo-temperatures similar to at present ($\sim 16^{\circ}\text{C}$); $n = 18$. See Appendix II for Δ_{47} data.

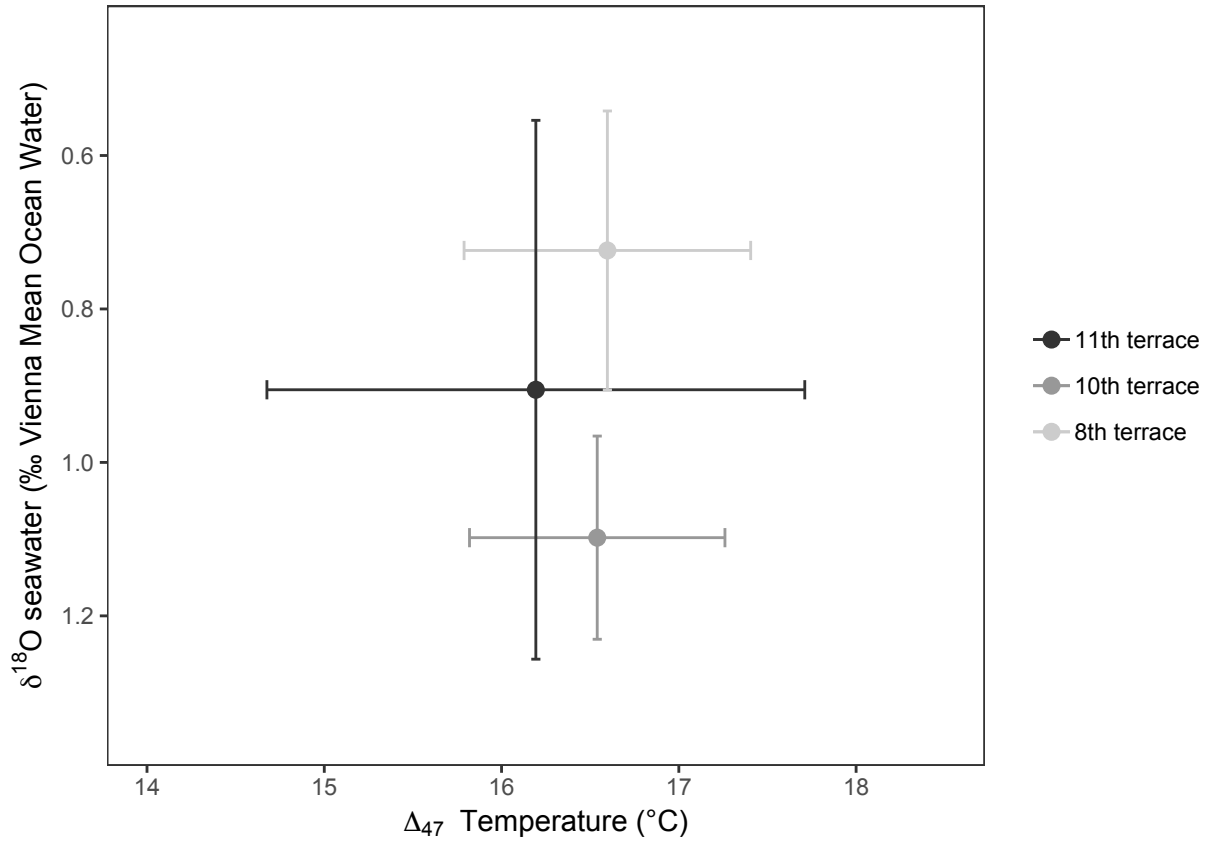


Figure 3.2: Δ_{47} & $\delta^{18}\text{O}_{\text{seawater}}$ for Early Pleistocene marine terraces on San Nicolas Island. Points represent means; horizontal and vertical bars represent the standard error of the mean for Δ_{47} and $\delta^{18}\text{O}_{\text{seawater}}$, respectively; $n = 18$. Please note that Δ_{47} and $\delta^{18}\text{O}_{\text{seawater}}$ errors are (inversely) correlated because Δ_{47} is used to construct $\delta^{18}\text{O}_{\text{seawater}}$ estimates (Equation 2.7). See Appendix II for Δ_{47} data.

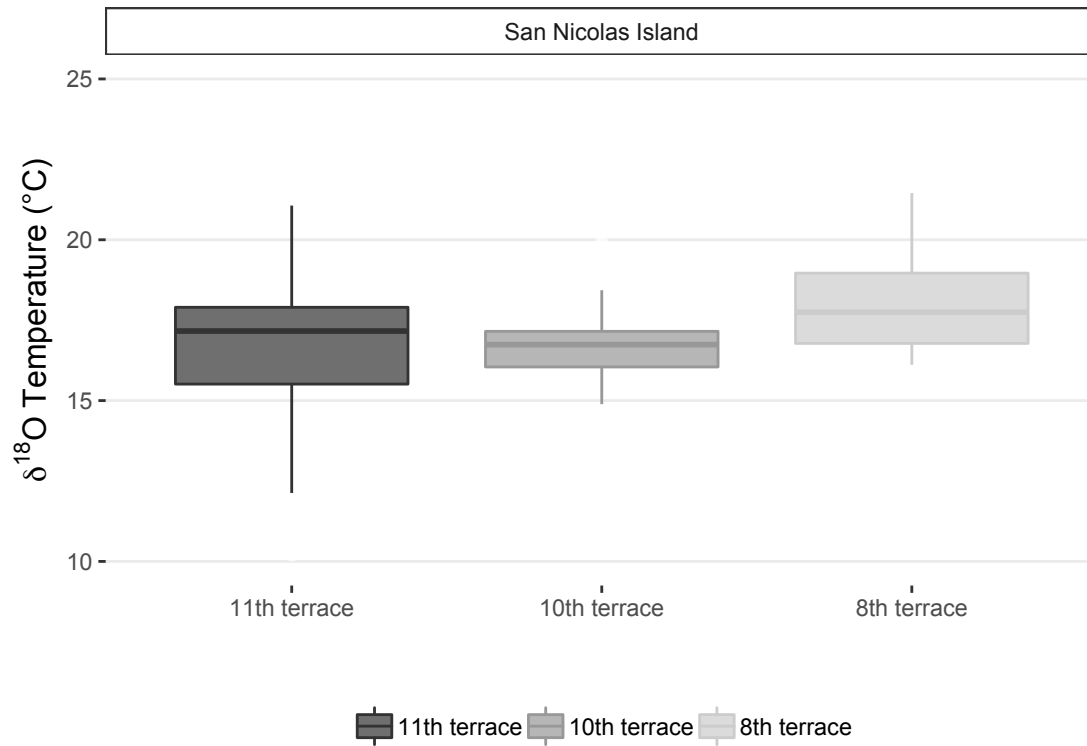


Figure 3.3: $\delta^{18}\text{O}$ temperatures for Early Pleistocene terraces on San Nicolas Island. Boxplots represent median (horizontal line) and interquartile range (upper and lower 25% represented by boxplot whiskers) for each climate state analyzed; $n = 18$. See Appendix I for $\delta^{18}\text{O}$ data.

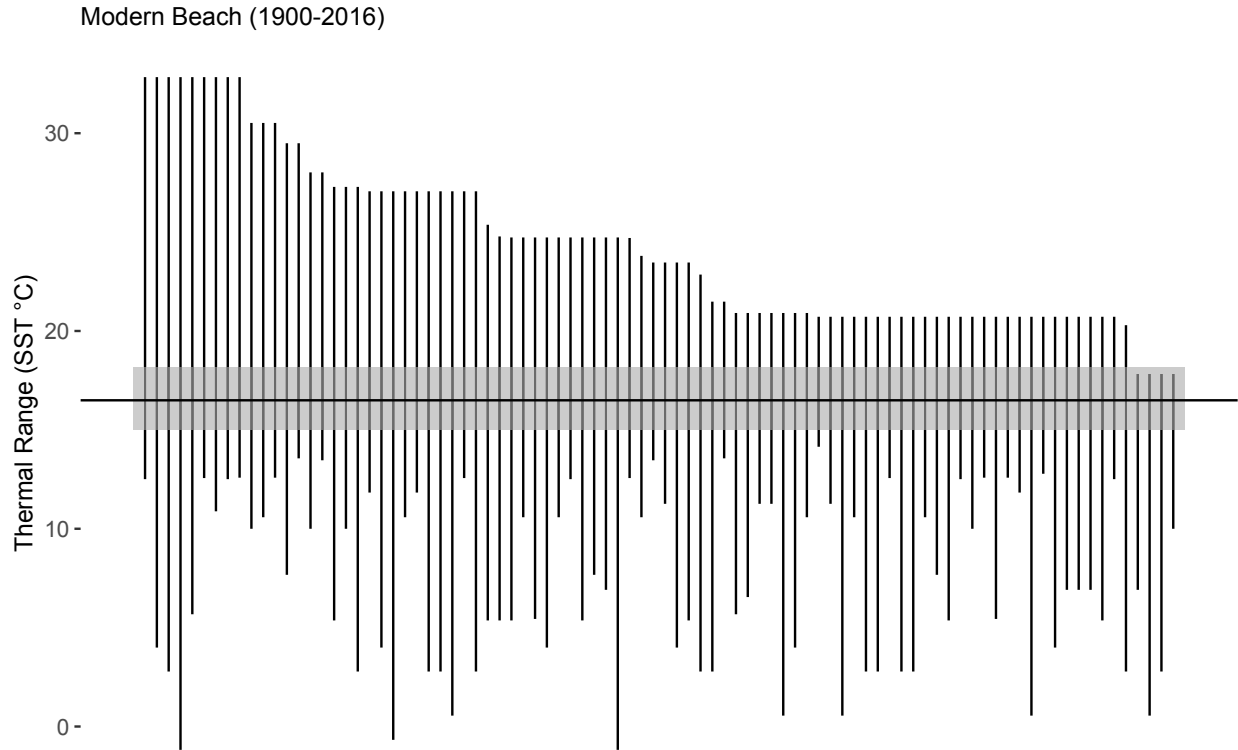


Figure 3.4: Contemporary thermal niche tracking on San Nicolas Island. Vertical bars represent the thermal ranges ($^{\circ}\text{C}$) for each species found on San Nicolas Island today (historical records dating to 1900 to collections made in 2016). Reconstructed $\delta^{18}\text{O}$ temperatures for modern (1900-2015) shells represented as the grey bar, which is bracketed by the upper and lower interquartile range, with the mean indicated in black. All species thermal ranges overlap with reconstructed paleo-temperatures. See Appendix III for species' geographic and thermal ranges; see Appendices II and III for stable isotope data used to reconstruct temperatures.

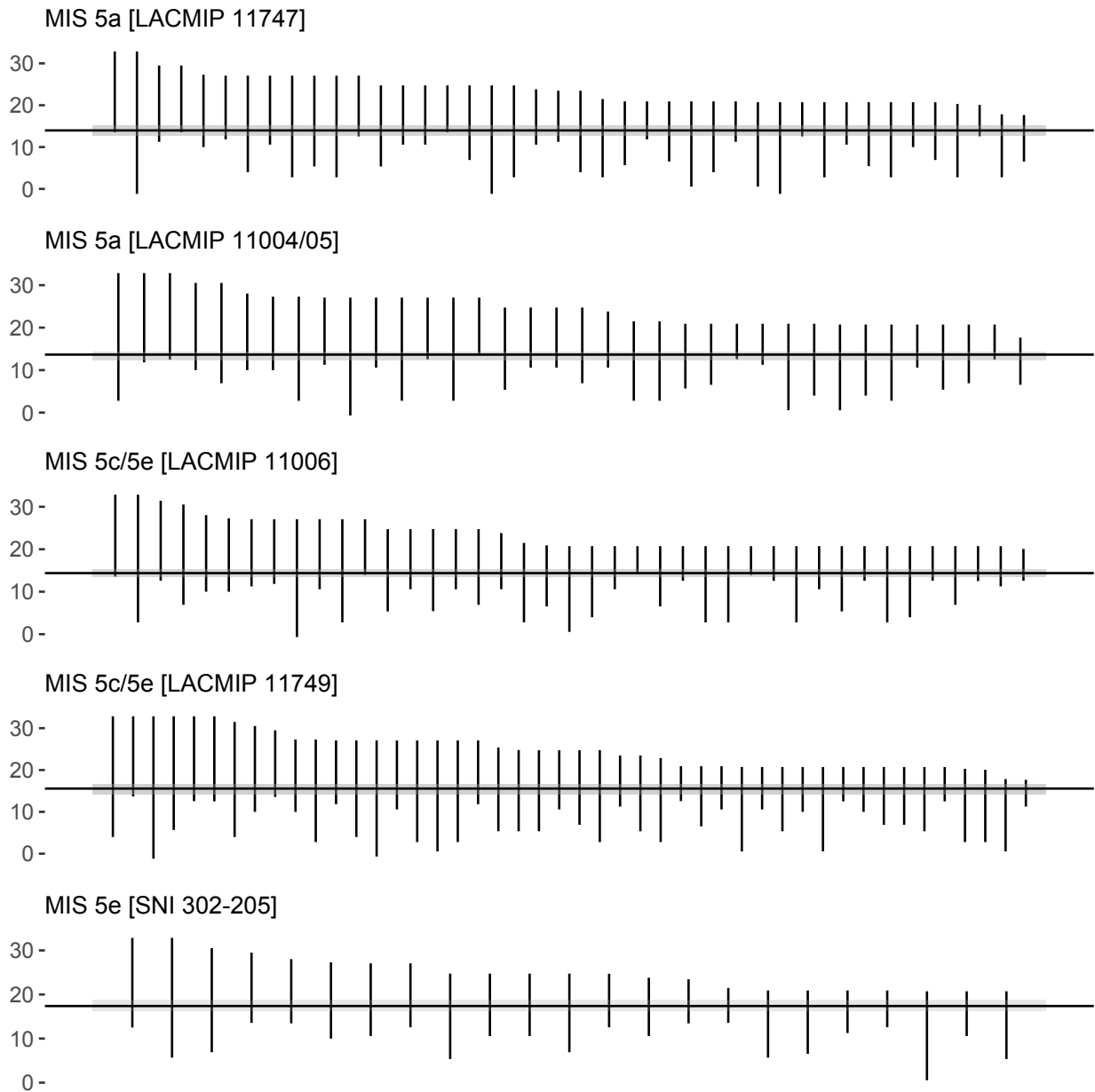


Figure 3.5: Late Pleistocene thermal niche tracking on San Nicolas Island. Y-axis represents thermal SST range in degrees Celsius; vertical bars represent the thermal ranges ($^{\circ}\text{C}$) for each species found at Late Pleistocene (MIS 5e, 5c/5e, and 5a) on San Nicolas. Reconstructed $\delta^{18}\text{O}$ paleo-temperatures represented as grey bars that are bracketed by the upper and lower interquartile range, with the mean indicated in black. All species lived within their contemporary thermal niches during the Late Pleistocene at these five localities. See Appendix III for species' geographic and thermal ranges; see Appendices II and III for stable isotope data used to reconstruct temperatures.

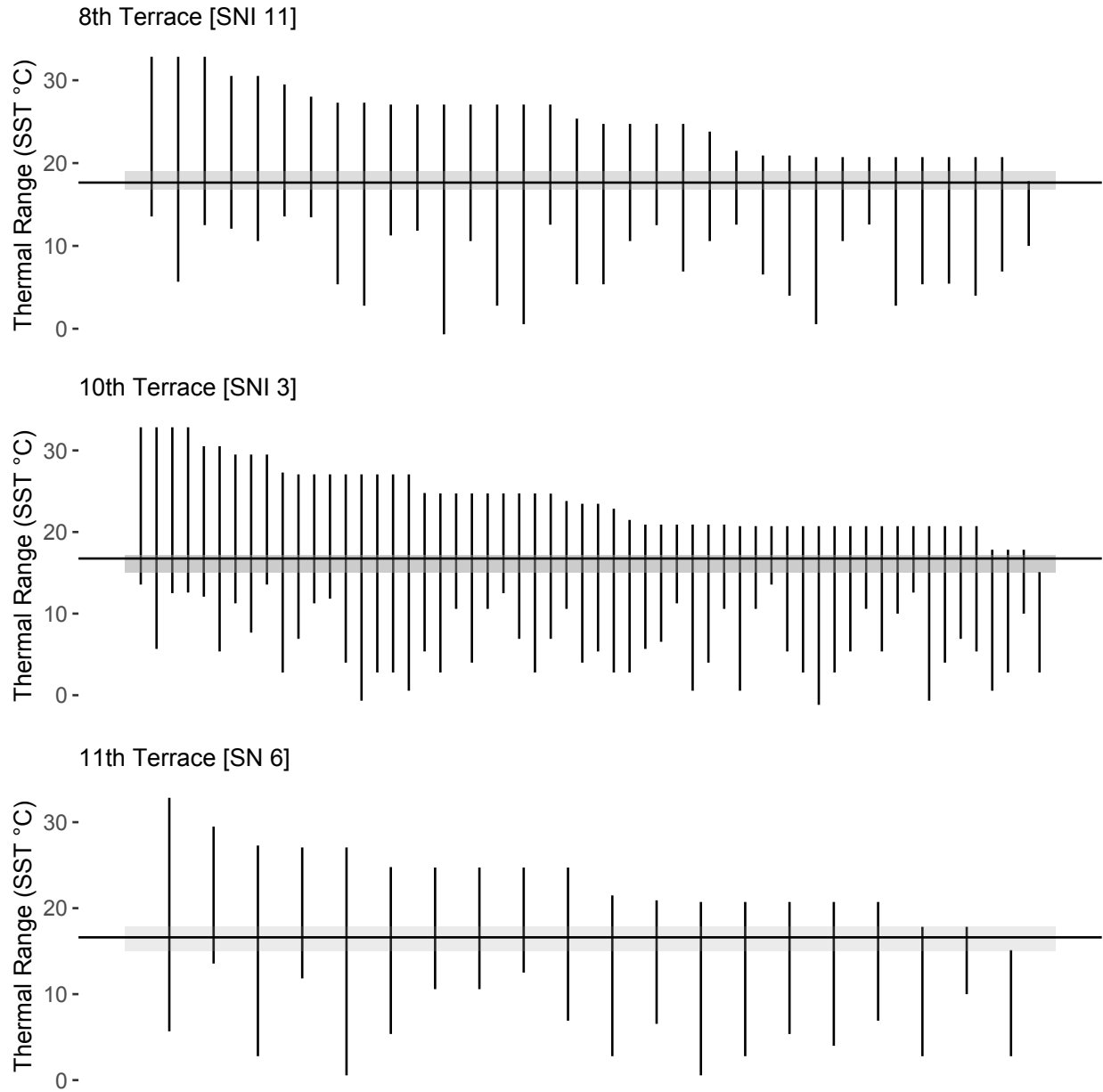


Figure 3.6: Early Pleistocene thermal niche tracking on San Nicolas Island. Vertical bars represent the thermal ranges ($^{\circ}\text{C}$) for each species found on the Early Pleistocene (11th, 10th, and 8th) marine terraces on San Nicolas. Reconstructed $\delta^{18}\text{O}$ paleo-temperatures represented as grey bars that are bracketed by the upper and lower interquartile range, with the mean indicated in black. All species lived within their contemporary thermal niches during the Early Pleistocene at these three localities. See Appendix III for species' geographic and thermal ranges; see Appendices II and III for stable isotope data used to reconstruct temperatures.

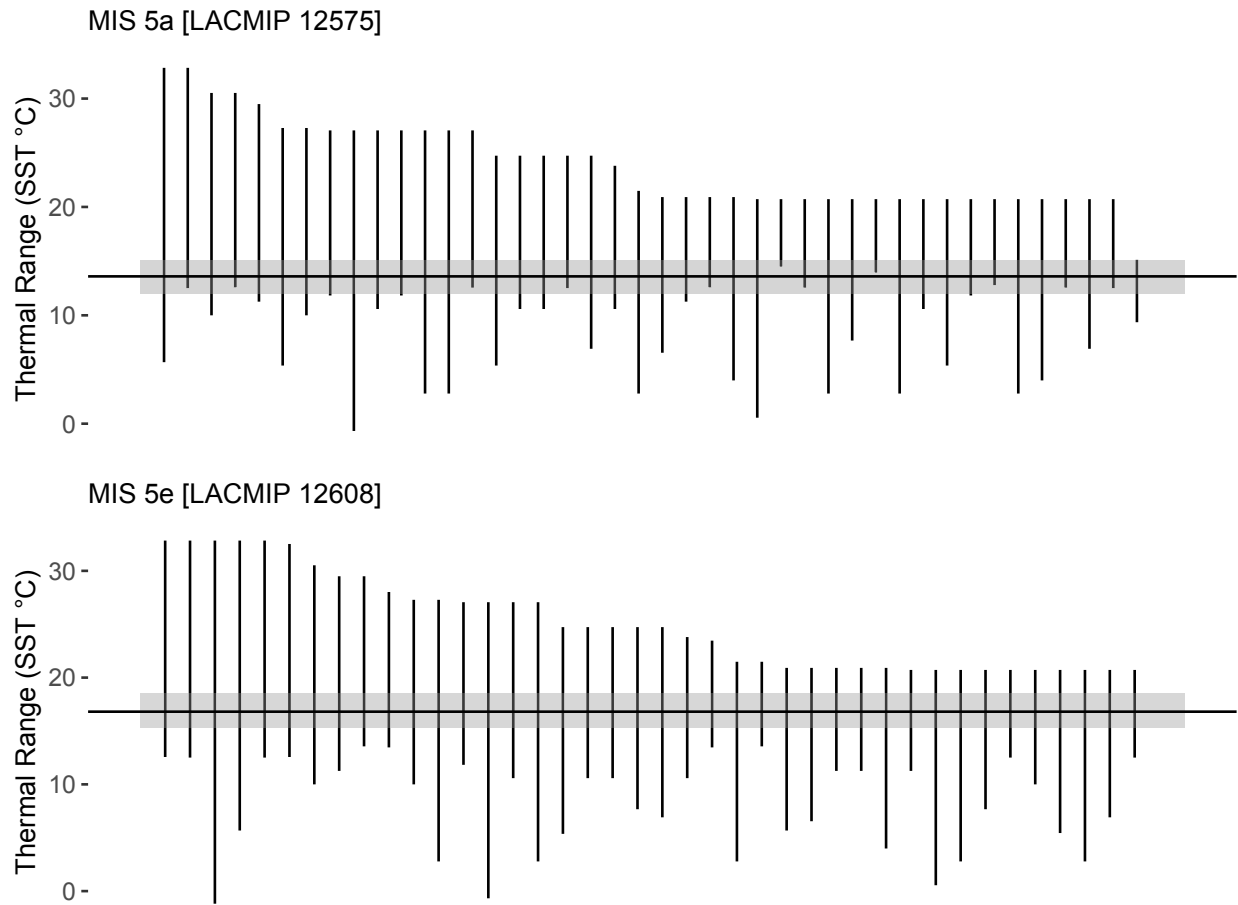


Figure 3.7: Thermal niche tracking at Palos Verdes Hills during MIS 5a and 5e. Vertical bars represent the thermal ranges (°C) for each species found on at Late Pleistocene (MIS 5e and 5a) marine terraces at Palos Verdes Hills. Reconstructed $\delta^{18}\text{O}$ paleo-temperatures represented as grey bars that are bracketed by the upper and lower interquartile range, with the mean indicated in black. All species lived within their contemporary thermal niches during the Late Pleistocene at these three localities. See Appendix III for species' geographic and thermal ranges; see Appendices II and III for stable isotope data used to reconstruct temperatures.

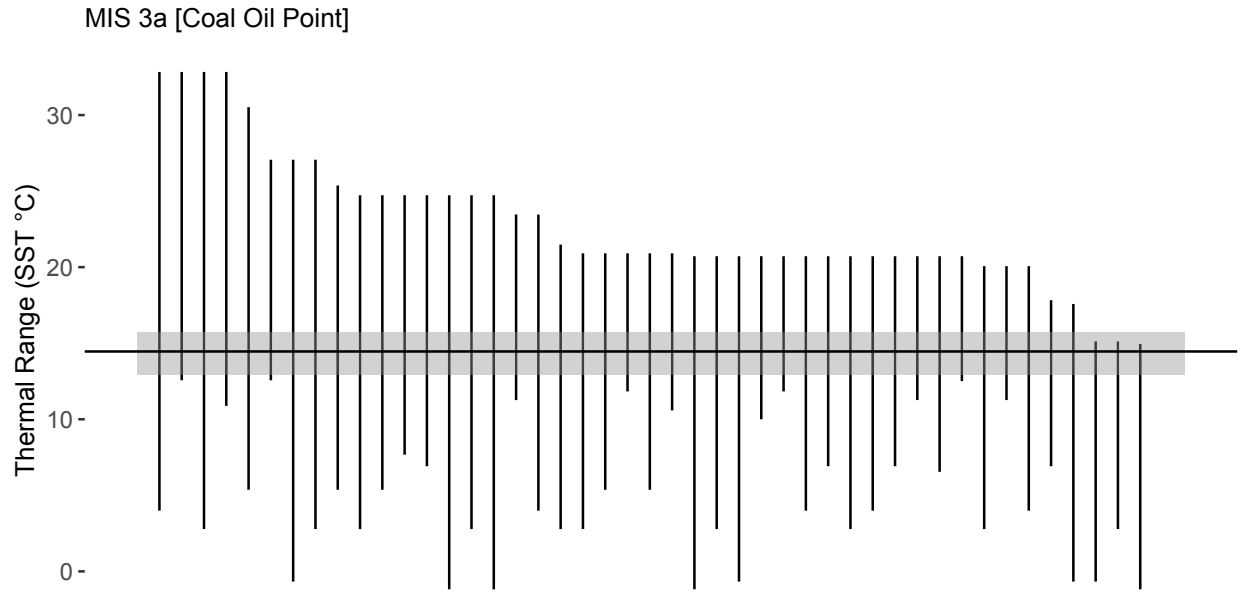


Figure 3.8: Thermal niche tracking at Isla Vista during MIS 3a. Vertical bars represent the thermal ranges (°C) for each species found at Coal Oil Point (MIS 3a) at Isla Vista. Reconstructed $\delta^{18}\text{O}$ paleo-temperatures represented as grey bars that are bracketed by the upper and lower interquartile range, with the mean indicated in black. All species lived within their contemporary thermal niches during MIS 3a at this locality. See Appendix III for species' geographic and thermal ranges; see Appendices II and III for stable isotope data used to reconstruct temperatures.

Chapter IV

Extralimitals from the Marine Isotope Substage 5e in coastal marine California

4.1 Abstract

As the most recent time in Earth history when global temperatures were warmer than at present, the peak of the last interglaciation (Marine Isotope Substage [MIS] 5e; ~120,000 years ago) can serve as a pre-anthropogenic baseline for a warmer near-future world. Here I use a new compilation of 22 MIS 5e fossil localities in California to establish baseline expectations for contemporary species invasions by identifying and analyzing bivalve species with present-day extralimital ranges, i.e. species that occupied the California region during MIS 5e but have since been restricted to adjacent regions. I find that 15% of species ($n = 142$) found in MIS 5e localities have extralimital ranges and that all currently occupy warmer waters to the south of California region. The majority of extralimital occurrences were found within paleo-embayments (all 9 paleo-embayment fossil localities house 17 extralimital species whereas only 3 of 13 open-coast habitats house 4 extralimital species); thus indicating that sheltered habitats harbored more ephemeral warm-water bivalves compared to exposed coasts during MIS 5e. I further find that these extralimital species tend to occur on more offshore oceanic islands and in cooler and more seasonally productive coastal habitats when compared to their conterminous fauna. These findings suggest that warm-water subtropical species with high dispersal potential and pre-existing tolerances to environmental conditions similar to California's comparatively cool and seasonally productive environments may have enabled extralimital bivalves to invade the California region during the ancient analog MIS 5e climate state.

4.2 Introduction

Pleistocene extralimital species—i.e., species that occupied regions outside of their present geographic limits—record a dynamic history of climatic and consequent biogeographical change (Valentine 1961; Valentine and Jablonski 1993; Roy et al 1996), and as such, have been used to biostatigraphically correlate deposits (e.g., Wehmiller et al 1977; Kennedy et al 1982), infer paleoenvironments (e.g., Woodring et al 1946; Valentine 1961; Addicott 1966; Kennedy et al 1982; Powell 2001; Powell et al 2004, 2009), and more recently, to examine the ecological and evolutionary attributes of range shifts (e.g., Roy et al 1995, 2001; Hellburg et al 2001). Although not widely discussed from a conservation standpoint, Pleistocene extralimital species also hold a special relevance for today because we may expect these contemporary expellees to recolonize once regional climates sufficiently change to allow them to track their environmental tolerances back into their paleo-ranges. In this sense, Pleistocene extralimitals can provide pre-anthropogenic baseline expectations for species invasions (and reinvasions) in response to regional climate change.

Extralimital marine invertebrates found within southern California's record of uplifted coastal marine terraces have been extensively studied for over 100 years (e.g., Conrad 1855; Valentine 1961; Muhs and Groves 2018) and offer an unparalleled opportunity to analyze the underpinnings of Pleistocene range shifts. Indeed, up to 17% of species found as fossils within this exceptionally complete fossil record (Valentine 1989) are presently extralimital (Valentine & Jablonski 1993). Emergent patterns of extralimital occurrences appear to follow climatic cycles during which northern extralimitals invade in colder climate states and southern extralimitals invade in warmer climate states (Valentine 1961; Valentine and Jablonski 1993; Roy et al 1996; Powell et al 2000; Muhs et al 2002, 2012, 2014, 2018). However, due to the historical difficulty of independently dating marine terrace deposits (see discussions Muhs et al 2002, 2012, 2014, 2018) previous investigations (e.g., Roy et al 1996, 2001) have been conducted at the composite Upper-Late Pleistocene level rather than focused on particular climate states.

Here I leverage advances in Late Pleistocene geochronology (Muhs et al 2002, 2006, 2012, 2014; Muhs and Groves 2018) to examine the characteristics of extralimital species that expanded their ranges into the California region during the warmest climate state of the last 300,000 years: the peak of the last interglaciation, Marine Isotope Substage "MIS" 5e, (~120,000 years ago; Shackleton and Opdike 1973). I focus on bivalve species because their biogeographic distributions are exceptionally well studied in the eastern Pacific (e.g., Coan et al 2000; Coan and Valentich-Scott 2012). My specific goals are to: 1) provide an exhaustive MIS 5e extralimital fauna of paleo-protected and paleo-open coast habitats, and 2) to test whether extralimitals show evidence of higher dispersal characteristics or of tolerating environmental conditions that are more similar to California's seasonally productive and cool coastal habitats when compared to their conterminous faunas. By investigating the characteristics of extralimital species from the globally warmer-than-at-present MIS 5e, I seek to establish a pre-anthropogenic baseline for species invasions in response to contemporary warming.

4.3 Methods

4.3.1 MIS 5e California region database

Only fossil collections from marine terrace localities that have been confidently dated to MIS 5e (or, MIS 5.5 of Martinson et al 1987; [130,000-115,000 years ago; Muhs and Groves 2018]) using uranium-thorium radiometric dating and/or amino acid racemization that show no evidence of substantial temporal mixing were included in MIS 5e California region database (Appendix V). Corresponding MIS 5e faunal lists were gathered by surveying the published literature and museum collections for the California region (Appendix VI). In total, MIS 5e database contains 142 taxonomically standardized (WoRMS Editorial Board 2018) bivalve species from 22 localities spread within and bounding the modern California region that ranges from Guadalupe Island (29°N) to Cayucos, California (35.4°N; Appendix V, VI). Importantly, because offshore islands can contain faunas distinct from the adjacent mainland coast (Valentine 1966; Lindberg et al 1980; McLean and Coan 1996), I also compiled exhaustive modern faunal lists for each

island in the MIS 5e dataset (i.e., Channel Islands and Guadalupe Island; Appendix VII). To identify MIS 5e extralimital species, modern geographic distributions and island occurrences were compared to MIS 5e distributions and island occurrences.

4.3.2 Contemporary Northern Panamic region database

To determine whether MIS 5e extralimitals share any distributional characteristics that distinguish them from their conterminous faunas I compared them to a pool of species with distributions that range up to or near to the Californian region today. To do this, I assembled a comprehensive database of marine bivalves that are known to occur within water depths shallower than 20-meters, a cut-off that is comparable to the maximum inferred depths of marine terrace deposits in MIS 5e dataset (Kanakoff and Emerson 1959 [~18 meters max]; Powell et al 2004 [~20 meters max]) in the Northern Panamic region (Baja California Sur and Golfo de California; Figure 4.1; Appendix VII). (Because the MIS 5e dataset ultimately contained only one northern extralimital species, I did not compile a Northern California/Oregon region fauna.) Please note that present-day bivalve depth ranges are minimum estimates. A few species in the dataset have their northernmost Pacific main coast range endpoints within the Northern Panamic region but also occur on Guadalupe Island (29°N); I include such species in the Northern Panamic fauna because offshore islands are known to house faunas of disjunct mainland regional affinities (Valentine 1961; Lindberg et al 1980). Species with maximum body sizes less than 5 mm are excluded from this study because such small-bodied species are substantially under-represented in the marine terrace fossil record (Valentine 1989). These constraints help to ensure that only species found within a reasonable distance from the modern California region (and therefore with a reasonably high probability of invading the California region compared to species living further south in the Panamic region) and from depths comparable to MIS 5e marine terrace record were included in the Northern Panamic species pool. The Northern Panamic region faunal database contains 355 bivalve species.

4.3.3 Contemporary species geographic distributions

Modern geographic distributions along the Pacific mainland coast and Golfo de California (eastern and western coasts, respectively) were gathered from scientific monographs and databases (Appendix VII). I collected occurrence data for eight major offshore Pacific islands with faunal affinities to North and South America (Guadalupe, Rocas Alijos, Tres Marias, Revillagigedo, Clipperton Atoll, Coco, Malpelo, and Galapagos islands) from published faunal surveys, monographs, and scientific papers (Appendix VII). Two aspects of geographic range were extracted from these data: latitudinal range and oceanic island occupancy. I focus on these geographic measures because latitudinal range is the most robust measure of geographic distribution along the mainland Pacific coast (which is primarily north-south trending) and the number of oceanic islands occupied is a measure of establishment success in offshore coastal habitats. Latitudinal range was taken as the maximum minus the minimum latitude at which each

species has been recorded. Oceanic island occupancy is taken as the number of major offshore island elements a species is known to occur on (see list above).

4.3.4 Contemporary species environmental distributions

To compute present-day environmental ranges, I assembled annual and seasonal (maximum and minimum average monthly) chlorophyll α concentration (a proxy for primary productivity) and sea surface temperature (SST) from Giovanni version 4.17.2 using the MODIS Aqua 4 km grid cell resolution data from 2003-2015 (Acker and Leptoukh 2007). SST and productivity are focused on here because they are the most important environmental variables that structure shallow coastal oceans today and are readily quantifiable using global compilations (Belanger et al 2012, Fenberg et al 2015). Each quarter-degree grid cell was merged with the ETOPO1 Global Relief Model (Amante and Eakins 2009). Only coastal marine grid cells were included to be comparable to the coastal depths preserved within the marine terrace record.

Maximum and minimum annual and seasonal SST and productivity values were computed by averaging the upper and lower 10% of values observed throughout a species' entire geographic distribution. This "range-through" approach is limited in its accuracy because sufficient and reliable species occurrence data for shallow marine mollusks are not currently available. Thus, this approach relies on a simplifying assumption that species range throughout their geographic ranges along the major coastlines of the eastern Pacific (see also Belanger et al 2013) in shallow marine habitats. This assumption is likely to introduce some distortion for species with patchy geographic distributions or specialized habitats. To address this potential inaccuracy, I also compute present-day "range-limiting" environmental conditions by taking the minimum SST and maximum and minimum productivity conditions observed at a species' most environmentally extreme geographic range endpoint; this endpoint could be on an oceanic island, within the Gulfo de California, or along the Pacific maincoast, depending on which of these endpoints had the most extreme temperature and productivity conditions, respectively. For instance, if a species ranges from Cabo San Lucas to Cedros Island, with Cedros Island representing the cooler of the two range endpoints, then the average annual and seasonal temperatures observed at Cedros Island were taken as the species' range-limiting temperature. This method holds promise in comparison to range-through calculations because it relies on the known occurrences of species at its biogeographic, and presumably, environmental extremes.

4.3.5 Statistical Analyses

The relative importance of oceanic island occupancy, latitudinal range, chlorophyll α concentration, and SST distributions (predictor variables) for MIS 5e extralimital status (response variable) was assessed using multiple logistic regressions as implemented in base R (R CoreTeam 2019). Two sets of multiple logistic regressions were run: one that contained combinations of geographic and range-through environmental conditions, and another that contained combinations of geographic and range-limiting environmental conditions. Collinear variables ($R^2 > 0.5$) were identified using the `corr.test` function as implemented in the 'psych' R

package (R CoreTeam 2019; Revelle 2017) and are provided in Table 4.2. Support for models with all non-collinear combinations of predictor variables were assessed using a stepwise (both forwards and backwards) regression framework ('MASS' R package). Relative model support was assessed using the comparison of sample size corrected Akaike Information Criteria (AICc values) as implemented in the 'AICcmodavg' R package (Mazerolle 2017; R CoreTeam 2019). Both unstandardized (Beta) and standardized (beta) coefficients were computed for the best-supported model using the multiple logistic regression framework in base R and the 'beta' function as implemented in the 'reghelper' R package for unstandardized and standardized coefficients, respectively. Predictions based on the best-supported multiple logistic regression model were obtained using the 'predict.glm' function as implemented in base R; these were used to qualitatively assess model performance and to cast baseline predictions for all Northern Panamic bivalve species.

4.4 Results

4.4.1 MIS 5e extralimital occurrences

Twenty-two species found as fossils in our MIS 5e database ($n = 142$) have southern extralimital ranges, i.e. they no longer exist in the California region and today occur exclusively to the south. Our MIS 5e dataset contains only one northern extralimital species (*Patinopecten caurinus*; from Kanakoff and Emerson 1959's 66-2 fossil locality), which is a robustly-shelled temperate-water species that is common in older fossil deposits in California but is not found in any other MIS 5e fossil deposits included herein. This ~15.5% species turnover between MIS 5e and present-day California region is comparable to previous faunal turnover estimates (~12%) for the marine terrace record over the Late Pleistocene (Roy et al 1995). Seventeen out of twenty-one southern MIS 5e extralimitals species in our dataset are found within paleo-bay fossil localities (in some San Pedro [Muhs and Groves 2018], Newport Beach [Kanakoff and Emerson 1959; Powell et al 2004], and Carmel Valley [Kern 1971] localities); the difference between paleo-bay ($n = 9$) vs. paleo open coast ($n = 13$) fossil localities in terms of extralimital occurrences is marked ($G = 16.27$; Table 4.1) and significant ($p < 0.001$; Table 4.1).

4.4.2 Extralimital characteristics

Of 21 pairwise-comparisons of environmental and geographic distribution predictor variables, I find that most SST predictor-pairs are correlated (Table 4.2); these pairs were thus excluded from multiple regression models and assessed separately. Models containing range-limiting environmental condition predictors (Table 4.3) are better supported than models containing range-through environmental conditions (Table 4.4). Both range-through and range-limiting models are qualitatively comparable in their ranking of each predictor variable's relative importance: overall, models containing annual SST perform better than winter and summer SST and all show the expected negative relationship (i.e., cooler temperatures differentiate extralimitals; Tables 4.3 and 4.4); seasonal minimum and maximum chlorophyll α concentrations

also show their expected positive relationships (i.e. higher chlorophyll α concentrations differentiate extralimitals), with minimum performing better than maximum chlorophyll α concentrations (Tables 4.3 and 4.4). Of the geographic predictors, latitudinal range shows no predictive value but the number of oceanic islands is well-supported, with extralimitals tending to occur on more oceanic islands compared to their conterminous fauna (Tables 4.2 and 4.4).

Both forward and backward regressions prefer models containing annual SST, minimum chlorophyll α concentration, and number of oceanic islands occupied (Table 4.5). Range-limiting annual SST most strongly differentiates MIS 5e extralimitals from their conterminous Northern Panamic fauna ($\beta = -1.43$ [Table 4.5; Figure 4.2]), followed by number of oceanic islands occupied ($\beta = 0.62$ [Table 4.5; Figure 4.2]), and minimum chlorophyll α ($\beta = 0.45$ [Table 4.5; Figure 4.2]); maximum chlorophyll α concentration is also marginally supported ($\beta = 0.27$; $p = 0.13$). Model predictions from the best-supported model (Figure 4.5) show the relative performance of the model in discriminating extralimital species from their conterminous Northern Panamic fauna and also highlights the species that are most similar to MIS 5e extralimital species (Figure 4.5).

4.5 Discussion

4.5.1 Regional climate implications of MIS 5e extralimital occurrences

The preponderance of southern extralimital species in the MIS 5e record of southern California (15%, $n = 142$; Appendix VI) may support the commonly held inference that global warming during MIS 5e resulted in warmer-than-present conditions within coastal Californian marine environments (Muhs et al 2002, 2012, 2014). However, these findings are also consistent with an alternative MIS 5e climate scenario, referred to as the “Bakun hypothesis,” that is consistent with the stable isotope paleo-thermometry presented herein (Chapter II; Figures 4.4 and 4.8) and has mixed support in some recent oceanographic models (Sydean et al 2014; Wang et al 2015). The “Bakun” scenario posits that warm continental temperatures intensified Ekman transport and coastal upwelling during MIS 5e, thus creating relatively cool conditions within exposed outer coast environments, but warmer-than-present conditions within protected embayments, which are sheltered from cool upwelling currents (Bakun 1990; Bakun et al 2015). This regional climate scenario is further bolstered by the notable pattern of MIS 5e southern extralimital occurrences (Table 4.1): 18 of 20 southern extralimital species in the confidently-dated MIS 5e database were found within protected paleo-embayment environments (in some San Pedro localities [Muhs and Groves 2018], Newport Beach [Kanakoff and Emerson 1959; Powell et al 2004], and Carmel Valley [Kern 1971] localities), thus suggesting that outer-coast sea surface temperatures were quite similar to today even while protected environments were warmer.

4.5.2 Study limitations and considerations

Range-through vs. range-limiting environmental ranges: A limitation of my present study is that sufficient and reliable species occurrence data for shallow marine bivalves is not available, which disables the construction of environmental niches from site-specific occurrences. Thus, I employ two methods to construct environmental ranges. The first, so-called “range-through” method (see also Belanger et al 2012) assumes that species range throughout their geographic ranges along the major coastlines of the eastern Pacific (see also Belanger et al 2013) in shallow marine habitats. This assumption is likely to introduce distortions for species with specific substrate preferences or with other specialized habitats. However, by assuming that species occur in all shallow coastal areas of their geographic range, the range-through assumption would overestimate environmental ranges for all species, thus biasing our results in a consistent manner across species. The second method, here referred to as “range-limiting,” constructs environmental ranges by analyzing the environmental characteristics of species only at their range endpoints. This method has the strength of relying exclusively on site-specific occurrences (i.e. by definition, species have verified occurrences at their range endpoints) but makes the assumption that range endpoints represent the extremes of a species’ environmental niche. For rare species that are not commonly collected or reported, this range-limiting method may underestimate environmental niches.

My analyses, which show stronger support for environmental ranges using range-limiting rather than range-through environmental conditions (Tables 4.3, 4.4, and 4.5), suggest that the range-through approach may obfuscate important distinctions by overestimating ranges. However, both range-through and range-limiting approaches are qualitatively similar, and rank the importance of environmental condition predictors similarly (Tables 4.3, 4.4, and 4.5). Hence, these findings appear to support the use of both approaches, although a goal of future work should be to test these findings when more robust and widespread site-specific data become available for marine mollusks.

Applying contemporary environmental ranges to understand MIS 5e environmental conditions: A further assumption of the present study is that contemporary environmental ranges of extralimital species can be used to make inferences about the climatic and consequent biogeographical dynamics of MIS 5e. There are two ways that this assumption could be misleading. First, if environmental conditions experienced in the Californian region during MIS 5e were drastically different from modern conditions, i.e. “no-analog”, then our analysis may be irrelevant for understanding MIS 5e range shifts (Jackson and Overpeck 2000; Williams and Jackson 2007). This concern is unlikely to strongly affect my conclusions because the core faunal composition of the Californian region today does not differ substantively from that of MIS 5e, thereby ruling out the probability of drastically different MIS 5e environmental conditions in the Californian region (75% faunal similarity between MIS 5e and today; Valentine 1989; Valentine and Jablonski 1996). Further, paleo-thermometry reconstructions on several of the sites analyzed herein (LACMIP localities SNI-128, SNI-302, SNI-205, 11749, and 12608) reconstruct temperatures similar to at present for exposed outer coast habitats during MIS 5e (Chapter II and Chapter III; Figures 2.1, 2.5, 3.5, and 3.7).

A second consideration with respect to drawing inferences about MIS 5e from contemporary environmental range data is that if environmental niches have evolved considerably since MIS 5e then using modern ranges to understand fossil distributions may be untenable. While investigating the stability of environmental niches over geological timescales is an area of much recent research (Pearman et al 2008; Nogués-Bravo 2009; Maguire et al 2015; Lieberman and Saupe 2016; Qiao et al 2016; Waterson et al 2017), most studies generally agree that environmental niches are relatively stable over Milankovitch scale cycles (Martinez-Meyer and Peterson 2006; Pearman et al 2008; Saupe et al 2014, 2015) although realized environmental niches may shift through time (Veloz et al 2012). These emerging findings, combined with the results presented here in Chapter III that all species occurrences found within 12 Early-Late Pleistocene marine terraces in southern California lived in paleo-temperature conditions well within their contemporary thermal ranges (Figures 3.4, 3.5, 3.6, 3.7, and 3.8), overwhelmingly support the use of contemporary environmental ranges to help infer the climatic and biogeographic dynamics of the past, at least on Holocene and Pleistocene timescales.

MIS 5e and MIS 5c marine terrace time-averaging: A final consideration of the present study is that although all localities studied herein are confidently dated to MIS 5e, many of these localities occur on marine terrace surfaces that show evidence of substantial temporal mixing at nearby sites due to terrace re-occupation at a subsequent sea-level highstand during the Marine Isotope Substage 5c (~105,000 years ago; Muhs et al 2002, Muhs et al 2012; Muhs et al 2014). One interpretation for this phenomenon is that complexities in local geomorphology and coastal uplift (partly the consequence of glacial isostatic adjustment; Muhs et al 2014; Muhs et al 2014; Simms et al 2015) expose some, even nearby, parts of marine terrace surfaces during terrace re-occupation but not others. While it is outside our present scope to test this idea, I note that complications arising from terrace re-occupation are unlikely to substantially distort my findings because faunal (Muhs et al 2002, Muhs et al 2012; Muhs et al 2014) and stable isotope paleothermometry (Chapter II; Figures 2.1 and 2.5) evidence indicates that the Marine Isotope Substage 5c was cooler than present-day, while MIS 5e appears to have been both thermally similar or warmer than at present, depending on paleo-habitat (again, with paleo-embayments appearing to have been warmer than open-coast habitats; Chapter II and Chapter III). This conclusion is further supported because many fossil localities that show substantial evidence of terrace reoccupation during MIS 5c contain a mixture of northern and southern extralimital species (see discussions in Muhs et al 2012; Muhs et al 2014). Long termed “thermally disjunct” assemblages (Woodring 1951; Valentine 1958, 1973; Valentine and Emerson 1961; Lindberg and Lipps 1993), the current and well-supported interpretation for these paleontological curiosities is that southern extralimital fossil occurrences were deposited during MIS 5e when warmer conditions facilitated tropical invasions and northern extralimital fossil occurrences were deposited during the 5c when cooler waters facilitated temperate invasions (e.g., Muhs et al 2002, Muhs et al 2012; Muhs et al 2014). Given that I find a preponderance of southern extralimital species in our MIS 5e dated fossil localities, I can thus confidently assume that the great majority of extralimital species analyzed herein are indeed from MIS 5e.

4.5.3 Environmental and geographic characteristics of MIS 5e extralimitals

Geographic predictors of MIS 5e extralimitals: Latitudinal range, which has been previously shown to non-randomly characterize southern Pleistocene extralimital species (Roy et al 1995), is not a meaningful predictor of MIS 5e extralimitals. But when the partially correlated (R^2 's range from 0.77-0.03 for pairwise correlations; Table 4.2) characteristics of environmental conditions are taken into account they emerge as the more powerful predictors (Tables 4.3, 4.4, and 4.5). The contrast between the present study and Roy et al 1995 may be due to a difference in how the conterminous faunal species pools were drawn: the study herein defines the conterminous fauna conservatively, and concentrates only on species that range into the Pacific coast of the southern Baja California Sur or the Gulf of California, whereas Roy et al 1995 defines the conterminous fauna as the entire Panamic region (Pacific coast of Baja California and Gulf of California to Peru). The difference between these two species pools would drive a difference in the relative importance of latitudinal range because many Panamic species are tropical insular and endemic species, whereas the Northern Panamic region contains mainly subtropical-tropical spanning species with relatively wide latitudinal ranges. Thus, because species with extralimital occurrences in southern California are overwhelmingly drawn from the adjacent shores of the Northern Panamic region rather than geographically disjunct Panamic shores (Appendix IV; Roy et al 1995) and hence, are characterized by having wide latitudinal ranges, extralimital species' wide latitudinal ranges would stand in contrast to the many endemic and insular species of the Panamic region.

In contrast to the unimportance of latitudinal range, I find that MIS 5e extralimital species have more occurrences on offshore oceanic islands compared to conterminous Northern Panamic region species (Tables 4.3 and 4.4; Figure 4.2). More numerous oceanic island occurrences in marine mollusks are strongly related to ecological traits such as long-lived planktonic larvae, rafting adult habitats (i.e., some wood-boring or kelp-inhabiting taxa), and generalist feeding ecologies (e.g., Hansen 1980; Jablonski 1986; Lester et al 2007) that influence larval and adult dispersal. Thus, the significance of this measure of wide geographic range, even while accounting for environmental ranges, points to key roles for ecological attributes influencing dispersal potential in facilitating climate-tracking and consequent species invasions (see also Lindberg and Lipps 1996 and Dobrowski et al 2011 for a related conclusions).

Environmental predictors of MIS 5e extralimitals: I find that cooler annual SST minima and more productive chlorophyll α concentration minima (and to a lesser extent, maxima) distinguish MIS 5e extralimitals from their conterminous fauna (Tables 4.3, 4.4, and 4.5; Figure 4.2). Low annual SSTs, in particular, most strongly improve regression model relative support (Tables 4.3, 4.4, and 4.5). The importance of annual SST and chlorophyll α concentration minima strongly suggest that MIS 5e extralimital species have an affinity or tolerance for relatively productive habitats and cool temperatures —both of which characterize the California region's environmental conditions (Belanger et al 2012; Fenberg et al 2015). The relative importance of

annual SST over seasonal SSTs (Tables 4.3 and 4.4) further points to an affinity to California-type climates because California is a relatively aseasonal climate in terms of temperature: in the Gulf of California, winter and summer temperatures average 16°C and 25°C, respectively, whereas in southern California winter and summer temperatures average 14°C and 19°C, respectively (Figures 1.4 and 1.5; NOAA World Ocean Atlas 2018). Thus, southern MIS 5e extralimitals show evidence of having thermal and environmental niches whose limits are quite similar to conditions experienced in the Californian region. I posit that as the contemporary Californian region climate continues to warm, these species will have a higher likelihood of successful establishment compared to their conterminous faunas because even small (~1°C) increases in temperature may allow them to track their thermal ranges back into the Californian region to re-establish their MIS 5e ranges; the findings of remarkably stable thermal niche tracking over fluctuating Pleistocene climate states presented in Chapter III herein further bolster this hypothesis.

4.5.4 A pre-anthropogenic baseline for contemporary warming

Globally, MIS 5e was a period of climatic warming — with the warmest temperatures of the last 300,000 years (Lisiecki and Raymo 2005). Thus, analysis of extralimitals during MIS 5e can serve as a pre-anthropogenic analog to make predictions for contemporary climate-change-driven (re)invasions into southern California. My analysis of MIS 5e extralimitals supports the dual importance of both environmental niches *and* life history attributes influencing dispersal, thus implying that both characteristics play complementary roles in determining which species responded to MIS 5e pre-anthropogenic warming by successfully tracking their niches into the Californian region. Modeled probabilities based on the best-supported regression predictors underscore the overall good model support and highlight several species with geographic and environmental characteristics similar to extralimital MIS 5e species that we may expect to imminently invade the Californian region if MIS 5e warming mirrors contemporary anthropogenic warming (Figure 4.3).

4.6 Conclusions

The MIS 5e bivalve fauna of southern California is characterized by the presence of southern extralimital species (15%), the majority of which occurred in paleo-embayment, rather than paleo-open coast settings (18 of 20; Table 4.1). Thus, MIS 5e appears to have coincided with warmer-than-at-present conditions within southern California's paleo-embayments, but similar conditions relative to today along the open-coast habitats. Extralimital bivalves differ from their conterminous fauna: extralimitals are distinguished by having more numerous offshore island occurrences, and cooler, more seasonally productive, environmental minima (Figure 4.2). These findings suggest that southern extralimitals that occupied the California region during MIS 5e have life history traits that enable high dispersal rates and environmental niches that include affinities to conditions quite similar to the California's more temperate habitats. Thus, MIS 5e

extralimitals, and non-extralimitals with similar characteristics (Figure 4.2; Appendix VII), may be more likely to (re)invade the California coast as the contemporary climate continues to warm.

Chapter IV Figures

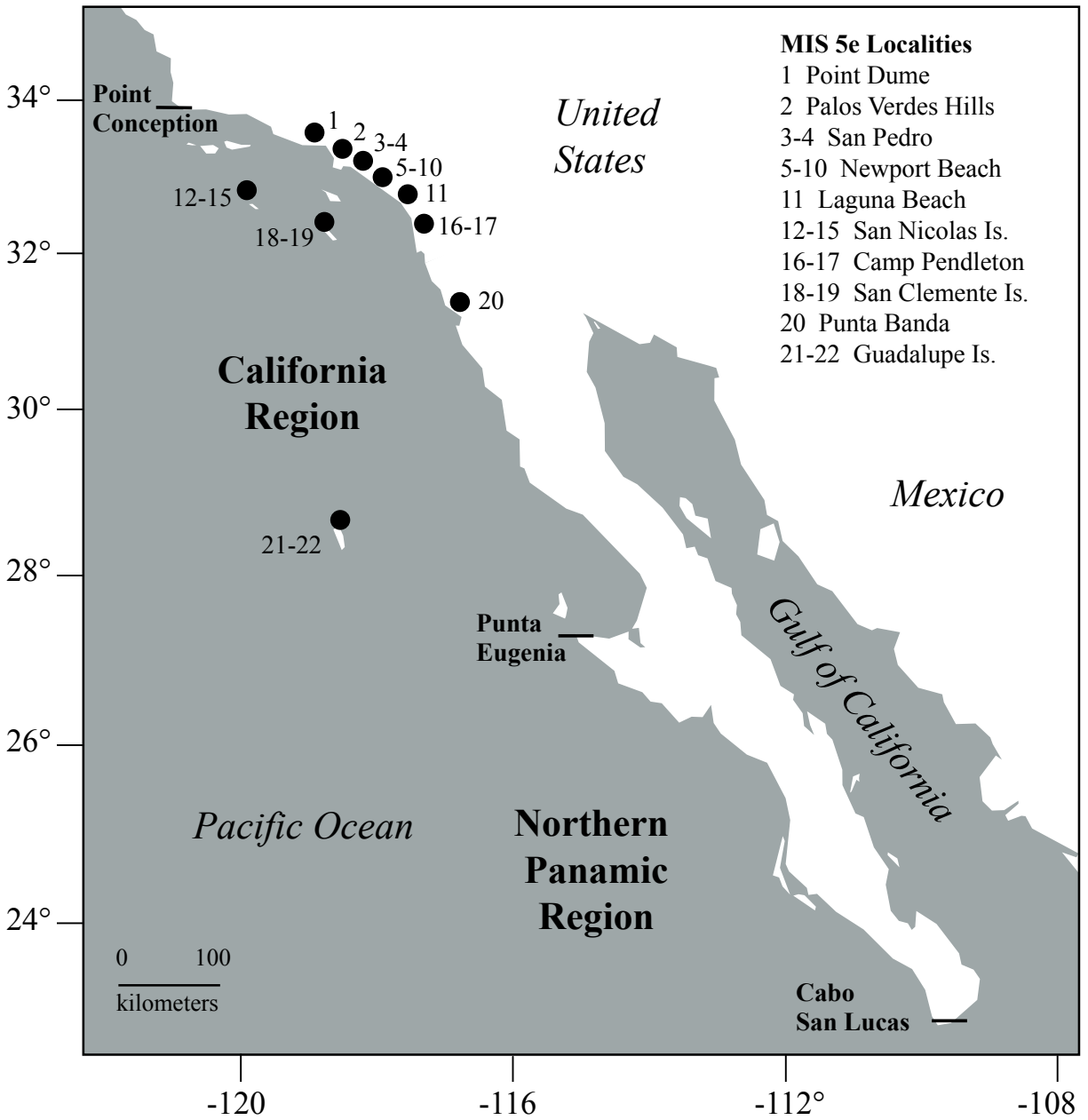


Figure 4.1: California & Northern Panamic region map with MIS 5e fossil localities. Paleoembayments indicated with asterisks.

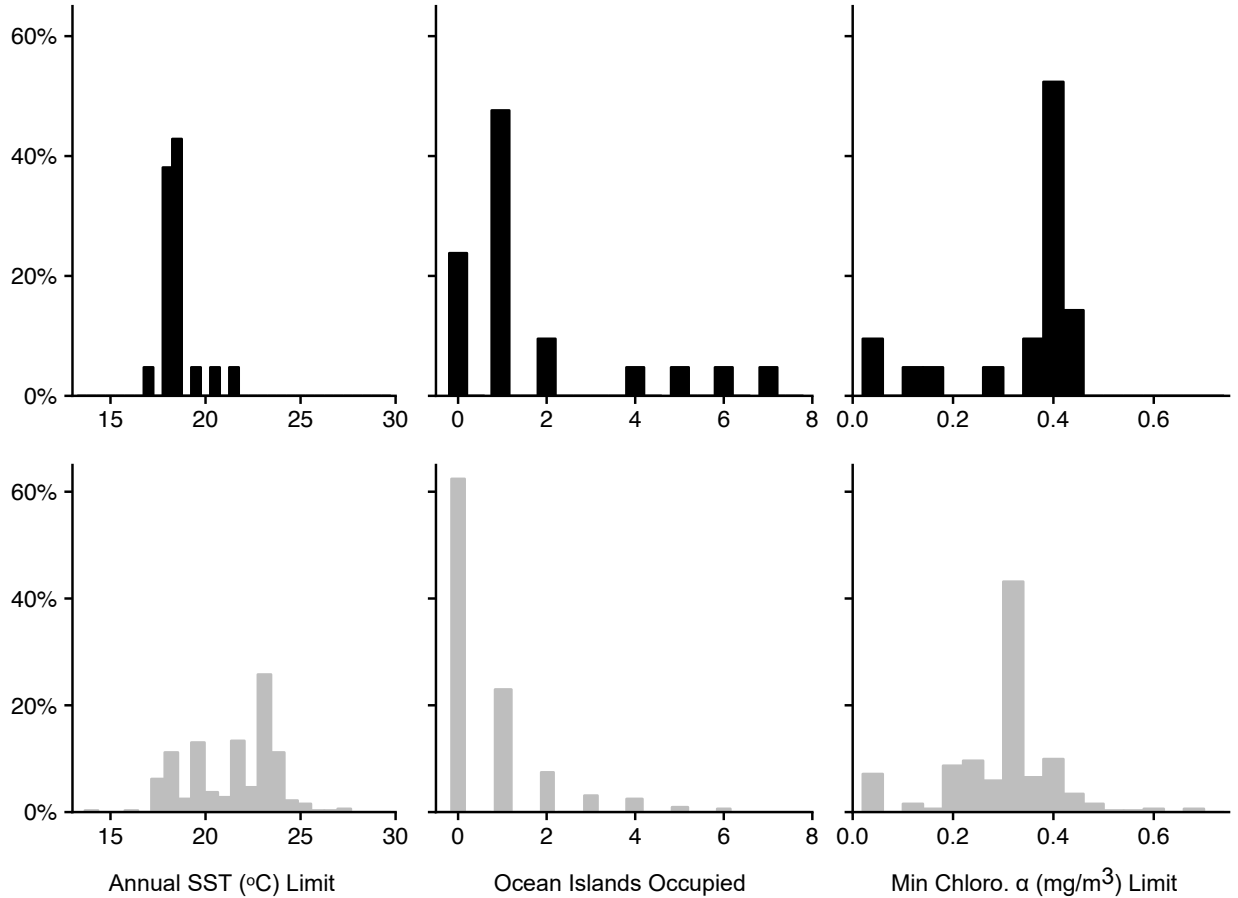


Figure 4.2: Best-supported MIS 5e extralimital model predictor frequency distributions.

Frequency distributions of Last Interglacial invasive species (top; n=20) compared to frequency distributions of Northern Panamic region species pool (bottom; n=130) for the three predictors included in the best-supported MIS 5e extralimital model: range-limiting minimum annual temperature (left), number of oceanic islands occupied (center), and range-limiting minimum chlorophyll α concentration (right).

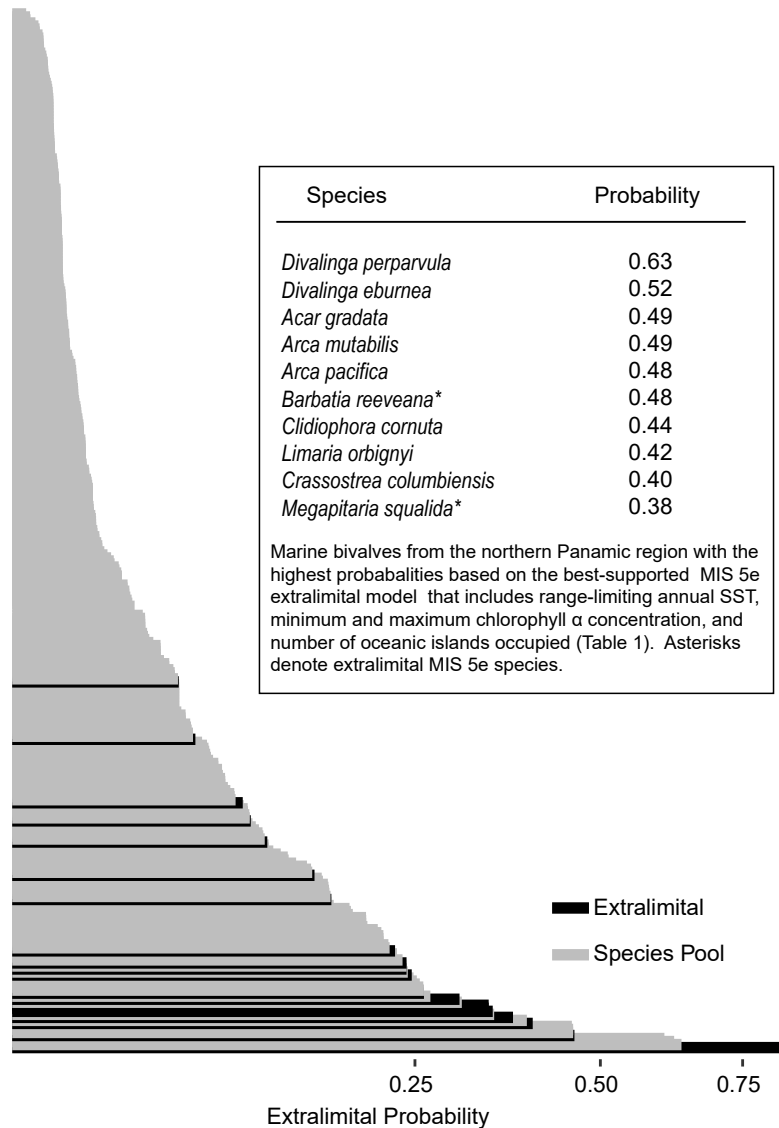


Figure 4.3: Best-supported MIS 5e extralimital model species probabilities. Probabilities calculated using the best-supported MIS 5e extralimital regression model (model predictors = range-limiting minimum annual temperature and minimum chlorophyll α concentration as well as number of oceanic islands occupied). Black distinguishes MIS 5e extralimital species from the Northern Panamic region species pool (grey). Inset: Species with the top ten highest modeled probabilities. Asterisks indicate MIS 5e extralimital species; full model results are listed in Appendix VII.

Chapter IV Tables

Locality paleo-coast type	Observed extralimital presence	Expected extralimital presence	<i>G</i>	<i>p</i>
Open coast	23% (3/13)	54% (7/13)	16.27	<.0001
Protected coast	100% (9/9)	55% (5/9)		

Table 4.1: Paleo-protected vs. paleo-open coast MIS 5e extralimital occurrences. *G*-test results for extralimital presence v. absence at paleo-protected (n = 9) and paleo-open coast (n = 13) MIS 5e localities. *G*: G-test statistic.

		Annual SST	# islands	Lat Range	Winter SST	Summer SST	Max chloro
Range-limiting	Annual SST						
	# islands	-0.25					
	Lat Range	-0.41	0.15				
	Winter SST	0.52	-0.14	-0.34			
	Summer SST	0.88	-0.24	-0.57	0.34		
	Max chloro	-0.22	0.02	0.1	-0.13	-0.1	
	Min chloro	-0.16	-0.44	0.22	-0.06	-0.16	0.12
		Annual SST	# islands	Lat Range	Winter SST	Summer SST	Max chloro
Range-through	Annual SST						
	# islands	-0.14					
	Lat Range	-0.47	0.18				
	Winter SST	0.62	-0.1	-0.34			
	Summer SST	0.73	-0.11	-0.77	0.24		
	Max chloro	-0.32	0.1	0.46	-0.23	-0.32	
	Min chloro	-0.06	-0.6	-0.03	-0.02	-0.04	0.04

Table 4.2: Environmental and geographic predictors correlation matrix. Pairs with statistically significant (i.e. $p < 0.05$) correlations that are greater than $|0.5|$ are shown in bold; these pairs were excluded from regression analyses.

Max Chloro.	Min Chloro.	Lat. Range	# Islands	Annual SST	Summer SST	Winter SST	df	logLik	AICc	delta AICc	weight
0.08	4.27		0.51	-0.61			5	-55.55	121.3	0	0.092
0.08	4.31		0.52		-0.44	-0.48	6	-54.71	121.7	0.4	0.075
0.09	4.41		0.53		-0.56		5	-55.82	121.8	0.54	0.07
	4.61		0.51	-0.64			4	-56.97	122.1	0.79	0.062
	4.66		0.52		-0.44	-0.60	5	-55.95	122.1	0.8	0.061
0.08			0.29	-0.69			4	-57.11	122.3	1.06	0.054
0.08			0.29		-0.50	-0.53	5	-56.17	122.5	1.25	0.049
0.11			0.31		-0.64		4	-57.48	123.1	1.81	0.037
0.08	4.48	-0.03	0.52		-0.48	-0.61	7	-54.39	123.1	1.85	0.036
0.08	4.29	-0.01	0.51	-0.63			6	-55.53	123.3	2.05	0.033
	4.90		0.54		-0.58		4	-57.67	123.5	2.18	0.031
			0.27		-0.51	-0.68	4	-57.7	123.5	2.26	0.03
			0.27	-0.73			3	-58.89	123.8	2.58	0.025
0.10	4.42	0.00	0.53		-0.57		6	-55.81	123.9	2.6	0.025
	4.77	-0.02	0.52		-0.46	-0.68	6	-55.82	123.9	2.62	0.025
0.08				-0.75			3	-59	124.1	2.81	0.023
	4.58	0.01	0.51	-0.62			5	-56.95	124.1	2.81	0.022
0.09		-0.02	0.29		-0.53	-0.61	6	-55.98	124.2	2.94	0.021
0.08					-0.54	-0.54	4	-58.09	124.3	3.03	0.02
0.08		0.00	0.29	-0.69			5	-57.11	124.4	3.12	0.019
					-0.55	-0.67	3	-59.42	124.9	3.63	0.015
				-0.78			2	-60.55	125.1	3.87	0.013
0.11		0.00	0.31		-0.63		5	-57.48	125.1	3.87	0.013
0.10					-0.68		3	-59.59	125.2	3.97	0.013

Table 4.3: AICc model comparisons for range-limiting regression models. AICc model comparisons for regression models (with delta AICc < 4) that include all combinations of non-correlated predictors from a global model containing latitudinal range, oceanic islands occupied, and range-limiting chlorophyll α concentration (seasonal max and minimum) and sea surface temperature (annual, January, and August) conditions. Beta (unstandardized) coefficients are shown for each predictor.

Annual SST	Lat Range	Max Chloro.	Min Chloro	# Islands	Summer SST	Winter SST	df	logLik	AICc	delta AICc	weight
-0.36			12.61	0.70			4	-64.60	137.3	0	0.23
-0.39				0.43			3	-66.37	138.8	1.51	0.11
-0.31	0.02		12.58	0.69			5	-64.41	139	1.69	0.10
-0.33		0.02	12.6	0.70			5	-64.53	139.2	1.92	0.09
-0.35	0.02			0.43			4	-66.17	140.5	3.15	0.05
-0.36		0.02		0.44			4	-66.28	140.7	3.36	0.04
	0.04		13.93	0.72		-0.34	5	-65.27	140.7	3.4	0.04
			13.52	0.73	-0.14	-0.36	5	-65.27	140.7	3.4	0.04
			14.42	0.75		-0.48	4	-66.31	140.7	3.41	0.04
-0.31	0.02	0.01	12.57	0.69			6	-64.41	141.1	3.75	0.04
		0.06	14.18	0.74		-0.37	5	-65.63	141.4	4.12	0.03

Table 4.4: AICc model comparisons for range-through regression models. AICc model support for regression models (with delta AICc < 4) including all combinations of non-correlated predictors from a global model of latitudinal range, oceanic islands occupied, and range-through chlorophyll α concentration (seasonal max and minimum) and sea surface temperature (annual, January, and August) conditions.

Model Type	Predictor	<i>beta</i> Coefficient	Standard Error	<i>z</i>	<i>p</i>
Range- Limiting Env. Conditions	Annual SST	-1.4253	0.4149	-3.436	0.000591
	# Islands Occupied	0.622	0.2401	2.591	0.009572
	Min Chloro α	0.451	0.2581	1.748	0.080494
	Max Chloro α	0.2671	0.1776	1.504	0.132465
Range- through Env. Conditions	Annual SST	-0.714	0.2025	-3.526	0.000421
	# Islands Occupied	0.8384	0.2366	3.544	0.000394
	Min. Chloro α	0.535	0.3082	1.736	0.082566

Table 4.5: Parameter estimates for the best-supported logistic regression models. Parameter estimates for the best-supported logistic regression models including range-limiting and range-through environmental conditions, respectively. Standardized *beta* coefficients shown. See Table 4.3 for comparison of models containing range-limiting environmental predictors and Table 4.4 for comparison of range-through environmental predictor models.

Chapter V

Lessons from the Pleistocene and predictions for the present

The geological axiom that "the present is the key to the past" has formed the basic assumption of paleoecology for the last century, but more recently, the field has asked: will the past be the key to the present? In answering this question, the Pleistocene has the power of geological youth: its major geomorphological features (e.g., mountains and island chains) are similar and its species are largely extant in contemporary coastal California (Valentine 1989b). This geological similarity allows paleoecologists to make specific predictions based on Pleistocene dynamics. Here, I synthesize my findings from the Pleistocene to offer three predictions for the present.

In Chapter II, I reconstructed paleo-temperatures during several late Pleistocene climates, including MIS 5e — which was, globally, the warmest climate state of the last 300,000 years (Lisiecki and Raymo 2005). My reconstructions of several MIS 5e open-coast habitats suggest that temperatures were similar to at present, and that upwelling may have been enhanced. These results imply that MIS 5e warming may have driven a large land-sea difference, thus causing open-coast habitats to experience strong upwelling and cooler temperatures than nearby land and embayment settings (Bakun 1990). This interpretation aligns with my finding in Chapter IV that most warm-water extralimitals lived in embayments during MIS 5e. Taken together, these results underlie my first prediction for the present: regional warming may coincide with stronger upwelling and cooler open coasts, alongside warmer paleo-embayments, in southern California.

In Chapter III, I found unanimous evidence that coastal marine mollusks have tracked stable niches over Early Pleistocene-recent timescales. Thus, my second prediction is that coastal marine mollusks will respond to contemporary change by shifting their latitudinal ranges in accordance with thermal isobar shifts. In Chapter IV, I found that MIS 5e extralimitals are characterized by having affinities for cooler, more seasonally productive, habitats as well as apparently higher dispersal potential than their conterminous Northern Panamic fauna. Using these characteristics, I cast specific probabilities for coastal California species invasions (Figure 4.3); these probabilities form my third prediction for the present.

But, how accurately Pleistocene, and deeper-time, dynamics predict contemporary change is an open question (Jackson and Blois 2015; Nogués-Bravo et al 2018). Human impacts such as coastal habitat degradation, pollution, introduced species and diseases, as well as food web disruption, will invariably alter the pre-Anthropocene rules of regional change. My Pleistocene predictions are grounded in pre-human regional changes, and as such, I hold no expectation that they should be exactly replicated in response to anthropogenic global change. However, as the pace of contemporary climate change accelerates, the character of environments and accompanying species that accumulate along California's shore — within our lifetimes — will serve to test my paleontological predictions.

References

- Acker, J.G., and G. Leptoukh. 2007. Online analysis enhances use of NASA Earth science data. *Eos, Transactions of the American Geophysical Union* 88:14-17.
- Addicott, W.O. 1966. Late Pleistocene marine paleoecology and zoogeography in central California. U.S. Geological Survey Professional Paper 523-C.
- Affeck, H.P., and J.M. Eiler. 2006. Abundance of mass 47 CO₂ in urban air, car exhaust, and human breath. *Geochemica et Cosmochimica Acta* 70: 1-12.
- Amante, C., and B.W. Eakins. 2009. ETOPOI 1 Arc-minute global relief model: procedures, data sources, and analysis. National Oceanographic and Atmospheric Administration Technical Memorandum, National Environment Satellite, Data, and Information Service National Geophysical Data Center-24, Boulder, Colorado.
- Arnold R. 1903. The paleontology and stratigraphy of the marine Pliocene and Pleistocene of San Pedro, California. *Contributions to Biology from the Hopkins Seaside Laboratory* 3.
- Bakun, A. 1990. Global climate change and intensification of coastal ocean upwelling. *Science* 247:198–201.
- Bakun, A., B.A. Black, S.J. Bograd, M. García-Reyes, A.J. Miller, R.R. Rykaczewski, and W.J. Sydeman. 2015. Anticipated effects of climate change on coastal upwelling ecosystems. *Current Climate Change Reports* 1:85–93.
- Barrick, R.E., A.E. Beveridge, R.T. Patterson, and J.K. Schubert. 1989. Reexamination of the benthic foraminiferal fauna from a Late Pleistocene marine terrace deposit near Goleta, California. *Journal of Paleontology* 63: 261-267.
- Barry, J.P., C.H. Baxter, R.D. Sagarin, and S.E. Gilman. 1995. Climate-Related, Long-Term Faunal Changes in a California Rocky Intertidal Community. *Science* 267: 672-675.
- Belanger, C.L. 2004. Preliminary environmental assessment of a Pleistocene marine deposit near Isla Vista, California. Unpublished fieldtrip guide for the Friends of the Pleistocene organized by L.D. Gurrola and E.A. Keller.
- Belanger, C.L., D. Jablonski, K. Roy, S.K. Berke, A.Z. Krug, and J.W. Valentine. 2012. Global environmental predictors of benthic marine biogeographic structure. *Proceedings of the National Academy of Sciences* 109:14046–14051.

- Burman, J., O. Gustafsson, M. Segl, and B. Schmitz, 2005, A simplified method of preparing phosphoric acid for stable isotope analyses of carbonates. *Mass Spectrometry* 19: 3086-3088.
- Coan, E.V., P.V. Scott and F.R. Bernard. 2000. Bivalve seashells of western North America. *Santa Barbara Museum of Natural History Monographs* 1-764 pp. Santa Barbara Museum of Natural History: Santa Barbara, CA.
- Coan, E.V. and P. Valentich-Scott. 2012. Bivalve seashells of tropical west America *Santa Barbara Museum of Natural History Monographs* 1-1258 pp. Santa Barbara Museum of Natural History: Santa Barbara, CA.
- Conrad, T. A. 1855. Report on the fossil shells collected in California by Wm. P. Blake, geologist of the expedition under the command of Lieutenant R. S. Williamson, United States Topographical Engineers. Appendix to the preliminary geological report of William P. Blake, Explorations and surveys for a railroad route from the Mississippi river to the Pacific Ocean, New York.
- Crickmay, C.H. 1929. The anomalous stratigraphy of Deadman's Island, California. *The Journal of Geology* 37: 617-638.
- Dall, W.H. 1921. Summary of the shell-bearing molluscs of the northwest coast of America, from San Diego, California to the Polar Sea. *United States National Museum Bulletin* 112: 1-217.
- Dincauze, D.F. 1987. Strategies for paleoenvironmental reconstruction in archaeology. *Advances in Archaeological Method and Theory* 11: 255-336.
- Dobrowski, S.Z., J.H. Thorne, J.A. Greenberg, H.D. Safford, A.R. Mynsberge, S.M. Crimmins, and A.K. Swanson. 2011. Modeling plant ranges over 75 years of climate change in California, USA: temporal transferability and species traits. *Ecological Monographs* 81:241–257.
- Dodd, J.R. 1966. The Influence of Salinity on Mollusk Shell Mineralogy: A Discussion. *Journal of Geology* 74: 85-89.
- Edwards, D.C. 1968. Reproduction in *Olivella biplicata*. *The Veliger* 10: 297-304.
- .1969a. Predators on *Olivella biplicata*, including a species-specific predator avoidance response. *The Veliger* 10: 326-333.

- .1969b. Zonation by size as an adaptation for intertidal life in *Olivella biplicata*. *American Zoologist* 9: 399-417.
- Eiler, J.M. 2007. "Clumped-isotope" geochemistry — the study of naturally-occurring, multiply-substituted isotopologues. *Earth and Planetary Science Letters* 262: 309-327.
- .2011. Paleoclimate reconstruction using carbonate clumped isotope thermometry. *Quaternary Science Reviews* 30: 3575-3588.
- Emerson, W.K. 1956a. Pleistocene invertebrates from Punta China, Baja California, Mexico. *Bulletin of the American Museum of Natural History* 111: 317-342.
- .1956b. Upwelling and associated marine life along Pacific Baja California, Mexico. *Journal of Paleontology* 30: 393-397.
- Epstein, S, R. Buchsbaum, H.A. Lowenstam, H.C. Urey. 1953. Revised carbonate-water isotopic temperature scale. *Bulletin of the Geological Society of America* 64: 1315-1326.
- Fenberg, P.B., B.A. Menge, P.T. Raimondi, M.M. Rivandeneira, 2014. Biogeographic structure of the northeastern Pacific rocky intertidal: the role of upwelling and dispersal to drive patterns. *Ecography* 38:83-95.
- Flato, G., J. Marotzke, B. Abiodun, P. Braconnot, S.C. Chou, W. Collins, P. Cox, F. Driouech, S. Emori, V. Eyring, C. Forest, P. Gleckler, E. Guilyardi, C. Jakob, V. Kattsov, C. Reason, and M. Rummukainen. 2013: Evaluation of Climate Models. *in* Stocker, T.F., D. Qin, G.-K. Plattner, M. Tignor, S.K. Allen, J. Boschung, A. Nauels, Y. Xia, V. Bex and P.M. Midgley (Eds.). *Climate Change 2013: The Physical Science Basis. Contribution of Working Group I to the Fifth Assessment Report of the Intergovernmental Panel on Climate Change*. Cambridge University Press, Cambridge, United Kingdom and New York, NY, USA.
- Gat, J.R. 1996. Oxygen and hydrogen isotopes in the hydrologic cycle. *Annual Review of Earth and Planetary Sciences* 24: 225-262.
- Grant, IV, U.I., and H. Gale. 1931. Catalogue of the marine Pliocene and Pleistocene Mollusca of California and adjacent regions. San Diego Society Natural History Museum Memoirs 1-1036.
- Grantham, B.A., G.L. Eckert, and A.L. Shanks. 2003. Dispersal potential of marine invertebrates in diverse habitats. *Ecological Applications* 13:S108–S116.

- Ghosh, P., J. Adkins, H. Affek, B. Balta, W. Guo, E.A. Schauble, D. Schrag, and J.M. Eiler. 2006. *Geochemica et Cosmochimica Acta* 70: 1439-1456.
- Grossman, E.L., T.L. Ku. 1986. Carbon and oxygen isotopic fractionation in biogenic aragonite — temp effects. *Chemical Geology (Isotope Geoscience Section)* 59: 59-74.
- Grossman, E.L. 2012. Oxygen isotope stratigraphy. *in* E.M. Gradstein, J.G. Ogg, M. Schmitz, G. Ogg (Eds.), *The Geologic Time Scale 2012* pp. 195-220.
- Gurrola, L.D., E.A. Keller, J.H. Chen, L.A. Owen, and J.Q. Spencer. 2014. Tectonic geomorphology of marine terraces: Santa Barbara fold belt, California. *Geological Society of America Bulletin* 126: 219-233.
- Hall, C.A. Jr., 2002, Nearshore marine paleoclimatic regions, increasing zoogeographic provinciality, molluscan extinctions, and paleoshorelines, California: late Oligocene (27 Ma) to late Pliocene (2.5 Ma). *Geological Society of America Special Paper* 357.
- Hansen, T. 1980. Influence of larval dispersal and geographic distribution on species longevity in neogastropods. *Paleobiology* 6:193–207.
- Haywood, A.M., P.J. Valdes, T. Aze, N. Barlow, A. Burke, A.M. Dolan, A.S. von de Heydt, D.J. Hill, S.S.R. Jamieson, B.L. Otto-Bliesner, U. Salzmann, E. Saupe, and J. Voss. 2019. What can paleoclimate modelling do for you? *Earth Systems and Environment* 3: 1-18.
- Hellburg, M.E., P.B. Deborah, and K. Roy. 2001. Climate-driven range expansion and morphological evolution in a marine gastropod. *Science* 292: 1707-1710.
- Hendy, I.L., and J.P. Kennett. 2000. Stable isotope stratigraphy and paleoceanography of the last 170 K.Y.: Site 1014, Tanner Basin, California. *in* L.M. Koizumi, I. Richter, and T.C. Moore (Eds.) *Proceedings of the Ocean Drilling Program, Scientific Reports* 167: 129-140.
- Hickman, C.S., and J.H. Lipps. 1983. Foraminiferivory: selective ingestion of foraminifera and test alterations produced by the neogastropod *Olivella*. *Journal of Foraminiferal Research* 13: 108-114.
- Holland, S.M. 2013. Relaxation time and the problem of the Pleistocene. *Diversity* 5: 276-292.
- Holt, J., P. Hyder, M. Ashworth, J. Harle, H.T. Hewitt, H. Liu, A.L. New, S. Pickles, A. Porter, E. Popova, J.I. Allen, J. Siddorn, and R. Wood. 2017. Prospects for the representation of

- coastal and shelf seas in global ocean models. *Geoscientific Model Development* 10: 499-523.
- Hudson, J.D. and T.F. Anderson. 1989. Ocean temperatures and isotopic compositions through time. *Transactions of the Royal Society of Edinburgh: Earth Sciences* 80: 183-192.
- Jablonski, D. 1986. Larval ecology and macroevolution in marine invertebrates. *Bulletin of Marine Science* 39:565–597.
- Jablonski, D., and J.J. Sepkoski. 1996. Paleobiology, community ecology, and scales of ecological pattern. *Ecology* 77:1367–1378.
- Jackson, S.T., and J.T. Overpeck. 2000. Responses of plant populations and communities to environmental changes of the late Quaternary. *Paleobiology* 26:194–220.
- Jackson, S.T. and J.L. Blois. 2015. Community ecology in a changing environment: perspectives from the Quaternary. *Proceedings of the National Academy of Sciences* 112: 4915-4921.
- Johnson, R.G. 1960a. Environmental interpretation of Pleistocene species. *The Journal of Geology* 68: 575-576.
- .1960b. Models and methods for analysis of the mode of formation of fossil assemblages. *Geological Society of America Bulletin* 71: 1075-1086.
- .1962. Mode of formation of marine fossil assemblages of the Pleistocene Millerton Formation of California. *Geological Society of America Bulletin* 73: 113-130.
- .1965a. Temperature variation in the infaunal environment of a sand flat. *Limnology and Oceanography* 10: 114-120.
- .1965b. Pelecypod death assemblages in Tomales Bay, California. *Journal of Paleontology* 39: 80-85.
- .Johnson, R.G. 1967. Salinity of interstitial water in a sandy beach. *Limnology and Oceanography* 12: 1-7.
- Johnson, M.E. 1988. Why are ancient rocky shores so uncommon? *Journal of Geology* 96: 469-480.
- .1992. Ancient rocky shores: a brief history and annotated bibliography. *Journal of Coastal Research* 8: 797-812.

- Johnson, M.E., and L.K. Libbey. 1997. Global review of Upper Pleistocene (Substage 5e) rocky shores: tectonic segregation, substrate variation, and biological diversity. *Journal of Coastal Research* 13:297-307.
- Kanakoff, G. P., and W. K. Emerson. 1959. Late Pleistocene invertebrates of the Newport Bay area, California. *Los Angeles County Museum, Contributions in Science* 31:1-47.
- Keen, A.M. 1971. *Seashells of tropical west America*. Stanford University Press. Stanford, California.
- Kennedy, G.L. 1978. Pleistocene paleoecology, paleozoogeography, and geochronology of marine invertebrate faunas of the Pacific Northwest Coast (San Francisco Bay to Puget Sound). Unpublished Ph.D. dissertation. University of California at Davis. Davis, California.
- Kennedy, G.L., K.R. Lajoie, and J.F. Wehmiller. 1982. Aminostratigraphy and faunal correlations of late Quaternary marine terraces, Pacific Coast, USA. *Nature* 299: 545-547.
- Kennedy, G.L., J.F. Wehmiller, and T.K. Rockwell. Paleoecology and paleozoogeography of Late Pleistocene marine-terrace faunas of southwestern Santa Barbara County, California. *Quaternary Coasts of the United States: Marine and Lacustrine Systems, SEPM Special Publications* 48: 343-361.
- Kennet, J.P., and K. Venz. 1995. Late Quaternary climatically related planktonic foraminiferal assemblage changes: hole 893A, Santa Barbara Basin, California. *Proceedings of the Ocean Drilling Program, Scientific Results* 146: 281-291.
- Kidwell, S.M., and D.W.J. Bosence. 1991. Taphonomy and time-averaging of shelly marine faunas. in P.A. Allison, and D.E.G. Briggs (Eds). *Taphonomy: Releasing the Data Locked in the Fossil Record, Topics in Geobiology*. Plenum Press, New York.
- Kern, P. 1971. Paleoenvironmental analysis of a Late Pleistocene estuary in southern California. *Journal of Paleontology* 45:810-823.
- Killingley, J.S., and W.H. Berger. 1979. Stable isotopes in a mollusk shell: detection of upwelling events. *Science* 205: 186-188.
- Krinsley, D. 1960. Magnesium, strontium, and aragonite in the shells of certain littoral gastropods. *Journal of Paleontology* 34: 744-755.

- Lester, S.E., S.D. Gaines, and B.P. Kinlan. 2007. Reproduction on the edge: large-scale patterns of individual performance in a marine invertebrate. *Ecology* 88:2229–2239.
- Libbey, L.K., and M.E. Johnson. 1997. Upper Pleistocene rocky shores and intertidal biotas at Playa La Palmita (Baja California, Sur, Mexico). *Journal of Coastal Research* 13: 216–225.
- Lieberman, B.S., and E.E. Saupe. 2016. Palaeoniches get stitches: analyses of niches informing macroevolutionary theory. *Lethaia* 49:145–149.
- Lindberg, D.R., B. Roth, M.G. Kellogg, and C.L. Hubbs. 1980. Invertebrate megafossils of Pleistocene (Sangamon interglacial) age from Isla de Guadalupe, Baja California, Mexico. *in* D. M. Powers (Ed). *The California Islands: Proceedings of a Multidisciplinary Symposium*. Santa Barbara Museum of Natural History, Santa Barbara.
- Lindberg, D.R., J.H. Lipps. 1996. Reading the chronicle of Quaternary temperate rocky shore faunas. *in* D. Jablonski, D.H. Erwin, and J.H. Lipps (Eds). *Evolutionary Paleobiology*. University of Chicago Press, Chicago.
- Lipps, J.H. 1967. Age and environment of a marine terrace fauna, San Clemente Island, California. *The Veliger* 9: 388-398.
- Lipps, J.H., J.W. Valentine, and E. Mitchell. 1968. Pleistocene paleoecology and biostratigraphy, Santa Barbara Island, California. *Journal of Paleontology* 42: 291-307.
- Lisiecki, L.E., and M.E. Raymo. 2005. A Pliocene-Pleistocene stack of 57 globally distributed benthic $\delta^{18}\text{O}$ records: Pliocene-Pleistocene benthic stack. *Paleoceanography* 20:3-17.
- Locarnini, R.A., A.V. Mishonov, O.K. Baranova, T.P. Boyer, M.M. Zweng, H.E. Garcia, J.R. Reagan, D. Seidov, K. Weathers, C.R. Paver, and I. Smolyar, 2018. *World Ocean Atlas 2018, Volume 1: Temperature*. A. Mishonov Technical Ed. in preparation.
- Maguire, K.C., J.L. Blois, D. Nieto-Lugilde, M.C. Fitzpatrick, and J.D. Williams. 2015. Modeling species and community responses to past, present, and future episodes of climatic and ecological change. *Annual Review of Ecology, Evolution, and Systematics* 46: 343-368.
- Marincovich, L. 1976. Late Pleistocene molluscan faunas from upper terraces of the Palos Verdes Hills, California. *Natural History Museum of Los Angeles County, Contributions to Science* 281.

- Martinez-Meyer, E., E. Townsend, A.T. Peterson, and W.W. Hargrove. 2004. Ecological niches as stable distributional constraints on mammal species, with implications for Pleistocene extinctions and climate change projections for biodiversity. *Global Ecology and Biogeography* 13: 305-314.
- Martinez-Meyer, E., and A.T. Peterson. 2006. Conservatism of ecological niche characteristics in North American plant species over the Pleistocene-to-recent transition. *Journal of Biogeography* 33:1779–1789.
- Martinson, D.G., N.G. Pisias, J.D. Hays, J. Imbrie, T.C. Moore, and N.J. Shackleton. 1987. Age dating and the orbital theory of the ice ages: development of a high-resolution 0 to 300,000-year chronostratigraphy. *Quaternary Research* 27: 1-19.
- Mazerolle, M. 2017. AICcmodavg: model selection and multimodel inference based on (Q) AIC (c). R package, Version 2.1-1. <https://cran.r-project.org/package=AICcmodavg>
- McKay, N.P., J.T. Overpeck, and L.O. Bette. 2011. The role of ocean thermal expansion in Last Interglacial sea level rise. *Geophysical Research Letters* 38: 1-6.
- McLean, J.H., and E.V. Coan. 1996. Marine mollusks of Rocas Alijos. *In Monographiae Biologicae* 75:305–318.
- Morris, R.H., D.P. Abbott, and E.C. Haderlie. 1980. *Intertidal Invertebrates of California*. Stanford University Press, Stanford, California.
- Muhs, D.R. 1992. The last interglacial-glacial transition in North America: evidence from uranium-thorium dating of coastal deposits. *Geological Society of America Special Paper* 270.
- Muhs, D.R., G.L. Kennedy, and T.K. Rockwell. 1994. Uranium-series ages of marine terrace corals from the Pacific coast of North America and implications for last-interglacial sea level history. *Quaternary Research* 42: 72-87.
- Muhs, D.R., and T.K. Kyser. 1987. Stable isotope compositions of fossil mollusks from southern California: Evidence for a cool last interglacial ocean. *Geology* 15:119-122.
- Muhs D.R., L.T. Groves. 2018. Little islands recording global events: late Quaternary sea level history and paleozoogeography of Santa Barbara and Anacapa Islands, Channel Islands National Park, California. *Western North American Naturalist* 78:540-589.
- Muhs, D.R., L.T. Groves, and R.R. Schumann. 2014. Interpreting the paleozoogeography and sea level history of thermally anomalous marine terrace faunas: a case study from the

- Last Interglacial complex of San Clemente Island, California. *Monographs of the Western North American Naturalist* 7:82-108.
- Muhs, D.R., T.K. Rockwell, and G.L. Kennedy. 1992. Late Quaternary uplift rates of marine terraces on the Pacific coast of North America, southern Oregon to Baja California Sur. *Quaternary International* 15/16: 121-133.
- Muhs, D.R., K.R. Simmons, R.R. Schumann, J.X. Mitrovica, and D.J. Laurel. 2015. Quaternary sea-level history on the Pacific coast of North America: effects of low uplift rate and glacial isostatic adjustment processes on the marine terrace record. *Geological Society of America Abstracts with Programs* 47: 626.
- Muhs, D.R., K.R. Simmons, and B. Steinke. 2002. The last interglacial period on the Pacific coast of North America: timing and paleoclimate. *Geological Society of America Bulletin* 114: 569-592.
- Muhs, D.R., K.R. Simmons, G.L. Kennedy, K.R. Ludwig, and L.T. Groves. 2006. A cool eastern Pacific Ocean at the close of the Last Interglacial complex. *Quaternary Science Reviews* 25:235-262.
- Muhs, D.R., K.R. Simmons, R.R. Schumann, L.T. Groves, J.X. Mitrovica, and D. Laurel. 2012. Sea-level history during the Last Interglacial complex on San Nicolas Island, California: Implications for glacial isostatic adjustment processes, paleozoogeography and tectonics. *Quaternary Science Reviews* 37:1-25.
- Nogués-Bravo, D. 2009. Predicting the past distribution of species climatic niches. *Global Ecology and Biogeography* 18:521-531.
- Nogués-Bravo, D., F. Rodríguez-Sánchez, L. Orsini, E. de Boer, R. Jansson, H. Morlon, D. Fordham, and S.T. Jackson. 2018. Cracking the code of biodiversity responses to past climate change. *Trends in Ecology & Evolution* 33:765-776.
- Onuf, C.P. 1972. Aspects of the population biology of the intertidal snail *Olivella biplicata*: distribution, nutrition, and effects of natural enemies. Ph.D. dissertation. University of California, Santa Barbara.
- Patzkowsky, M.E. and S.M. Holland. 2016. Biotic invasion, niche stability, and the assembly of regional biotas in deep time: comparison between faunal provinces. *Paleobiology* 42: 359-379.
- Pearce, T.A. 1988. Evolutionary relationships among the helminthoglyptid land-snails *Micrarionta micromphala* Pilsbry, 1939, *M. opunitia* Roth, 1975, and *M. sodalis*

- (Hemphill, 1901) on San Nicolas Island. Masters thesis, University of California, Berkeley.
- Pearman, P.B., A. Guisan, O. Broennimann, and C.F. Randin. 2008a. Niche dynamics in space and time. *Trends in Ecology and Evolution* 23:149-158.
- Pearman, P.B., C.F. Randin, O. Broennimann, W.O. van der Knaap, R. Engler, G. Le Lay, N.E. Zimmermann, and A. Guisan. 2008b. Prediction of plant species distributions across six millennia. *Ecology Letters* 11: 357-369.
- Peterson, A.T. 2011. Ecological niche conservatism: a time-structured review of evidence. *Journal of Biogeography* 38: 817-827.
- Phillips, D.W. 1977. Activity of the gastropod mollusk *Olivella biplicata* in response to a natural light/ dark cycle. *The Veliger* 20: 137-143.
- Powell, II, C.L. 1994. Molluscan evidence for a late Pleistocene sea level lowstand from Monterey Bay, central California. *The Veliger* 37: 69-80.
- . 2000. A preliminary chronostratigraphy based on molluscan biogeography for the Late Quaternary of southern California. *Western Society of Malacologists* 32: 23-36.
- . 2001. Geologic and molluscan evidence for a previously misunderstood late Pleistocene, cool water, open coast terrace at Newport Bay, southern California. *The Veliger* 44: 340-347.
- . 2004. Paleoecologic analysis and age of a Late Pleistocene fossil assemblage at a locality in Newport Beach, Upper Newport Bay, Orange County, California. *The Veliger* 47: 171-180.
- . 2013. Pliocene fossil mollusks collected from a shrimp trap off San Clemente Island, southern California. *The Festivus*: 19-23.
- Powell, C.L., II, and M. McGann. 2008. Late Pleistocene mollusks and foraminifers from near Cordell Bank, offshore central California: their age and environmental significance. *The Festivus*, 40: 101-114.
- Powell, II, C.L., M. McGann and D.A. Trimble. 1992. Molluscan and foraminiferal evidence of a late Pleistocene sea level lowstand at Cordell Bank, central California. *Eos Transactions of the American Geophysical Union*, 73: 273-274.

- Powell, C.L., II, and Ponti, D.J., 2007, Paleontologic and stratigraphic reevaluation of Deadman Island, formerly in San Pedro Bay, California, *in* Brown, A.R., Shlemon, R.J., and Cooper, J.D., (Eds). *Geology and paleontology of Palos Verdes Hills, California: A 60th anniversary revisit to commemorate the 1946 publication of U.S. Geological Survey Professional Paper 207: Pacific Section SEPM, book 103*, p. 101-120.
- Powell, C.L., II, R.J. Stanton, Jr., M. Vendrasco, and P. Liff-Grief. 2009. Warm extralimital fossil mollusks used to recognize the mid-Pliocene warm event in southern California. *The Western Society of Malacologists, Annual Report for 2008*. 41: 70-91.
- Qiao, H., E.E. Saupe, J. Soberón, A.T. Peterson, and C.E. Myers. 2016. Impacts of niche breadth and dispersal ability on macroevolutionary patterns. *The American Naturalist* 188:149-162.
- Quay, P.D., B. Tilbrook, and C.S. Wong. 1992. Oceanic uptake of fossil fuel CO₂: Carbon-13 evidence. *Science* 256: 74-79.
- R Core Team. 2017. R: a language and environment for statistical computing. R Foundation for Statistical Computing, Vienna, Austria.
- Randall, D.A., S. Bony, R. Colman, T. Fichefet, J. Fyfe, V. Kattsov, A. Pitman, J. Shukla, J. Srinivasan, R.J. Stouffer, A. Sumi and K.E. Taylor, 2007. *Climate Models and Their Evaluation*. *in* Solomon, S., D. Qin, M. Manning, Z. Chen, M. Marquis, K.B. Averyt, M. Tignor and H.L. Miller (Eds). *Climate Change 2007: The Physical Science Basis. Contribution of Working Group I to the Fourth Assessment Report of the Intergovernmental Panel on Climate Change*. Cambridge University Press, Cambridge, United Kingdom and New York, NY, USA.
- Revelle, W. 2017. Psych: procedures for personality and psychological research. R package, Version 1.8.3.3. <https://cran.r-project.org/package=psych>.
- Ricketts, E.F., and J. Calvin. Rev. by J.W. Hedgpeth. 1985. *Between Pacific tides*. Stanford University Press, Stanford, CA.
- Roy, K., D. Jablonski, and J.W. Valentine. 1995. Thermally anomalous assemblages revisited: patterns in the extraprovincial latitudinal range shifts of Pleistocene marine mollusks. *Geology* 23:1071–1074.
- . 2001. Climate change, species range limits and body size in marine bivalves. *Ecology Letters* 4:366–370.

- Roy, K., J.W. Valentine, D. Jablonski, and S.M. Kidwell. 1996. Scales of climatic variability and time averaging in Pleistocene biotas: implications for ecology and evolution. *Trends in Ecology and Evolution* 11:458–463.
- Russell, M.P. 1991. Modern death assemblages and Pleistocene fossil assemblages in open coast high energy environments, San Nicolas Island, California. *PALAIOS* 6: 179-191.
- Sanford, E., J.L. Sones, M. Gracia-Reyes, J.H.R. Goddard, and J.L. Largier. Widespread shifts in the coastal biota of northern California during the 2014-2016 marine heatwaves. *Scientific Reports* 9: 4216.
- Saupe, E.E., J.R. Hendricks, R.W. Portell, H.J. Dowsett, A. Haywood, S.J. Hunter, and B.S. Lieberman. 2014. Macroevolutionary consequences of profound climate change on niche evolution in marine mollusks over the past three million years. *Proceedings of the Royal Society of London B: Biological Sciences* 281:20160654.
- Saupe, E.E., H. Qiao, J.R. Hendricks, R.W. Portell, S.J. Hunter, J. Soberón, and B.S. Lieberman. 2015. Niche breadth and geographic range size as determinants of species survival on geological time scales: determinants of species survival. *Global Ecology and Biogeography* 24:1159–1169.
- Schauble, E.A., P. Ghosh, and J.M. Eiler. 2006. Preferential formation of ^{13}C - ^{18}O bonds in carbonate minerals, estimated using first-principles lattice dynamics. *Geochimica et Cosmochimica Acta* 70: 2510-2529.
- Schmidt, G.A. 1999. Forward modeling of carbonate proxy data from planktonic foraminifera using oxygen isotope tracers in a global ocean model. *Paleoceanography* 14: 482-497.
- Schopf, T.J.M. 1978. Fossilization potential of an intertidal fauna: Friday Harbor, Washington. *Paleobiology* 4: 261-270.
- Shackleton, N.J., N.D. Opdike. 1973. Oxygen isotope and paleomagnetic stratigraphy of equatorial Pacific core V28-238: oxygen isotope temperatures and ice volumes on a 105 year and 106 year scale*. 1973. *Quaternary Research* 3: 39-55.
- Simms, A.R., H. Rouby, and K. Lambeck. 2015. Marine terraces and rates of vertical tectonic motion: the importance of glacio-isostatic adjustment along the Pacific coast of central North America. *Geological Society of America Bulletin* 128:81-93.
- Sokal, R., and E.J. Rohlf. 2012. *Biometry: the principles and practice of statistics in biological research*. W. H. Freeman and Co., New York.

- Stigall, A.L. 2014. When and how do species achieve niche stability over long time scales? *Ecography* 37: 1123-1132.
- Stohler, R. 1962. Preliminary report on growth studies in *Olivella biplicata*. *The Veliger* 4: 150-151.
- . 1969. Growth study in *Olivella biplicata* (Sowerby, 1825). *The Veliger* 11: 259-267.
- Strathmann, M.F. 1987. Reproduction and development of marine invertebrates of the northern Pacific coast: data and methods for the study of eggs, embryos, and larvae. University of Washington Press, Seattle.
- Staudigel, P.T., and P.K. Swart. 2016. Isotopic behavior during the aragonite-calcite transition: implications for sample preparation and proxy interpretation. *Chemical Geology* 442: 130-138.
- Suess, H.E. 1953. Natural radiocarbon and the rate of exchange of carbon dioxide between the atmosphere and the sea. Proceedings of the Conference on Nuclear Processes in Geologic Settings, National Academy of Sciences, National Research Council, Washington, D.C.
- . 1955. Radiocarbon concentration in modern wood. *Science* 122: 415-417.
- Sunday, J.M., A.E. Bates, and N.K. Dulvy. 2011. Global analysis of thermal tolerance and latitude in ectotherms. *Proceedings of the Royal Society Biological Sciences* 278: 1823-1830.
- . 2012. Thermal tolerances and the global redistribution of animals. *Nature Climate Change* 2: 686-690
- Svenning, J., C. Flojgaard, K.A. Marske, D. Nogues-Bravo, and S. Normand. 2011. Applications of species distribution modeling to paleobiology. *Quaternary Science Reviews* 30: 1-18.
- Sydeman, W.J., M. Garcia-Reyes, D.S. Schoeman, R.R. Rykaczewski, S.A. Thompson, B.A. Black, and S.J. Bograd. 2014. Climate change and wind intensification in coastal upwelling ecosystems. *Science* 345:77-80.
- Takesue, R.K., and A. Geen. 2004. Mg/Ca, Sr/Ca, and stable isotopes in modern and Holocene *Protothaca staminea* shells from a northern California coastal upwelling region. *Geochimica et Cosmochimica* 68: 3845-3861.
- Trecker, M.A., L.D. Gurrola, and E.A. Keller. 1999. Oxygen-isotope correlation of marine terrace uplift of the Mesa hills, Santa Barbara, California, USA. *in* I.S. Stewart and C.

- Vita-Finzi (Eds.) *Coastal Tectonics*. Geological Society, London Species Publications 146: 57-69.
- Tukey, J.W. 1949. Comparing individual means in the analysis of variance. *Biometrics* 5: 99-114.
- Turney, C.S.M., and R.T. Jones. 2010. Does the Agulhas Current amplify global temperatures during super-interglacials? *Journal of Quaternary Science* 25: 839-843.
- Urey, H.C. 1947. The thermodynamic properties of isotopic substances. *Journal of the Chemical Society (Resumed)* 562-581.
- Valentine, J.W. 1959. Marine climatic record of northwest American epicontinental Pleistocene, in Sears, M., ed. *International Oceanographic Congress, Washington, D.C., American Association for the Advancement of Science*, p. 295-296.
- . 1955. Upwelling and thermally anomalous Pacific coast Pleistocene molluscan faunas. *American Journal of Science* 253: 452-474.
- . 1958. Late Pleistocene megafauna of Cayucos, California, and its zoogeographic significance. *Journal of Paleontology* 32: 678-696.
- . 1961. Paleoecologic molluscan geography of the Californian Pleistocene. *University of California. Publications in Geological Sciences* 34:309-442
- . 1966. Numerical analysis of marine molluscan ranges on the extratropical northeastern Pacific shelf. *Limnology and Oceanography* 11:198–211.
- . 1973. *Evolutionary paleoecology of the marine biosphere*. Prentice Hall, Englewood Cliffs, N.J.
- . 1980. Camalu: A Pleistocene terrace fauna from Baja California. *Journal of Paleontology* 54: 1310-1318.
- . 1989a. How good was the fossil record - clues from the Californian Pleistocene. *Paleobiology* 15:83–94.
- . 1989b. Phanerozoic marine faunas and the stability of the Earth system. *Palaeogeography, Palaeoclimatology, and Palaeoecology* 75: 137–155.
- Valentine, J.W., and W.K. Emerson. 1961. Environmental interpretation of Pleistocene marine species: a discussion. *The Journal of Geology* 69: 616-618.

- Valentine, J.W., and D. Jablonski. 1993. Fossil communities: compositional variation at many time scales. *in* R.E. Ricklefs and D. Schluter (Eds). *Species Diversity in Ecological Communities: Historical and Geographic Perspectives*. University of Chicago Press, Chicago.
- Valentine, J.W. and J.H. Lipps. 1967. Late Cenozoic history of the southern California islands. *in* *Proceedings of the Symposium on the Biology of the California Islands*. Santa Barbara, California.
- Valentine, J.W., and R.F. Meade. 1960. Isotopic and zoogeographic paleotemperatures of Californian Pleistocene Mollusca. *Science* 132: 810-811.
- Valentine, J.W., and E.M. Moores. 1970. Plate-tectonic regulation of faunal diversity and sea level: a model. *Nature* 228: 657-659.
- Veddar, J.G., and R.M. Norris. 1963. Geology of San Nicolas Island California. Geological Survey Professional Paper 369.
- Veloz, S.D., J.W. Williams, J.L. Blois, F. He, B. Otto-Bliesner, and Z. Liu. 2012. No-analogue climates and shifting realized niches during the late Quaternary: implications for 21st-century predictions by species distribution models. *Global Change Biology* 18: 1698–1713.
- Walker, S.E. 1988. Taphonomic significance of hermit crabs (Anomura: Paguridea): epifaunal hermit crab - infaunal gastropod example. *Palaeogeography, Palaeoclimatology, Palaeoecology* 63: 45-71.
- . 1989. Hermit crabs as taphonomic agents. *PALAIOS* 4: 439-452.
- Wang, D., T.C. Gouhier, B.A. Menge, and A.R. Ganguly. 2015. Intensification and spatial homogenization of coastal upwelling under climate change. *Nature* 518:390–394.
- Warne, J.E. 1971. Paleoeological aspects of a modern coastal lagoon. *University of California Publications in Geological Sciences* 87: 1-112.
- Waterson, A.M., K.M. Edgar, D.N. Schmidt, and P.J. Valdes. 2017. Quantifying the stability of planktic foraminiferal physical niches between the Holocene and Last Glacial Maximum: niche stability of Planktic Foraminifera. *Paleoceanography* 32:74–89.
- Wehmiller, J.F. 1977. Correlation and chronology of Pacific coast marine deposits of continental United States by fossil amino acid stereochemistry-technique evaluation, relative ages,

- kinetic model ages, and geologic implications. Geological Survey Open-file Report 77-680.
- Williams, J.W., and S.T. Jackson. 2007. Novel climates, no-analogue communities, and ecological surprises. *Frontiers in Ecology and the Environment* 5:475–482.
- Woodring, W.P., M. Bramlette, and W.S.W. Kew. 1946. Geology and Paleontology of Palos Verdes Hills, California. U.S. Geological Survey Professional Paper 20753-55.
- .1951. Basic assumption underlying paleoecology. *Science* 113: 482-483.
- WoRMS Editorial Board. 2018. World Register of Marine Species. Available from <http://www.marinespecies.org>. Accessed 2017-04-23. doi:10.14284/170
- Worth, J.R.P., G.J. Williamson, S. Sakaguchi, P.G. Nevill, G.J. Jordan. 2014. Environmental niche modeling fails to predict Last Glacial Maximum refugia: niche shifts, microrefugia, or incorrect paleoclimate estimates? *Global Ecology and Biogeography* 23: 1198-1197.
- Wright, R.H. 1972. Late Pleistocene marine fauna, Goleta, California. *Journal of Paleontology* 46: 688-695.
- Zacherl, D., S.D. Gaines, and S.I. Lonhart. 2003. The limits to biogeographical distributions: insights from the northward range extension of the marine snail, *Kelletia kelletii* (Forbes, 1852). *Journal of Biogeography* 30: 913-924.
- Zinsmeister, W.J. 1974. A new interpretation of thermally anomalous molluscan assemblages of the Californian Pleistocene. *Journal of Paleontology* 48: 84-91.

Appendix I: Bulk isotopes and $\delta^{18}\text{O}$ paleo-temperatures. Individual measurements and computed parameters for biogenic aragonite *C. biplicata* powders, showing: specimen, location, locality, time period, stable isotope ratios for $\delta^{13}\text{C}_{\text{aragonite}}$ and $\delta^{18}\text{O}_{\text{aragonite}}$, and temperatures derived from $\delta^{18}\text{O}$ with associated mean $\delta^{18}\text{O}_{\text{seawater}}$ for each locality and time period. $\delta^{18}\text{O}$ temperatures were computed after adding a +0.5‰ correction to $\delta^{18}\text{O}_{\text{aragonite}}$ to account for an apparent vital effect. Data from the Center for Stable Isotope Biogeochemistry in the Department of Integrative Biology at the University of California, Berkeley.

Location	Time Period	Locality	Specimen	$\delta^{13}\text{C}$ ‰ VPDB	$\delta^{18}\text{O}_{\text{aragonite}}$ ‰ VPDB	$\delta^{18}\text{O}_{\text{seawater}}$ ‰ VPDB	$\delta^{18}\text{O}$ temperature
SNI	8th terrace	SNI 11	SNI-11.1	0.67	0.67	0.72	17.77
SNI	8th terrace	SNI 11	SNI-11.1	0.39	0.39	0.72	18.96
SNI	8th terrace	SNI 11	SNI-11.1	0.94	0.94	0.72	16.60
SNI	8th terrace	SNI 11	SNI-11.1	0.79	0.79	0.72	17.24
SNI	8th terrace	SNI 11	SNI-11.1	0.93	0.93	0.72	16.64
SNI	8th terrace	SNI 11	SNI-11.1	1.75	1.75	0.72	13.09
SNI	8th terrace	SNI 11	SNI-11.1	-0.18	-0.18	0.72	21.45
SNI	8th terrace	SNI 11	SNI-11.1	0.22	0.22	0.72	19.72
SNI	8th terrace	SNI 11	SNI-11.1	0.49	0.49	0.72	18.54
SNI	8th terrace	SNI 11	SNI-11.1	0.49	0.49	0.72	18.54
SNI	8th terrace	SNI 11	SNI-11.1	0.84	0.84	0.72	17.03
SNI	8th terrace	SNI 11	SNI-11.2	0.38	0.38	0.72	19.02
SNI	8th terrace	SNI 11	SNI-11.2	0.76	0.76	0.72	17.39
SNI	8th terrace	SNI 11	SNI-11.2	0.89	0.89	0.72	16.82
SNI	8th terrace	SNI 11	SNI-11.2	0.29	0.29	0.72	19.41
SNI	8th terrace	SNI 11	SNI-11.2	0.85	0.85	0.72	16.98
SNI	8th terrace	SNI 11	SNI-11.2	2.20	2.20	0.72	11.12
SNI	8th terrace	SNI 11	SNI-11.2	1.04	1.04	0.72	16.16
SNI	8th terrace	SNI 11	SNI-11.2	0.51	0.51	0.72	18.46
SNI	8th terrace	SNI 11	SNI-11.2	1.01	1.01	0.72	16.29
SNI	8th terrace	SNI 11	SNI-11.2	1.05	1.05	0.72	16.11
SNI	8th terrace	SNI 11	SNI-11.3	0.20	0.20	0.72	19.79
SNI	8th terrace	SNI 11	SNI-11.3	0.78	0.78	0.72	17.30
SNI	8th terrace	SNI 11	SNI-11.3	2.05	2.05	0.72	11.79
SNI	8th terrace	SNI 11	SNI-11.3	0.68	0.68	0.72	17.73
SNI	8th terrace	SNI 11	SNI-11.3	0.39	0.39	0.72	18.97
SNI	8th terrace	SNI 11	SNI-11.3	0.59	0.59	0.72	18.11

SNI	8th terrace	SNI 11	SNI-11.3	0.31	0.31	0.72	19.33
SNI	8th terrace	SNI 11	SNI-11.3	0.42	0.42	0.72	18.85
SNI	8th terrace	SNI 11	SNI-11.3	0.57	0.57	0.72	18.20
SNI	8th terrace	SNI 11	SNI-11.3	0.48	0.48	0.72	18.59
SNI	8th terrace	SNI 11	SNI-11.3	0.32	0.32	0.72	19.28
SNI	10th terrace	SNI 3	SNI-3.F1	1.65	1.65	1.10	15.13
SNI	10th terrace	SNI 3	SNI-3.F1	1.19	1.19	1.10	17.13
SNI	10th terrace	SNI 3	SNI-3.F1	1.44	1.44	1.10	16.05
SNI	10th terrace	SNI 3	SNI-3.F1	1.22	1.22	1.10	17.00
SNI	10th terrace	SNI 3	SNI-3.F1	1.41	1.41	1.10	16.18
SNI	10th terrace	SNI 3	SNI-3.F1	1.44	1.44	1.10	16.05
SNI	10th terrace	SNI 3	SNI-3.F1	1.17	1.17	1.10	17.22
SNI	10th terrace	SNI 3	SNI-3.F1	1.13	1.13	1.10	17.39
SNI	10th terrace	SNI 3	SNI-3.F1	1.23	1.23	1.10	16.96
SNI	10th terrace	SNI 3	SNI-3.F1	1.39	1.39	1.10	16.26
SNI	10th terrace	SNI 3	SNI-3.F1	1.58	1.58	1.10	15.44
SNI	10th terrace	SNI 3	SNI-3.F1	1.44	1.44	1.10	16.05
SNI	10th terrace	SNI 3	SNI-3.F1	1.43	1.43	1.10	16.09
SNI	10th terrace	SNI 3	SNI-3.F1	1.47	1.47	1.10	15.92
SNI	10th terrace	SNI 3	SNI-3.F1	1.19	1.19	1.10	17.13
SNI	10th terrace	SNI 3	SNI-3.F1	1.25	1.25	1.10	16.87
SNI	10th terrace	SNI 3	SNI-3.F2	1.02	1.02	1.10	17.87
SNI	10th terrace	SNI 3	SNI-3.F2	1.41	1.41	1.10	16.18
SNI	10th terrace	SNI 3	SNI-3.F2	1.30	1.30	1.10	16.65
SNI	10th terrace	SNI 3	SNI-3.F2	1.12	1.12	1.10	17.43
SNI	10th terrace	SNI 3	SNI-3.F2	1.24	1.24	1.10	16.91
SNI	10th terrace	SNI 3	SNI-3.F2	1.07	1.07	1.10	17.65
SNI	10th terrace	SNI 3	SNI-3.F2	0.95	0.95	1.10	18.17
SNI	10th terrace	SNI 3	SNI-3.F2	1.30	1.30	1.10	16.65
SNI	10th terrace	SNI 3	SNI-3.F2	1.04	1.04	1.10	17.78
SNI	10th terrace	SNI 3	SNI-3.F2	1.23	1.23	1.10	16.96
SNI	10th terrace	SNI 3	SNI-3.F3	1.19	1.19	1.10	17.13
SNI	10th terrace	SNI 3	SNI-3.F3	1.38	1.38	1.10	16.31
SNI	10th terrace	SNI 3	SNI-3.F3	1.47	1.47	1.10	15.92
SNI	10th terrace	SNI 3	SNI-3.F3	1.41	1.41	1.10	16.18
SNI	10th terrace	SNI 3	SNI-3.F3	1.23	1.23	1.10	16.96

SNI	10th terrace	SNI 3	SNI-3.F3	1.19	1.19	1.10	17.13
SNI	10th terrace	SNI 3	SNI-3.F3	1.25	1.25	1.10	16.87
SNI	10th terrace	SNI 3	SNI-3.F3	1.58	1.58	1.10	15.44
SNI	10th terrace	SNI 3	SNI-3.F3	1.94	1.94	1.10	13.88
SNI	10th terrace	SNI 3	SNI-3.F3	1.51	1.51	1.10	15.74
SNI	10th terrace	SNI 3	SNI-3.F4	1.36	1.36	1.10	16.39
SNI	10th terrace	SNI 3	SNI-3.F4	1.48	1.48	1.10	15.87
SNI	10th terrace	SNI 3	SNI-3.F4	1.68	1.68	1.10	15.00
SNI	10th terrace	SNI 3	SNI-3.F4	0.54	0.54	1.10	19.95
SNI	10th terrace	SNI 3	SNI-3.F4	1.39	1.39	1.10	16.26
SNI	10th terrace	SNI 3	SNI-3.F4	1.40	1.40	1.10	16.22
SNI	10th terrace	SNI 3	SNI-3.F4	1.13	1.13	1.10	17.39
SNI	10th terrace	SNI 3	SNI-3.F4	1.26	1.26	1.10	16.83
SNI	10th terrace	SNI 3	SNI-3.F4	1.22	1.22	1.10	17.00
SNI	10th terrace	SNI 3	SNI-3.F4	1.15	1.15	1.10	17.30
SNI	11th terrace	SNI 519	SNI-519.F1	1.31	1.31	0.91	15.77
SNI	11th terrace	SNI 519	SNI-519.F1	2.15	2.15	0.91	12.13
SNI	11th terrace	SNI 519	SNI-519.F1	1.41	1.41	0.91	15.34
SNI	11th terrace	SNI 519	SNI-519.F1	1.53	1.53	0.91	14.82
SNI	11th terrace	SNI 519	SNI-519.F1	2.24	2.24	0.91	11.74
SNI	11th terrace	SNI 519	SNI-519.F1	1.85	1.85	0.91	13.43
SNI	11th terrace	SNI 519	SNI-519.F1	1.51	1.51	0.91	14.91
SNI	11th terrace	SNI 519	SNI-519.F1	1.37	1.37	0.91	15.51
SNI	11th terrace	SNI 519	SNI-519.F2	0.76	0.76	0.91	18.16
SNI	11th terrace	SNI 519	SNI-519.F2	1.37	1.37	0.91	15.51
SNI	11th terrace	SNI 519	SNI-519.F2	1.37	1.37	0.91	15.51
SNI	11th terrace	SNI 519	SNI-519.F2	0.85	0.85	0.91	17.77
SNI	11th terrace	SNI 519	SNI-519.F2	0.91	0.91	0.91	17.51
SNI	11th terrace	SNI 519	SNI-519.F2	1.43	1.43	0.91	15.25
SNI	11th terrace	SNI 519	SNI-519.F2	0.95	0.95	0.91	17.34
SNI	11th terrace	SNI 519	SNI-519.F2	0.86	0.86	0.91	17.73
SNI	11th terrace	SNI 519	SNI-519.F2	1.16	1.16	0.91	16.42
SNI	11th terrace	SNI 519	SNI-519.F2	0.58	0.58	0.91	18.94
SNI	11th terrace	SNI 519	SNI-519.F3	0.56	0.56	0.91	19.03
SNI	11th terrace	SNI 519	SNI-519.F3	0.92	0.92	0.91	17.47
SNI	11th terrace	SNI 519	SNI-519.F3	-2.39	-2.39	0.91	31.83

SNI	11th terrace	SNI 519	SNI-519.F3	0.64	0.64	0.91	18.68
SNI	11th terrace	SNI 519	SNI-519.F3	0.60	0.60	0.91	18.86
SNI	11th terrace	SNI 519	SNI-519.F3	1.04	1.04	0.91	16.95
SNI	11th terrace	SNI 519	SNI-519.F3	1.02	1.02	0.91	17.03
SNI	11th terrace	SNI 519	SNI-519.F3	1.02	1.02	0.91	17.03
SNI	11th terrace	SNI 519	SNI-519.F3	1.06	1.06	0.91	16.86
SNI	11th terrace	SNI 519	SNI-519.F4	0.67	0.67	0.91	18.55
SNI	11th terrace	SNI 519	SNI-519.F4	0.85	0.85	0.91	17.77
SNI	11th terrace	SNI 519	SNI-519.F4	0.89	0.89	0.91	17.60
SNI	11th terrace	SNI 519	SNI-519.F4	1.64	1.64	0.91	14.34
SNI	11th terrace	SNI 519	SNI-519.F4	0.96	0.96	0.91	17.29
SNI	11th terrace	SNI 519	SNI-519.F4	0.63	0.63	0.91	18.72
SNI	11th terrace	SNI 519	SNI-519.F4	0.81	0.81	0.91	17.94
SNI	11th terrace	SNI 519	SNI-519.F4	0.66	0.66	0.91	18.59
SNI	11th terrace	SNI 519	SNI-519.F4	0.90	0.90	0.91	17.55
IV	2000-2015	Isla Vista	IV.M1	0.32	0.32	-0.10	15.72
IV	2000-2015	Isla Vista	IV.M1	0.30	0.30	-0.10	15.79
IV	2000-2015	Isla Vista	IV.M1	0.81	0.81	-0.10	13.57
IV	2000-2015	Isla Vista	IV.M1	0.35	0.35	-0.10	15.58
IV	2000-2015	Isla Vista	IV.M1	0.18	0.18	-0.10	16.34
IV	2000-2015	Isla Vista	IV.M1	0.13	0.13	-0.10	16.52
PVH	2000-2015	Point Fermin	SP.M1	1.10	1.10	0.35	14.29
PVH	2000-2015	Point Fermin	SP.M1	1.02	1.02	0.35	14.61
PVH	2000-2015	Point Fermin	SP.M1	1.12	1.12	0.35	14.19
PVH	2000-2015	Point Fermin	SP.M1	0.92	0.92	0.35	15.04
PVH	2000-2015	Point Fermin	SP.M1	0.77	0.77	0.35	15.72
IV	2000-2015	Isla Vista	IV.M1	0.57	0.57	-0.10	14.62
IV	2000-2015	Isla Vista	IV.M1	-0.29	-0.29	-0.10	18.35
IV	2000-2015	Isla Vista	IV.M1	-0.46	-0.46	-0.10	19.09
IV	2000-2015	Isla Vista	IV.M1	1.65	1.65	-0.10	9.94
IV	2000-2015	Isla Vista	IV.M1	0.49	0.49	-0.10	14.97
IV	2000-2015	Isla Vista	IV.M1	0.72	0.72	-0.10	13.97
IV	2000-2015	Isla Vista	IV.M1	-0.29	-0.29	-0.10	18.35
IV	2000-2015	Isla Vista	IV.M1	-0.01	-0.01	-0.10	17.14
IV	2000-2015	Isla Vista	IV.M1	-1.29	-1.29	-0.10	22.69
IV	2000-2015	Isla Vista	IV.M1	0.06	0.06	-0.10	16.85

IV	2000-2015	Isla Vista	IV.M1	-1.18	-1.18	-0.10	22.23
IV	2000-2015	Isla Vista	IV.M1	-0.35	-0.35	-0.10	18.60
IV	2000-2015	Isla Vista	IV.M1	-0.22	-0.22	-0.10	18.04
IV	2000-2015	Isla Vista	IV.M1	-0.86	-0.86	-0.10	20.81
IV	2000-2015	Isla Vista	IV.M2	2.53	2.53	-0.10	6.12
IV	2000-2015	Isla Vista	IV.M2	0.62	0.62	-0.10	14.41
IV	2000-2015	Isla Vista	IV.M2	0.28	0.28	-0.10	15.88
IV	2000-2015	Isla Vista	IV.M2	0.99	0.99	-0.10	12.80
IV	2000-2015	Isla Vista	IV.M2	0.48	0.48	-0.10	14.99
IV	2000-2015	Isla Vista	IV.M2	-0.79	-0.79	-0.10	20.52
IV	2000-2015	Isla Vista	IV.M2	-0.64	-0.64	-0.10	19.89
IV	2000-2015	Isla Vista	IV.M2	-1.02	-1.02	-0.10	21.53
IV	2000-2015	Isla Vista	IV.M2	-1.12	-1.12	-0.10	21.97
IV	2000-2015	Isla Vista	IV.M2	-0.73	-0.73	-0.10	20.26
IV	2000-2015	Isla Vista	IV.M2	-0.83	-0.83	-0.10	20.70
IV	2000-2015	Isla Vista	IV.M2	-0.80	-0.80	-0.10	20.57
IV	2000-2015	Isla Vista	IV.M2	-0.52	-0.52	-0.10	19.35
IV	2000-2015	Isla Vista	IV.M2	-0.60	-0.60	-0.10	19.70
IV	2000-2015	Isla Vista	IV.M3	-0.04	-0.04	-0.10	17.27
IV	2000-2015	Isla Vista	IV.M3	0.39	0.39	-0.10	15.40
IV	2000-2015	Isla Vista	IV.M3	0.57	0.57	-0.10	14.62
IV	2000-2015	Isla Vista	IV.M3	-0.04	-0.04	-0.10	17.27
IV	2000-2015	Isla Vista	IV.M3	-0.32	-0.32	-0.10	18.48
IV	2000-2015	Isla Vista	IV.M3	-0.41	-0.41	-0.10	18.88
IV	2000-2015	Isla Vista	IV.M3	0.12	0.12	-0.10	16.58
IV	2000-2015	Isla Vista	IV.M3	0.63	0.63	-0.10	14.37
IV	2000-2015	Isla Vista	IV.M3	-0.28	-0.28	-0.10	18.31
IV	2000-2015	Isla Vista	IV.M3	-0.10	-0.10	-0.10	17.53
IV	2000-2015	Isla Vista	IV.M3	0.02	0.02	-0.10	17.01
IV	2000-2015	Isla Vista	IV.M3	0.34	0.34	-0.10	15.62
IV	2000-2015	Isla Vista	IV.M4	0.68	0.68	-0.10	14.14
IV	2000-2015	Isla Vista	IV.M4	0.56	0.56	-0.10	14.67
IV	2000-2015	Isla Vista	IV.M4	0.47	0.47	-0.10	15.06
IV	2000-2015	Isla Vista	IV.M4	0.24	0.24	-0.10	16.05
IV	2000-2015	Isla Vista	IV.M4	0.44	0.44	-0.10	15.19
IV	2000-2015	Isla Vista	IV.M4	1.16	1.16	-0.10	12.08

IV	2000-2015	Isla Vista	IV.M4	-0.51	-0.51	-0.10	19.29
IV	2000-2015	Isla Vista	IV.M4	-0.44	-0.44	-0.10	19.03
IV	2000-2015	Isla Vista	IV.M5	0.20	0.20	-0.10	16.23
IV	2000-2015	Isla Vista	IV.M5	0.11	0.11	-0.10	16.62
IV	2000-2015	Isla Vista	IV.M5	0.42	0.42	-0.10	15.27
IV	2000-2015	Isla Vista	IV.M5	0.06	0.06	-0.10	16.84
IV	2000-2015	Isla Vista	IV.M5	0.09	0.09	-0.10	16.71
IV	2000-2015	Isla Vista	IV.M5	1.39	1.39	-0.10	11.08
IV	2000-2015	Isla Vista	IV.M5	0.83	0.83	-0.10	13.48
IV	2000-2015	Isla Vista	IV.M5	2.44	2.44	-0.10	6.52
IV	2000-2015	Isla Vista	IV.M6	1.07	1.07	-0.10	12.43
IV	2000-2015	Isla Vista	IV.M6	0.96	0.96	-0.10	12.92
IV	2000-2015	Isla Vista	IV.M6	1.32	1.32	-0.10	11.36
IV	2000-2015	Isla Vista	IV.M6	0.73	0.73	-0.10	13.94
IV	2000-2015	Isla Vista	IV.M6	0.26	0.26	-0.10	15.96
IV	2000-2015	Isla Vista	IV.M6	0.28	0.28	-0.10	15.88
SNI	2000-2015	NavFac	Navac.M1	1.81	1.81	-0.10	9.24
SNI	2000-2015	NavFac	Navac.M1	1.68	1.68	-0.10	9.80
SNI	2000-2015	NavFac	Navac.M1	0.21	0.21	-0.10	16.18
SNI	2000-2015	NavFac	Navac.M1	0.46	0.46	-0.10	15.10
SNI	2000-2015	NavFac	Navac.M1	0.02	0.02	-0.10	17.01
SNI	2000-2015	NavFac	Navac.M1	0.06	0.06	-0.10	16.84
SNI	2000-2015	NavFac	Navac.M1	0.20	0.20	-0.10	16.23
SNI	2000-2015	NavFac	Navac.M1	-0.37	-0.37	-0.10	18.70
SNI	2000-2015	NavFac	Navac.M1	-0.26	-0.26	-0.10	18.22
SNI	2000-2015	NavFac	Navac.M1	0.46	0.46	-0.10	15.10
SNI	2000-2015	NavFac	Navac.M1	0.21	0.21	-0.10	16.18
SNI	2000-2015	NavFac	Navac.M1	-0.81	-0.81	-0.10	20.61
SNI	2000-2015	NavFac	Navac.M1	-0.35	-0.35	-0.10	18.62
SNI	2000-2015	NavFac	Navac.M1	-1.51	-1.51	-0.10	23.65
SNI	2000-2015	NavFac	Navac.M1	-0.24	-0.24	-0.10	18.14
SNI	2000-2015	NavFac	Navac.M1	-0.32	-0.32	-0.10	18.48
SNI	2000-2015	NavFac	Navac.M1	-0.79	-0.79	-0.10	20.52
SNI	2000-2015	NavFac	Navac.M1	-0.16	-0.16	-0.10	17.79
SNI	2000-2015	NavFac	Navac.M1	-0.32	-0.32	-0.10	18.48
SNI	2000-2015	NavFac	Navac.M1	-0.40	-0.40	-0.10	18.83

SNI	2000-2015	NavFac	Navac.M1	-0.46	-0.46	-0.10	19.09
SNI	2000-2015	NavFac	Navac.M1	-0.62	-0.62	-0.10	19.79
SNI	2000-2015	NavFac	Navac.M1	-0.30	-0.30	-0.10	18.40
SNI	2000-2015	NavFac	Navac.M1	0.17	0.17	-0.10	16.36
SNI	2000-2015	NavFac	Navac.M2	0.57	0.57	-0.10	14.62
SNI	2000-2015	NavFac	Navac.M2	-0.13	-0.13	-0.10	17.66
SNI	2000-2015	NavFac	Navac.M2	-0.03	-0.03	-0.10	17.23
SNI	2000-2015	NavFac	Navac.M2	-0.05	-0.05	-0.10	17.31
SNI	2000-2015	NavFac	Navac.M2	0.01	0.01	-0.10	17.05
SNI	2000-2015	NavFac	Navac.M2	0.05	0.05	-0.10	16.88
SNI	2000-2015	NavFac	Navac.M2	0.15	0.15	-0.10	16.45
SNI	2000-2015	NavFac	Navac.M2	0.24	0.24	-0.10	16.05
SNI	2000-2015	NavFac	Navac.M2	0.03	0.03	-0.10	16.97
SNI	2000-2015	NavFac	NavFac.M3	0.85	0.85	-0.10	13.41
SNI	2000-2015	NavFac	NavFac.M3	0.34	0.34	-0.10	15.62
SNI	2000-2015	NavFac	NavFac.M3	0.16	0.16	-0.10	16.40
SNI	2000-2015	NavFac	NavFac.M3	0.34	0.34	-0.10	15.62
SNI	2000-2015	NavFac	NavFac.M3	0.17	0.17	-0.10	16.36
SNI	2000-2015	NavFac	NavFac.M3	0.04	0.04	-0.10	16.92
SNI	2000-2015	NavFac	NavFac.M3	0.23	0.23	-0.10	16.10
SNI	2000-2015	NavFac	NavFac.M3	0.25	0.25	-0.10	16.01
SNI	2000-2015	NavFac	NavFac.M3	0.69	0.69	-0.10	14.10
SNI	2000-2015	NavFac	NavFac.M3	0.32	0.32	-0.10	15.71
SNI	2000-2015	NavFac	NavFac.M4	0.70	0.70	-0.10	14.06
SNI	2000-2015	NavFac	NavFac.M4	0.41	0.41	-0.10	15.32
SNI	2000-2015	NavFac	NavFac.M4	0.12	0.12	-0.10	16.58
SNI	2000-2015	NavFac	NavFac.M4	0.19	0.19	-0.10	16.27
SNI	2000-2015	NavFac	NavFac.M4	0.44	0.44	-0.10	15.19
SNI	2000-2015	NavFac	NavFac.M4	0.69	0.69	-0.10	14.10
SNI	2000-2015	NavFac	NavFac.M4	0.54	0.54	-0.10	14.75
SNI	2000-2015	NavFac	NavFac.M4	0.37	0.37	-0.10	15.49
SNI	2000-2015	NavFac	NavFac.M4	0.42	0.42	-0.10	15.27
SNI	2000-2015	NavFac	NavFac.M4	0.09	0.09	-0.10	16.71
PVH	2000-2015	Point Fermin	SP.M1	1.00	1.00	0.35	14.71
PVH	2000-2015	Point Fermin	SP.M1	0.45	0.45	0.35	17.10
PVH	2000-2015	Point Fermin	SP.M1	0.10	0.10	0.35	18.62

PVH	2000-2015	Point Fermin	SP.M1	1.39	1.39	0.35	13.02
PVH	2000-2015	Point Fermin	SP.M1	1.74	1.74	0.35	11.50
PVH	2000-2015	Point Fermin	SP.M1	0.69	0.69	0.35	16.05
PVH	2000-2015	Point Fermin	SP.M1	0.76	0.76	0.35	15.75
PVH	2000-2015	Point Fermin	SP.M1	0.81	0.81	0.35	15.53
PVH	2000-2015	Point Fermin	SP.M1	0.58	0.58	0.35	16.53
PVH	2000-2015	Point Fermin	SP.M1	1.17	1.17	0.35	13.97
PVH	2000-2015	Point Fermin	SP.M1	0.27	0.27	0.35	17.88
PVH	2000-2015	Point Fermin	SP.M1	0.39	0.39	0.35	17.36
PVH	2000-2015	Point Fermin	SP.M1	0.07	0.07	0.35	18.75
PVH	2000-2015	Point Fermin	SP.M1	0.52	0.52	0.35	16.79
PVH	2000-2015	Point Fermin	SP.M1	0.09	0.09	0.35	18.66
PVH	2000-2015	Point Fermin	SP.M1	-0.46	-0.46	0.35	21.05
PVH	2000-2015	Point Fermin	SP.M1	0.16	0.16	0.35	18.35
PVH	2000-2015	Point Fermin	SP.M2	0.57	0.57	0.35	16.58
PVH	2000-2015	Point Fermin	SP.M2	0.47	0.47	0.35	17.01
PVH	2000-2015	Point Fermin	SP.M2	0.89	0.89	0.35	15.19
PVH	2000-2015	Point Fermin	SP.M2	0.77	0.77	0.35	15.71
PVH	2000-2015	Point Fermin	SP.M2	0.05	0.05	0.35	18.83
PVH	2000-2015	Point Fermin	SP.M2	0.18	0.18	0.35	18.27
PVH	2000-2015	Point Fermin	SP.M2	0.22	0.22	0.35	18.09
PVH	2000-2015	Point Fermin	SP.M2	0.22	0.22	0.35	18.09
PVH	2000-2015	Point Fermin	SP.M3	0.55	0.55	0.35	16.66
PVH	2000-2015	Point Fermin	SP.M3	0.90	0.90	0.35	15.14
PVH	2000-2015	Point Fermin	SP.M3	0.91	0.91	0.35	15.10
PVH	2000-2015	Point Fermin	SP.M3	1.09	1.09	0.35	14.32
PVH	2000-2015	Point Fermin	SP.M3	0.65	0.65	0.35	16.23
PVH	2000-2015	Point Fermin	SP.M3	1.67	1.67	0.35	11.78
PVH	2000-2015	Point Fermin	SP.M3	1.10	1.10	0.35	14.27
PVH	2000-2015	Point Fermin	SP.M3	1.54	1.54	0.35	12.36
PVH	2000-2015	Point Fermin	SP.M4	0.80	0.80	0.35	15.58
PVH	2000-2015	Point Fermin	SP.M4	0.90	0.90	0.35	15.14
PVH	2000-2015	Point Fermin	SP.M4	1.37	1.37	0.35	13.10
PVH	2000-2015	Point Fermin	SP.M4	1.22	1.22	0.35	13.75
PVH	2000-2015	Point Fermin	SP.M4	0.99	0.99	0.35	14.75
PVH	2000-2015	Point Fermin	SP.M4	0.45	0.45	0.35	17.10

PVH	2000-2015	Point Fermin	SP.M4	0.22	0.22	0.35	18.09
PVH	2000-2015	Point Fermin	SP.M4	0.00	0.00	0.35	19.05
PVH	2000-2015	Point Fermin	SP.M5	0.76	0.76	0.35	15.75
PVH	2000-2015	Point Fermin	SP.M5	1.73	1.73	0.35	11.54
PVH	2000-2015	Point Fermin	SP.M5	0.03	0.03	0.35	18.92
PVH	2000-2015	Point Fermin	SP.M5	1.08	1.08	0.35	14.36
SNI	2000-2015	Sandspit	Sandspit.M1	0.46	0.46	-0.10	15.10
SNI	2000-2015	Sandspit	Sandspit.M1	0.29	0.29	-0.10	15.84
SNI	2000-2015	Sandspit	Sandspit.M1	0.82	0.82	-0.10	13.54
SNI	2000-2015	Sandspit	Sandspit.M1	0.58	0.58	-0.10	14.58
SNI	2000-2015	Sandspit	Sandspit.M1	1.07	1.07	-0.10	12.45
SNI	2000-2015	Sandspit	Sandspit.M1	0.58	0.58	-0.10	14.58
SNI	2000-2015	Sandspit	Sandspit.M1	0.71	0.71	-0.10	14.01
SNI	2000-2015	Sandspit	Sandspit.M1	0.70	0.70	-0.10	14.06
SNI	2000-2015	Sandspit	Sandspit.M1	0.66	0.66	-0.10	14.23
SNI	2000-2015	Sandspit	Sandspit.M1	0.85	0.85	-0.10	13.41
SNI	2000-2015	Sandspit	Sandspit.M2	0.36	0.36	-0.10	15.53
SNI	2000-2015	Sandspit	Sandspit.M2	0.18	0.18	-0.10	16.31
SNI	2000-2015	Sandspit	Sandspit.M2	-0.02	-0.02	-0.10	17.18
SNI	2000-2015	Sandspit	Sandspit.M2	0.05	0.05	-0.10	16.88
SNI	2000-2015	Sandspit	Sandspit.M2	0.10	0.10	-0.10	16.66
SNI	2000-2015	Sandspit	Sandspit.M2	0.40	0.40	-0.10	15.36
SNI	2000-2015	Sandspit	Sandspit.M2	0.09	0.09	-0.10	16.71
SNI	2000-2015	Sandspit	Sandspit.M2	0.02	0.02	-0.10	17.01
SNI	2000-2015	Sandspit	Sandspit.M2	0.15	0.15	-0.10	16.45
SNI	2000-2015	Sandspit	Sandspit.M2	-0.06	-0.06	-0.10	17.36
SNI	2000-2015	Sandspit	sandspit.m3	0.97	0.97	-0.10	12.89
SNI	2000-2015	Sandspit	sandspit.m3	0.96	0.96	-0.10	12.93
SNI	2000-2015	Sandspit	sandspit.m3	0.66	0.66	-0.10	14.23
SNI	2000-2015	Sandspit	sandspit.m3	0.74	0.74	-0.10	13.88
SNI	2000-2015	Sandspit	sandspit.m3	0.84	0.84	-0.10	13.45
SNI	2000-2015	Sandspit	sandspit.m3	0.92	0.92	-0.10	13.10
SNI	2000-2015	Sandspit	sandspit.m3	1.08	1.08	-0.10	12.41
SNI	2000-2015	Sandspit	sandspit.m3	0.82	0.82	-0.10	13.54
SNI	2000-2015	Sandspit	sandspit.m3	0.72	0.72	-0.10	13.97
SNI	2000-2015	Sandspit	sandspit.m3	0.88	0.88	-0.10	13.28

SNI	2000-2015	Sandspit	Sandspit.M4	0.78	0.78	-0.10	13.71
SNI	2000-2015	Sandspit	Sandspit.M4	0.72	0.72	-0.10	13.97
SNI	2000-2015	Sandspit	Sandspit.M4	0.47	0.47	-0.10	15.06
SNI	2000-2015	Sandspit	Sandspit.M4	0.32	0.32	-0.10	15.71
SNI	2000-2015	Sandspit	Sandspit.M4	0.69	0.69	-0.10	14.10
SNI	2000-2015	Sandspit	Sandspit.M4	0.30	0.30	-0.10	15.79
SNI	2000-2015	Sandspit	Sandspit.M4	0.72	0.72	-0.10	13.97
SNI	2000-2015	Sandspit	Sandspit.M4	1.20	1.20	-0.10	11.89
SNI	1900	UCMP 2433	2433.M1	0.94	0.94	-0.10	13.02
SNI	1900	UCMP 2433	2433.M1	-0.32	-0.32	-0.10	18.48
SNI	1900	UCMP 2433	2433.M1	0.12	0.12	-0.10	16.58
SNI	1900	UCMP 2433	2433.M1	0.83	0.83	-0.10	13.49
SNI	1900	UCMP 2433	2433.M1	-0.29	-0.29	-0.10	18.35
SNI	1900	UCMP 2433	2433.M1	0.30	0.30	-0.10	15.79
SNI	1900	UCMP 2433	2433.M1	0.80	0.80	-0.10	13.62
SNI	1900	UCMP 2433	2433.M1	0.60	0.60	-0.10	14.49
SNI	1900	UCMP 2433	2433.M1	0.96	0.96	-0.10	12.93
SNI	1900	UCMP 2433	2433.M1	-0.27	-0.27	-0.10	18.27
SNI	1900	UCMP 2433	2433.M1	0.47	0.47	-0.10	15.06
SNI	1900	UCMP 2433	2433.M1	-0.52	-0.52	-0.10	19.35
SNI	1900	UCMP 2433	2433.M1	-0.27	-0.27	-0.10	18.27
SNI	1900	UCMP 2433	2433.M1	-0.50	-0.50	-0.10	19.27
SNI	1900	UCMP 2433	2433.M1	0.76	0.76	-0.10	13.80
SNI	1900	UCMP 2433	2433.M1	0.99	0.99	-0.10	12.80
SNI	1900	UCMP 2433	2433.M1	-0.52	-0.52	-0.10	19.35
SNI	1900	UCMP 2433	2433.M1	0.31	0.31	-0.10	15.75
SNI	1900	UCMP 2433	2433.M1	0.43	0.43	-0.10	15.23
SNI	1900	UCMP 2433	2433.M1	-0.53	-0.53	-0.10	19.40
SNI	1900	UCMP 2433	2433.M1	-0.56	-0.56	-0.10	19.53
SNI	1900	UCMP 2433	2433.M1	-0.46	-0.46	-0.10	19.09
SNI	1900	UCMP 2433	2433.M1	-0.24	-0.24	-0.10	18.14
SNI	1900	UCMP 2433	2433.M1	-0.49	-0.49	-0.10	19.22
SNI	1900	UCMP 2433	2433.M1	-0.66	-0.66	-0.10	19.96
SNI	1900	UCMP 2433	2433.M1	-0.62	-0.62	-0.10	19.79
SNI	1900	UCMP 2433	2433.M1	-0.36	-0.36	-0.10	18.66
SNI	1900	UCMP 2433	2433.M1	-0.16	-0.16	-0.10	17.79

SNI	1900	UCMP 2433	2433.M1	-1.28	-1.28	-0.10	22.65
SNI	1900	UCMP 2433	2433.M1	-0.54	-0.54	-0.10	19.44
SNI	1900	UCMP 2433	2433.M1	-0.81	-0.81	-0.10	20.61
SNI	1900	UCMP 2433	2433.M1	-0.72	-0.72	-0.10	20.22
SNI	1900	UCMP 2433	2433.M1	0.26	0.26	-0.10	15.97
SNI	1900	UCMP 2433	2433.M1	-0.23	-0.23	-0.10	18.09
SNI	1900	UCMP 2433	2433.M1	-0.20	-0.20	-0.10	17.96
SNI	1900	UCMP 2433	2433.M1	-0.23	-0.23	-0.10	18.09
SNI	1900	UCMP 2433	2433.M1	-0.22	-0.22	-0.10	18.05
SNI	1900	UCMP 2433	2433.M2	0.54	0.54	-0.10	14.75
SNI	1900	UCMP 2433	2433.M2	0.37	0.37	-0.10	15.49
SNI	1900	UCMP 2433	2433.M2	1.09	1.09	-0.10	12.37
SNI	1900	UCMP 2433	2433.M2	1.42	1.42	-0.10	10.93
SNI	1900	UCMP 2433	2433.M2	0.18	0.18	-0.10	16.31
SNI	1900	UCMP 2433	2433.M2	0.48	0.48	-0.10	15.01
SNI	1900	UCMP 2433	2433.M2	-0.11	-0.11	-0.10	17.57
SNI	1900	UCMP 2433	2433.M2	-0.29	-0.29	-0.10	18.35
SNI	1900	UCMP 2433	2433.M2	0.09	0.09	-0.10	16.71
SNI	1900	UCMP 2433	2433.M2	0.09	0.09	-0.10	16.71
SNI	1900	UCMP 2433	2433.M2	-0.25	-0.25	-0.10	18.18
SNI	1900	UCMP 2433	2433.M2	-0.50	-0.50	-0.10	19.27
SNI	1900	UCMP 2433	2433.M2	0.04	0.04	-0.10	16.92
SNI	1900	UCMP 2433	2433.M2	-0.29	-0.29	-0.10	18.35
SNI	1900	UCMP 2433	2433.M2	-0.23	-0.23	-0.10	18.09
SNI	1900	UCMP 2433	2433.M2	-0.95	-0.95	-0.10	21.22
SNI	1900	UCMP 2433	2433.M2	-0.75	-0.75	-0.10	20.35
SNI	1900	UCMP 2433	2433.M2	-1.18	-1.18	-0.10	22.22
SNI	1900	UCMP 2433	2433.M2	-0.40	-0.40	-0.10	18.83
SNI	1900	UCMP 2433	2433.M2	0.37	0.37	-0.10	15.49
SNI	1900	UCMP 2433	2433.M2	-0.08	-0.08	-0.10	17.44
SNI	1900	UCMP 2433	2433.M2	0.09	0.09	-0.10	16.71
SNI	1900	UCMP 2433	2433.M2	-0.34	-0.34	-0.10	18.57
SNI	1900	UCMP 2433	2433.M2	-0.36	-0.36	-0.10	18.66
SNI	1900	UCMP 2433	2433.M2	0.06	0.06	-0.10	16.84
SNI	1900	UCMP 2433	2433.M2	-0.20	-0.20	-0.10	17.96
SNI	1900	UCMP 2433	2433.M2	-0.48	-0.48	-0.10	19.18

SNI	1900	UCMP 2433	2433.M2	-0.83	-0.83	-0.10	20.70
SNI	1900	UCMP 2433	2433.M2	-0.06	-0.06	-0.10	17.36
SNI	1900	UCMP 2433	2433.M2	0.03	0.03	-0.10	16.97
SNI	1900	UCMP 2433	2433.M2	-0.25	-0.25	-0.10	18.18
SNI	1900	UCMP 2433	2433.M3	0.07	0.07	-0.10	16.79
SNI	1900	UCMP 2433	2433.M3	-0.27	-0.27	-0.10	18.27
SNI	1900	UCMP 2433	2433.M3	0.00	0.00	-0.10	17.10
SNI	1900	UCMP 2433	2433.M3	0.67	0.67	-0.10	14.19
SNI	1900	UCMP 2433	2433.M3	0.04	0.04	-0.10	16.92
SNI	1900	UCMP 2433	2433.M4	-0.22	-0.22	-0.10	18.05
SNI	1900	UCMP 2433	2433.M4	0.03	0.03	-0.10	16.97
SNI	1900	UCMP 2433	2433.M4	0.00	0.00	-0.10	17.10
SNI	1900	UCMP 2433	2433.M4	0.37	0.37	-0.10	15.49
SNI	1900	UCMP 2433	2433.M4	0.29	0.29	-0.10	15.84
SNI	5c/5e	11006	11006.2	1.54	1.54	0.54	13.19
SNI	5c/5e	11006	11006.2	1.18	1.18	0.54	14.75
SNI	5c/5e	11006	11006.2	1.38	1.38	0.54	13.89
SNI	5c/5e	11006	11006.2	1.25	1.25	0.54	14.45
SNI	5c/5e	11006	11006.2	1.21	1.21	0.54	14.62
SNI	5c/5e	11006	11006.2	1.59	1.59	0.54	12.97
SNI	5c/5e	11006	11006.2	1.24	1.24	0.54	14.49
SNI	5c/5e	11006	11006.2	0.55	0.55	0.54	17.49
SNI	5c/5e	11006	11006.2	1.35	1.35	0.54	14.02
SNI	5c/5e	11006	11006.2	1.12	1.12	0.54	15.01
SNI	5c/5e	11006	11006.F1	1.38	1.38	0.54	13.89
SNI	5c/5e	11006	11006.F1	1.68	1.68	0.54	12.58
SNI	5c/5e	11006	11006.F1	1.56	1.56	0.54	13.10
SNI	5c/5e	11006	11006.F1	1.63	1.63	0.54	12.80
SNI	5c/5e	11006	11006.F1	1.60	1.60	0.54	12.93
SNI	5c/5e	11006	11006.F1	1.40	1.40	0.54	13.80
SNI	5c/5e	11006	11006.F1	1.44	1.44	0.54	13.63
SNI	5c/5e	11006	11006.F1	1.45	1.45	0.54	13.58
SNI	5c/5e	11006	11006.F3	1.43	1.43	0.54	13.67
SNI	5c/5e	11006	11006.F3	1.35	1.35	0.54	14.02
SNI	5c/5e	11006	11006.F3	1.53	1.53	0.54	13.23
SNI	5c/5e	11006	11006.F3	1.43	1.43	0.54	13.67

SNI	5c/5e	11006	11006.F3	1.35	1.35	0.54	14.02
SNI	5c/5e	11006	11006.F3	1.32	1.32	0.54	14.15
SNI	5c/5e	11006	11006.F3	1.32	1.32	0.54	14.15
SNI	5c/5e	11006	11006.F3	1.31	1.31	0.54	14.19
SNI	5c/5e	11006	11006.F3	1.37	1.37	0.54	13.93
SNI	5c/5e	11006	11006.F3	1.36	1.36	0.54	13.97
SNI	5c/5e	11006	11006.F4	0.83	0.83	0.54	16.27
SNI	5c/5e	11006	11006.F4	1.06	1.06	0.54	15.27
SNI	5c/5e	11006	11006.F4	1.06	1.06	0.54	15.27
SNI	5c/5e	11006	11006.F4	0.98	0.98	0.54	15.62
SNI	5c/5e	11006	11006.F4	1.04	1.04	0.54	15.36
SNI	5c/5e	11006	11006.F4	0.86	0.86	0.54	16.14
SNI	5c/5e	11006	11006.F4	0.88	0.88	0.54	16.06
SNI	5c/5e	11006	11006.F4	0.92	0.92	0.54	15.88
SNI	5c/5e	11006	11006.F4	0.88	0.88	0.54	16.06
SNI	5c/5e	11006	11006.F4	0.94	0.94	0.54	15.80
SNI	5a	11747	11747.1	1.20	1.20	0.22	13.28
SNI	5a	11747	11747.1	0.00	0.00	0.22	18.48
SNI	5a	11747	11747.1	2.04	2.04	0.22	9.63
SNI	5a	11747	11747.1	0.36	0.36	0.22	16.92
SNI	5a	11747	11747.1	1.36	1.36	0.22	12.58
SNI	5a	11747	11747.1	1.97	1.97	0.22	9.93
SNI	5a	11747	11747.1	1.37	1.37	0.22	12.54
SNI	5a	11747	11747.1	1.55	1.55	0.22	11.76
SNI	5a	11747	11747.1	0.80	0.80	0.22	15.01
SNI	5a	11747	11747.1	2.44	2.44	0.22	7.89
SNI	5a	11747	11747.1	0.76	0.76	0.22	15.19
SNI	5a	11747	11747.1	0.80	0.80	0.22	15.01
SNI	5a	11747	11747.1	0.69	0.69	0.22	15.49
SNI	5a	11747	11747.2	1.49	1.49	0.22	12.02
SNI	5a	11747	11747.2	1.00	1.00	0.22	14.14
SNI	5a	11747	11747.2	1.15	1.15	0.22	13.49
SNI	5a	11747	11747.2	1.03	1.03	0.22	14.01
SNI	5a	11747	11747.2	1.03	1.03	0.22	14.01
SNI	5a	11747	11747.2	0.86	0.86	0.22	14.75
SNI	5a	11747	11747.2	1.01	1.01	0.22	14.10

SNI	5a	11747	11747.2	0.51	0.51	0.22	16.27
SNI	5a	11747	11747.2	0.94	0.94	0.22	14.40
SNI	5a	11747	11747.2	1.40	1.40	0.22	12.41
SNI	5a	11747	11747.F3	0.91	0.91	0.22	14.54
SNI	5a	11747	11747.F3	0.91	0.91	0.22	14.54
SNI	5a	11747	11747.F3	1.00	1.00	0.22	14.14
SNI	5a	11747	11747.F3	1.21	1.21	0.22	13.23
SNI	5a	11747	11747.F3	1.13	1.13	0.22	13.58
SNI	5a	11747	11747.F3	1.19	1.19	0.22	13.32
SNI	5a	11747	11747.F3	1.14	1.14	0.22	13.54
SNI	5a	11747	11747.F3	1.23	1.23	0.22	13.15
SNI	5a	11747	11747.F3	1.31	1.31	0.22	12.80
SNI	5a	11747	11747.F3	1.37	1.37	0.22	12.54
SNI	5a	11747	11747.F4	0.90	0.90	0.22	14.58
SNI	5a	11747	11747.F4	0.61	0.61	0.22	15.84
SNI	5a	11747	11747.F4	0.75	0.75	0.22	15.23
SNI	5a	11747	11747.F4	0.80	0.80	0.22	15.01
SNI	5a	11747	11747.F4	0.77	0.77	0.22	15.14
SNI	5a	11747	11747.F4	0.65	0.65	0.22	15.66
SNI	5a	11747	11747.F4	0.47	0.47	0.22	16.44
SNI	5a	11747	11747.F4	0.69	0.69	0.22	15.49
SNI	5a	11747	11747.F4	0.87	0.87	0.22	14.71
SNI	5c/5e	11749	11749.1	0.25	0.25	0.05	16.66
SNI	5c/5e	11749	11749.1	0.39	0.39	0.05	16.05
SNI	5c/5e	11749	11749.1	0.96	0.96	0.05	13.58
SNI	5c/5e	11749	11749.1	0.18	0.18	0.05	16.97
SNI	5c/5e	11749	11749.1	0.51	0.51	0.05	15.53
SNI	5c/5e	11749	11749.1	0.28	0.28	0.05	16.53
SNI	5c/5e	11749	11749.1	0.74	0.74	0.05	14.54
SNI	5c/5e	11749	11749.1	1.02	1.02	0.05	13.32
SNI	5c/5e	11749	11749.1	-0.30	-0.30	0.05	19.05
SNI	5c/5e	11749	11749.1	0.79	0.79	0.05	14.32
SNI	5c/5e	11749	11749.1	-0.51	-0.51	0.05	19.96
SNI	5c/5e	11749	11749.1	0.52	0.52	0.05	15.49
SNI	5c/5e	11749	11749.1	-0.38	-0.38	0.05	19.40
SNI	5c/5e	11749	11749.1	0.09	0.09	0.05	17.36

SNI	5c/5e	11749	11749.1	0.53	0.53	0.05	15.45
SNI	5c/5e	11749	11749.1	0.56	0.56	0.05	15.32
SNI	5c/5e	11749	11749.1	-1.29	-1.29	0.05	23.35
SNI	5c/5e	11749	11749.1	-0.89	-0.89	0.05	21.61
SNI	5c/5e	11749	11749.1	0.23	0.23	0.05	16.75
SNI	5c/5e	11749	11749.1	0.34	0.34	0.05	16.27
SNI	5c/5e	11749	11749.1	0.45	0.45	0.05	15.79
SNI	5c/5e	11749	11749.1	0.57	0.57	0.05	15.27
SNI	5c/5e	11749	11749.1	2.01	2.01	0.05	9.02
SNI	5c/5e	11749	11749.1	-0.01	-0.01	0.05	17.79
SNI	5c/5e	11749	11749.1	0.13	0.13	0.05	17.18
SNI	5c/5e	11749	11749.1	0.29	0.29	0.05	16.49
SNI	5c/5e	11749	11749.1	0.43	0.43	0.05	15.88
SNI	5c/5e	11749	11749.1	-0.63	-0.63	0.05	20.48
SNI	5c/5e	11749	11749.1	0.61	0.61	0.05	15.10
SNI	5c/5e	11749	11749.1	0.63	0.63	0.05	15.01
SNI	5c/5e	11749	11749.1	0.78	0.78	0.05	14.36
SNI	5c/5e	11749	11749.1	0.79	0.79	0.05	14.32
SNI	5c/5e	11749	11749.1	0.38	0.38	0.05	16.10
SNI	5c/5e	11749	11749.1	0.14	0.14	0.05	17.14
SNI	5c/5e	11749	11749.1	0.46	0.46	0.05	15.75
SNI	5c/5e	11749	11749.1	0.42	0.42	0.05	15.92
SNI	5c/5e	11749	11749.1	0.60	0.60	0.05	15.14
SNI	5c/5e	11749	11749.2	0.71	0.71	0.05	14.67
SNI	5c/5e	11749	11749.2	0.82	0.82	0.05	14.19
SNI	5c/5e	11749	11749.2	0.51	0.51	0.05	15.53
SNI	5c/5e	11749	11749.2	1.00	1.00	0.05	13.41
SNI	5c/5e	11749	11749.2	0.78	0.78	0.05	14.36
SNI	5c/5e	11749	11749.2	1.79	1.79	0.05	9.98
SNI	5c/5e	11749	11749.2	0.96	0.96	0.05	13.58
SNI	5c/5e	11749	11749.2	0.50	0.50	0.05	15.58
SNI	5c/5e	11749	11749.2	-0.09	-0.09	0.05	18.14
SNI	5c/5e	11749	11749.2	-0.07	-0.07	0.05	18.05
SNI	5c/5e	11749	11749.2	0.19	0.19	0.05	16.92
SNI	5c/5e	11749	11749.2	0.35	0.35	0.05	16.23
SNI	5c/5e	11749	11749.2	-0.01	-0.01	0.05	17.79

SNI	5c/5e	11749	11749.2	-0.01	-0.01	0.05	17.79
SNI	5c/5e	11749	11749.2	0.09	0.09	0.05	17.36
SNI	5c/5e	11749	11749.2	0.51	0.51	0.05	15.53
SNI	5c/5e	11749	11749.2	0.32	0.32	0.05	16.36
SNI	5c/5e	11749	11749.2	0.80	0.80	0.05	14.28
SNI	5c/5e	11749	11749.2	0.29	0.29	0.05	16.49
SNI	5c/5e	11749	11749.2	0.36	0.36	0.05	16.18
SNI	5c/5e	11749	11749.4	0.76	0.76	0.05	14.45
SNI	5c/5e	11749	11749.4	0.76	0.76	0.05	14.45
SNI	5c/5e	11749	11749.4	0.66	0.66	0.05	14.88
SNI	5c/5e	11749	11749.4	0.59	0.59	0.05	15.19
SNI	5c/5e	11749	11749.4	0.78	0.78	0.05	14.36
SNI	5c/5e	11749	11749.4	0.74	0.74	0.05	14.54
SNI	5c/5e	11749	11749.4	0.53	0.53	0.05	15.45
SNI	5c/5e	11749	11749.4	0.74	0.74	0.05	14.54
SNI	5c/5e	11749	11749.4	0.95	0.95	0.05	13.62
SNI	5c/5e	11749	11749.4	0.79	0.79	0.05	14.32
SNI	5c/5e	11749	11749.F3	0.82	0.82	0.05	14.19
SNI	5c/5e	11749	11749.F3	0.81	0.81	0.05	14.23
SNI	5c/5e	11749	11749.F3	0.86	0.86	0.05	14.01
SNI	5c/5e	11749	11749.F3	1.01	1.01	0.05	13.36
SNI	5c/5e	11749	11749.F3	0.96	0.96	0.05	13.58
SNI	5c/5e	11749	11749.F3	0.89	0.89	0.05	13.88
SNI	5c/5e	11749	11749.F3	0.88	0.88	0.05	13.93
SNI	5c/5e	11749	11749.F3	0.94	0.94	0.05	13.67
PVH	5a	12575	12575.2	1.05	1.05	0.50	15.14
PVH	5a	12575	12575.2	1.16	1.16	0.50	14.67
PVH	5a	12575	12575.2	1.57	1.57	0.50	12.89
PVH	5a	12575	12575.2	1.12	1.12	0.50	14.84
PVH	5a	12575	12575.2	1.31	1.31	0.50	14.01
PVH	5a	12575	12575.2	1.12	1.12	0.50	14.84
PVH	5a	12575	12575.4	0.70	0.70	0.50	16.66
PVH	5a	12575	12575.4	0.81	0.81	0.50	16.18
PVH	5a	12575	12575.4	0.78	0.78	0.50	16.31
PVH	5a	12575	12575.4	0.99	0.99	0.50	15.40
PVH	5a	12575	12575.4	0.86	0.86	0.50	15.97

PVH	5a	12575	12575.4	0.69	0.69	0.50	16.71
PVH	5a	12575	12575.4	0.95	0.95	0.50	15.58
PVH	5a	12575	12575.4	0.79	0.79	0.50	16.27
PVH	5a	12575	12575.5	1.60	1.60	0.50	12.76
PVH	5a	12575	12575.5	1.70	1.70	0.50	12.32
PVH	5a	12575	12575.5	1.77	1.77	0.50	12.02
PVH	5a	12575	12575.5	1.38	1.38	0.50	13.71
PVH	5e	12608	12608.1	0.88	0.88	0.35	15.23
PVH	5e	12608	12608.1	0.87	0.87	0.35	15.27
PVH	5e	12608	12608.1	0.94	0.94	0.35	14.97
PVH	5e	12608	12608.1	0.82	0.82	0.35	15.49
PVH	5e	12608	12608.1	0.77	0.77	0.35	15.71
PVH	5e	12608	12608.1	0.88	0.88	0.35	15.23
PVH	5e	12608	12608.1	2.70	2.70	0.35	7.33
PVH	5e	12608	12608.1	0.33	0.33	0.35	17.62
PVH	5e	12608	12608.1	0.06	0.06	0.35	18.79
PVH	5e	12608	12608.1	0.36	0.36	0.35	17.49
PVH	5e	12608	12608.1	0.88	0.88	0.35	15.23
PVH	5e	12608	12608.1	0.69	0.69	0.35	16.05
PVH	5e	12608	12608.1	0.65	0.65	0.35	16.23
PVH	5e	12608	12608.1	0.87	0.87	0.35	15.27
PVH	5e	12608	12608.1	0.21	0.21	0.35	18.14
PVH	5e	12608	12608.3	1.69	1.69	0.35	11.71
PVH	5e	12608	12608.3	1.27	1.27	0.35	13.54
PVH	5e	12608	12608.3	1.77	1.77	0.35	11.37
PVH	5e	12608	12608.3	0.73	0.73	0.35	15.88
PVH	5e	12608	12608.3	1.60	1.60	0.35	12.10
PVH	5e	12608	12608.3	2.52	2.52	0.35	8.12
PVH	5e	12608	12608.3	1.03	1.03	0.35	14.57
PVH	5e	12608	12608.3	0.65	0.65	0.35	16.24
PVH	5e	12608	12608.3	0.94	0.94	0.35	14.98
PVH	5e	12608	12608.4	0.67	0.67	0.35	16.14
PVH	5e	12608	12608.4	1.57	1.57	0.35	12.24
PVH	5e	12608	12608.4	0.36	0.36	0.35	17.49
PVH	5e	12608	12608.4	1.00	1.00	0.35	14.71
PVH	5e	12608	12608.4	0.57	0.57	0.35	16.58

PVH	5e	12608	12608.4	0.98	0.98	0.35	14.80
PVH	5e	12608	12608.4	0.99	0.99	0.35	14.75
PVH	5e	12608	12608.4	0.54	0.54	0.35	16.71
PVH	5e	12608	12608.4	0.72	0.72	0.35	15.92
PVH	5e	12608	12608.4	0.78	0.78	0.35	15.66
PVH	5e	12608	12608.4	1.23	1.23	0.35	13.71
PVH	5e	12608	12608.4	1.39	1.39	0.35	13.02
PVH	5e	12608	12608.4	0.37	0.37	0.35	17.44
PVH	5e	12608	12608.4	0.60	0.60	0.35	16.45
PVH	5e	12608	12608.4	0.75	0.75	0.35	15.79
PVH	5e	12608	12608.4	0.26	0.26	0.35	17.92
PVH	5e	12608	12608.4	0.25	0.25	0.35	17.96
PVH	5e	12608	12608.4	1.31	1.31	0.35	13.36
PVH	5e	12608	12608.4	0.62	0.62	0.35	16.36
PVH	5e	12608	12608.4	0.22	0.22	0.35	18.09
PVH	5e	12608	12608.5	0.17	0.17	0.35	18.31
PVH	5e	12608	12608.5	0.46	0.46	0.35	17.05
PVH	5e	12608	12608.5	0.74	0.74	0.35	15.84
PVH	5e	12608	12608.5	0.66	0.66	0.35	16.18
PVH	5e	12608	12608.5	-0.14	-0.14	0.35	19.66
PVH	5e	12608	12608.5	-0.44	-0.44	0.35	20.96
PVH	5e	12608	12608.5	-0.46	-0.46	0.35	21.05
PVH	5e	12608	12608.5	-0.45	-0.45	0.35	21.00
PVH	5e	12608	12608.5	0.04	0.04	0.35	18.88
PVH	5e	12608	12608.5	0.01	0.01	0.35	19.01
PVH	5e	12608	12608.5	0.51	0.51	0.35	16.84
PVH	5e	12608	12608.5	0.11	0.11	0.35	18.57
PVH	5e	12608	12608.5	-0.14	-0.14	0.35	19.66
PVH	5e	12608	12608.5	-0.18	-0.18	0.35	19.83
PVH	5e	12608	12608.5	-0.16	-0.16	0.35	19.74
PVH	5e	12608	12608.5	-0.60	-0.60	0.35	21.65
PVH	5e	12608	12608.5	-0.53	-0.53	0.35	21.35
PVH	5e	12608	12608.5	0.09	0.09	0.35	18.66
PVH	5e	12608	12608.5	-0.53	-0.53	0.35	21.35
PVH	5e	12608	12608.5	0.37	0.37	0.35	17.44
PVH	5e	12608	12608.5	0.55	0.55	0.35	16.66

PVH	5e	12608	12608.5	-0.25	-0.25	0.35	20.13
PVH	5e	12608	12608.5	-1.01	-1.01	0.35	23.43
PVH	5a	12575	12575.1	1.42	1.42	0.50	13.54
PVH	5a	12575	12575.1	1.23	1.23	0.50	14.36
PVH	5a	12575	12575.1	1.73	1.73	0.50	12.19
PVH	5a	12575	12575.1	1.45	1.45	0.50	13.41
PVH	5a	12575	12575.1	1.29	1.29	0.50	14.10
PVH	5a	12575	12575.1	2.57	2.57	0.50	8.55
PVH	5a	12575	12575.1	2.03	2.03	0.50	10.90
PVH	5a	12575	12575.1	1.79	1.79	0.50	11.94
PVH	5a	12575	12575.1	2.19	2.19	0.50	10.21
PVH	5a	12575	12575.1	1.22	1.22	0.50	14.41
PVH	5a	12575	12575.1	1.33	1.33	0.50	13.94
PVH	5a	12575	12575.1	1.50	1.50	0.50	13.20
PVH	5a	12575	12575.1	0.21	0.21	0.50	18.81
PVH	5a	12575	12575.1	1.68	1.68	0.50	12.39
PVH	5a	12575	12575.1	2.02	2.02	0.50	10.91
PVH	5a	12575	12575.1	1.74	1.74	0.50	12.16
PVH	5a	12575	12575.2	2.31	2.31	0.50	9.68
PVH	5a	12575	12575.2	2.22	2.22	0.50	10.06
PVH	5a	12575	12575.2	1.62	1.62	0.50	12.66
PVH	5a	12575	12575.2	1.77	1.77	0.50	12.02
PVH	5a	12575	12575.2	1.07	1.07	0.50	15.07
PVH	5a	12575	12575.2	2.78	2.78	0.50	7.64
PVH	5a	12575	12575.2	2.18	2.18	0.50	10.25
PVH	5a	12575	12575.4	1.36	1.36	0.50	13.78
PVH	5a	12575	12575.4	2.01	2.01	0.50	10.96
PVH	5a	12575	12575.5	2.67	2.67	0.50	8.13
PVH	5a	12575	12575.5	2.46	2.46	0.50	9.01
PVH	5a	12575	12575.5	2.62	2.62	0.50	8.31
PVH	5a	12575	12575.5	1.59	1.59	0.50	12.81
PVH	5a	12575	12575.5	2.69	2.69	0.50	8.04
PVH	5a	12575	12575.5	2.06	2.06	0.50	10.77
SNI	5a	11004/05	11004/05.1	1.37	1.37	0.25	12.66
SNI	5a	11004/05	11004/05.1	1.91	1.91	0.25	10.32
SNI	5a	11004/05	11004/05.1	1.91	1.91	0.25	10.32

SNI	5a	11004/05	11004/05.1	1.91	1.91	0.25	10.32
SNI	5a	11004/05	11004/05.1	2.06	2.06	0.25	9.67
SNI	5a	11004/05	11004/05.1	1.45	1.45	0.25	12.32
SNI	5a	11004/05	11004/05.1	1.19	1.19	0.25	13.45
SNI	5a	11004/05	11004/05.1	1.34	1.34	0.25	12.79
SNI	5a	11004/05	11004/05.1	0.32	0.32	0.25	17.22
SNI	5a	11004/05	11004/05.1	2.33	2.33	0.25	8.50
SNI	5a	11004/05	11004/05.1	1.78	1.78	0.25	10.88
SNI	5a	11004/05	11004/05.1	1.50	1.50	0.25	12.10
SNI	5a	11004/05	11004/05.1	0.61	0.61	0.25	15.96
SNI	5a	11004/05	11004/05.1	0.96	0.96	0.25	14.44
SNI	5a	11004/05	11004/05.2	1.03	1.03	0.25	14.14
SNI	5a	11004/05	11004/05.2	0.73	0.73	0.25	15.44
SNI	5a	11004/05	11004/05.2	1.22	1.22	0.25	13.32
SNI	5a	11004/05	11004/05.2	1.30	1.30	0.25	12.97
SNI	5a	11004/05	11004/05.2	0.65	0.65	0.25	15.79
SNI	5a	11004/05	11004/05.2	1.18	1.18	0.25	13.49
SNI	5a	11004/05	11004/05.2	0.96	0.96	0.25	14.44
SNI	5a	11004/05	11004/05.2	0.87	0.87	0.25	14.83
SNI	5a	11004/05	11004/05.2	1.65	1.65	0.25	11.45
SNI	5a	11004/05	11004/05.2	1.24	1.24	0.25	13.23
SNI	5a	11004/05	11004/05.3	1.14	1.14	0.25	13.66
SNI	5a	11004/05	11004/05.3	1.29	1.29	0.25	13.01
SNI	5a	11004/05	11004/05.3	0.72	0.72	0.25	15.49
SNI	5a	11004/05	11004/05.3	1.23	1.23	0.25	13.27
SNI	5a	11004/05	11004/05.3	1.01	1.01	0.25	14.23
SNI	5a	11004/05	11004/05.3	1.26	1.26	0.25	13.14
SNI	5a	11004/05	11004/05.3	1.00	1.00	0.25	14.27
SNI	5a	11004/05	11004/05.3	1.11	1.11	0.25	13.79
SNI	5a	11004/05	11004/05.3	0.12	0.12	0.25	18.09
SNI	5a	11004/05	11004/05.4	1.63	1.63	0.25	11.54
SNI	5a	11004/05	11004/05.4	1.62	1.62	0.25	11.58
SNI	5a	11004/05	11004/05.4	1.28	1.28	0.25	13.05
SNI	5a	11004/05	11004/05.4	1.58	1.58	0.25	11.75
SNI	5a	11004/05	11004/05.4	1.34	1.34	0.25	12.79
SNI	5a	11004/05	11004/05.4	1.29	1.29	0.25	13.01

SNI	5a	11004/05	11004/05.4	1.14	1.14	0.25	13.66
SNI	5a	11004/05	11004/05.4	1.09	1.09	0.25	13.88
SNI	5a	11004/05	11004/05.4	1.16	1.16	0.25	13.58
IV	3a	Isla Vista	IV.F1	0.86	0.86	0.11	14.28
IV	3a	Isla Vista	IV.F1	1.14	1.14	0.11	13.03
IV	3a	Isla Vista	IV.F1	0.59	0.59	0.11	15.43
IV	3a	Isla Vista	IV.F1	0.24	0.24	0.11	16.95
IV	3a	Isla Vista	IV.F1	0.29	0.29	0.11	16.75
IV	3a	Isla Vista	IV.F1	0.56	0.56	0.11	15.55
IV	3a	Isla Vista	IV.F1	0.20	0.20	0.11	17.15
IV	3a	Isla Vista	IV.F1	0.55	0.55	0.11	15.63
IV	3a	Isla Vista	IV.F1	0.69	0.69	0.11	15.00
IV	3a	Isla Vista	IV.F1	1.04	1.04	0.11	13.48
IV	3a	Isla Vista	IV.F1	1.21	1.21	0.11	12.75
IV	3a	Isla Vista	IV.F1	0.76	0.76	0.11	14.70
IV	3a	Isla Vista	IV.F2	1.49	1.49	0.11	11.53
IV	3a	Isla Vista	IV.F2	1.12	1.12	0.11	13.14
IV	3a	Isla Vista	IV.F2	1.16	1.16	0.11	12.96
IV	3a	Isla Vista	IV.F2	1.01	1.01	0.11	13.61
IV	3a	Isla Vista	IV.F2	2.17	2.17	0.11	8.58
IV	3a	Isla Vista	IV.F2	0.58	0.58	0.11	15.50
IV	3a	Isla Vista	IV.F2	0.51	0.51	0.11	15.77
IV	3a	Isla Vista	IV.F2	1.06	1.06	0.11	13.39
IV	3a	Isla Vista	IV.F2	0.25	0.25	0.11	16.89
IV	3a	Isla Vista	IV.F2	0.91	0.91	0.11	14.05
IV	3a	Isla Vista	IV.F2	0.94	0.94	0.11	13.92
IV	3a	Isla Vista	IV.F2	1.19	1.19	0.11	12.83
IV	3a	Isla Vista	IV.F2	1.10	1.10	0.11	13.22
IV	3a	Isla Vista	IV.F2	1.08	1.08	0.11	13.31
IV	3a	Isla Vista	IV.F3	0.97	0.97	0.11	13.79
IV	3a	Isla Vista	IV.F3	1.17	1.17	0.11	12.92
IV	3a	Isla Vista	IV.F3	1.28	1.28	0.11	12.44
IV	3a	Isla Vista	IV.F3	0.91	0.91	0.11	14.05
IV	3a	Isla Vista	IV.F3	0.86	0.86	0.11	14.26
IV	3a	Isla Vista	IV.F3	0.75	0.75	0.11	14.74
IV	3a	Isla Vista	IV.F3	0.84	0.84	0.11	14.35

IV	3a	Isla Vista	IV.F3	0.98	0.98	0.11	13.74
IV	3a	Isla Vista	IV.F3	1.13	1.13	0.11	13.09
IV	3a	Isla Vista	IV.F3	1.27	1.27	0.11	12.49
IV	3a	Isla Vista	IV.F3	1.35	1.35	0.11	12.14
IV	3a	Isla Vista	IV.F3	0.96	0.96	0.11	13.83
IV	3a	Isla Vista	IV.F3	1.28	1.28	0.11	12.44
IV	3a	Isla Vista	IV.F3	0.86	0.86	0.11	14.26
IV	3a	Isla Vista	IV.F3	0.35	0.35	0.11	16.48
IV	3a	Isla Vista	IV.F3	0.52	0.52	0.11	15.74
IV	3a	Isla Vista	IV.F3	-0.19	-0.19	0.11	18.82
IV	3a	Isla Vista	IV.F3	-1.55	-1.55	0.11	24.72
IV	3a	Isla Vista	IV.F3	-0.04	-0.04	0.11	18.17
IV	3a	Isla Vista	IV.F3	0.31	0.31	0.11	16.65
IV	3a	Isla Vista	IV.F4	2.52	2.52	0.11	7.05
IV	3a	Isla Vista	IV.F4	0.27	0.27	0.11	16.81
IV	3a	Isla Vista	IV.F4	0.25	0.25	0.11	16.89
IV	3a	Isla Vista	IV.F4	0.92	0.92	0.11	14.02
IV	3a	Isla Vista	IV.F4	1.45	1.45	0.11	11.71
IV	3a	Isla Vista	IV.F4	1.41	1.41	0.11	11.86
IV	3a	Isla Vista	IV.F4	1.71	1.71	0.11	10.58
IV	3a	Isla Vista	IV.F4	0.65	0.65	0.11	15.18
IV	3a	Isla Vista	IV.F4	1.41	1.41	0.11	11.88
IV	3a	Isla Vista	IV.F4	1.40	1.40	0.11	11.94
IV	3a	Isla Vista	IV.F4	0.55	0.55	0.11	15.61
IV	3a	Isla Vista	IV.F4	1.16	1.16	0.11	12.96
IV	3a	Isla Vista	IV.F4	0.61	0.61	0.11	15.35
IV	3a	Isla Vista	IV.F4	1.11	1.11	0.11	13.18
IV	3a	Isla Vista	IV.F4	0.44	0.44	0.11	16.09
IV	3a	Isla Vista	IV.F5	1.02	1.02	0.11	13.57
IV	3a	Isla Vista	IV.F5	1.07	1.07	0.11	13.35
IV	3a	Isla Vista	IV.F5	1.47	1.47	0.11	11.62
IV	3a	Isla Vista	IV.F5	0.91	0.91	0.11	14.05
IV	3a	Isla Vista	IV.F5	0.80	0.80	0.11	14.52
IV	3a	Isla Vista	IV.F5	1.06	1.06	0.11	13.40
IV	3a	Isla Vista	IV.F5	1.47	1.47	0.11	11.61
IV	3a	Isla Vista	IV.F5	1.67	1.67	0.11	10.76

IV	3a	Isla Vista	IV.F5	1.54	1.54	0.11	11.31
IV	3a	Isla Vista	IV.F5	0.95	0.95	0.11	13.87
IV	3a	Isla Vista	IV.F5	0.59	0.59	0.11	15.44
IV	3a	Isla Vista	IV.F5	0.72	0.72	0.11	14.87
IV	3a	Isla Vista	IV.F6	1.13	1.13	0.11	13.09
IV	3a	Isla Vista	IV.F6	0.74	0.74	0.11	14.79
IV	3a	Isla Vista	IV.F6	0.85	0.85	0.11	14.31
IV	3a	Isla Vista	IV.F6	1.26	1.26	0.11	12.53
IV	3a	Isla Vista	IV.F6	0.47	0.47	0.11	15.96
IV	3a	Isla Vista	IV.F6	0.64	0.64	0.11	15.22
IV	3a	Isla Vista	IV.F6	2.26	2.26	0.11	8.19
IV	3a	Isla Vista	IV.F6	2.33	2.33	0.11	7.87
IV	3a	Isla Vista	IV.F6	0.97	0.97	0.11	13.77
IV	3a	Isla Vista	IV.F6	0.44	0.44	0.11	16.09
IV	3a	Isla Vista	IV.F6	0.09	0.09	0.11	17.61
IV	3a	Isla Vista	IV.F6	0.21	0.21	0.11	17.09
IV	3a	Isla Vista	IV.F6	0.16	0.16	0.11	17.30
IV	3a	Isla Vista	IV.F6	0.33	0.33	0.11	16.56
SNI	5e	SNI 302	302.1	0.69	0.69	0.61	17.17
SNI	5e	SNI 302	302.1	1.35	1.35	0.61	14.30
SNI	5e	SNI 302	302.1	1.38	1.38	0.61	14.17
SNI	5e	SNI 302	302.1	0.70	0.70	0.61	17.12
SNI	5e	SNI 302	302.1	0.94	0.94	0.61	16.08
SNI	5e	SNI 302	302.1	0.23	0.23	0.61	19.16
SNI	5e	SNI 302	302.1	0.81	0.81	0.61	16.65
SNI	5e	SNI 302	302.1	1.26	1.26	0.61	14.69
SNI	5e	SNI 302	302.1	0.85	0.85	0.61	16.47
SNI	5e	SNI 302	302.F2	0.64	0.64	0.61	17.38
SNI	5e	SNI 302	302.F2	0.15	0.15	0.61	19.51
SNI	5e	SNI 302	302.F2	0.27	0.27	0.61	18.99
SNI	5e	SNI 302	302.F2	0.74	0.74	0.61	16.95
SNI	5e	SNI 302	302.F2	1.42	1.42	0.61	14.00
SNI	5e	SNI 302	302.F3	0.98	0.98	0.61	15.91
SNI	5e	SNI 302	302.F3	0.94	0.94	0.61	16.08
SNI	5e	SNI 302	302.F3	0.68	0.68	0.61	17.21
SNI	5e	SNI 302	302.F3	0.98	0.98	0.61	15.91

SNI	5e	SNI 302	302.F3	0.64	0.64	0.61	17.38
SNI	5e	SNI 302	302.F3	0.54	0.54	0.61	17.82
SNI	5e	SNI 302	302.F3	0.95	0.95	0.61	16.04
SNI	5e	SNI 302	302.F3	0.88	0.88	0.61	16.34
SNI	5e	SNI 302	302.F3	0.91	0.91	0.61	16.21
SNI	5e	SNI 302	302.F3	0.71	0.71	0.61	17.08
SNI	5e	SNI 302	302.F3	0.40	0.40	0.61	18.43
SNI	5e	SNI 302	302.F3	0.61	0.61	0.61	17.51
SNI	5e	SNI 302	302.F4	0.03	0.03	0.61	20.03
SNI	5e	SNI 302	302.F4	1.54	1.54	0.61	13.48
SNI	5e	SNI 302	302.F4	0.22	0.22	0.61	19.21
SNI	5e	SNI 302	302.F4	0.38	0.38	0.61	18.51
SNI	5e	SNI 302	302.F4	0.65	0.65	0.61	17.34
SNI	5e	SNI 302	302.F4	0.45	0.45	0.61	18.21
SNI	5e	SNI 302	302.F4	0.64	0.64	0.61	17.38
SNI	5e	SNI 302	302.F4	0.43	0.43	0.61	18.30
SNI	5e	SNI 302	302.F4	0.57	0.57	0.61	17.69
SNI	5e	SNI 302	302.F4	0.57	0.57	0.61	17.69
SNI	5e	SNI 302	302.F4	0.54	0.54	0.61	17.82
SNI	5e	SNI 302	302.F4	0.63	0.63	0.61	17.43
SNI	5e	SNI 302	302.F4	0.20	0.20	0.61	19.29
SNI	5e	SNI 302	302.F4	0.25	0.25	0.61	19.08
SNI	5e	SNI 302	302.F4	0.34	0.34	0.61	18.69
SNI	5e	SNI 302	302.F4	0.35	0.35	0.61	18.64
SNI	5e	SNI 302	302.F4	0.37	0.37	0.61	18.56

Appendix II: Clumped isotopes and Δ_{47} paleo-temperatures. Individual measurements and computed parameters for biogenic aragonite *C. biplicata* powders, showing: specimen, location, locality, time period, stable and clumped isotope ratios for $\delta^{13}\text{C}_{\text{aragonite}}$, $\delta^{18}\text{O}_{\text{aragonite}}$, Δ_{47} (both raw and corrected to the Eth reference frame), Δ_{48} , and temperatures derived from Δ_{47} . Data from the Department of Earth and Planetary Sciences at the University of California, Berkeley.

Location	Time Period	Locality	Specimen	$\delta^{13}\text{C}$ ‰ VPDB	$\delta^{18}\text{O}$ ‰ VPDB	Δ_{47} ‰ pbl	Δ_{47} standard deviation	Δ_{48} ‰	Δ_{48} standard deviation	Δ_{47} corrected to ETH	Δ_{47} temperature
SNI	5a	11004/05	11004/05.3	1.74	1.82	-0.26	0.03	2.12	0.08	0.71	12.71
SNI	5a	11004/05	11004/05.3	1.79	1.87	-0.27	0.01	2.06	0.09	0.67	22.55
SNI	5a	11004/05	11004/05.3	1.86	1.94	-0.24	0.02	2.11	0.11	0.72	10.50
SNI	5a	11004/05	11004/05.3	1.84	1.92	-0.25	0.03	2.76	0.12	0.70	17.80
SNI	5a	11004/05	11004/05.3	1.79	1.87	-0.25	0.02	2.41	0.09	0.70	12.90
SNI	5a	11004/05	11004/05.3	1.78	1.86	-0.26	0.02	2.47	0.07	0.71	11.36
SNI	5a	11004/05	11004/05.4	1.79	1.87	-0.27	0.03	1.73	0.09	0.67	22.46
SNI	5a	11004/05	11004/05.4	1.92	1.99	-0.26	0.02	1.98	0.06	0.71	13.67
SNI	5a	11004/05	11004/05.4	1.93	2.01	-0.25	0.02	2.30	0.09	0.71	12.53
SNI	5a	11004/05	11004/05.4	1.89	1.97	-0.24	0.02	2.74	0.11	0.73	9.91
SNI	5a	11004/05	11004/05.4	1.78	1.86	-0.27	0.02	2.70	0.08	0.70	19.09
SNI	5a	11004/05	11004/05.4	1.92	2.00	-0.24	0.02	2.43	0.12	0.70	12.54
SNI	5c/5e	11006	11006.F3	2.10	2.17	-0.26	0.02	2.04	0.10	0.71	12.91
SNI	5c/5e	11006	11006.F3	2.08	2.15	-0.27	0.02	2.09	0.08	0.70	15.30
SNI	5c/5e	11006	11006.F3	2.00	2.08	-0.26	0.02	2.16	0.05	0.71	11.57
SNI	5c/5e	11006	11006.F4	1.90	1.98	-0.27	0.01	1.91	0.15	0.70	16.16
SNI	5c/5e	11006	11006.F4	1.82	1.90	-0.26	0.03	1.90	0.12	0.68	19.57
SNI	5c/5e	11006	11006.F4	1.88	1.96	-0.25	0.02	2.30	0.11	0.72	9.06
SNI	5c/5e	11006	11006.F4	1.90	1.98	-0.25	0.02	2.46	0.13	0.70	12.96
SNI	5c/5e	11006	11006.F4	1.82	1.90	-0.26	0.02	2.66	0.07	0.71	15.85
SNI	5a	11747	11747.1	1.86	1.94	-0.24	0.02	2.94	0.11	0.73	11.04
SNI	5a	11747	11747.1	1.83	1.90	-0.26	0.02	1.86	0.08	0.71	13.55
SNI	5a	11747	11747.1	1.87	1.94	-0.25	0.03	2.12	0.12	0.72	9.82
SNI	5a	11747	11747.1	1.85	1.93	-0.26	0.03	2.43	0.11	0.71	12.28
SNI	5a	11747	11747.1	1.94	2.02	-0.27	0.02	2.54	0.09	0.69	16.78
SNI	5a	11747	11747.F4	1.76	1.84	-0.24	0.02	2.38	0.12	0.71	12.05
SNI	5a	11747	11747.F4	1.81	1.89	-0.25	0.02	2.43	0.13	0.69	17.12
SNI	5a	11747	11747.F4	1.76	1.84	-0.23	0.02	2.30	0.10	0.72	9.60
SNI	5a	11747	11747.F4	1.62	1.69	-0.26	0.02	2.61	0.09	0.70	17.68
SNI	5c/5e	11749	11749.1	1.09	1.17	-0.27	0.03	2.47	0.07	0.68	18.19
SNI	5c/5e	11749	11749.1	1.11	1.20	-0.25	0.02	2.55	0.07	0.70	17.12
SNI	5c/5e	11749	11749.4	1.59	1.67	-0.26	0.02	2.44	0.05	0.70	12.81
SNI	5c/5e	11749	11749.4	1.56	1.64	-0.26	0.02	2.52	0.06	0.71	11.13
SNI	5c/5e	11749	11749.4	1.63	1.71	-0.25	0.02	2.65	0.06	0.72	12.56
PVH	5a	12575	12575.1	1.96	2.03	-0.26	0.02	2.18	0.10	0.70	13.59
PVH	5a	12575	12575.1	2.00	2.08	-0.27	0.02	2.36	0.12	0.70	14.91
PVH	5a	12575	12575.1	2.02	2.09	-0.26	0.01	2.29	0.10	0.70	13.83

PVH	5e	12608	12608.3	1.28	1.36	-0.26	0.02	1.78	0.08	0.70	14.43
PVH	5e	12608	12608.3	1.08	1.17	-0.27	0.02	1.84	0.09	0.68	21.13
PVH	5e	12608	12608.3	1.21	1.29	-0.27	0.03	2.12	0.09	0.69	16.87
PVH	5e	12608	12608.4	1.49	1.57	-0.26	0.03	1.76	0.09	0.68	20.08
PVH	5e	12608	12608.4	1.48	1.56	-0.26	0.02	2.23	0.11	0.69	15.89
PVH	5e	12608	12608.4	1.40	1.48	-0.28	0.02	2.40	0.10	0.69	17.26
SNI	5e	SNI 128	128.F1	1.32	1.40	-0.25	0.02	2.77	0.13	0.71	15.49
SNI	5e	SNI 128	128.F2	0.53	0.62	-0.24	0.04	2.56	0.09	0.72	12.55
SNI	5e	SNI 128	128.F1	1.28	1.36	-0.26	0.02	2.18	0.10	0.68	19.42
SNI	5e	SNI 128	128.F1	1.20	1.28	-0.27	0.03	2.27	0.15	0.70	14.59
SNI	5e	SNI 128	128.F1	1.30	1.38	-0.27	0.02	2.28	0.05	0.70	14.45
SNI	5e	SNI 128	128.F2	0.53	0.62	-0.26	0.02	2.26	0.09	0.71	11.64
SNI	5e	SNI 128	128.F2	0.52	0.61	-0.24	0.02	2.24	0.08	0.72	9.28
SNI	5e	SNI 128	128.F2	0.54	0.62	-0.26	0.02	2.41	0.08	0.71	11.85
SNI	5e	SNI 302	302.1	1.52	1.60	-0.27	0.02	2.13	0.09	0.69	17.60
SNI	5e	SNI 302	302.1	1.51	1.59	-0.26	0.02	2.17	0.09	0.71	12.57
SNI	5e	SNI 302	302.1	1.25	1.34	-0.26	0.01	2.25	0.20	0.70	14.61
SNI	5e	SNI 302	302.1	1.52	1.60	-0.26	0.02	2.77	0.08	0.70	18.71
SNI	5e	SNI 302	302.F2	0.97	1.05	-0.26	0.02	2.49	0.10	0.69	19.44
SNI	5e	SNI 302	302.F2	0.95	1.04	-0.27	0.02	1.97	0.10	0.68	21.87
SNI	5e	SNI 302	302.F2	0.93	1.01	-0.27	0.02	2.20	0.11	0.70	14.92
SNI	5e	SNI 302	302.F2	0.90	0.98	-0.28	0.02	2.03	0.11	0.67	21.76
SNI	5e	SNI 302	302.F2	0.95	1.03	-0.26	0.03	2.77	0.11	0.69	20.03
SNI	5e	SNI 302	302.F2	0.86	0.94	-0.27	0.03	2.57	0.09	0.70	17.65
PVH	5a	12575	12575.2	1.98	2.06	-0.26	0.02	1.78	0.13	0.68	20.36
PVH	5a	12575	12575.2	1.95	2.02	-0.26	0.02	1.79	0.14	0.69	18.65
PVH	5a	12575	12575.2	1.99	2.07	-0.25	0.03	1.98	0.14	0.72	11.85
PVH	5a	12575	12575.2	1.93	2.01	-0.26	0.02	2.26	0.10	0.69	15.98
PVH	5a	12575	12575.2	1.72	1.79	-0.24	0.02	2.26	0.17	0.72	8.41
IV	3a	Isla Vista	IV.F3	1.34	1.42	-0.26	0.01	2.68	0.10	0.71	15.54
IV	3a	Isla Vista	IV.F3	1.12	1.20	-0.25	0.02	2.54	0.07	0.71	16.05
IV	3a	Isla Vista	IV.F3	1.02	1.11	-0.26	0.02	2.50	0.09	0.70	18.32
IV	3a	Isla Vista	IV.F3	1.07	1.15	-0.25	0.04	2.57	0.13	0.72	11.37
IV	3a	Isla Vista	IV.F6	1.05	1.13	-0.27	0.02	2.42	0.14	0.70	18.12
IV	3a	Isla Vista	IV.F6	1.18	1.26	-0.27	0.02	1.66	0.08	0.67	22.59
IV	3a	Isla Vista	IV.F6	1.09	1.17	-0.26	0.02	1.83	0.13	0.71	13.81
IV	3a	Isla Vista	IV.F6	1.07	1.15	-0.25	0.02	2.19	0.08	0.71	12.94
IV	3a	Isla Vista	IV.F6	1.05	1.13	-0.25	0.02	2.47	0.13	0.70	15.92
IV	3a	Isla Vista	IV.F6	1.09	1.17	-0.24	0.03	2.54	0.11	0.73	5.35
SNI	8th terrace	SNI 11	SNI-11.2	1.37	1.45	-0.27	0.02	2.44	0.07	0.68	22.24
SNI	8th terrace	SNI 11	SNI-11.2	1.45	1.53	-0.27	0.03	2.55	0.09	0.70	16.61
SNI	8th terrace	SNI 11	SNI-11.2	1.50	1.58	-0.26	0.02	2.51	0.13	0.70	17.52
SNI	8th terrace	SNI 11	SNI-11.2	1.43	1.51	-0.25	0.03	2.64	0.07	0.72	12.65
SNI	8th terrace	SNI 11	SNI-11.2	1.40	1.48	-0.26	0.02	2.53	0.11	0.70	17.90
SNI	8th terrace	SNI 11	SNI-11.3	1.09	1.17	-0.26	0.02	2.44	0.10	0.68	22.69
SNI	8th terrace	SNI 11	SNI-11.3	1.02	1.11	-0.27	0.02	2.42	0.11	0.70	17.60

SNI	8th terrace	SNI 11	SNI-11.3	1.35	1.43	-0.26	0.01	2.51	0.12	0.70	17.29
SNI	10th terrace	SNI 3	SNI-3.F2	1.66	1.74	-0.26	0.02	2.38	0.11	0.68	18.07
SNI	10th terrace	SNI 3	SNI-3.F2	1.66	1.74	-0.26	0.03	2.45	0.08	0.70	18.43
SNI	10th terrace	SNI 3	SNI-3.F2	1.66	1.74	-0.26	0.02	2.62	0.14	0.68	23.66
SNI	10th terrace	SNI 3	SNI-3.F3	1.80	1.87	-0.26	0.02	2.50	0.11	0.69	14.89
SNI	10th terrace	SNI 3	SNI-3.F3	1.81	1.89	-0.25	0.02	2.74	0.08	0.71	15.94
SNI	10th terrace	SNI 3	SNI-3.F3	1.81	1.89	-0.25	0.02	2.64	0.09	0.71	15.37
SNI	11th terrace	SNI 519	SNI-519.F3	1.58	1.66	-0.26	0.03	2.52	0.10	0.71	15.85
SNI	11th terrace	SNI 519	SNI-519.F3	1.57	1.65	-0.25	0.02	2.59	0.13	0.72	12.30
SNI	11th terrace	SNI 519	SNI-519.F3	1.61	1.69	-0.27	0.01	2.48	0.13	0.69	20.65
SNI	11th terrace	SNI 519	SNI-519.F3	1.53	1.61	-0.25	0.02	2.58	0.13	0.70	15.83
SNI	11th terrace	SNI 519	SNI-519.F4	1.73	1.81	-0.25	0.02	2.42	0.15	0.71	10.19
SNI	11th terrace	SNI 519	SNI-519.F4	1.69	1.77	-0.26	0.02	2.49	0.12	0.69	21.06
SNI	11th terrace	SNI 519	SNI-519.F4	1.72	1.80	-0.27	0.02	2.69	0.10	0.70	17.48

Appendix III: Pleistocene faunas of Isla Vista, Palos Verdes Hills, and San Nicolas Island. Fossil bivalves and gastropods from Pleistocene localities in Palos Verdes Hills (12575 and 12608), Isla Vista (Coal Oil Point), and San Nicolas Island (SN-6; SN-11; SN-3; SNI-128; 11004/05; 11006; 11749; 11747 SNI-302/205); modern faunal list for San Nicolas Island (SNI modern). Species names are taxonomically standardized (see Chapter II for standardization description).

Taxonomy		Pleistocene Fossil Locality												
Class	Scientific name	SNI modern	SN-6	SN-11	SN-3	Coal Oil Point	12575	12608	SNI-128	11004/05	11006	11749	11747	SNI-302/05
Bivalvia	Ameritella modesta	0	0	0	0	1	0	0	0	0	0	0	0	0
Bivalvia	Bernardina bakeri	0	0	1	0	0	0	0	0	0	1	0	0	0
Bivalvia	Callithaca tenerrima	0	0	0	0	1	0	0	0	0	0	0	0	0
Bivalvia	Caryocorbula luteola	0	0	0	0	0	0	1	0	0	0	0	0	0
Bivalvia	Chacea ovoidea	0	0	0	0	1	0	0	0	0	0	0	1	0
Bivalvia	Chama arcana	1	0	0	0	0	0	1	0	0	0	0	0	1
Bivalvia	Chlamys hastata	1	0	0	1	0	1	0	0	0	1	0	0	0
Bivalvia	Clinocardium nuttallii	0	0	0	1	1	0	0	0	0	0	0	1	0
Bivalvia	Crassadoma gigantea	1	0	0	1	0	0	0	0	0	0	1	1	0
Bivalvia	Cryptomya californica	1	0	0	0	1	0	0	0	0	0	1	0	0
Bivalvia	Cumingia californica	1	0	1	1	0	1	1	0	1	1	0	1	1
Bivalvia	Dallocardia quadragenaria	0	0	0	0	0	0	0	0	0	0	1	0	0
Bivalvia	Epilucina californica	1	1	1	1	0	1	1	1	1	1	1	1	1
Bivalvia	Gari californica	1	0	0	1	0	0	0	0	0	0	0	0	0
Bivalvia	Gari fucata	0	0	0	0	0	0	0	0	0	0	0	1	0
Bivalvia	Glans carpenteri	1	1	1	1	0	1	1	1	1	1	1	1	1
Bivalvia	Glycymeris septentrionalis	1	0	0	1	0	0	0	0	0	0	1	0	0
Bivalvia	Here excavata	0	0	0	0	0	0	0	0	0	0	1	0	0
Bivalvia	Hiatella arctica	1	0	0	0	0	0	1	0	0	0	1	1	0
Bivalvia	Irusella lamellifera	1	0	0	1	1	0	1	0	0	0	1	0	0
Bivalvia	Leptopecten latiauratus	1	0	0	0	0	1	0	0	0	0	0	0	0
Bivalvia	Leukoma staminea	1	0	1	1	1	1	1	0	1	0	1	1	0
Bivalvia	Lucinisca nuttalli	1	0	0	0	1	0	0	0	0	0	1	0	0
Bivalvia	Lucinoma annulata	0	0	0	0	0	0	0	0	0	0	1	0	0
Bivalvia	Macoma inquinata	0	0	0	0	1	0	0	0	0	0	0	0	0
Bivalvia	Macoma nasuta	0	0	0	0	1	0	0	0	0	0	0	0	0
Bivalvia	Macoma obliqua	0	0	0	0	1	0	0	0	0	0	0	0	0
Bivalvia	Macoploma acolasta	0	0	0	0	1	0	0	0	0	0	0	0	0

Bivalvia	<i>Macoploma yoldiformis</i>	0	0	0	0	1	0	0	0	0	0	0	0	0
Bivalvia	<i>Megangulus bodegensis</i>	1	0	0	0	1	0	0	0	0	0	0	0	0
Bivalvia	<i>Milneria minima</i>	0	0	0	1	0	0	0	0	0	0	0	0	0
Bivalvia	<i>Mytilisepta bifurcata</i>	1	0	1	0	0	1	0	0	1	0	0	1	1
Bivalvia	<i>Mytilus californianus</i>	1	1	1	1	0	0	1	0	1	0	1	0	0
Bivalvia	<i>Nutricola cymata</i>	0	0	0	0	0	0	0	0	0	0	0	1	0
Bivalvia	<i>Nutricola ovalis</i>	0	0	0	0	0	0	0	0	0	0	0	1	0
Bivalvia	<i>Nutricola tantilla</i>	1	1	1	1	1	1	0	0	0	1	0	0	0
Bivalvia	<i>Ostrea lurida</i>	0	0	0	0	1	0	0	0	0	0	0	0	0
Bivalvia	<i>Panopea generosa</i>	1	0	0	0	0	0	0	0	0	0	1	1	0
Bivalvia	<i>Parapholas californica</i>	1	0	0	0	1	0	0	0	0	0	1	1	0
Bivalvia	<i>Penitella penita</i>	1	0	0	1	1	0	0	0	0	0	0	1	0
Bivalvia	<i>Penitella turnae</i>	0	0	0	0	0	1	0	0	0	0	0	0	0
Bivalvia	<i>Petricola californiensis</i>	0	0	0	0	0	0	0	0	1	0	0	0	0
Bivalvia	<i>Petricola carditoides</i>	1	0	0	1	0	0	0	0	0	0	1	0	0
Bivalvia	<i>Platyodon cancellatus</i>	1	0	0	0	1	0	0	0	0	0	0	0	0
Bivalvia	<i>Pododesmus macrochisma</i>	1	0	0	0	1	0	0	0	0	0	0	1	0
Bivalvia	<i>Rexithaerus expansa</i>	0	0	0	0	1	0	0	0	0	0	0	0	0
Bivalvia	<i>Rexithaerus indentata</i>	1	0	0	0	1	0	0	0	0	0	0	0	0
Bivalvia	<i>Saccella taphria</i>	0	0	0	0	1	0	0	0	0	0	0	0	0
Bivalvia	<i>Saxidomus gigantea</i>	0	0	0	0	1	0	0	0	0	0	0	0	0
Bivalvia	<i>Saxidomus nuttalli</i>	1	0	0	1	1	0	0	0	0	0	1	0	0
Bivalvia	<i>Simomactra planulata</i>	0	0	0	0	0	0	0	0	0	0	1	0	0
Bivalvia	<i>Solen sicarius</i>	0	0	0	0	1	0	0	0	0	0	0	0	0
Bivalvia	<i>Tresus capax</i>	0	0	0	0	1	0	0	0	0	0	0	0	0
Bivalvia	<i>Tresus nuttallii</i>	0	0	0	1	1	0	0	0	0	0	1	1	0
Bivalvia	<i>Zemysina orbella</i>	1	0	0	1	0	0	0	0	0	0	0	0	0
Bivalvia	<i>Zirfaea pilsbryi</i>	0	0	0	0	1	0	0	0	0	0	0	0	0
Gastropoda	<i>Acanthinucella paucilirata</i>	1	0	0	0	0	0	0	0	0	0	0	0	0
Gastropoda	<i>Acanthinucella spirata</i>	1	0	0	0	0	0	1	0	0	0	0	0	0
Gastropoda	<i>Acmaea mitra</i>	1	1	1	1	0	1	1	1	1	1	1	1	1
Gastropoda	<i>Acteocina inculta</i>	0	0	0	0	0	0	0	0	0	1	0	0	0
Gastropoda	<i>Alia carinata</i>	1	1	0	1	1	1	1	0	1	0	0	1	0
Gastropoda	<i>Alvania compacta</i>	0	0	0	0	0	0	0	0	1	1	0	0	0
Gastropoda	<i>Amphissa columbiana</i>	0	0	0	0	1	0	0	0	0	0	1	0	0
Gastropoda	<i>Amphissa versicolor</i>	1	0	0	1	0	0	1	0	1	0	0	1	1
Gastropoda	<i>Amphithalamus inclusus</i>	0	0	1	1	0	0	0	0	0	1	0	0	0
Gastropoda	<i>Assiminea translucens</i>	0	0	0	1	0	0	0	0	0	0	0	0	0
Gastropoda	<i>Atrimitra idae</i>	1	0	1	1	0	0	0	1	0	1	1	0	0

Gastropoda	Barbarofusus barbarentis	0	0	0	0	1	0	0	0	0	0	0	0	0
Gastropoda	Barbarofusus kobelti	0	0	0	1	0	0	0	0	0	0	0	0	0
Gastropoda	Barleeia californica	0	0	0	0	0	1	0	0	0	1	0	0	0
Gastropoda	Barleeia haliotiphila	0	0	0	0	0	0	0	0	0	1	0	0	0
Gastropoda	Caecum californicum	0	0	1	1	0	0	0	0	1	1	0	0	0
Gastropoda	Caecum crebricinctum	0	0	0	0	0	0	0	0	1	1	0	0	0
Gastropoda	Caecum dextroversum	0	0	0	1	1	0	0	0	0	0	0	0	0
Gastropoda	Caecum quadratum	0	0	1	1	0	0	0	0	0	0	0	0	0
Gastropoda	Californiconus californicus	1	1	1	1	0	1	1	0	0	1	1	1	0
Gastropoda	Calliostoma annulatum	1	0	0	0	0	0	0	0	1	0	0	0	0
Gastropoda	Calliostoma ligatum	1	0	0	0	0	0	0	0	0	1	0	0	0
Gastropoda	Ceratostoma foliatum	0	0	0	1	0	0	0	0	0	0	0	0	0
Gastropoda	Cerithiopsisidella cosmia	1	0	0	0	0	1	0	0	0	0	0	0	0
Gastropoda	Clathromangelia rhyssa	0	0	0	0	0	0	0	0	0	1	0	0	0
Gastropoda	Crepidula naticarum	0	0	0	0	0	0	0	0	0	1	0	1	0
Gastropoda	Crepidula norrisiarum	0	0	0	0	0	1	0	0	0	0	0	0	0
Gastropoda	Crepidula nummaria	1	0	0	0	1	0	0	0	0	0	0	0	0
Gastropoda	Crepidula perforans	0	0	0	1	0	1	1	0	0	0	0	1	0
Gastropoda	Crepidatella lingulata	1	0	1	1	1	1	1	0	1	1	1	0	0
Gastropoda	Crockerella conradiana	0	0	0	0	0	1	0	0	0	0	0	0	0
Gastropoda	Crossata californica	0	0	0	0	0	0	1	0	0	0	0	0	0
Gastropoda	Diodora arnoldi	1	0	0	0	0	1	1	0	1	0	1	0	0
Gastropoda	Diodora aspera	1	1	1	1	1	1	1	0	0	1	0	1	0
Gastropoda	Discurria inessa	1	0	1	0	0	1	1	0	1	1	1	1	1
Gastropoda	Epitonium tinctum	1	0	0	0	0	0	0	0	0	1	0	0	0
Gastropoda	Fissurella volcano	1	0	1	0	0	1	1	1	1	1	1	1	1
Gastropoda	Fissurellidea bimaculata	1	0	1	0	1	0	0	0	0	0	1	0	0
Gastropoda	Fusitriton oregonensis	0	0	0	0	1	0	0	0	0	0	0	0	0
Gastropoda	Granulina margaritula	1	0	0	0	0	0	0	0	1	1	0	0	0
Gastropoda	Haliotis cracherodii	1	0	0	1	0	1	1	0	0	0	0	0	1
Gastropoda	Haliotis kamtschatkana	0	0	0	1	0	0	0	0	0	0	0	0	0
Gastropoda	Haliotis rufescens	1	0	0	1	0	1	0	0	1	1	0	1	1
Gastropoda	Halistylus pupoideus	0	0	0	1	0	0	0	0	0	0	0	0	0
Gastropoda	Harfordia harfordii	0	0	0	0	0	0	0	0	1	0	0	1	0
Gastropoda	Hipponix antiquatus	1	1	1	1	0	1	1	0	0	0	1	0	1
Gastropoda	Hipponix panamensis	0	0	0	0	0	0	0	0	1	1	0	0	1
Gastropoda	Hipponix tumens	1	1	0	1	0	1	1	0	1	1	0	1	1
Gastropoda	Homalopoma baculum	1	0	0	0	0	0	1	0	0	0	0	0	0
Gastropoda	Homalopoma luridum	1	1	1	1	0	1	0	0	1	1	1	0	1

Gastropoda	Homalopoma paucicostatum	1	0	0	0	0	0	1	0	0	0	0	0
Gastropoda	Lacuna unifasciata	1	1	1	1	0	1	0	0	0	0	0	0
Gastropoda	Liotia fenestrata	1	0	0	1	0	0	0	0	0	0	0	0
Gastropoda	Lirabuccinum dirum	0	1	0	1	0	0	0	0	0	0	0	0
Gastropoda	Lirobittium attenuatum	1	0	1	0	0	0	1	0	0	0	0	1
Gastropoda	Lirobittium interfossa	1	0	0	0	0	0	0	0	0	1	0	0
Gastropoda	Lirobittium purpureum	1	0	0	0	1	1	0	0	0	0	0	0
Gastropoda	Lirobittium quadrifilatum	0	0	0	0	0	1	0	0	1	0	0	1
Gastropoda	Lirularia lirulata	0	0	0	0	1	0	0	0	0	0	0	0
Gastropoda	Littorina keenae	1	0	0	0	0	0	0	0	1	1	0	0
Gastropoda	Littorina plena	0	0	0	0	0	0	0	0	0	0	0	1
Gastropoda	Littorina scutulata	1	0	0	1	0	1	0	0	0	1	0	1
Gastropoda	Lottia asmi	1	0	1	0	0	1	0	0	0	0	0	0
Gastropoda	Lottia digitalis	1	1	1	1	0	0	0	0	0	0	1	0
Gastropoda	Lottia gigantea	1	0	0	0	0	0	1	0	1	0	0	0
Gastropoda	Lottia instabilis	1	0	0	0	0	0	0	0	0	0	1	0
Gastropoda	Lottia limatula	1	0	0	1	0	0	0	0	0	0	0	0
Gastropoda	Lottia pelta	1	0	0	1	0	0	0	0	1	0	0	1
Gastropoda	Lottia scabra	1	0	0	0	0	1	1	1	1	1	1	1
Gastropoda	Lottia scutum	1	0	0	1	0	0	0	0	0	0	1	0
Gastropoda	Marsenina rhombica	0	0	0	1	0	0	0	0	0	0	0	0
Gastropoda	Megastraea undosa	1	0	0	0	0	0	1	0	0	0	0	0
Gastropoda	Melanella thersites	0	0	1	0	0	0	0	0	0	0	0	0
Gastropoda	Mitrella tuberosa	1	0	1	1	0	1	1	0	1	0	0	1
Gastropoda	Nassarina penicillata	1	0	0	0	0	1	0	0	0	0	0	0
Gastropoda	Nassarius fossatus	0	0	0	0	1	0	0	0	0	0	0	0
Gastropoda	Nassarius mendicus	0	0	0	0	1	1	1	0	0	1	0	1
Gastropoda	Nassarius perpinguis	1	0	0	0	1	0	1	0	0	0	0	0
Gastropoda	Neobernaya spadicea	1	0	0	0	0	0	0	0	0	0	0	0
Gastropoda	Neostylidium eschrichtii	1	1	0	1	0	0	0	0	0	0	0	1
Gastropoda	Neverita reclusiana	0	0	0	0	0	0	0	0	0	0	0	0
Gastropoda	Norrisia norrisii	1	0	0	0	0	0	1	0	0	0	0	0
Gastropoda	Ocinebrina gracillima	0	0	0	0	0	0	0	0	0	0	1	0
Gastropoda	Odostomia gravida	0	0	0	0	0	1	0	0	0	0	0	0
Gastropoda	Odostomia turricula	0	0	0	0	0	0	0	0	0	1	0	0
Gastropoda	Olivella baetica	1	0	0	0	0	0	0	0	1	0	1	0
Gastropoda	Olivella biplicata	1	1	1	1	1	1	1	1	1	1	1	1
Gastropoda	Opalia montereyensis	0	0	0	0	0	0	0	0	0	1	0	1
Gastropoda	Pomaulax gibberosus	1	1	0	1	0	0	0	0	0	0	1	0

Gastropoda	<i>Pseudomelatoma torosa</i>	0	0	0	0	0	0	0	0	0	0	1	1	0
Gastropoda	<i>Pseudopusula californiana</i>	1	0	1	0	0	0	0	0	0	0	0	0	0
Gastropoda	<i>Seila montereyensis</i>	1	0	0	0	0	1	0	0	0	0	0	0	0
Gastropoda	<i>Tectura depicta</i>	0	0	0	0	0	0	0	0	1	1	0	0	0
Gastropoda	<i>Tectura paleacea</i>	1	0	0	0	0	0	0	0	0	0	1	0	0
Gastropoda	<i>Tegula brunnea</i>	1	1	1	1	0	0	0	0	0	0	0	0	0
Gastropoda	<i>Tegula funebris</i>	1	1	1	1	0	1	1	0	1	1	1	1	0
Gastropoda	<i>Tegula gallina</i>	1	0	1	0	0	0	1	0	0	0	0	0	1
Gastropoda	<i>Tegula montereyi</i>	0	0	0	0	0	0	0	0	0	0	1	0	0
Gastropoda	<i>Tegula pulligo</i>	1	0	0	1	0	0	0	0	0	0	1	0	0
Gastropoda	<i>Thylacodes squamigerus</i>	1	1	1	1	0	0	1	1	0	0	1	1	1
Gastropoda	<i>Trimusculus reticulatus</i>	1	0	1	1	0	1	1	0	1	0	1	0	0
Gastropoda	<i>Triphora pedroana</i>	1	0	0	0	0	1	1	0	1	1	1	0	0
Gastropoda	<i>Turritella cooperi</i>	0	0	0	0	1	0	0	0	0	0	0	0	0
Gastropoda	<i>Vitrinella oldroydi</i>	0	0	0	0	0	0	0	0	0	1	0	0	0

Appendix IV: Present-day ranges of Pleistocene mollusks from California. Present-day thermal maxima and minima; maincoast, and Gulfo de California latitudinal endpoints; and offshore island occurrences for Pleistocene bivalve and gastropod species from California. Abbreviations: sum max = summer maximum temperature (°C), win min = winter minimum temperature (°C); N.M = northern maincoast latitude; S.M = southern maincoast latitude; NW = northwest Gulfo de California latitude; NE = southwest Gulfo de California latitude; SW = southwest Gulfo de California latitude; SE = southeast Gulfo de California latitude; Sni = San Nicolas Island; Roc = Rocas Alijos; Coc = Coco Island; Rev = Islas Revillagigedo; Gal = Galapagos Islands; Gua = Guadalupe Island; Smi = San Miguel Island; Sro = Santa Rosa Island; Scr = Santa Cruz Island; Ana = Anacapa Island; Sca = Santa Catalina Island; Scl = San Clemente Island.

Scientific name	Thermal Range		Maincoast		Gulfo de California				Islands												
	Sum max	Win min	N.M	S.M	NW	NE	SW	SE	Sni	Roc	Coc	Rev	Gal	Gua	Smi	Sro	Scr	Ana	Sba	Sca	Scl
<i>Ameritella modesta</i>	20.91	2.781	59.2	27.7	NA	NA	NA	NA	0	0	0	0	0	0	0	0	0	0	0	0	0
<i>Bernardina bakeri</i>	20.719	12.583	36.6	27.9	NA	NA	NA	NA	0	0	0	0	0	1	0	0	0	0	0	0	0
<i>Callithaca tenerrima</i>	20.91	5.364	57.3	27.6	NA	NA	NA	NA	0	0	0	0	0	0	0	0	0	0	0	0	0
<i>Caryocorbula luteola</i>	32.836	12.563	36.7	22.9	24.2	30	22.9	26.3	0	0	0	0	0	0	0	0	0	0	0	0	0
<i>Chaceia ovoidea</i>	20.91	11.83	37.9	27.7	NA	NA	NA	NA	0	0	0	0	0	0	0	0	0	0	0	0	0
<i>Chama arcana</i>	32.836	12.508	37.1	9.7	29	31.1	22.9	22.9	1	0	0	0	0	0	1	1	1	1	1	1	0
<i>Chlamys hastata</i>	20.719	2.781	58.7	32.7	NA	NA	NA	NA	1	0	0	0	0	0	0	0	1	0	0	0	0
<i>Clinocardium nuttallii</i>	20.719	-1.18	63.1	32.7	NA	NA	NA	NA	0	0	0	0	0	0	0	0	0	0	0	0	0

<i>Crassadoma gigantea</i>	27.063	3.992	60.2	22.9	NA	27.9	NA	27.9	1	0	0	0	0	1	0	0	1	0	1	0	0	
<i>Cryptomya californica</i>	32.836	3.992	59.5	-5.8	31.7	31.7	22.9	22.9	1	0	0	0	0	0	0	0	0	0	0	1	0	
<i>Cumingia californica</i>	23.798	10.582	41.8	26.1	NA	NA	NA	NA	1	0	0	0	0	0	0	0	0	0	0	0	0	
<i>Dallocardia quadragenaria</i>	20.91	12.583	36.6	27.7	NA	NA	NA	NA	0	0	0	0	0	0	0	0	0	0	0	0	0	
<i>Epilucina californica</i>	24.729	10.582	41.8	24.5	NA	NA	NA	NA	1	1	0	0	0	1	0	0	0	0	0	0	0	
<i>Gari californica</i>	24.729	3.992	60.8	24.6	NA	NA	NA	NA	1	0	0	0	0	0	0	0	0	0	0	0	0	
<i>Gari fucata</i>	32.836	13.56	34	24.6	30.3	30.2	30.3	23.1	0	0	0	0	0	0	0	0	1	0	0	0	0	
<i>Glans carpenteri</i>	20.91	6.546	53.9	27.7	NA	NA	NA	NA	1	0	0	0	0	1	0	0	1	0	1	1	1	
<i>Glycymeris septentrionalis</i>	22.852	2.781	59.2	32.7	29.1	NA	29.1	NA	1	1	0	0	0	1	0	0	0	0	0	0	0	
<i>Here excavata</i>	32.836	13.666	34.4	23.2	31.1	28	29	23.2	0	0	0	0	0	0	0	0	0	0	0	0	0	
<i>Hiatella arctica</i>	32.836	-1.18	71.4	-55	31.7	31.7	22.9	22.9	1	0	0	0	1	0	1	1	1	1	1	1	0	0
<i>Irusella lamellifera</i>	20.719	9.999	43.4	30.5	NA	NA	NA	NA	1	0	0	0	0	0	0	0	0	0	0	0	0	0
<i>Leptopecten latiauratus</i>	27.063	11.83	38	22.9	NA	NA	NA	NA	1	0	0	0	0	0	0	0	0	0	0	0	0	0
<i>Leukoma staminea</i>	27.063	2.781	60.8	22.9	NA	NA	NA	NA	1	0	0	0	0	0	0	0	0	0	0	0	0	0

<i>Lucinisca nuttalli</i>	32.836	12.563	36.7	20.4	31	31.3	26.1	20.4	1	0	0	0	0	0	0	0	0	0	0	0	0
<i>Lucinoma annulata</i>	31.49	3.992	60.8	22.9	29.5	27.9	25.7	27.9	0	0	1	0	0	0	0	0	0	0	0	0	0
<i>Macoma inquinata</i>	17.58	-0.673	60	34.1	NA	NA	NA	NA	0	0	0	0	0	0	0	0	0	0	0	0	0
<i>Macoma nasuta</i>	32.836	2.781	59.2	20.4	31.1	31.1	31.1	20.4	0	0	0	0	0	0	0	0	0	0	0	0	0
<i>Macoma obliqua</i>	14.946	-1.18	71.4	47.5	NA	NA	NA	NA	0	0	0	0	0	0	0	0	0	0	0	0	0
<i>Macoploma acolasta</i>	20.066	11.261	38.3	33.7	NA	NA	NA	NA	0	0	0	0	0	0	0	0	0	0	0	0	0
<i>Macoploma yoldiformis</i>	20.91	5.364	57.1	27.7	NA	NA	NA	NA	0	0	0	0	0	0	0	0	0	0	0	0	0
<i>Megangulus bodegensis</i>	24.729	5.364	57.1	24.6	NA	NA	NA	NA	1	0	0	0	0	0	0	0	0	0	0	0	0
<i>Milneria minima</i>	24.703	6.912	50.8	25	NA	NA	NA	NA	0	1	0	0	0	1	0	0	0	0	0	0	0
<i>Mytilisepta bifurcata</i>	27.063	12.563	36.7	22.9	NA	NA	NA	NA	1	0	0	0	0	0	1	1	1	1	1	1	1
<i>Mytilus californianus</i>	27.286	2.781	59.2	27.7	NA	NA	NA	NA	1	0	0	1	0	0	1	1	1	1	1	1	1
<i>Nutricola cymata</i>	24.729	13.56	34.4	24.5	31.3	NA	31.2	NA	0	1	0	0	0	1	0	1	0	0	0	0	0
<i>Nutricola ovalis</i>	20.91	11.261	39.5	27.7	NA	NA	NA	NA	0	0	0	0	0	0	0	0	0	0	0	0	0
<i>Nutricola tantilla</i>	20.719	3.992	60.8	28.2	NA	NA	NA	NA	1	0	0	0	0	0	0	0	0	0	0	0	0

<i>Ostrea lurida</i>	30.52	5.364	57.1	7	NA	NA	NA	NA	0	0	0	0	0	0	0	0	0	0	0	0	1	0
<i>Panopea generosa</i>	20.293	2.781	58	33.6	NA	NA	NA	NA	1	0	0	0	0	0	0	0	0	0	0	0	0	0
<i>Parapholas californica</i>	23.462	11.261	38.3	26.2	NA	NA	NA	NA	1	0	0	0	0	0	0	0	0	0	0	0	0	0
<i>Penitella penita</i>	23.462	3.992	60.8	26.2	NA	NA	NA	NA	1	0	0	0	0	0	0	0	0	0	0	0	0	0
<i>Penitella turnae</i>	15.118	9.363	46.9	34.9	NA	NA	NA	NA	0	0	0	0	0	0	0	0	0	0	0	0	0	0
<i>Petricola californiensis</i>	32.836	11.83	37.9	16.2	NA	31.2	NA	16.2	0	0	0	0	0	0	0	0	0	0	0	0	0	0
<i>Petricola carditoides</i>	23.462	5.364	57.1	26.2	NA	NA	NA	NA	1	0	0	0	0	0	0	0	0	0	0	0	0	0
<i>Platyodon cancellatus</i>	20.719	6.912	53.6	28.3	NA	NA	NA	NA	1	0	0	0	0	0	0	0	0	0	0	0	0	0
<i>Pododesmus macrochisma</i>	24.729	-1.18	70.6	24.6	NA	NA	NA	NA	1	0	0	0	0	0	0	0	0	0	0	0	0	0
<i>Rexithaerus expansa</i>	15.118	-0.673	60	35.1	NA	NA	NA	NA	0	0	0	0	0	0	0	0	0	0	0	0	0	0
<i>Rexithaerus indentata</i>	32.836	10.882	41	24.5	31.4	27.9	23.2	22.9	1	0	0	0	0	0	0	0	0	0	0	0	0	0
<i>Saccella taphria</i>	20.719	11.261	39.5	28.2	NA	NA	NA	NA	0	0	0	0	0	0	0	0	0	0	0	0	0	0
<i>Saxidomus gigantea</i>	20.066	3.992	60.2	33.7	NA	NA	NA	NA	0	0	0	0	0	0	0	0	0	0	0	0	0	0
<i>Saxidomus nuttalli</i>	20.91	10.582	41.8	27.7	NA	NA	NA	NA	1	0	0	0	0	0	0	0	0	0	0	0	0	0

<i>Simomactra planulata</i>	27.063	11.83	38	22.9	NA	NA	NA	NA	0	0	0	0	0	0	0	0	0	0	0	0	0	
<i>Solen sicarius</i>	20.719	6.546	54	30.4	NA	NA	NA	NA	0	0	0	0	0	0	0	0	0	0	0	0	0	
<i>Tresus capax</i>	15.118	2.781	59.2	35.1	NA	NA	NA	NA	0	0	0	0	0	0	0	0	0	0	0	0	0	
<i>Tresus nuttallii</i>	24.729	2.781	58	24.6	NA	27.9	NA	27.9	0	0	0	0	0	0	0	0	0	0	0	0	0	
<i>Zemysina orbella</i>	32.836	12.583	36.6	7.4	30.8	31.3	27.1	20.4	1	0	0	0	0	0	0	0	0	0	0	0	0	
<i>Zirfaea pilsbryi</i>	24.729	-1.18	69.7	24.6	NA	NA	NA	NA	0	0	0	0	0	0	0	0	0	0	0	0	0	
<i>Acanthinucella paucilirata</i>	20.719	14.146	33.8	28	NA	NA	NA	NA	1	0	0	0	0	0	0	0	0	0	0	0	0	
<i>Acanthinucella spirata</i>	20.719	11.261	38.2	29.9	NA	NA	NA	NA	1	0	0	0	0	0	1	1	1	1	1	0	0	1
<i>Acmaea mitra</i>	20.719	0.551	57	31.9	NA	NA	NA	NA	1	0	0	0	0	0	0	1	0	0	0	0	0	
<i>Acteocina inculta</i>	31.417	12.583	36.6	28.3	28.5	30.3	24.5	30.3	0	0	0	0	0	0	0	0	0	0	0	0	0	
<i>Alia carinata</i>	21.483	2.781	60.3	26.7	NA	NA	NA	NA	1	0	0	0	0	1	1	1	1	1	1	0	1	1
<i>Alvania compacta</i>	20.719	3.992	60.3	28	NA	NA	NA	NA	0	0	0	0	0	0	0	0	0	0	0	0	0	
<i>Amphissa columbiana</i>	20.066	2.781	58	33.7	NA	NA	NA	NA	0	0	0	0	0	0	0	0	0	0	0	0	0	
<i>Amphissa versicolor</i>	20.91	5.676	54.2	27.7	NA	NA	NA	NA	1	0	0	0	0	0	1	1	1	1	1	1	1	0

<i>Amphithalamus inclusus</i>	32.836	13.56	33.7	20.4	24.2	28	24.2	20.4	0	1	1	0	1	1	0	1	0	0	0	1	1
<i>Assimineia translucens</i>	27.063	6.912	49.9	22.9	NA	NA	NA	NA	0	0	0	0	0	0	0	0	0	0	0	0	0
<i>Atrimitra idae</i>	20.719	10.582	41.75	28	NA	NA	NA	NA	1	0	0	0	0	0	0	1	1	0	1	1	1
<i>Barbarofusus barborensis</i>	27.063	12.563	36.7	22.9	NA	NA	NA	NA	0	0	0	0	0	1	0	0	0	0	0	0	0
<i>Barbarofusus kobelti</i>	20.719	13.56	34.4	28.3	NA	NA	NA	NA	0	0	0	0	0	1	0	0	0	0	1	1	0
<i>Barleeia californica</i>	20.719	14.489	33.7	28	NA	NA	NA	NA	0	0	0	0	0	1	0	0	0	0	0	0	0
<i>Barleeia haliotiphila</i>	20.719	6.546	54	28	NA	NA	NA	NA	0	0	0	0	0	0	0	0	0	0	0	0	0
<i>Caecum californicum</i>	27.063	11.261	38.7	22.9	NA	NA	NA	NA	0	1	0	0	0	1	0	0	0	0	0	0	0
<i>Caecum crebricinctum</i>	21.483	2.781	59.8	26.7	NA	NA	NA	NA	0	0	0	0	0	0	0	0	0	0	0	0	0
<i>Caecum dextroversum</i>	24.729	2.781	59.8	24.6	NA	NA	NA	NA	0	1	0	0	0	1	0	0	0	0	0	0	0
<i>Caecum quadratum</i>	30.52	12.076	37.7	18.7	NA	NA	NA	NA	0	0	0	0	0	0	0	0	0	0	0	0	0
<i>Californiconus californicus</i>	27.063	11.83	38	22.9	24.2	NA	24.2	NA	1	1	0	0	0	1	0	1	1	1	0	1	1
<i>Calliostoma annulatum</i>	20.719	2.781	58.7	30	NA	NA	NA	NA	1	0	0	0	0	0	0	0	0	0	0	0	0
<i>Calliostoma ligatum</i>	20.719	2.781	58.7	28	NA	NA	NA	NA	1	0	0	0	0	0	0	0	0	0	0	0	0

Ceratostoma foliatum	20.719	5.364	57.1	32.7	NA	NA	NA	NA	0	0	0	0	0	0	0	0	0	0	0	0	0
Cerithiopsidella cosmia	20.719	12.563	36.7	28	NA	NA	NA	NA	1	0	0	0	0	0	0	1	0	0	0	0	1
Clathromangeli a rhyssa	20.719	13.95	34	28	NA	NA	NA	NA	0	0	0	0	0	0	0	0	0	0	0	0	0
Crepidula naticarum	20.719	12.563	36.7	31.7	NA	NA	NA	NA	0	0	0	0	0	0	0	0	0	0	0	0	0
Crepidula norrisiarum	20.719	7.671	48.5	31.7	NA	NA	NA	NA	0	0	0	0	0	0	0	0	1	1	0	0	0
Crepidula nummaria	17.827	6.912	51	35	NA	NA	NA	NA	1	0	0	0	0	0	0	0	0	0	0	0	0
Crepidula perforans	29.493	11.261	39.2	33.7	NA	NA	NA	NA	0	0	0	0	1	1	0	1	1	0	0	1	0
Crepipatella lingulata	27.063	-0.673	60	23.2	NA	NA	NA	NA	1	0	0	0	0	1	1	1	1	0	1	1	1
Crockerella conradiana	20.719	13.95	34	28	NA	NA	NA	NA	0	0	0	0	0	0	0	0	0	0	0	0	0
Crossata californica	32.517	12.563	36.7	22.9	NA	30.3	NA	27.9	0	0	0	0	0	0	0	0	0	0	0	0	0
Diodora arnoldi	30.52	9.999	43.3	21	NA	NA	NA	NA	1	0	0	0	0	0	0	0	0	0	0	0	0
Diodora aspera	20.719	2.781	58.7	30.8	NA	NA	NA	NA	1	0	0	0	0	0	0	0	0	0	0	0	0
Discurria insessa	24.729	5.364	56.3	24.6	NA	NA	NA	NA	1	0	0	0	0	0	1	1	1	1	0	0	1
Epitonium tinctum	24.729	5.44	54.8	24.6	NA	NA	NA	NA	1	0	0	0	0	0	1	1	1	1	1	1	1

<i>Fissurella</i> <i>volcano</i>	27.063	10.582	41.8	22.9	NA	NA	NA	NA	1	1	0	0	0	1	1	1	1	1	1	1	1
<i>Fissurellidea</i> <i>bimaculata</i>	25.371	5.364	55	24	NA	NA	NA	NA	1	0	0	0	0	0	0	0	0	0	0	0	0
<i>Fusitriton</i> <i>oregonensis</i>	20.719	-0.673	60	32.7	NA	NA	NA	NA	0	0	0	0	0	0	0	0	0	0	0	0	0
<i>Granulina</i> <i>margaritula</i>	32.836	2.781	58.2	7	31	28	22.9	20.4	1	1	0	0	1	1	0	0	0	0	0	0	0
<i>Haliotis</i> <i>cracherodii</i>	20.91	11.261	38.9	27.6	NA	NA	NA	NA	1	0	0	0	0	1	1	1	1	1	0	1	1
<i>Haliotis</i> <i>kamtschatkana</i>	20.719	5.364	57.1	28	NA	NA	NA	NA	0	0	0	0	0	0	0	0	0	0	0	0	0
<i>Haliotis</i> <i>rufescens</i>	20.719	10.582	41.8	28	NA	NA	NA	NA	1	0	0	0	0	0	0	0	0	0	0	0	0
<i>Halistylus</i> <i>pupoideus</i>	30.52	5.364	55	8	NA	NA	NA	NA	0	0	0	0	0	0	0	0	0	0	0	0	0
<i>Harfordia</i> <i>harfordii</i>	17.653	6.546	54	36.5	NA	NA	NA	NA	0	0	0	0	0	0	0	0	1	0	0	0	0
<i>Hipponix</i> <i>antiquatus</i>	32.836	5.676	54.2	-9.2	NA	28	NA	20.4	1	0	1	1	1	1	0	0	1	1	1	1	1
<i>Hipponix</i> <i>panamensis</i>	30.52	6.912	49.8	-9.2	NA	NA	NA	NA	0	0	0	0	0	0	0	0	0	0	0	0	0
<i>Hipponix</i> <i>tumens</i>	24.729	10.582	41.8	24.6	NA	NA	NA	NA	1	1	0	0	0	1	0	0	1	0	0	1	1
<i>Homalopoma</i> <i>baculum</i>	20.719	7.671	48.5	28	NA	NA	NA	NA	1	0	0	0	0	0	0	0	1	1	1	1	1
<i>Homalopoma</i> <i>luridum</i>	20.719	5.364	57.1	30	NA	NA	NA	NA	1	0	0	0	0	1	0	1	1	1	1	1	1

<i>Homalopoma paucicostatum</i>	20.719	12.508	37	31	NA	NA	NA	NA	1	0	0	0	0	1	0	0	0	0	0	0	0	
<i>Lacuna unifasciata</i>	24.729	12.508	36.9	24.6	NA	NA	NA	NA	1	0	0	0	0	0	1	1	1	1	1	1	0	0
<i>Liotia fenestrata</i>	20.719	12.583	36.6	30.5	NA	NA	NA	NA	1	0	0	0	0	1	0	0	0	0	0	0	0	0
<i>Lirabuccinum dirum</i>	15.118	2.781	56	36.6	NA	NA	NA	NA	0	0	0	0	0	0	0	0	0	0	0	0	0	0
<i>Lirobittium attenuatum</i>	20.719	5.44	54.8	28	NA	NA	NA	NA	1	0	0	0	0	0	0	0	0	0	0	0	0	1
<i>Lirobittium interfossa</i>	20.719	12.583	36.6	28	NA	NA	NA	NA	1	0	0	0	0	1	0	0	0	0	0	0	1	0
<i>Lirobittium purpureum</i>	20.719	11.83	38	32	NA	NA	NA	NA	1	0	0	0	0	0	0	0	0	0	0	0	0	0
<i>Lirobittium quadrifilatum</i>	20.91	12.583	36.6	27	NA	NA	NA	NA	0	0	0	0	0	0	0	0	0	0	0	0	0	0
<i>Lirularia lirulata</i>	20.719	3.992	60.6	32.7	NA	NA	NA	NA	0	0	0	0	0	0	0	0	0	0	0	0	0	0
<i>Littorina keenae</i>	28.019	9.999	43.2	24.5	NA	NA	NA	NA	1	0	1	0	0	0	1	1	1	1	1	1	1	1
<i>Littorina plena</i>	27.063	5.364	57.1	22.9	NA	NA	NA	NA	0	0	0	0	0	0	0	0	0	0	0	0	0	0
<i>Littorina scutulata</i>	27.063	2.781	58	22.9	NA	NA	NA	NA	1	0	0	0	0	0	1	1	1	1	1	1	1	1
<i>Lottia asmi</i>	27.286	5.364	55	22.9	NA	NA	NA	NA	1	0	0	1	0	0	1	1	0	0	0	0	1	0
<i>Lottia digitalis</i>	27.063	0.551	52.9	22.9	NA	NA	NA	NA	1	1	0	0	0	1	1	1	1	1	1	1	1	1

<i>Lottia gigantea</i>	20.91	11.261	38.7	27.8	NA	NA	NA	NA	1	0	0	0	0	1	1	1	1	1	1	1	1
<i>Lottia instabilis</i>	20.719	0.551	51.7	32.7	NA	NA	NA	NA	1	0	0	0	0	0	1	1	0	1	0	0	0
<i>Lottia limatula</i>	29.493	7.671	48.5	22.9	NA	NA	NA	NA	1	0	0	1	0	1	1	1	1	1	1	1	1
<i>Lottia pelta</i>	20.91	0.551	57	27.4	NA	NA	NA	NA	1	0	0	0	0	1	1	1	1	1	1	1	1
<i>Lottia scabra</i>	27.286	9.999	43.3	22.9	NA	NA	NA	NA	1	0	0	1	0	0	1	1	1	1	1	1	1
<i>Lottia scutum</i>	17.827	0.551	57	34.4	NA	NA	NA	NA	1	0	0	0	0	0	1	1	0	0	0	0	0
<i>Marsenina rhombica</i>	20.719	-0.673	60	30	NA	NA	NA	NA	0	0	0	0	0	0	0	0	0	0	0	0	0
<i>Megastraea undosa</i>	23.462	13.462	35.1	26.2	NA	NA	NA	NA	1	0	0	0	0	1	0	0	1	0	0	1	0
<i>Melanella thersites</i>	21.483	12.563	36.7	26.7	NA	NA	NA	NA	0	0	0	0	0	0	0	0	0	0	0	0	0
<i>Mitrella tuberosa</i>	20.91	3.992	60.2	27.2	NA	NA	NA	NA	1	0	0	0	0	0	0	0	0	0	0	0	0
<i>Nassarina penicillata</i>	20.719	12.781	35.6	32.5	NA	NA	NA	NA	1	0	0	0	0	0	1	0	0	0	0	1	0
<i>Nassarius fossatus</i>	20.719	6.912	49.8	32.6	NA	NA	NA	NA	0	0	0	0	0	0	0	0	0	0	0	0	0
<i>Nassarius mendicus</i>	20.719	2.781	58	32.5	NA	NA	NA	NA	0	0	0	0	0	0	0	0	0	0	0	0	0
<i>Nassarius perpinguis</i>	24.729	7.671	48.5	24.6	NA	NA	NA	NA	1	0	0	0	0	0	0	0	0	0	0	0	0

<i>Neobernaya spadicea</i>	24.703	12.563	36.7	24.9	NA	NA	NA	NA	1	0	0	0	0	1	0	0	0	0	0	1	0
<i>Neostylidium eschrichtii</i>	17.827	2.781	60.3	34.9	NA	NA	NA	NA	1	0	0	0	0	0	0	0	0	0	0	0	0
<i>Neverita reclusiana</i>	32.836	13.95	34.1	21.5	31.2	28	22.9	21.5	0	0	0	0	0	0	0	0	0	0	0	0	0
<i>Norrisia norrisii</i>	21.483	13.56	34.4	26.7	NA	NA	NA	NA	1	0	0	0	0	1	0	1	1	1	1	1	1
<i>Ocinebrina gracillima</i>	20.719	12.508	37	31	NA	NA	NA	NA	0	0	0	0	0	1	0	0	0	0	1	1	1
<i>Odostomia gravida</i>	20.719	12.563	36.7	28	NA	NA	NA	NA	0	0	0	0	0	0	0	0	0	0	0	0	0
<i>Odostomia turricula</i>	20.719	12.583	36.6	28	NA	NA	NA	NA	0	0	0	0	0	1	0	0	0	0	0	0	0
<i>Olivella baetica</i>	27.063	2.781	58	22.9	NA	NA	NA	NA	1	0	0	0	0	0	0	0	0	0	0	0	0
<i>Olivella biplicata</i>	24.729	6.912	49.8	24.6	NA	NA	NA	NA	1	0	0	0	0	0	0	1	0	0	0	0	0
<i>Opalia montereyensis</i>	20.066	12.583	36.6	33.7	NA	NA	NA	NA	0	0	0	0	0	0	0	0	0	0	0	0	0
<i>Pomaulax gibberosus</i>	24.78	5.364	55	24.3	NA	NA	NA	NA	1	1	0	0	0	1	0	0	0	0	0	0	0
<i>Pseudomelatom a torosa</i>	20.719	9.999	44	32.6	NA	NA	NA	NA	0	0	0	0	0	0	0	0	0	0	0	0	0
<i>Pseudopusula californiana</i>	30.52	10.582	41.8	16.8	30.3	28	30.3	28	1	1	0	0	0	1	0	0	0	0	0	0	0
<i>Seila montereyensis</i>	30.52	12.583	36.6	20.4	27.3	28	27.3	28	1	1	0	0	0	1	0	1	1	1	1	1	0

<i>Tectura depicta</i>	27.063	13.95	34.1	22.9	NA	NA	NA	NA	0	0	0	0	0	0	0	0	0	0	0	0	0
<i>Tectura paleacea</i>	20.719	6.912	49.8	30.8	NA	NA	NA	NA	1	0	0	0	0	1	0	1	0	1	0	0	1
<i>Tegula brunnea</i>	17.827	9.999	43.3	35.3	NA	NA	NA	NA	1	0	0	0	0	0	1	0	0	0	0	0	0
<i>Tegula funebris</i>	20.719	6.912	51	30	NA	NA	NA	NA	1	0	0	0	0	0	1	1	1	1	0	1	1
<i>Tegula gallina</i>	28.019	13.462	35	25	NA	NA	NA	NA	1	0	1	0	0	1	0	0	1	0	0	1	1
<i>Tegula montereyi</i>	17.653	11.261	38.6	35.4	NA	NA	NA	NA	0	0	0	0	0	0	1	0	0	0	0	0	0
<i>Tegula pulligo</i>	20.719	5.364	58	32	NA	NA	NA	NA	1	0	0	0	0	0	0	0	0	0	0	0	0
<i>Thylacodes squamigerus</i>	29.493	13.56	34.4	26	NA	NA	NA	NA	1	0	0	0	0	1	0	1	1	1	1	1	1
<i>Trimusculus reticulatus</i>	32.836	12.508	37	18	NA	27.9	NA	20.4	1	0	0	0	0	0	1	0	0	1	0	0	1
<i>Triphora pedroana</i>	20.719	12.508	37	30	NA	NA	NA	NA	1	0	0	0	0	1	0	1	0	1	1	1	1
<i>Turritella cooperi</i>	20.719	12.508	37	28	NA	NA	NA	NA	0	0	0	0	0	1	0	0	0	0	0	0	0
<i>Vitrinella oldroydi</i>	20.719	11.261	39.5	32	NA	NA	NA	NA	0	0	0	0	0	0	0	0	0	0	0	0	0

Appendix V: Marine Isotope Substage 5e fossil localities. Fossil localities from the California Region (northern Pacific coast of Baja California to Point Conception, California) dated to the Marine Isotope Substage 5e. Locality sources, locations, and paleo-habitats indicated. For associated extralimital species, see Appendix VI.

Latitude	Locality ID	Date Source	Locality	Paleo-habitat	Paleoecology & Faunal Source
34.05	1710	Wehmiller <i>et al.</i> 1977; Kennedy <i>et al.</i> 1982	Point Dume, California	Open coast	UC Museum of Paleontology
33.75	12608	Muhs <i>et al.</i> 2006	Palos Verdes Hills, California	Open coast	Muhs <i>et al.</i> 2006
33.7	12576	Muhs <i>et al.</i> 2018	San Pedro, California	Embayment	Muhs <i>et al.</i> 2018
33.7	66-2	Grant <i>et al.</i> 1999	Newport Bay, California	Embayment	Kanakoff and Emerson 1959
33.65	2601	Powell <i>et al.</i> 2004	Newport Bay, California	Embayment	Powell <i>et al.</i> 2004
33.65	2602	Powell <i>et al.</i> 2004	Newport Bay, California	Embayment	Powell <i>et al.</i> 2004
33.65	2603	Powell <i>et al.</i> 2004	Newport Bay, California	Embayment	Powell <i>et al.</i> 2004
33.65	2604	Powell <i>et al.</i> 2004	Newport Bay, California	Embayment	Powell <i>et al.</i> 2004
33.65	2605	Powell <i>et al.</i> 2004	Newport Bay, California	Embayment	Powell <i>et al.</i> 2004
33.65	2606	Powell <i>et al.</i> 2004	Newport Bay, California	Embayment	Powell <i>et al.</i> 2004

33.64	1722	Wehmiller <i>et al.</i> 1977; Kennedy <i>et al.</i> 1982	Laguna Beach, California	Open coast	UC Museum of Paleontology
33.25	11749	Muhs <i>et al.</i> 2012	San Nicolas Island, California	Open coast	LA County Museum
33.25	11750	Muhs <i>et al.</i> 1994	San Nicolas Island, California	Open coast	LA County Museum
33.25	10622	Muhs <i>et al.</i> 2006	San Nicolas Island, California	Open coast	Muhs <i>et al.</i> 2006
33.25	302	Muhs <i>et al.</i> 2012	San Nicolas Island, California	Open coast	Muhs <i>et al.</i> 2012
33.2	5574	Kennedy <i>et al.</i> 1982	Camp Pendleton, California	Open coast	LA County Museum; Shlemon 1978
32.9	318	Muhs and Simmons 2018, personal comm.	Carmel Valley (San Diego), California	Embayment	Kern 1971
32.9	10725	Muhs <i>et al.</i> 2002	San Clemente Island, California	Open coast	LA County Museum
32.9	12007	Muhs <i>et al.</i> 2002	San Clemente Island, California	Open coast	LA County Museum
31.7	10130	Muhs <i>et al.</i> 2002	Punta Banda, Baja California Norte	Open coast	Muhs <i>et al.</i> 2002
29.03	0633	Muhs <i>et al.</i> 2002	Guadalupe Island, Baja California Norte	Open coast	Lindberg <i>et al.</i> 1980
29.03	2465	Muhs <i>et al.</i> 2002	Guadalupe Island, Baja California Norte	Open coast	Lindberg <i>et al.</i> 1980

Appendix VI: Marine Isotope Substage 5e extralimital mollusc occurrences. Extralimital bivalve and gastropod species from MIS 5e localities in the California Region. For further information on fossil localities, see Appendix V.

Extralimital species	318	12608	1710	12576	66-2	2601	2602	2603	2604	2605	2606	1722	5574	11749	11750	10622	302	10725	12007	10130	633	2465	
<i>Anadara perlabiata</i>	0	0	0	0	1	1	0	1	1	0	0	0	0	0	0	0	0	0	0	0	0	0	0
<i>Barbatia reeveana</i>	0	0	0	0	0	0	0	0	0	0	0	0	0	0	0	0	0	0	0	0	1	0	0
<i>Chama echinata</i>	0	0	0	0	0	0	0	0	0	0	0	0	0	0	0	0	0	0	0	0	1	1	0
<i>Chioneryx squamosa</i>	0	0	0	1	1	0	0	0	0	0	0	0	0	0	0	0	0	0	0	0	0	0	0
<i>Chionopsis gnidia</i>	1	0	0	0	1	1	1	1	0	1	1	0	0	0	0	0	0	0	0	0	0	0	0
<i>Codakia distinguenda</i>	0	0	0	0	0	0	0	0	0	0	0	0	0	0	0	0	0	0	0	0	1	1	0
<i>Crassinella nuculiformis</i>	0	0	0	0	1	1	1	1	1	0	1	0	0	0	0	0	0	0	0	0	0	0	0
<i>Ctena mexicana</i>	0	0	0	0	0	0	0	0	0	0	0	0	0	0	0	0	0	0	0	0	1	0	0
<i>Cyathodonta undulata</i>	0	0	0	0	1	0	0	0	0	0	0	0	0	0	0	0	0	0	0	0	0	0	0
<i>Cyclinella subquadrata</i>	0	0	0	0	1	0	0	0	0	0	0	0	0	0	0	0	0	0	0	0	0	0	0
<i>Dosinia ponderosa</i>	0	0	0	0	1	0	0	1	0	0	1	0	0	0	0	0	0	0	0	0	0	0	0

<i>Euvola vogdesi</i>	0	0	0	0	1	0	0	1	0	0	1	0	0	0	0	0	0	0	0	0	0	0
<i>Leukoma grata</i>	0	0	0	0	1	0	0	0	0	0	0	0	0	0	0	0	0	0	0	0	0	0
<i>Megapitaria squalida</i>	0	0	0	0	1	0	0	1	1	0	1	0	0	0	0	0	0	0	0	0	0	0
<i>Mulinia pallida</i>	0	0	0	0	1	0	0	0	0	0	0	1	0	0	0	0	0	0	0	0	0	0
<i>Petricolaria cognata</i>	0	0	0	0	1	1	1	1	1	0	1	0	0	0	0	0	0	0	0	0	0	0
<i>Psammotreta pura</i>	0	0	0	0	0	0	0	0	0	0	0	1	0	0	0	0	0	0	0	0	0	0
<i>Trachycardium procerum</i>	0	0	0	1	1	0	0	0	0	0	0	0	0	0	0	0	0	0	0	0	0	0
<i>Undulostrea megodon</i>	0	0	0	0	1	0	0	0	0	0	0	0	0	0	0	0	0	0	0	0	0	0
<i>Cyclinella producta</i>	1	0	0	0	0	0	0	0	0	0	0	0	0	0	0	0	0	0	0	0	0	0
<i>Asthenothaerus villosior</i>	1	0	0	0	0	0	0	0	0	0	0	0	0	0	0	0	0	0	0	0	0	0

Appendix VII: Present-day ranges of Northern Panamic region mollusks. Present-day thermal maxima and minima; maincoast, and Gulfo de California latitudinal endpoints; and offshore island occurrences for Pleistocene bivalve and gastropod species from California. Abbreviations: North = northern maincoast latitude; South = southern maincoast latitude; Pool = extralimital v. conterminous species pool; Shall. = shallowest recorded depth; Max Size = maximum body size (millimeters); NW = northwest Gulfo de California latitude; NE = southwest Gulfo de California latitude; SW = southwest Gulfo de California latitude; SE = southeast Gulfo de California latitude; RL Ann Temp = range-limiting annual temperature (°C); RL Min Chlo = range-limiting minimum chlorophyll α concentration; RL Max Chlo = range-limiting maximum chlorophyll α concentration; Lat = latitudinal range; Island = number of offshore islands occupied; Prob = modeled probabilities based on best-supported MIS 5e extralimital regression.

Family	Scientific Name	North	South	Pool	Shall.	Max size	NW	NE	SW	SE	RL Ann Temp	RL Min Chlo	RL Max Chlo	Lat	Island	Prob
Semelidae	<i>Abra palmeri</i>	26.8	-3.7	Species	0	10	31.00	31.30	25.90	20.42	19.55	0.35	16.19	35.00	0	0.06
Arcidae	<i>Acar gradata</i>	27.8	8.3	Pool	0	41	26.12	31.33	22.88	20.42	17.78	0.05	8.97	23.03	6	0.49
Tellinidae	<i>Acorylus rickettsi</i>	22.375	7.6	Species	9	12	25.80	27.90	22.10	20.42	23.95	0.21	8.64	20.30	0	0.00
Cardiidae	<i>Acrosterigma pristipleura</i>	22.375	-1.8	Pool	0	81	26.10	21.50	22.10	20.42	24.08	0.05	7.16	27.90	2	0.00
Nuculanidae	<i>Adrana crenifera</i>	22.375	-3.8	Species	8	36	NA	23.30	NA	20.42	24.18	0.33	7.16	27.10	0	0.00
Nuculanidae	<i>Adrana metcalfei</i>	22.375	-0.4	Pool	7	24	30.30	27.90	22.10	20.42	22.61	0.24	7.16	30.70	0	0.00
Mytilidae	<i>Adula soleniformis</i>	22.375	-5.1	Species	0	40	NA	23.20	NA	20.42	19.67	0.33	7.16	28.30	0	0.03
Veneridae	<i>Agriopoma catharium</i>	23.5	-12	Pool	13	67	29.50	27.93	23.12	20.42	18.02	0.21	14.76	41.50	1	0.18
Tellinidae	<i>Ameritella amianta</i>	22.375	-2.2	Species	0	15	NA	31.70	NA	20.42	23.00	0.33	7.16	33.90	0	0.00
Tellinidae	<i>Ameritella coani</i>	22.375	8	Pool	0	10	28.90	31.40	22.10	20.42	21.84	0.32	9.31	23.40	2	0.01
Tellinidae	<i>Ameritella felix</i>	24.6	-3.7	Species	0	17	26.70	27.90	22.10	20.42	21.56	0.44	7.96	31.60	0	0.03
Mytilidae	<i>Amygdalum americanum</i>	22.375	-5.1	Pool	4	32	25.80	27.93	22.10	20.42	19.67	0.21	7.16	33.03	0	0.03
Arcidae	<i>Anadara adamsi</i>	22.375	-2.2	Species	8	30	28.97	22.68	22.10	20.42	21.84	0.33	8.38	31.17	0	0.01
Arcidae	<i>Anadara aequatorialis</i>	22.375	-3.7	Pool	0	48	30.30	23.23	22.10	20.42	23.04	0.33	7.16	34.00	0	0.00
Arcidae	<i>Anadara biangulata</i>	22.375	-3.7	Species	10	68	27.00	27.90	22.10	20.42	23.95	0.33	7.16	31.60	0	0.00
Arcidae	<i>Anadara cepoides</i>	22.375	1	Pool	10	90	29.80	27.95	22.10	20.42	22.84	0.33	7.16	28.80	0	0.00
Arcidae	<i>Anadara concinna</i>	22.375	-1.1	Species	6	54	31.00	29.90	22.10	20.42	22.79	0.26	7.16	32.10	0	0.00

Arcidae	<i>Anadara emarginata</i>	24.1	-5.9	Species Pool	0	51	28.40	28.80	22.10	20.42	19.41	0.35	8.29	34.70	0	0.09
Arcidae	<i>Anadara formosa</i>	28.3	-5.1	Species Pool	10	121	28.97	27.95	25.75	20.42	18.35	0.42	8.38	34.07	1	0.10
Arcidae	<i>Anadara mazatlanica</i>	22.375	-4.1	Species Pool	7	87	27.05	27.95	22.10	20.42	23.38	0.33	8.40	32.05	0	0.00
Arcidae	<i>Anadara nux</i>	22.375	-5.2	Species Pool	4	24	27.05	23.20	22.10	20.42	19.30	0.33	8.40	32.25	0	0.04
Arcidae	<i>Anadara obesa</i>	22.9	-4.7	Species Pool	10	43	23.88	28.78	22.88	20.42	20.04	0.28	7.03	33.48	0	0.02
Arcidae	<i>Anadara perlabiata</i>	27.8	-4.7	Extralimital	0	50	28.40	27.93	22.10	20.42	17.78	0.44	8.97	33.10	1	0.31
Arcidae	<i>Anadara reinharti</i>	22.375	-3.5	Species Pool	2	68	28.97	31.33	26.62	20.42	21.84	0.33	8.38	34.83	0	0.01
Arcidae	<i>Anadara similis</i>	22.375	-3.6	Species Pool	0	66	NA	24.25	NA	20.42	24.51	0.33	8.47	27.85	0	0.00
Arcidae	<i>Anadara tuberculosa</i>	26.8	-5.1	Species Pool	0	97	28.97	28.80	24.17	20.42	19.55	0.46	16.19	34.07	0	0.10
Mastridae	<i>Anatina cyprinus</i>	22.375	-2.2	Species Pool	15	57	29.97	27.93	22.10	20.42	22.95	0.33	7.16	32.17	0	0.00
Lucinidae	<i>Anodontia edentuloides</i>	25.9	12.6	Species Pool	9	52	31.00	31.30	30.00	20.42	21.60	0.35	4.83	18.70	1	0.01
Cardiidae	<i>Apiocardia obovalis</i>	24.6	10.7	Species Pool	0	25	23.00	23.22	22.10	20.42	21.56	0.19	7.03	13.90	1	0.02
Arcidae	<i>Arca mutabilis</i>	27.8	-5.1	Species Pool	0	44	30.33	31.40	29.80	20.42	17.78	0.05	8.97	36.50	6	0.49
Arcidae	<i>Arca pacifica</i>	27.8	-5.1	Species Pool	0	128	31.03	31.40	22.88	20.42	17.78	0.41	8.97	36.50	3	0.48
Chamidae	<i>Arcinella californica</i>	28.3	-3.6	Species Pool	10	74	29.53	31.30	28.53	20.42	18.35	0.35	5.67	34.90	0	0.04
Thraciidae	<i>Asthenothaerus villosior</i>	28.3	9.4	Extralimital	0	10	31.33	31.40	22.87	20.42	18.35	0.28	4.83	22.00	0	0.03
Pinnidae	<i>Atrina cumingii</i>	22.375	-3.5	Species Pool	0	290	27.80	31.50	22.10	20.42	22.84	0.33	7.54	35.00	1	0.01
Pinnidae	<i>Atrina maura</i>	24.6	-6.9	Species Pool	0	175	31.50	31.40	30.50	20.42	18.46	0.41	7.52	38.40	0	0.11
Pinnidae	<i>Atrina tuberculosa</i>	27.8	7.1	Species Pool	0	290	31.13	27.93	25.78	20.42	17.78	0.32	8.97	24.03	2	0.20
Glycymerididae	<i>Axinactis delessertii</i>	24.6	-6.4	Species Pool	8	45	NA	NA	NA	NA	19.05	0.67	6.98	31.00	1	0.17
Glycymerididae	<i>Axinactis inaequalis</i>	22.375	-6.9	Species Pool	0	46	27.20	NA	22.10	NA	18.46	0.05	8.40	34.10	2	0.06
Arcidae	<i>Barbatia lurida</i>	22.375	-3.7	Species Pool	0	51	29.77	31.40	25.57	20.42	22.84	0.33	7.16	35.10	1	0.01
Arcidae	<i>Barbatia reeveana</i>	28.3	-5.1	Extralimital	0	95	29.80	31.33	23.03	20.42	18.35	0.05	6.92	36.43	7	0.48
Basterotiidae	<i>Basterotia californica</i>	28.3	19.2	Species Pool	0	13	29.80	31.40	23.37	27.95	18.35	0.41	4.83	12.20	0	0.05
Basterotiidae	<i>Basterotia panamica</i>	27.2	-2.2	Species Pool	0	11	29.80	31.40	22.88	30.35	18.67	0.41	16.66	33.60	1	0.08

Basterotiidae	<i>Basterotina rectangularis</i>	28.3	-1.6	Species Pool	9	11	30.33	27.97	23.37	26.97	18.35	0.26	7.07	31.93	1	0.06
Mytilidae	<i>Botula cylista</i>	22.375	-3.9	Species Pool	0	28	NA	23.20	NA	20.42	23.82	0.33	7.16	27.10	0	0.00
Mytilidae	<i>Brachidontes semilaevis</i>	28.3	-5.1	Species Pool	0	13	31.03	31.30	28.97	20.42	18.35	0.35	6.92	36.40	2	0.15
Arcidae	<i>Calloarca alternata</i>	22.375	-0.9	Species Pool	10	41	NA	31.40	NA	20.42	22.15	0.28	7.16	32.30	1	0.01
Cuspidariidae	<i>Cardiomya costata</i>	28.3	-2.2	Species Pool	4	11	29.83	31.40	28.83	20.62	18.35	0.41	4.83	33.60	2	0.07
Cuspidariidae	<i>Cardiomya didyma</i>	22.375	-2.5	Species Pool	6	10	31.20	31.30	28.53	20.42	23.24	0.33	7.16	33.80	0	0.00
Carditidae	<i>Carditamera affinis</i>	26.2	-5.1	Species Pool	0	100	31.02	31.30	22.88	20.42	19.67	0.35	6.92	36.40	1	0.10
Carditidae	<i>Carditamera radiata</i>	24.6	-4.7	Species Pool	0	56	NA	NA	NA	NA	20.04	0.67	6.98	29.30	0	0.07
Carditidae	<i>Cardites crassicosatus</i>	22.375	-3.6	Species Pool	0	68	29.80	31.40	24.17	20.42	22.84	0.33	7.16	35.00	1	0.01
Carditidae	<i>Cardites grayi</i>	22.375	7.7	Species Pool	0	47	23.88	23.23	22.10	20.42	25.67	0.22	7.16	16.18	2	0.00
Carditidae	<i>Cardites laticostatus</i>	24.6	-4.1	Species Pool	0	60	26.90	28.80	22.10	20.42	21.56	0.46	7.03	32.90	3	0.09
Corbulidae	<i>Caryocorbula amethystina</i>	22.375	-2.6	Species Pool	0	31	24.20	23.30	22.10	20.42	23.99	0.33	7.16	26.80	0	0.00
Corbulidae	<i>Caryocorbula biradiata</i>	27.8	-4.1	Species Pool	0	21	29.80	31.00	27.15	20.42	17.78	0.41	8.97	35.10	1	0.31
Corbulidae	<i>Caryocorbula ira</i>	22.375	-12	Species Pool	15	14	29.80	29.90	22.10	20.42	18.02	0.33	14.76	41.90	1	0.17
Corbulidae	<i>Caryocorbula marmorata</i>	24.6	-12.1	Species Pool	0	8	30.07	31.40	28.80	20.42	18.02	0.41	12.03	43.50	1	0.31
Corbulidae	<i>Caryocorbula nasuta</i>	27.9	-12.1	Species Pool	0	18	27.32	31.40	26.07	20.42	17.78	0.41	12.03	43.50	2	0.29
Corbulidae	<i>Caryocorbula otra</i>	22.375	-2.2	Species Pool	0	26	26.00	27.90	22.10	20.42	23.90	0.25	7.16	30.10	0	0.00
Lucinidae	<i>Cavilinga lampra</i>	22.375	6	Species Pool	0	25	31.00	31.50	22.10	20.42	23.25	0.05	7.16	25.50	1	0.00
Lucinidae	<i>Cavilinga lingualis</i>	28.3	-3.1	Species Pool	0	18	31.30	31.50	22.10	20.42	18.35	0.45	11.89	34.60	0	0.06
Chamidae	<i>Chama buddiana</i>	22.375	-0.9	Species Pool	0	125	31.13	31.40	26.02	20.42	22.15	0.28	7.16	32.30	1	0.01
Chamidae	<i>Chama coralloides</i>	24.6	-4.3	Species Pool	0	85	29.60	31.30	22.10	20.42	21.56	0.35	6.98	35.60	0	0.02
Chamidae	<i>Chama echinata</i>	28.3	-3.5	Species Pool	0	38	29.53	31.40	22.88	20.42	18.35	0.14	7.54	34.90	4	0.27
Chamidae	<i>Chama frondosa</i>	22.375	-1.6	Species Pool	0	90	31.02	31.30	22.88	20.42	23.24	0.05	7.16	32.90	2	0.00
Chamidae	<i>Chama hicksi</i>	22.375	3	Species Pool	12	90	29.00	29.00	16.00	0.00	21.52	0.33	8.38	29.00	0	0.01
Chamidae	<i>Chama tinctoria</i>	22.375	7.7	Species Pool	15	37	NA	NA	NA	NA	27.46	0.22	7.16	14.68	1	0.00

Veneridae	<i>Chione compta</i>	22.375	-6.5	Species Pool	18	50	26.70	27.95	22.10	20.42	19.02	0.33	8.89	34.45	1	0.06
Veneridae	<i>Chione guatulcoensis</i>	22.375	9	Species Pool	0	24	25.17	27.90	22.10	20.42	23.95	0.33	8.05	18.90	1	0.00
Veneridae	<i>Chione subimbricata</i>	24.6	-7.7	Species Pool	0	49	24.47	27.93	24.17	20.42	17.87	0.36	11.66	35.63	1	0.17
Veneridae	<i>Chione tumens</i>	25	11.7	Species Pool	0	47	29.80	31.40	22.88	26.95	21.75	0.29	10.38	19.70	0	0.01
Veneridae	<i>Chioneryx squamosa</i>	27.8	-5.9	Extralimital	0	11	31.02	31.40	28.17	20.42	17.78	0.41	8.97	37.30	1	0.29
Veneridae	<i>Chionopsis amathusia</i>	22.375	-4.1	Species Pool	0	74	28.97	27.95	22.10	20.42	21.84	0.33	8.38	33.07	0	0.01
Veneridae	<i>Chionopsis gnidia</i>	28.3	-5.1	Extralimital	0	120	31.02	31.40	26.67	20.42	18.35	0.41	6.92	36.50	0	0.07
Veneridae	<i>Chionopsis lilacina</i>	22.375	-2.6	Species Pool	0	71	28.90	30.30	22.10	20.42	21.84	0.33	7.16	32.90	0	0.01
Veneridae	<i>Chionopsis pulicaria</i>	22.375	-2.6	Species Pool	0	62	31.70	31.70	22.10	20.42	23.00	0.33	7.16	34.30	0	0.00
Veneridae	<i>Choristodon robustus</i>	27.8	-5.1	Species Pool	0	43	26.12	31.30	25.12	20.42	17.78	0.25	8.97	36.40	2	0.32
Mytilidae	<i>Choromytilus palliopunctatus</i>	27.1	7.6	Species Pool	0	92	23.88	31.50	22.88	20.42	18.88	0.22	16.66	23.90	0	0.05
Pandoridae	<i>Clidiophora claviculata</i>	28.2	23.2	Species Pool	15	45	31.00	31.30	22.10	20.42	18.34	0.21	4.83	10.88	0	0.04
Pandoridae	<i>Clidiophora cornuta</i>	27.8	-14.1	Species Pool	0	36	31.02	31.40	28.97	20.42	17.22	0.41	15.71	45.50	0	0.44
Lucinidae	<i>Codakia distinguenda</i>	28	-3.6	Extralimital	0	150	31.02	31.50	24.20	20.42	18.04	0.05	6.18	35.10	6	0.34
Corbulidae	<i>Corbula speciosa</i>	22.375	6	Species Pool	0	21	31.00	28.70	22.10	20.42	22.50	0.05	7.16	25.00	1	0.00
Crassatellidae	<i>Crassinella nuculiformis</i>	28.3	-3.1	Extralimital	0	6	31.50	31.40	22.10	20.42	18.35	0.41	11.89	34.60	0	0.06
Ostreidae	<i>Crassostrea columbiensis</i>	27.7	-5	Species Pool	0	80	28.40	27.90	22.10	20.42	17.78	0.44	8.97	33.40	1	0.40
Ostreidae	<i>Crassostrea corteziensis</i>	22.375	9	Species Pool	0	250	NA	28.80	NA	20.42	22.50	0.33	8.05	19.80	0	0.00
Lucinidae	<i>Ctena chiquita</i>	26.1	-1.6	Species Pool	0	14	31.00	30.30	26.07	20.42	21.55	0.26	3.44	32.60	1	0.01
Lucinidae	<i>Ctena mexicana</i>	27.2	-4.1	Extralimital	0	21	30.33	31.30	23.55	20.42	18.67	0.10	16.66	35.40	5	0.17
Semelidae	<i>Cumingia lamellosa</i>	22.375	-5.1	Species Pool	0	24	30.92	31.70	29.80	20.42	19.67	0.33	7.16	36.80	0	0.03
Thraciidae	<i>Cyathodonta dubiosa</i>	22.375	7.6	Species Pool	13	44	29.10	27.95	22.10	20.42	21.52	0.22	8.64	21.50	0	0.01
Thraciidae	<i>Cyathodonta undulata</i>	24.6	-4.2	Extralimital	0	50	30.77	31.40	24.17	20.42	21.56	0.41	6.98	35.60	1	0.03
Veneridae	<i>Cyclinella jadisi</i>	22.375	-2.7	Species Pool	0	70	NA	31.40	NA	20.42	23.24	0.33	7.16	34.10	0	0.00
Veneridae	<i>Cyclinella producta</i>	27.8	-3.8	Extralimital	0	43	29.80	31.40	28.80	21.22	17.78	0.41	8.97	35.20	0	0.21

Veneridae	<i>Cyclinella subquadrata</i>	28.3	-13.1	Extralimital	0	81	31.50	31.70	22.10	20.42	18.35	0.45	49.97	44.80	1	0.29
Propeamussiidae	<i>Cyclopecten pernokus</i>	28.3	-2.2	Pool	2	10	29.60	27.98	23.55	20.42	18.35	0.10	7.07	31.80	4	0.16
Tellinidae	<i>Cymatoica undulata</i>	22.375	-2.2	Species	7	17	31.27	31.70	27.05	20.42	23.00	0.33	7.16	33.90	0	0.00
Pholadidae	<i>Cyrtopleura crucigera</i>	22.375	-3.5	Pool	0	44	NA	27.93	NA	20.42	23.94	0.33	7.54	31.43	0	0.00
Cardiidae	<i>Dallocardia senticosa</i>	22.375	-5.8	Species	0	60	31.05	31.30	30.68	20.42	19.41	0.33	8.29	37.10	0	0.03
Pectinidae	<i>Delectopecten zacaе</i>	22.9	-6.6	Pool	10	22	28.97	NA	22.88	NA	19.00	0.10	8.89	35.57	2	0.07
Ostreidae	<i>Dendostrea folium</i>	22.375	9	Species	8	24	24.47	NA	22.10	NA	24.97	0.33	8.05	15.47	3	0.00
Pholadidae	<i>Diplothyra curta</i>	22.375	-2.2	Pool	0	15	31.67	31.50	31.03	20.42	23.12	0.33	7.16	33.87	0	0.00
Lucinidae	<i>Divalinga eburnea</i>	27.7	-4.1	Species	0	31	29.80	31.50	28.97	20.42	17.78	0.59	8.97	35.60	3	0.52
Lucinidae	<i>Divalinga perparvula</i>	24.6	-14.3	Pool	7	23	26.90	28.80	22.88	20.42	16.43	0.46	11.29	43.10	2	0.63
Donacidae	<i>Donax caelatus</i>	22.375	8.6	Species	0	49	28.83	27.92	22.10	20.42	22.14	0.23	11.44	20.23	0	0.01
Donacidae	<i>Donax carinatus</i>	24.6	-4.1	Pool	0	52	24.20	24.60	22.10	20.42	21.56	0.27	9.14	28.70	0	0.02
Donacidae	<i>Donax culter</i>	22.375	16.8	Species	0	47	25.17	25.42	22.10	20.42	24.90	0.21	7.16	8.62	0	0.00
Donacidae	<i>Donax gracilis</i>	27.7	-4.7	Pool	0	29	30.77	31.40	29.77	20.42	17.78	0.41	8.97	36.10	1	0.29
Donacidae	<i>Donax punctatostratus</i>	26.8	19.1	Species	0	48	27.05	31.40	26.05	20.42	19.55	0.27	21.03	12.30	0	0.06
Donacidae	<i>Donax transversus</i>	22.375	-5.1	Pool	0	42	25.67	24.60	24.67	20.42	19.67	0.25	9.14	30.77	0	0.04
Veneridae	<i>Dosinia dunkeri</i>	24.6	-6.9	Species	0	60	31.50	31.40	22.10	20.42	18.46	0.41	7.52	38.40	1	0.16
Veneridae	<i>Dosinia ponderosa</i>	27.8	-3.7	Extralimital	0	147	31.03	31.40	26.07	20.42	17.78	0.41	8.97	35.10	1	0.29
Veneridae	<i>Dosinia semiobliterata</i>	22.375	0.4	Species	0	53	NA	23.23	NA	20.42	24.60	0.24	7.16	22.83	0	0.00
Nuculidae	<i>Ennucula colombiana</i>	22.375	-5.1	Pool	11	9	31.03	27.93	22.10	20.42	19.67	0.05	7.16	36.13	1	0.03
Pharidae	<i>Ensis californicus</i>	24.6	19.2	Species	0	85	31.50	31.70	22.10	20.42	21.56	0.45	6.98	12.50	0	0.03
Pharidae	<i>Ensis nitidus</i>	22.375	9.7	Pool	0	92	31.02	NA	22.10	NA	23.29	0.33	15.90	21.32	0	0.01
Pharidae	<i>Ensis tropicalis</i>	22.375	8.7	Species	0	98	24.20	31.70	22.10	20.42	23.00	0.23	11.44	23.00	0	0.00
Lyonsiidae	<i>Entodesma inflatum</i>	26.8	-12	Pool	0	40	31.50	31.40	22.10	20.42	18.02	0.41	16.19	43.50	0	0.23
Lyonsiidae	<i>Entodesma pictum</i>	22.9	-6.5	Species	0	70	31.02	31.40	22.88	20.42	19.02	0.34	8.89	37.90	1	0.06

Lucinidae	<i>Epicodakia clarionensis</i>	24.6	-3.7	Species Pool	0	17	29.90	27.95	22.10	26.95	20.47	0.05	7.07	33.60	4	0.06
Tellinidae	<i>Eurytellina eburnea</i>	22.375	-5.9	Species Pool	9	61	NA	27.90	NA	20.42	19.41	0.33	8.29	33.80	0	0.03
Tellinidae	<i>Eurytellina hiberna</i>	22.375	-4.6	Species Pool	0	19	NA	31.70	NA	20.42	20.68	0.33	7.16	36.30	0	0.01
Tellinidae	<i>Eurytellina inaequistriata</i>	22.375	-2.3	Species Pool	1	34	NA	31.40	NA	20.42	23.24	0.33	7.16	33.70	0	0.00
Tellinidae	<i>Eurytellina prora</i>	22.375	-3.7	Species Pool	0	72	31.00	27.90	22.10	20.42	23.29	0.33	7.16	34.70	0	0.00
Tellinidae	<i>Eurytellina regia</i>	27.8	-4.1	Species Pool	0	52	30.77	31.70	29.77	20.42	17.78	0.51	8.97	35.80	0	0.22
Tellinidae	<i>Eurytellina rubescens</i>	22.375	-3.7	Species Pool	0	47	30.30	NA	22.10	NA	23.04	0.33	7.16	34.00	0	0.00
Pectinidae	<i>Euvola perula</i>	22.375	-4.5	Species Pool	2	39	NA	27.90	NA	20.42	20.68	0.33	7.16	32.40	2	0.03
Pectinidae	<i>Euvola vogdesi</i>	27.8	-2.2	Species Pool	0	117	29.53	31.40	22.10	20.42	17.78	0.41	8.97	33.60	2	0.29
Ungulinidae	<i>Foveamysia soror</i>	26.2	-0.9	Species Pool	0	15	31.00	31.30	22.10	20.42	21.44	0.28	4.83	32.20	0	0.01
Pandoridae	<i>Frenamya arcuata</i>	22.375	-4.1	Species Pool	15	26	24.70	NA	22.10	NA	23.38	0.33	7.16	28.80	0	0.00
Pandoridae	<i>Frenamya radians</i>	26.7	-3.7	Species Pool	4	24	NA	NA	NA	NA	19.79	0.61	16.19	30.40	0	0.05
Arcidae	<i>Fugleria illota</i>	26.8	-4.5	Species Pool	0	51	31.02	31.40	22.88	20.42	19.55	0.41	16.19	35.90	1	0.09
Psammobiidae	<i>Gari helenae</i>	27.8	-1.6	Species Pool	0	61	31.02	30.30	28.97	20.42	17.78	0.26	8.97	32.62	1	0.12
Psammobiidae	<i>Gari lata</i>	24.6	-2.2	Species Pool	0	66	30.00	30.30	22.10	20.42	21.56	0.38	6.98	32.50	0	0.01
Gastrochaenidae	<i>Gastrochaena denticulata</i>	22.375	-41.8	Species Pool	0	18	NA	NA	NA	NA	27.46	0.33	7.16	64.18	1	0.00
Gastrochaenidae	<i>Gastrochaena ovata</i>	22.375	-2.2	Species Pool	0	31	31.03	31.00	22.10	20.42	23.29	0.05	7.16	33.23	4	0.01
Veneridae	<i>Globivenus isocardia</i>	22.375	-3.8	Species Pool	8	127	28.97	27.95	23.13	20.77	20.47	0.05	8.38	32.77	5	0.10
Glycymerididae	<i>Glycymeris gigantea</i>	24.6	11.1	Species Pool	0	105	29.80	31.40	28.97	21.40	21.56	0.27	15.60	20.30	1	0.04
Glycymerididae	<i>Glycymeris maculata</i>	22.375	-8.5	Species Pool	0	84	31.02	31.40	29.53	20.42	18.16	0.33	9.11	39.90	0	0.06
Veneridae	<i>Gouldia californica</i>	24.6	-13.6	Species Pool	0	8	25.97	28.40	24.17	20.42	19.55	0.21	14.70	42.00	2	0.25
Periplomatidae	<i>Halistrepta myrae</i>	22.375	19.1	Species Pool	16	30	26.00	27.90	22.10	20.42	23.95	0.25	21.03	8.80	0	0.00
Mastridae	<i>Harvella elegans</i>	22.375	-4	Species Pool	0	76	NA	23.20	NA	20.42	23.81	0.33	7.16	27.20	0	0.00
Crassatellidae	<i>Hybolophus gibbosus</i>	26.1	-5.6	Species Pool	5	93	31.10	27.93	27.05	20.42	19.64	0.44	8.66	36.70	1	0.13
Gryphaeidae	<i>Hyotissa fisheri</i>	22.375	-1.3	Species Pool	0	230	29.80	NA	22.10	NA	22.84	0.31	7.16	31.10	4	0.01

Gryphaeidae	<i>Hyotissa quercina</i>	22.375	-6.4	Species Pool	0	89	31.02	31.40	22.10	20.42	19.05	0.05	7.16	37.80	4	0.10
Veneridae	<i>Hyphantosoma aletes</i>	28.3	9.5	Species Pool	15	54	25.80	28.30	23.48	20.42	18.35	0.21	3.34	18.80	0	0.04
Veneridae	<i>Hyphantosoma pollicaris</i>	22.375	-5.1	Species Pool	0	67	31.02	27.90	22.10	20.42	19.67	0.33	7.16	36.12	1	0.05
Veneridae	<i>Hysteroconcha lupanaria</i>	26.2	-5.9	Species Pool	0	78	NA	28.80	NA	20.42	19.41	0.46	8.29	34.70	0	0.09
Veneridae	<i>Hysteroconcha multispinosa</i>	22.375	-3.5	Species Pool	8	41	NA	22.40	NA	20.42	23.94	0.33	7.54	25.90	0	0.00
Veneridae	<i>Iliochione subrugosa</i>	24.6	-5.9	Species Pool	0	50	26.12	31.40	22.88	20.42	19.41	0.25	8.29	37.30	1	0.08
Donacidae	<i>Iphigenia altior</i>	22.375	-5.8	Species Pool	0	84	NA	23.23	NA	20.42	19.41	0.33	8.29	29.03	0	0.03
Pholadidae	<i>Jouannetia pectinata</i>	28.3	-2.2	Species Pool	0	52	24.20	27.90	22.10	20.42	18.35	0.41	7.07	30.50	1	0.07
Corbulidae	<i>Juliacorbulina bicarinata</i>	22.375	-3.7	Species Pool	0	13	NA	31.40	NA	20.42	23.24	0.33	7.16	35.10	1	0.00
Crassatellidae	<i>Kalolophus antillarum</i>	22.9	-2.7	Species Pool	5	105	29.50	30.30	22.88	20.42	22.61	0.34	6.07	33.00	0	0.01
Tellinidae	<i>Laciolina ochracea</i>	22.375	-1.4	Species Pool	0	65	26.70	27.90	22.10	20.42	23.23	0.25	7.96	29.30	2	0.01
Veneridae	<i>Lamelliconcha alternata</i>	22.9	-4.3	Species Pool	0	56	31.27	31.30	30.27	23.22	22.82	0.34	5.87	35.60	0	0.00
Veneridae	<i>Lamelliconcha callicomata</i>	22	-2.8	Species Pool	12	47	NA	NA	NA	NA	24.13	0.56	9.58	24.80	0	0.00
Veneridae	<i>Lamelliconcha concinna</i>	24.8	-3.7	Species Pool	0	52	31.50	31.40	22.10	20.42	21.24	0.41	8.77	35.20	0	0.04
Veneridae	<i>Lamelliconcha unicolor</i>	22.375	-1.3	Species Pool	0	55	NA	22.50	NA	20.42	23.23	0.31	7.16	23.80	0	0.00
Veneridae	<i>Lamelliconcha vinacea</i>	22.375	-2.2	Species Pool	0	40	NA	27.90	NA	20.42	23.90	0.33	7.16	30.10	0	0.00
Arcidae	<i>Larkinia grandis</i>	24.6	-5.6	Species Pool	0	156	24.20	27.90	22.10	20.42	19.64	0.41	8.66	33.50	1	0.05
Mytilidae	<i>Leiosolenus calyculatus</i>	22.375	-0.7	Species Pool	0	15	24.90	27.90	22.10	20.42	21.92	0.05	7.16	28.60	3	0.01
Mytilidae	<i>Leiosolenus hastasius</i>	22.375	-4.7	Species Pool	0	39	NA	23.20	NA	20.42	20.04	0.33	7.16	27.90	0	0.02
Mytilidae	<i>Leiosolenus levigatus</i>	22.375	-0.5	Species Pool	0	56	NA	27.90	NA	20.42	21.92	0.27	7.16	28.40	1	0.01
Mytilidae	<i>Leiosolenus spatiosus</i>	22.375	-3.7	Species Pool	0	63	31.02	31.40	30.02	20.42	23.24	0.33	7.16	35.10	0	0.00
Pectinidae	<i>Leopecten sericeus</i>	22.375	-3.6	Species Pool	13	88	29.50	28.30	22.10	20.42	22.61	0.05	7.16	33.10	3	0.01
Tellinidae	<i>Leporimetis cognata</i>	24.6	-5.9	Species Pool	0	80	29.90	31.30	28.90	20.42	19.41	0.35	8.29	37.20	1	0.10
Semelidae	<i>Leptomya ecuadoriana</i>	22.375	-3.5	Species Pool	0	37	NA	25.60	NA	20.42	23.94	0.27	11.06	29.10	0	0.00
Pectinidae	<i>Leptopecten biolleyi</i>	26.7	-3.1	Species Pool	18	12	26.10	27.90	22.10	20.42	19.79	0.25	16.19	31.00	0	0.04

Pectinidae	<i>Leptopecten tumbezensis</i>	22.375	-4.7	Species Pool	0	45	31.10	27.90	22.10	20.42	20.04	0.33	7.16	35.80	0	0.02
Pectinidae	<i>Leptopecten velero</i>	22.375	-4.6	Species Pool	5	17	30.30	NA	22.10	NA	20.68	0.33	7.16	34.90	1	0.02
Veneridae	<i>Leukoma asperrima</i>	22.375	-5.8	Species Pool	0	51	NA	28.80	NA	20.42	19.41	0.33	8.29	34.60	0	0.03
Veneridae	<i>Leukoma beili</i>	22.375	-2.3	Species Pool	0	57	NA	23.20	NA	20.42	23.90	0.33	7.16	25.50	0	0.00
Veneridae	<i>Leukoma columbiensis</i>	22.375	-4.5	Species Pool	0	60	NA	27.90	NA	20.42	20.68	0.33	7.16	32.40	0	0.01
Veneridae	<i>Leukoma grata</i>	24.6	-4.5	Extralimital	0	53	31.02	31.40	24.17	20.42	20.68	0.41	6.98	35.90	1	0.05
Veneridae	<i>Leukoma histrionica</i>	22.375	-5.9	Species Pool	0	56	NA	27.90	NA	20.42	19.41	0.33	8.29	33.80	0	0.03
Veneridae	<i>Leukoma metodon</i>	22.375	-5.8	Species Pool	0	43	NA	NA	NA	NA	19.41	0.33	8.29	28.18	0	0.03
Limidae	<i>Lima tetrica</i>	22.375	-1.3	Species Pool	0	73	29.90	30.30	22.10	20.42	22.89	0.31	7.16	31.60	2	0.01
Limidae	<i>Limaria orbigny</i>	22.375	-33.6	Species Pool	0	50	31.03	31.30	28.15	20.42	14.27	0.33	7.16	64.90	1	0.42
Limidae	<i>Limaria pacifica</i>	22.375	-5.8	Species Pool	0	41	29.80	31.30	28.80	20.42	19.41	0.33	8.29	37.10	1	0.05
Mytilidae	<i>Lioberus salvadoricus</i>	22.375	8.1	Species Pool	0	42	31.03	31.70	22.10	20.42	23.00	0.32	9.31	23.60	0	0.00
Veneridae	<i>Lirophora mariae</i>	28.3	-4.5	Species Pool	6	37	31.33	31.40	23.55	20.42	18.35	0.41	4.83	35.90	1	0.05
Cardiidae	<i>Lophocardium annettae</i>	28.3	10.7	Species Pool	0	57	31.02	27.90	26.85	20.42	18.35	0.19	7.07	20.32	0	0.07
Cardiidae	<i>Lophocardium cumingii</i>	22.375	6	Species Pool	10	51	25.50	25.60	22.10	20.42	24.98	0.27	11.06	19.60	0	0.00
Lucinidae	<i>Lucinisca centrifuga</i>	27.7	-5.9	Species Pool	0	20	26.95	31.30	25.97	20.42	17.78	0.35	8.97	37.20	1	0.28
Lucinidae	<i>Lucinisca fenestrata</i>	22.375	-1	Species Pool	13	55	30.00	27.90	22.10	20.42	22.95	0.26	7.16	31.00	0	0.00
Arcidae	<i>Lunarca brevifrons</i>	22.375	-4.7	Species Pool	0	43	NA	27.95	NA	20.42	20.04	0.33	7.16	32.65	0	0.02
Tellinidae	<i>Lyratellina lyrica</i>	22.375	-3.6	Species Pool	15	60	31.00	27.90	22.10	20.42	23.29	0.33	7.16	34.60	0	0.00
Tellinidae	<i>Macoploma ecuadoriana</i>	22.375	-5.1	Species Pool	0	101	31.00	27.90	22.10	20.42	19.67	0.33	7.16	36.10	0	0.03
Tellinidae	<i>Macoploma elytrum</i>	22.375	-3.6	Species Pool	1	52	31.20	NA	22.10	NA	23.24	0.33	7.16	34.80	0	0.00
Tellinidae	<i>Macoploma lamproleuca</i>	22.375	-4.1	Species Pool	0	97	NA	27.90	NA	20.42	23.38	0.33	7.16	32.00	0	0.00
Tellinidae	<i>Macoploma siliqua</i>	22.375	1	Species Pool	18	30	31.00	NA	22.10	NA	23.29	0.33	7.16	30.00	0	0.00
Macluridae	<i>Mactrellona clisia</i>	22.375	-4.1	Species Pool	0	100	NA	27.40	NA	20.42	23.38	0.33	7.16	31.50	0	0.00
Macluridae	<i>Mactrellona exoleta</i>	22.375	-4.1	Species Pool	0	131	NA	23.22	NA	20.42	23.38	0.33	7.16	27.32	0	0.00

Mastridae	<i>Mactrellona subalata</i>	22.375	-3.5	Species Pool	0	85	NA	24.25	NA	20.42	23.94	0.33	8.47	27.75	0	0.00
Mastridae	<i>Mactrotoma angusta</i>	22.375	-4.1	Species Pool	0	54	NA	23.20	NA	20.42	23.38	0.33	7.16	27.30	0	0.00
Malleidae	<i>Malleus regula</i>	22.375	7.3	Species Pool	10	120	25.10	23.23	22.10	20.42	24.86	0.05	7.16	17.80	5	0.01
Pholadidae	<i>Martesia striata</i>	24.6	-3.5	Species Pool	0	44	31.50	31.40	22.10	20.42	21.56	0.14	7.54	35.00	2	0.02
Veneridae	<i>Megapitaria aurantiaca</i>	28	-6.5	Species Pool	0.5	128	28.97	31.40	24.10	20.42	18.04	0.41	8.89	37.90	1	0.13
Veneridae	<i>Megapitaria squalida</i>	27.8	-5.1	Extralimital	0	130	31.02	31.40	22.88	20.42	17.78	0.41	8.97	36.50	2	0.38
Lucinidae	<i>Merisca cristallina</i>	28.3	-6.9	Species Pool	18	6	29.60	29.90	22.10	20.42	18.35	0.44	7.52	36.80	0	0.04
Ungulinidae	<i>Microstagon obliquum</i>	24.1	-2.4	Species Pool	6	6	23.50	25.60	22.10	20.42	22.87	0.21	11.06	28.00	0	0.01
Mytilidae	<i>Modiolatus pacificus</i>	22.375	-5.8	Species Pool	0	98	NA	26.00	NA	20.42	19.41	0.33	8.29	31.80	0	0.03
Mytilidae	<i>Modiolus americanus</i>	24.6	-5.1	Species Pool	0	85	24.20	27.90	22.10	20.42	19.67	0.41	7.07	33.00	0	0.04
Mytilidae	<i>Modiolus eiseni</i>	22.375	-5.1	Species Pool	4	55	25.80	27.93	22.10	20.42	19.67	0.21	7.16	33.03	0	0.03
Mastridae	<i>Mulinia pallida</i>	26.3	-13.8	Extralimital	0	93	31.00	31.40	22.10	20.42	18.46	0.41	21.43	45.20	1	0.30
Mytilidae	<i>Mytella charruana</i>	24.6	-3.5	Species Pool	0	80	24.20	27.90	22.10	20.42	21.56	0.41	7.54	31.40	1	0.03
Mytilidae	<i>Mytella guyanensis</i>	24.6	-3.5	Species Pool	0	70	31.02	31.40	30.02	20.42	21.56	0.41	7.54	34.90	0	0.03
Mytilidae	<i>Mytella tumbezensis</i>	24.6	-3.5	Species Pool	0	46	25.80	27.90	22.10	20.42	21.56	0.21	7.54	31.40	0	0.02
Lucinidae	<i>Neophysema aphanes</i>	25.5	-1.5	Species Pool	4	21	25.80	30.30	22.10	20.42	21.73	0.21	5.00	31.80	1	0.01
Noetiidae	<i>Noetia reversa</i>	22.375	-4.1	Species Pool	0	70	29.80	23.20	26.80	20.42	22.84	0.33	7.16	33.90	0	0.00
Nuculanidae	<i>Nuculana costellata</i>	22.375	5.5	Species Pool	15	25	31.02	27.90	22.10	20.42	23.29	0.33	7.16	25.52	0	0.00
Veneridae	<i>Nutricula humilis</i>	28.3	23.3	Species Pool	0	7	28.97	24.23	24.17	23.23	18.35	0.21	8.47	5.74	0	0.07
Ostreidae	<i>Ostrea angelica</i>	22.375	10.9	Species Pool	0.5	100	31.02	31.30	28.80	20.42	20.47	0.10	15.60	20.40	3	0.05
Ostreidae	<i>Ostrea conchaphila</i>	22.375	-3.5	Species Pool	0	80	31.33	31.40	28.17	20.42	23.24	0.33	7.54	34.90	0	0.01
Ostreidae	<i>Ostrea megodon</i>	27.7	-5.9	Extralimital	0	103	31.15	27.95	23.13	20.42	17.78	0.42	8.97	37.05	1	0.36
Tellinidae	<i>Oudardia varilineata</i>	22.375	-3.7	Species Pool	7	25	NA	22.40	NA	20.42	24.38	0.33	7.16	26.10	0	0.00
Tellinidae	<i>Oudardia virgo</i>	24.8	-3.5	Species Pool	0	23	30.77	31.40	29.77	20.42	21.24	0.41	8.77	34.90	0	0.03
Corbulidae	<i>Panamicorbula ventricosa</i>	22.375	-3.5	Species Pool	0	35	24.20	27.95	22.10	20.42	23.94	0.33	7.54	31.45	0	0.00

Pandoridae	<i>Pandora rachaelae</i>	22.375	15.8	Species Pool	0	14	23.40	31.00	22.10	20.42	23.29	0.05	11.99	15.20	1	0.00
Pandoridae	<i>Pandora sarahae</i>	24.6	22.9	Species Pool	2	12	31.00	31.30	30.00	30.30	21.56	0.26	6.98	8.40	0	0.01
Pandoridae	<i>Pandora uncifera</i>	22.375	-0.9	Species Pool	5	13	29.80	30.30	22.88	20.42	22.15	0.28	7.16	31.20	0	0.00
Hiatellidae	<i>Panopea globosa</i>	24.6	22.9	Species Pool	10	164	31.02	27.90	27.23	23.22	21.56	0.26	7.07	8.12	0	0.01
Veneridae	<i>Paphonotia elliptica</i>	22.375	-18.5	Species Pool	0	40	NA	NA	NA	NA	18.90	0.33	10.45	40.88	0	0.05
Cardiidae	<i>Papyridea aspersa</i>	28.3	-2.2	Species Pool	0	52	29.80	31.40	26.12	20.42	18.35	0.41	4.83	33.60	2	0.07
Cardiidae	<i>Papyridea hiulca</i>	22.375	-4.5	Species Pool	0	50	25.80	NA	22.10	NA	20.68	0.21	7.16	30.30	0	0.01
Pholadidae	<i>Parapholas acuminata</i>	22.375	-3.9	Species Pool	0	62	30.50	27.90	22.10	20.42	23.13	0.33	7.16	34.40	1	0.00
Pholadidae	<i>Parapholas calva</i>	22.375	1.4	Species Pool	0	50	NA	27.93	NA	20.42	23.95	0.33	7.71	26.53	1	0.00
Lucinidae	<i>Pegophysema blanquita</i>	24.6	17.7	Species Pool	18	90	31.00	30.50	30.00	29.50	21.56	0.21	6.98	13.30	0	0.03
Veneridae	<i>Periglypta multicostata</i>	22.375	-4.2	Species Pool	0	137	28.15	30.30	22.10	20.42	22.40	0.33	7.16	34.50	1	0.01
Periplomatidae	<i>Periploma stearnsii</i>	22.9	22.9	Species Pool	0	51	30.50	NA	22.10	NA	23.13	0.42	2.90	8.40	0	0.01
Veneridae	<i>Petricola botula</i>	22.375	-2.2	Species Pool	0	16	NA	23.20	NA	20.42	23.90	0.33	7.16	25.40	0	0.00
Veneridae	<i>Petricola denticulata</i>	24.8	-6.8	Species Pool	0	42	31.50	31.40	22.10	20.42	18.55	0.41	10.08	38.30	1	0.23
Veneridae	<i>Petricola exarata</i>	22.375	-3.5	Species Pool	0	15	NA	27.90	NA	20.42	23.94	0.33	7.54	31.40	0	0.00
Veneridae	<i>Petricola insignis</i>	22.375	-2.2	Species Pool	0	44	30.77	31.33	22.88	20.42	23.24	0.33	7.16	33.53	0	0.00
Veneridae	<i>Petricola linguafelis</i>	22.375	-3.7	Species Pool	0	7	23.50	23.70	22.10	20.42	24.38	0.21	7.16	27.40	0	0.00
Veneridae	<i>Petricolaria cognata</i>	28.3	-3.5	Species Extralimital	0	80	31.00	31.30	22.10	20.42	18.35	0.35	7.54	34.80	0	0.09
Ungulinidae	<i>Phlyctiderma caelatum</i>	22.375	-4.2	Species Pool	0	24	NA	23.50	NA	20.42	22.82	0.33	7.16	27.70	1	0.01
Ungulinidae	<i>Phlyctiderma semirugosum</i>	26.2	-4.1	Species Pool	0	14	31.00	31.40	23.50	20.42	21.44	0.41	4.83	35.50	1	0.02
Pholadidae	<i>Pholas chiloensis</i>	27.8	-41.9	Species Pool	0	131	31.02	31.30	30.77	20.42	17.78	0.35	8.97	73.20	0	0.20
Tellinidae	<i>Phyllodella insculpta</i>	22.375	-2.2	Species Pool	6	35	28.90	NA	22.10	NA	21.84	0.33	7.16	31.10	0	0.01
Pteriidae	<i>Pinctada mazatlanica</i>	22.9	-5.1	Species Pool	0	150	27.20	29.00	24.17	20.42	19.67	0.05	8.40	34.10	4	0.11
Pinnidae	<i>Pinna rugosa</i>	28.2	-5.6	Species Pool	0	430	31.02	31.40	24.17	20.42	18.34	0.14	8.66	37.00	2	0.09
Veneridae	<i>Pitar berryi</i>	22.375	-2.2	Species Pool	7	55	NA	27.95	NA	20.42	23.90	0.33	7.16	30.15	0	0.00

Veneridae	<i>Pitar consanguineus</i>	22.375	-3.7	Species Pool	0	47	28.20	23.30	22.10	20.42	22.40	0.05	7.16	31.90	1	0.00
Veneridae	<i>Pitar helenae</i>	22.375	-3.5	Species Pool	0	33	31.33	31.40	28.15	20.42	23.24	0.33	7.54	34.90	1	0.01
Veneridae	<i>Pitar perfragilis</i>	22.375	-2.5	Species Pool	6	28	31.00	27.95	22.10	20.42	23.29	0.33	7.16	33.50	0	0.00
Placunidae	<i>Placunanomia cumingii</i>	22.375	-3.6	Species Pool	0	100	28.90	28.30	22.10	20.42	21.84	0.21	7.16	32.50	0	0.01
Placunidae	<i>Placunanomia panamensis</i>	22.375	9	Species Pool	2	70	27.00	27.90	22.10	20.42	23.95	0.33	8.05	18.90	0	0.00
Lucinidae	<i>Pleurolocina leucocymoides</i>	27.7	-2.5	Species Pool	9	27	31.00	27.95	28.97	20.42	17.78	0.42	8.97	33.50	2	0.30
Lucinidae	<i>Pleurolocina taylori</i>	22.9	22.9	Species Pool	0	15	25.80	NA	22.90	NA	24.78	0.21	2.48	2.90	1	0.00
Plicatulidae	<i>Plicatula anomiooides</i>	22.375	13.5	Species Pool	0	42	30.30	27.90	22.10	20.42	23.04	0.33	12.55	16.80	0	0.00
Plicatulidae	<i>Plicatula penicillata</i>	22.375	-2.2	Species Pool	0	24	28.97	27.95	22.10	20.42	21.84	0.33	8.38	31.17	0	0.01
Plicatulidae	<i>Plicatula spondylopsis</i>	22.375	-3.6	Species Pool	0	50	31.00	29.90	22.10	20.42	22.79	0.33	7.16	34.60	1	0.01
Anomiidae	<i>Pododesmus foliatus</i>	22.375	-4.5	Species Pool	0	95	30.00	27.90	22.10	20.42	20.68	0.33	7.16	34.50	0	0.01
Psammobiidae	<i>Psammotella bertini</i>	27.8	-5	Species Pool	0	93	24.20	28.00	22.10	20.42	17.78	0.41	8.97	33.00	0	0.13
Tellinidae	<i>Psammotreta dombei</i>	22.375	-3.5	Species Pool	0	69	NA	25.60	NA	20.42	23.94	0.27	11.06	29.10	0	0.00
Tellinidae	<i>Psammotreta dombei</i>	22.375	-3.5	Species Pool	0	70	NA	27.90	NA	20.42	23.94	0.33	7.54	31.40	0	0.00
Tellinidae	<i>Psammotrella psammotrella</i>	22.375	-1.1	Species Pool	0	33	NA	31.40	NA	20.42	23.05	0.26	7.16	32.50	0	0.00
Tellinidae	<i>Psammotreta pura</i>	24.6	-5.6	Species Extralimital	0	55	30.77	31.40	24.17	20.42	19.64	0.41	8.66	37.00	1	0.09
Chamidae	<i>Pseudochama corrugata</i>	22.375	-5.8	Species Pool	0	87	29.53	27.92	22.10	20.42	19.41	0.33	8.29	35.33	1	0.05
Chamidae	<i>Pseudochama inermis</i>	22.375	7.2	Species Pool	0	79	NA	31.40	NA	20.42	23.24	0.32	7.16	24.20	0	0.00
Chamidae	<i>Pseudochama panamensis</i>	22.375	3	Species Pool	0	52	29.80	22.80	24.17	20.42	22.84	0.33	7.16	26.80	0	0.00
Chamidae	<i>Pseudochama saavedrai</i>	22.375	-3.6	Species Pool	0	65	29.80	31.33	22.10	20.42	22.84	0.33	7.16	34.93	1	0.01
Lucinidae	<i>Radiolucina cancellaris</i>	28.3	-12.1	Species Pool	0	8	28.80	31.30	26.07	20.42	18.02	0.35	12.03	43.40	0	0.12
Mastridae	<i>Raeta plicatella</i>	22.375	7.6	Species Pool	0	79	31.00	30.30	22.10	20.42	23.06	0.22	8.64	23.40	0	0.00
Mastridae	<i>Rangia mendica</i>	22.375	16.9	Species Pool	0	25	31.02	31.33	22.88	20.42	23.24	0.21	7.16	14.43	0	0.00
Nuculanidae	<i>Saccella acapulcensis</i>	22.375	1	Species Pool	4	14	NA	31.40	NA	20.42	23.24	0.33	7.16	30.40	1	0.00
Nuculanidae	<i>Saccella eburnea</i>	25.3	-4.7	Species Pool	10	17	25.30	27.87	23.20	20.42	20.04	0.33	7.07	32.57	0	0.02

Nuculanidae	<i>Saccella elenensis</i>	22.375	-5.2	Species Pool	15	14	31.03	28.00	25.97	20.42	19.30	0.33	7.16	36.23	0	0.04
Nuculanidae	<i>Saccella fastigata</i>	22.375	-5.9	Species Pool	9	40	NA	27.93	NA	20.42	19.41	0.33	8.29	33.83	0	0.03
Nuculanidae	<i>Saccella hindsii</i>	22.375	7.6	Species Pool	16	15	NA	27.90	NA	20.42	23.95	0.22	8.64	20.30	0	0.00
Nuculanidae	<i>Saccella impar</i>	22.375	-2.5	Species Pool	3	19	31.02	31.40	30.07	20.42	23.24	0.33	7.16	33.90	0	0.00
Nuculanidae	<i>Saccella laeviradius</i>	22.375	-5.8	Species Pool	7	8	NA	31.40	NA	20.42	19.41	0.33	8.29	37.20	0	0.03
Ostreidae	<i>Saccostrea palmula</i>	26.8	-5.9	Species Pool	0	75	31.20	31.40	26.67	20.42	19.41	0.41	16.19	37.30	2	0.14
Psammobiidae	<i>Sanguinolaria ovalis</i>	22.375	7.2	Species Pool	0	34	NA	27.90	NA	20.42	23.95	0.32	7.16	20.70	0	0.00
Psammobiidae	<i>Sanguinolaria tellinoides</i>	23.3	0.4	Species Pool	0	75	30.90	29.90	29.77	20.42	22.79	0.24	4.22	30.50	0	0.00
Semelidae	<i>Semele barbarae</i>	22.375	-2.7	Species Pool	0	54	27.23	NA	22.10	NA	23.64	0.33	8.40	29.93	0	0.00
Semelidae	<i>Semele bicolor</i>	22.375	-4.1	Species Pool	0	31	29.90	30.22	22.10	20.42	22.89	0.33	7.16	34.32	0	0.00
Semelidae	<i>Semele californica</i>	24.8	22.9	Species Pool	0	44	29.97	27.93	24.17	27.67	21.24	0.26	8.77	7.07	0	0.02
Semelidae	<i>Semele flavescens</i>	24.6	-4.7	Species Pool	0	69	31.02	31.40	22.88	20.42	20.04	0.41	6.98	36.10	1	0.07
Semelidae	<i>Semele formosa</i>	22.375	-2.2	Species Pool	0	77	28.37	28.40	22.10	20.42	21.89	0.23	7.50	30.60	1	0.01
Semelidae	<i>Semele hanleyi</i>	22.375	19.5	Species Pool	0	28	31.10	31.40	24.17	20.42	23.24	0.33	7.16	11.90	0	0.00
Semelidae	<i>Semele jamesi</i>	22.375	1.6	Species Pool	4	7	30.33	27.93	22.10	20.42	23.04	0.05	7.16	28.73	3	0.01
Semelidae	<i>Semele jovis</i>	22.375	9.7	Species Pool	0	71	31.12	31.50	24.17	20.42	23.24	0.33	15.90	21.80	0	0.01
Semelidae	<i>Semele laevis</i>	22.375	-3.7	Species Pool	0	89	NA	27.93	NA	20.42	23.95	0.33	7.16	31.63	0	0.00
Semelidae	<i>Semele lenticularis</i>	27.8	-3.9	Species Pool	0	30	30.33	31.40	22.87	20.42	17.78	0.41	8.97	35.30	0	0.21
Semelidae	<i>Semele pallida</i>	22.375	-3.5	Species Pool	13	41	26.67	27.95	22.10	20.42	23.93	0.33	7.96	31.45	0	0.00
Semelidae	<i>Semele pilsbryi</i>	22.375	-1.3	Species Pool	0	54	NA	27.93	NA	20.42	23.23	0.31	7.16	29.23	0	0.00
Semelidae	<i>Semele purpurascens</i>	22.375	-2.3	Species Pool	0	34	NA	27.93	NA	20.42	23.90	0.33	7.16	30.23	2	0.00
Semelidae	<i>Semele rosea</i>	24.6	-3.5	Species Pool	0	83	28.97	27.95	27.97	20.42	21.56	0.42	8.38	32.47	1	0.04
Semelidae	<i>Semele tortuosa</i>	22.375	-2	Species Pool	0	62	25.80	27.93	22.10	20.42	23.95	0.21	7.16	29.93	0	0.00
Semelidae	<i>Semele verrucosa</i>	28.3	2	Species Pool	0	27	31.08	31.50	24.27	20.42	18.35	0.20	5.25	29.50	0	0.03
Semelidae	<i>Semelina campbellorum</i>	22.375	-6.9	Species Pool	5	7	29.10	25.40	22.10	20.42	18.46	0.05	8.38	36.00	1	0.06

Semelidae	<i>Semelina subquadrata</i>	24.6	-2.2	Species Pool	0	7	25.80	27.90	22.10	20.42	21.56	0.21	7.07	30.10	1	0.02
Mytilidae	<i>Septifer zeteki</i>	22.9	-5.9	Species Pool	0	11	31.13	27.95	24.17	20.42	19.41	0.05	8.29	37.03	5	0.14
Tellinidae	<i>Serratina brevirostris</i>	22.375	-3.5	Species Pool	0	19	NA	27.90	NA	20.42	23.94	0.33	7.54	31.40	0	0.00
Tellinidae	<i>Serratina martinicensis</i>	24.6	1	Species Pool	10	13	31.02	27.90	30.68	20.42	21.56	0.37	7.07	30.02	1	0.01
Tellinidae	<i>Serratina reclusa</i>	22.375	6.4	Species Pool	0	23	NA	31.40	NA	20.42	23.24	0.29	7.16	25.00	0	0.00
Macridae	<i>Simomactra dolabriformis</i>	24.6	0.9	Species Pool	0	94	31.02	31.30	30.02	20.42	21.56	0.35	6.98	30.40	0	0.01
Thraciidae	<i>Skoglundia colpoica</i>	22.375	-3.7	Species Pool	0	24	25.17	30.03	22.10	20.42	22.79	0.33	7.16	33.73	0	0.00
Solenidae	<i>Solen pazensis</i>	22.375	15.8	Species Pool	0	58	24.20	NA	22.10	NA	25.12	0.30	11.99	8.40	0	0.00
Solenidae	<i>Solen pfeifferi</i>	22.375	-3.5	Species Pool	0	49	31.02	28.80	22.10	20.42	22.50	0.33	7.54	34.52	0	0.01
Myidae	<i>Sphenia gulfensis</i>	22.375	23.2	Species Pool	0	13	25.80	31.40	22.10	23.20	23.24	0.21	4.83	9.30	0	0.00
Spondylidae	<i>Spondylus crassisquama</i>	28.3	-6.7	Species Pool	10	145	28.90	27.92	23.03	20.42	18.35	0.44	10.08	35.60	1	0.08
Spondylidae	<i>Spondylus leucacanthus</i>	28.3	-1.3	Species Pool	10	156	29.53	28.70	28.97	26.95	18.35	0.31	6.42	30.83	0	0.03
Spondylidae	<i>Spondylus limbatus</i>	22.375	-3.9	Species Pool	0.5	249	31.02	31.40	24.17	20.42	20.47	0.10	7.16	35.30	4	0.04
Tellinidae	<i>Strigilla chroma</i>	22.375	-4.1	Species Pool	0	25	NA	31.70	NA	20.42	23.00	0.33	7.16	35.80	0	0.00
Tellinidae	<i>Strigilla cicercula</i>	22.375	0	Species Pool	0	12	31.13	27.92	22.10	20.42	23.20	0.25	7.16	31.13	0	0.00
Tellinidae	<i>Strigilla dichotoma</i>	22.375	-1.1	Species Pool	0	9	30.30	30.60	22.10	20.42	23.04	0.26	7.16	31.70	0	0.00
Tellinidae	<i>Strigilla ervilia</i>	22.375	-2.2	Species Pool	0	11	23.88	27.87	22.88	20.42	23.90	0.28	7.16	30.07	0	0.00
Tellinidae	<i>Strigilla interrupta</i>	21.6	-2.2	Species Pool	9	8	NA	NA	NA	NA	23.90	0.39	11.25	23.80	0	0.01
Tellinidae	<i>Strigilla serrata</i>	24.1	-1.1	Species Pool	0	10	31.02	31.70	30.02	20.42	22.87	0.26	5.33	32.80	1	0.00
Ostreidae	<i>Striostrea prismatica</i>	22.375	-4.1	Species Pool	0	190	24.20	23.22	22.10	20.42	23.38	0.33	7.16	28.30	0	0.00
Carditidae	<i>Strophocardia megastropa</i>	22.375	-1.9	Species Pool	0	54	29.60	27.95	22.10	20.42	22.61	0.05	7.16	31.50	3	0.01
Solecurtidae	<i>Tagelus longisinuatus</i>	22.375	16.2	Species Pool	0	62	NA	23.22	NA	20.42	26.54	0.33	7.16	7.02	0	0.00
Solecurtidae	<i>Tagelus peruanus</i>	22.375	-12	Species Pool	0	48	NA	23.42	NA	20.42	18.02	0.33	14.76	35.42	0	0.12
Solecurtidae	<i>Tagelus peruvianus</i>	22.375	-3.7	Species Pool	0	85	31.00	27.90	22.10	20.42	23.29	0.33	7.16	34.70	0	0.00
Solecurtidae	<i>Tagelus politus</i>	24.6	-3.5	Species Pool	0	50	31.20	27.95	27.05	20.42	21.56	0.42	7.54	34.70	1	0.04

Tellinidae	<i>Tellidora burneti</i>	22.375	-2.2	Species Pool	0	49	31.02	31.40	26.88	20.42	23.24	0.33	7.16	33.60	0	0.00
Tellinidae	<i>Tellina subangulata</i>	24.6	7.9	Species Pool	0	25	NA	NA	NA	NA	21.56	0.29	9.31	16.70	0	0.01
Tellinidae	<i>Tellinella cumingii</i>	22.375	-2.5	Species Pool	4	69	NA	31.40	NA	20.42	23.24	0.33	7.16	33.90	0	0.00
Tellinidae	<i>Tellinidella purpurea</i>	22.375	-4.1	Species Pool	0	72	24.20	23.20	22.10	20.42	23.38	0.33	7.16	28.30	0	0.00
Tellinidae	<i>Temnoconcha cognata</i>	22.375	-3.9	Species Pool	0	66	29.90	27.90	22.10	20.42	22.89	0.33	7.16	33.80	0	0.00
Corbulidae	<i>Tenuicorbula tenuis</i>	22.375	-3.7	Species Pool	0	25	NA	28.90	NA	20.42	22.31	0.33	7.71	32.60	0	0.01
Thraciidae	<i>Thracia bereniceae</i>	22.375	9.7	Species Pool	0	25	26.67	31.40	24.17	20.42	23.24	0.33	15.90	21.70	0	0.01
Thraciidae	<i>Thracia squamosa</i>	24.6	7.8	Species Pool	0	36	31.00	28.00	23.17	20.42	20.47	0.10	7.07	23.20	2	0.03
Ungulinidae	<i>Timothyus inezensis</i>	24.6	-1.6	Species Pool	6	20	31.00	30.30	26.90	20.42	21.56	0.26	6.98	32.60	0	0.01
Veneridae	<i>Tivela argentina</i>	22.375	-3.5	Species Pool	0	68	31.02	31.30	30.02	20.42	23.24	0.33	7.54	34.80	0	0.01
Veneridae	<i>Tivela byronensis</i>	27.8	-4.2	Species Pool	0	63	31.02	31.30	26.02	20.58	17.78	0.35	8.97	35.50	1	0.28
Veneridae	<i>Tivela delessertii</i>	22.375	8.5	Species Pool	0	41	27.05	23.30	22.10	20.42	24.18	0.23	8.40	18.55	0	0.00
Veneridae	<i>Tivela lessonii</i>	22.375	-5.1	Species Pool	0	70	NA	22.40	NA	20.42	19.67	0.33	7.16	27.50	0	0.03
Veneridae	<i>Tivela lineata</i>	22.9	0.5	Species Pool	0	31	25.80	28.00	22.10	20.42	23.95	0.21	7.07	27.50	0	0.00
Veneridae	<i>Tivela planulata</i>	24.6	-5.1	Species Pool	0	65	27.33	28.85	22.88	20.42	19.67	0.46	7.53	33.95	0	0.10
Cardiidae	<i>Trachycardium belcheri</i>	28.3	-3.5	Species Pool	14	44	27.05	28.22	23.55	20.42	18.35	0.21	8.40	31.80	0	0.09
Cardiidae	<i>Trachycardium consors</i>	22.375	-2.2	Species Pool	0	84	29.53	31.50	23.55	20.42	22.61	0.33	7.16	33.70	1	0.01
Cardiidae	<i>Trachycardium procerum</i>	27.8	-14.2	Species Extralimital	0	117	31.02	31.30	24.17	20.42	17.22	0.35	12.32	45.50	1	0.37
Veneridae	<i>Transennella caryonautes</i>	22.9	15.8	Species Pool	10	46	24.13	27.90	23.13	23.22	23.95	0.29	11.99	12.10	0	0.00
Veneridae	<i>Transennella modesta</i>	22.375	-1.3	Species Pool	0	35	27.32	27.95	22.10	20.42	23.23	0.31	7.16	29.25	1	0.00
Veneridae	<i>Transennella vulnerata</i>	22.9	-5.6	Species Pool	0	48	26.60	27.90	22.10	20.42	19.64	0.34	8.66	33.50	0	0.03
Cardiidae	<i>Trigoniocardia granifera</i>	24.1	-3.5	Species Pool	0	18	30.77	31.50	29.77	20.42	22.87	0.35	7.54	35.00	2	0.03
Glycymerididae	<i>Tucetona multicostata</i>	24.6	-2.2	Species Pool	8	46	30.07	31.40	23.55	20.42	21.56	0.41	6.98	33.60	3	0.05
Glycymerididae	<i>Tucetona strigilata</i>	22.375	-3.7	Species Pool	10	49	28.97	27.93	22.10	20.42	21.84	0.33	8.38	32.67	0	0.01
Corbulidae	<i>Varicorbula obesa</i>	28.3	6.7	Species Pool	14	13	25.50	27.95	22.10	20.42	18.35	0.27	7.07	21.60	0	0.05